U.PORTO

DOUTORAMENTO

BIOLOGIA BÁSICA E APLICADA

Gene Regulation in the Tumor - Immune System Microenvironment Crosstalk

Joana Fernandes Alberto Wilton Pereira

D

2021

U.PORTO

Joana Fernandes Alberto Wilton Pereira. Gene Regulation in the Tumor - Immune System Microenvironment Crosstalk

D.ICBAS **2021**

Gene Regulation in the Tumor - Immune System Microenvironment Crosstalk

Joana Fernandes Alberto Wilton Pereira

SEDE ADMINISTRATIVA

INSTITUTO DE CIÊNCIAS BIOMÉDICAS ABEL SALAZAR

FACULDADE DE CIÊNCIAS

FACULDADE DE MEDICINA

GENE REGULATION IN THE TUMOR-IMMUNE SYSTEM MICROENVIRONMENT CROSSTALK

Tese de candidatura ao grau de Doutor em Biologia Básica e Aplicada (GABBA), Programa Doutoral da Universidade do Porto
(Instituto de Ciências Biomédicas Abel Salazar, Faculdade de Ciências e Faculdade de Medicina da Universidade do Porto)

Orientadora – Doutora Maria Alexandra Marques Moreira
Categoria – Investigadora Principal
Afiliação – Instituto de Ciências Biomédicas Abel Salazar, Instituto de Biologia Molecular e Celular e Universidade do Porto, Porto, Portugal

Co-orientadora – Doutora Maria José Cardoso Oliveira
Categoria – Investigadora Principal
Afiliação – Faculdade de Medicina, Instituto Nacional de Engenharia Biomédica e Universidade do Porto, Porto, Portugal

“Nothing in life is to be feared, it is only to be understood. Now is the time to understand more, so that we may fear less.” - Marie Skłodowska-Curie

De acordo com o disposto na alínea A, ponto número 2 do Artigo 31.º do Decreto-Lei n.º 230/2009, de 14 de Setembro, a autora declara que na elaboração desta tese foram incluídos resultados descritos e aceites na publicação abaixo indicada. A autora participou ativamente na concepção, execução, interpretação e discussão dos trabalhos que estiveram envolvidos em todo o documento, bem como na sua redação na integra.

As contribuições de análise de dados que não foram realizadas pela autora são as seguintes: no artigo submetido à revista *Cell Reports* (subchapter 4.2), o co-autor Michael Tellier fez o gráfico do metaperfil da expressão genética de M1 e M1 + RKO (Seccao 4.2 Painel 1D), e a co-autora Angela Margarida Costa realizou a análise dos genes por mim identificados utilizando a base de dados The Cancer Genome Atlas Program (TCGA) para identificar diferenças na expressão de RNA e correlacionar com a sobrevivência de doentes com cancro (Seccao 4.2, painéis centro e direito 1I 1J 2D 2E, e Painel 2H).

According to the above-mentioned Portuguese legislation, the author declares that the present thesis includes described and accepted data in the publication indicated below. The author actively participated in the conception, execution, interpretation and discussion of all data present in this thesis, as well as the entirety of its writing.

Contributions of data analysis that were not performed by the author are as following: in the article submitted to the *Cell Reports* paper (subchapter 4.2), co-author Michael Tellier made the metaprofile graph of differences in gene expression of M1 and M1 + RKO, and co-author Angela Margarida Costa made the data analyses graphs from the databases on The Cancer Genome Atlas (TCGA) to identify differences in protein expression and patient survival of the identified DEGs.

Published article included in this thesis / Publicação incluída nesta tese

Joana Wilton, M Tellier, T Nojima, AM Costa, MJ Oliveira, AM Moreira (2021), *Simultaneous studies of gene expression and alternative polyadenylation in primary human immune cells*, *Methods in Enzymology*, 655:349-399.
doi: 10.1016/bs.mie.2021.04.004.

Article in revision / Publicação em fase de revisão:

Joana Wilton, Michael Tellier, Takayuki Nojima, Isabel Pereira-Castro, Angela M Costa, Jaime Freitas, Ricardo Pinto, Luísa Pereira, Shona Murphy, Maria Jose Oliveira, Nicholas J Proudfoot, Alexandra Moreira, *Proximity to colorectal cancer cells modulates macrophage alternative polyadenylation, in revision.*

The research described in this thesis was developed at the:

- Gene Regulation and Tumor and Microenvironment Interaction research groups at i3S – Instituto de Investigação e Inovação em Saúde da Universidade do Porto, Porto, Portugal
- Prof. Nicholas Proudfoot laboratory at the Sir William Dunn School of Pathology, University of Oxford, Oxford, United Kingdom

Methods in Enzymology is part of Elsevier publishing. The article included herein is authorized by its Copyright policy, which states that the authors: "(…) retain the rights to use their research data freely without any restriction, re-use their own material in new works without permission or payment (with full acknowledgement of the original article): Extend an article to book length, Include an article in a subsequent compilation of their own work, Re-use portions, excerpts, and their own figures or tables in other works, use and share their works for scholarly purposes (with full acknowledgement of the original article); **Include in a thesis or dissertation (provided this is not published commercially)**"

See full copyright policy information at https://www.elsevier.com/about/policies/copyright

Financial Support

Work in Moreira's laboratory was funded by the National Funds through Fundação para a Ciência e Tecnologia (FCT), I.P., under the project UIDB/04293/2020, through project Norte-01-0145-FEDER-000008 - Porto Neurosciences and Neurologic Disease Research Initiative at I3S, and NORTE-01-0145-FEDER-000051 – "Cancer Research on Therapy Resistance: From Basic Mechanisms to Novel Targets", through support by Norte Portugal Regional Operational Programme (NORTE 2020), under the PORTUGAL 2020 Partnership Agreement, through the European Regional Development Fund (ERDF)"; HORIZON2020 EU Grant Agreement No. 68335: "FOLSMART - Folate-Target Nanodevices To Activated Macrophages For Rheumatoid Arthritis", and by Programa Operacional Regional do Norte and co-funded by European Regional Development Fund under the project "The Porto Comprehensive Cancer Center" with the reference NORTE-01-0145-FEDER-072678 - Consórcio PORTO.CCC – Porto Comprehensive Cancer Center.

Joana Wilton was awarded a PhD fellowship (PD/BD/114168/2016) by FCT-Portuguese Foundation for Science and Technology from January 2016 to December 2019, and a fellowship (H2020-NMP-PILOTS-2015-683356-FOLSMART) from January 2020 to July 2020.

U.PORTO
ICBAS INSTITUTO DE CIÊNCIAS BIOMÉDICAS ABEL SALAZAR
SCHOOL OF MEDICINE AND BIOMEDICAL SCIENCES
3S INSTITUTO DE INVESTIGAÇÃO E INOVAÇÃO EM SAÚDE UNIVERSIDADE DO PORTO
FCT Fundação para a Ciência e a Tecnologia
PCCC PORTO. COMPREHENSIVE CANCER CENTRE
A·B·B·A
NORTE 2020 PROGRAMA OPERACIONAL REGIONAL DO NORTE
Horizon 2020 European Union Funding for Research & Innovation

Acknowledgements

First and foremost, my eternal gratitude is due to the GABBA Coordinating Committee: Professors António Amorim, Alexandre do Carmo, Fátima Carneiro, Maria de Sousa, João Relvas, Manuel Sobrinho Simões e Claudio Sunkel, that inspire me to embody the GABBA spirit every day. I would also like to take this opportunity and thank the funding agency FCT for financial support.

Secondly, I would like to thank my main supervisor, Professor Alexandra Moreira, for the opportunity to tackle my late-blooming passion for gene regulation in her lab. I'd like to thank her for the fruitful discussions, late-night enthusiastic pep talks and for always challenging me to become a better scientist. Thank you for always keeping your door open to my questions and for always keeping our eyes on the prize: truthful, slow science.

I'm also grateful to my co-supervisor, Maria Jose Oliveira, for encouraging me throughout the years, and for generously explaining the intricacies of the tumor microenvironment to a naïve first-year PhD student. Thank you for seeing unforeseen links between this project and others', and for the detail and effort you put into your work.

Thank you both for having accepted the marriage of ideas that became this project.

As no (wo)man is an island, there are a few people I wish to acknowledge. I will keep this as concise as possible.

To the GR lab: thank you all for encouraging critical thinking, teamwork and integrity at all times. Isabel Castro, my sister from another father, thanks for the tough-love warmth and for sharing your broad knowledge. Beatriz Garcia, I love your persistence, inventiveness, enthusiasm, and grit. Thanks for telling me what I needed – not what I wanted – to hear. Marta Oliveira, there are no words for your discrete generosity and friendship. I wish you all the best and I miss the yin to my yang all the time. Jaime Freitas, thank you for the support only a Whatsapp message away. Past members Ana, Andreia, Joana, and Olena, your companionship will not be forgotten.

To the TMI lab: thank you Angela for the help about co-cultures. Thanks Flavia P and Andreia for the help in ELISA. To the CAGE lab: thank you Sonia, Emma and Diana for all the good moments in the 118 room during the long macrophage isolation days. To my i3S neighbors Sofia Valente, Rita Matos, Renata Carrico, Fábio Ferreira, Mafalda Pinho, Claudia Brito, Ana Almeida and many others, thanks for always lending a kind ear. To the Lab Support and Maintenance Units, thank you for making our jobs easier every day, with grace and professionalism.

Thank you to my MSc thesis supervisors, Cristina Cordas and Pedro Tavares, for being the first people to motivate me to continue in science. Don't worry, I won't hold it against you!

À Anabela, pela empatia aleatoriamente descoberta numa tarde de Verão. Às inóvias Catarina Spratley e Núria Amorim: pela amizade sem cobranças – "¡*os quiero muchísimo*!".

As meninas do i3S Diagnostics, o meu mais recente desafio – Gina, Margarida, Rute, Susete e Diana – obrigada pelos bons momentos entre pipetagens.

Às minhas amigas mais antigas, Inês, Cláudia, Mafalda, Diana, obrigada por me proporcionarem o retorno a normalidade. À GABBinha Rita Gomes, por ser por vezes a pessoa que melhor compreendeu. Às Filipas M e V, pelos conselhos sempre certeiros.

À Diana e ao Luís, pela amizade recente mas intensa. À comadre Inês, por termos crescido tanto juntas. À Teresa e à sua mãe Antónia, obrigada por serem a minha casa longe de casa. À Maria João pela sua extraordinária perspicácia e amizade férrea.

À minha família: aos meus pais pelo incentivo em embarcar nesta aventura e pelos valores incutidos, e ao meu irmão, por trazer um pouco do seu frenesim tão confortável nas suas visitas. Obrigada a todos pelos conselhos e pela perspectiva.

Ao João, pelo amor e apoio contínuos e incondicionais que tornaram possível ter feito este processo com saúde, alegria e lucidez. Obrigada por teres sido um *sounding board* para ideias e ensaios. A tua calma e carinho foram o porto seguro de que não sabia precisar.

Esta tese é dedicada aos meus avós, Belmira, Maria José, Rui e Vasco.

Presentations in Conferences in the scope of this PhD

a. Oral communications

- **Joana Wilton**, J Freitas, I Pereira-Castro, AM Costa, K Kamieniarz-Gdula, T Nojima, M Tellier, S Murphy, N J Proudfoot, MJ Oliveira, A Moreira, *Transcriptomics in primary human macrophages: from polarization to tumor co-cultures*, SICR 2019, Symposium on Immunomodulation in Cancer and Regeneration, 25th June 2019, i3S, Porto, Portugal. Selected Oral Presentation. Best Oral Presentation Award.
- **Joana Wilton**, *Don't shoot the messenger: RNA at the center of unraveling mechanisms of gene regulation in the cancer – macrophage microenvironment*, i3S Retreat, November 29th 2018, Póvoa do Varzim, Portugal. Speed talk.

b. Poster communications

- **Joana Wilton**, M Tellier, T Nojima, I Pereira-Castro, J Freitas, AM Costa, S Murphy, NJ Proudfoot, MJ Oliveira, AM Moreira, *SRSF12 and cancer cells modulate macrophage alternative polyadenylation*, RNA 2021 Virtual Meeting, Session 5, May 25th-June 5th 2021. Online-led event.
- **Joana Wilton**, J Freitas, I Pereira-Castro, K Kamieniarz-Gdula, T Nojima, M Tellier, AM Carmo, S Murphy, NJ Proudfoot, MJ Oliveira, AM Moreira, *Transcriptomics in primary human macrophages: from pro-inflammatory polarization to tumor interactions*, Cold Spring Harbor Meeting - Eukaryotic mRNA Processing, Aug 20th - 24th 2019, Cold Spring Harbor, New York, USA.
- Freitas J, **Joana Wilton**, Lager F, Renault G, Nogueira, E, Guimarães D, Cavaco-Paulo A, Bismuth, G, Carmo, AM, Moreira, A (2018), *Rheumatoid Arthritis treatment with folate-based liposomes encapsulating MTX reveals specific mRNA signatures*, ptRNA Meeting, January 24th-25th 2019, i3S, Porto, Portugal.
- **Joana Wilton**, J Freitas, I Pereira-Castro, AM Costa, K Kamieniarz-Gdula, T Nojima, M Tellier, Murphy, N J Proudfoot, MJ Oliveira, A Moreira, *mRNA at the center of gene regulation in macrophages: from polarization to tumor co-cultures*, ptRNA Meeting, January 24th-25th 2019, i3S, Porto, Portugal. Best Poster Award.
- Freitas J, **Joana Wilton**, Lager F, Renault G, Nogueira E, Cavaco-Paulo A, Bismuth G, Carmo AM, Moreira A (2018), *RNA-Seq analysis reveals unique transcriptional signatures associated with Rheumatoid Arthritis treatment with targeted liposomes encapsulating MTX, RNA and Disease Meeting*, November 17th-20th 2018, Uppsala, Sweden.
- **Joana Wilton**, Freitas, J, Pereira-Castro, I, Costa, AM, Castro, F, Oliveira, MJ, Moreira, A, *Don't shoot the messenger: RNA at the center of unraveling mechanisms of gene regulation in the cancer – macrophage microenvironment*, 8th conference of the International Cancer Microenvironment Society (ICMS), June 10th -14th 2018, Lisbon, Portugal.
- **Joana Wilton**, I Pereira-Castro, J Freitas, AM Costa, F Castro, MJ Oliveira, AM Moreira, *Mechanisms of gene regulation in the crosstalk of the cancer – macrophage microenvironment*, SICR2017 – Symposium on Immunomodulation in Cancer and Regeneration, 23rd June 2017, i3S, Porto, Portugal. Best Poster Award.

Table of Contents

Published article included in this thesis / Publicação incluída nesta tese 5

Financial Support 7

Acknowledgements 9

Presentations in Conferences in the scope of this PhD 11

Abstract 15

List of Figures 25

List of Tables 27

Chapter I – General Introduction 29

1. Hallmarks of cancer 30

1.1 Colorectal cancer 30

1.2 The tumor microenvironment 31

1.2.1 Tumor Microenvironment: cellular components 32

1.2.1.1 Stromal Cells 33

1.2.1.2 Macrophages 34

1.2.1.3 Other immune cells 44

1.2.2 Physico-chemical properties of the Tumor Microenvironment 46

1.2.2.1 Oxygen content: hypoxia and angiogenesis 46

1.2.2.2 Epithelial to mesenchymal transition 47

1.2.2.3 Extracellular matrix: cellular architecture 48

1.3 Mimetizing the Tumor Microenvironment: Co-cultures 49

2. Transcription and alternative 3' UTR regulation 51

2.1 Transcription: initiation, elongation and termination 51

2.2 Pre-mRNA 5' capping and splicing 56

2.3 Pre-mRNA 3' end processing – cleavage and polyadenylation 58

2.3.2 Auxiliary regulatory elements: 60

2.3.3 Alternative Polyadenylation (APA) and alternative 3' UTRs 61

3. Alternative 3' UTR mRNA isoforms produced by Alternative Polyadenylation 66

3.1 Alternative 3' UTR mRNA isoforms in macrophages _____ 66
3.2 Alternative 3' UTR mRNA isoforms in cancer _____ 68

Chapter II – Thesis Aims _____ ***71***

Chapter III – Results _____ ***75***

3.1 ***Simultaneous studies of gene expression and alternative polyadenylation in primary human immune cells*** _____ **77**

3.2 ***Proximity to colorectal cancer cells modulates macrophage alternative polyadenylation*** _____ **129**

3.3 ***Expression of RAC1 alternative 3' UTR depends on macrophages and CRC cells state*** _____ **183**

Chapter IV – General Discussion _____ ***205***

Chapter V – Future work _____ ***219***

Chapter VI - References _____ ***222***

Abstract

Primary human macrophages are very plastic and their transcriptome may be affected by neighboring cell types and RNA metabolism factors.

Through several RNA-Seq methodologies in steady-state and fractionated RNA, we demonstrate that pro-inflammatory M1 macrophages change both gene expression and alternative polyadenylation profiles, producing mRNAs with shorter 3'UTRs, in comparison to naïve M0 macrophages. Furthermore, exposure of M1 macrophages to colorectal cancer cells (CRC) induces a pro-inflammatory to anti-inflammatory (M2) alterations, illustrated by the macrophage gene expression profile. This allowed us to identify a 35 gene signature panel – including *LRP5*, *MRC1*, and *THBS1* – consisting of genes that promote tumor progression and whose expression is increased upon co-culture with CRC cells.

Simultaneously, we quantified the number of alternative 3'UTR mRNA isoforms in all macrophage populations – the naïve M0, the pro-inflammatory M1, and pro-inflammatory macrophages co-cultured with CRC cells. We observed that while M0 and M1 macrophages express similar numbers of alternative 3' UTR mRNA isoforms, when co-cultured with CRC cells, macrophages present an increase in the number of genes producing only one mRNA isoform. Curiously, this occurred mainly in RNA metabolism-related genes.

When comparing the expression profile of M1 pro-inflammatory with that of M0 macrophages, we also identified a 46 gene signature consisting of 33 genes with increased expression of the short 3' UTR mRNA that are involved in macrophage biology such as *MAP3K8* and *MXD1*. The other 13 genes showed an increase in the long 3' UTR mRNA expression, and this subset includes genes connected to the immune system such as *IL12RB1*. Interestingly, 45 of the 46 genes maintained their differential 3' UTR mRNA expression in macrophages upon co-culture with CRC cells.

These two transcriptomic signatures – gene expression modifications upon CRC co-culture and 3' UTR mRNA isoform expression in M1 and co-cultured macrophages – were validated *in vitro*. Additionally, *in silico* analyses of CRC patient databases we suggest that some of these signatures are correlated with patient survival. For instance, upregulated *LRP5* and *SEMA6B* expression in tumor-associated

macrophages mat be protective, increasing patient survival, while upregulation of *MAP3K8*, *MXD1* and *IL12RB1* were probably deleterious to tumor patients.

These findings prompted us to investigate the molecular mechanisms involved in the transcriptomic modifications detected. We observed that SRSF12, an SR protein, is upregulated in pro-inflammatory M1 macrophages in comparison to M0 macrophages, therefore we asked if this protein was involved in the mechanism. SRSF12 siRNA depletion in M1 macrophages caused a decrease in the expression of innate immune response genes and in genes involved in RNA metabolism. Furthermore, SRSF12 depletion led to a decrease in the number of APA mRNA isoforms expressed in M1 macrophages, suggesting a function in proximal polyA signal selection.

Hypoxia and inflammation are known drivers in gene expression. Here, we present a single-gene study on the expression and APA in macrophages polarized to distinct inflammatory profiles and CRC cells upon hypoxia. We focused on *RAC1, MCL1,* and *CD47* as these genes are expressed in the CRC cell line RKO, and also in primary human macrophages. IL1B was also analyzed in macrophages due to its importance for the innate immune response, and HIF1A in CRC cells, as HIF1A is involved in the hypoxia response. Our results evidenced a trend towards upregulation of *RAC1, MCL1, IL1B, CD47* mRNAs with short 3' UTRs in pro-inflammatory M1 macrophages, but not in CRC cells. We also show in M1 macrophages that YBX1 binds to the 3'UTR of *Rac1* mRNA. Moreover, by ChIP analysis, we show that RNAPII occupancy increases on *RAC1* gene in RKO cells upon hypoxia. In conclusion, we show that hypoxia causes transcriptomic alterations in CRC cells and that pro-inflammatory polarization causes transcriptomic changes in macrophages, and reinforce that alternative polyadenylation is a gene, cell-type and cell-state-specific mechanism.

Overall, we show that pro-inflammatory polarization, CRC co-culture and SRSF12 all modulate gene expression and APA mRNA profiles in macrophages, affecting their inflammatory and anti-tumor properties. We propose that SRSF12 activates proximal polyA signal selection and influences the expression of macrophage-related genes and of RNA metabolism-associated genes, suggesting a new role for SRSF12 in macrophage function.

Keywords: Alternative polyadenylation; 3' UTR; mRNA isoforms; 3' mRNA-Seq; Chromatin-bound RNA-Seq; Nucleoplasm RNA-Seq; Subcellular fractionation; DGE; primary human macrophages differentiation and polarization; macrophage-cancer cells co-culture; *SRSF12*; *LRP5*; *MRC1*; *THBS1*; *MAP3K8*; *MXD1*; IL12RB1; *RAC1*; *MCL1*; *IL1B*; *CD47*.

Sumário

Os macrófagos primarios humanos são muito plásticos, e o seu transcriptoma pode ser afectado por células adjacentes e factores de metabolismo de RNA.

Através de RNA-Seq *steady state* e em amostras fraccionadas, este trabalho demonstra que os macrófagos M1 pro-inflamatórios mudam os seus perfis de expressão genética e poliadenilação alternativa, produzindo mRNAs com 3' UTRs mais curtas, em comparação com macrófagos M0 não estimulados. Além disso, a estimulação dos macrófagos M1 com células de cancro colorectal (CRC) induz mudanças no perfil de expressão genética dos macrófagos, alterando o seu perfil de pro-inflamatório para anti-inflamatório (M2). Esta estratégia permitiu a identificação de uma assinatura com 35 genes cuja expressão genética aumenta após co-cultura com células de CRC, incluindo genes que promovem a progressão tumoral, como *LRP5*, *MRC1* e *THBS1*.

Simultaneamente, o número de isoformas de mRNA com APA em todas as populações de macrófagos foram quantificadas – M0, M1, e macrófagos após co-cultura com células de CRC. M0 e M1 apresentam números semelhantes de isoformas de mRNA com e sem APA, mas os macrófagos após co-cultura evidenciaram um aumento no número de genes que produzem apenas uma isoforma de mRNA. Curiosamente, esta observação ocorreu principalmente em genes ligados ao metabolismo de RNA.

Ao comparar o perfil de expressão genetica de macrófagos M0 e M1, foi identificada uma assinatura de 46 genes, consistindo em 33 genes que apresentam um aumento na expressão de mRNAs com 3' UTRs curtas, incluindo genes envolvidos na biologia dos macrófagos, como *MAP3K8* e *MXD1*. Os restantes 13 genes identificados apresentam um aumento na expressão de mRNAs com 3' UTRs longas, incluindo genes ligados ao sistema imunitário, como *IL12RB1*. Curiosamente, 45 dos 46 genes mantiveram a sua isoforma 3' UTR predominante em macrófagos após co-cultura com células de CRC.

Estas duas assinaturas transcriptómicas, consistindo em diferenças de expressão genética após co-cultura com células de CRC e diferenças na expressão de isoformas de mRNA em M1 e macrófagos após co-cultura, foram validadas *in vitro*. Adicionalmente, análises *in silico* de bases de dados de pacientes com CRC sugerem que alguns genes estavam correlacionados com sobrevivência de pacientes. Por exemplo, a sobre-expressão de *LRP5* e *SEMA6B* em macrófagos associados a tumores pode ser protetora, aumentando a sobrevivência de pacientes, enquanto a sobre-expressão de *MAP3K8*, *MXD1* e *IL12RB1* pode ser perniciosa para pacientes com cancro.

Estas descobertas levaram-nos a investigar os mecanismos moleculares envolvidos nestas diferenças. O gene *SRSF12* é sobre-expresso em macrófagos M1 em comparação com macrófagos M0, e assim questionamos se este gene poderia estar envolvida nas alterações transcriptómicas observados. A depleção de SRSF12 por siRNA em macrófagos M1 provocou uma diminuição na expressão de genes da resposta imunitária inata, e em genes envolvidos no metabolismo de RNA. Além

disso, a depleção de SRSF12 provoca uma diminuição no número de isoformas de mRNA com APA em macrófagos M1, sugerindo uma função na selecção de sinais de poliadenilação proximais.
A hipóxia e a inflamação são moduladoras da expressão genética. Consequentemente, realizou-se um estudo de expressão genética e APA de genes em macrófagos polarizados para perfis inflamatórios distintos e na linha celular de CRC RKO em hipóxia. Os genes escolhidos foram *RAC1*, *MCL1* e *CD47*, visto que são expressos em ambos os tipos de células. Adicionalmente, incluiu-se o gene *IL1B* em macrófagos devido a sua importância para a resposta imune inata, e o gene *HIF1A* em células de CRC devido ao seu envolvimento na resposta de hipóxia. Descobriu-se uma tendência em macrófagos para a sobre-expressão das isoformas de 3' UTR curtas de *MCL1*, *IL1B*, *CD47* e a sobre-expressão da isoforma longa de 3' UTR de *RAC1*, o que não ocorre em células de CRC. Adicionalmente, caracterizamos a ligação da proteína YBX1 ao mRNA com a 3' UTR de *RAC1* em M1. Adicionalmente, por análise de ChIP mostramos que a ocupação da RNAPII aumenta no gene de RAC1 em células de RKO em hipóxia. Concluímos que a hipóxia provoca modificações transcriptómicas em células de CRC e que a polarização pro-inflamatória provoca alterações transcriptómicas nos macrófagos, reforçando que a poliadenilação alternativa é específica em cada gene, tipos e estado celular.
Em suma, mostramos que a polarização pro-inflamatória, a co-cultura com células CRC, e a presença de SRSF12 modulam a expressão genética e os perfis de APA, afectando as funções de inflamação e ação anti-tumoral. Propomos que o SRSF12 activa a seleção de sinais de poliadenilação proximal e influencia a expressão de genes relacionados com macrófagos e genes de metabolismo de RNA, sugerindo um novo papel para SRSF12 em macrófagos.

Palavras-chave: Poliadenilação alternativa; 3' UTR; isoformas de mRNA; 3' mRNA-Seq; Chromatin-bound RNA-Seq; Nucleoplasm RNA-Seq; Fracionamento subcelular; diferencial de expressão genetica; diferenciação e polarização de macrófagos humanos primarios; co-cultura de macrófagos com células de cancro; *SRSF12*; *LRP5; MRC1; THBS1; MAP3K8; MXD1; IL12RB1; RAC1*; *MCL1*; *IL1B*; *CD47*; Hipóxia.

List of Abbreviations

0-9

16S – prokaryotic small-subunit ribosomal RNA

18S – nuclear small-subunit ribosomal RNA

3' UTR – 3' untranslated region

3'Seq – 3' RNA sequencing

3D – three-dimensional

A

APA – alternative polyadenylation

APC [standalone] – antigen presenting cell

APC [standalone] – adenomatous polyposis coli gene

APC [when suffixed] – allophycocyanin

AREs – AT-rich elements

ATCC – American Type Culture Collection

AS – antisense

ASO – antisense oligonucleotide

B

bp – base pairs

C

CCL – chemokine (C-C motif) ligand

CCR – chemokine (C-C motif) receptor

CD – cluster of differentiation

cDNA – complementary DNA

CDK – cyclin-dependent kinase

CDS – coding sequence

CFIm – mammalian cleavage factor I

CFIIm – mammalian cleavage factor II

ChIP – chromatin immunoprecipitation

ChrRNA – chromatin-bound RNA

ChrRNA-Seq – chromatin-bound RNA sequencing

CPA – cleavage and polyadenylation

CPSF – cleavage and polyadenylation specificity factor

CR-APA – coding region APA

CRC – colorectal cancer

CS – cleavage site

CstF – cleavage stimulation factor

CTD – carboxy-terminal domain

CXCL – chemokine (C-X-C motif) ligand

CXCR – chemokine (C-X-C motif) receptor

D

DAPI – 4',6-diamidino-2-phenylindole

DC – dendritic cell

DESeq – differential analysis of count data

DEG – differentially-expressed genes

DEXSeq – differential use of exons in RNA-sequencing data

Dfx - desferrioxamine

DGE – differential gene expression

DNA – deoxyribonucleic acid

DNase – deoxyribonuclease

dNTPs – deoxyribonucleotide triphosphate

dPAS – distal polyadenylation signal

DSE – downstream sequence element

E

ECL – enhanced chemiluminescence

ECM – extracellular matrix

EDTA – ethylene diamine tetra-acetic acid

EGF – epithelial growth factor

EGFR – epithelial growth factor receptor

ELISA – enzyme-linked immunosorbent assay

ELAVL1 – embryonic lethal abnormal vision-like 1
EMT – epithelial-mesenchymal transition

F
FBS – fetal bovine serum
FC – flow cytometry
FDR – false discovery rate
FITC – fluorescein isothiocyanate

G
GAPDH – glyceraldehyde 3-phosphate dehydrogenase
GLOBOCAN – Global Cancer Observatory
GO – gene ontology
GSEA – gene set enrichment analysis

H
HIF-1A – hypoxia-inducible factor 1-alpha
hnRNP – heterogenous nuclear ribonucleic protein
HRP – horseradish peroxidase
HSC – hematopoietic stem cell
Htseq-count – analyzing high-throughput sequencing data

I
IF – immunofluorescence
IFN – interferon
Ig – immunoglobulin
IGV – Integrative Genomics Viewer
IL – interleukin
IP - immunoprecipitation

K
kb – kilobase
kDa – kilodalton

L
lincRNA – long intergenic non-coding RNA
LNA – locked nucleic acid
LPS – lipopolysaccharide
LRP5 – low-density lipoprotein receptor-related protein 5

M
M0 – naïve macrophages
M1 – pro-inflammatory macrophages
M2 – anti-inflammatory macrophages
M-CSF – macrophage colony-stimulating factor
Mac – macrophages
MAPK – mitogen-activated protein kinase
MCL1 – myeloid cell leukemia 1
MFI – median fluorescence intensity
miRNA - microRNA
MHC – major histocompatibility complex
MMR – mismatch repair system
Mox – detoxifying macrophages
MRC1 – C-type mannose receptor 1
mRNA – messenger RNA
MSI – microsatellite instability
MSS – microsatellite stability

N
NF-kB – nuclear factor kappa B
NGS – next generation sequencing
nt - nucleotide

P
P-Ser – phosphatidyl serine
pA – polyadenylation site

PAGE – polyacrylamide gel electrophoresis
PAP – polyA polymerase
PAS – polyadenylation signal
PBMCs – peripheral blood mononuclear cells
PBS – phosphate-buffered saline
PCR – polymerase chain reaction
PD-L1 – programmed cell death ligand 1
PE – Phycoerythrin
PFA – Paraformaldehyde
PI – propidium iodide
polyA – poly-adenosine tail
pPAS – proximal polyadenylation signal
pre-mRNA – precursor messenger RNA
Pro – proline
PRR – pattern recognition receptors
PTBP1- polypyrimidine tract binding protein 1

R
RAC1 – Rac family small GTPase
RACE – rapid amplification of cDNA ends
RBPs – RNA binding proteins
RIP – RNA immunoprecipitation
RIPA – radioimmunoprecipitation assay buffer
RNA – ribonucleic acid
RNA Pol II – RNA Polymerase II
RNase - ribonuclease
ROS – reactive oxygen species
RPM – reads per million
rpm – rotations per minute
rRNA – ribosomal RNA
RT-qPCR – real time-quantitative PCR

S
SAMtools – sequence alignment/map tools
SDS – sodium dodecyl sulfate
Ser – serine
siRNA – small interfering RNA
SRrp – serine-arginine repressor protein
SRSF – serine and arginine splicing factor
STAR – ultrafast universal RNA-Seq aligner

T
TAMs – tumor-associated macrophages
TBS – tris-buffered saline
TF – transcription factor
TGF – transforming growth factor
Th – T helper cell
Thr – threonine
TLR – Toll-like receptor
TM – transmembrane
TME – tumor Microenvironment
TNF – tumor necrosis alpha
TNM – Tumor/Node lymph invasion/Metastasis classification
Tris – trishydromethylaminomethane
Tyr – tyrosine

U
USE – upstream sequence element
UTR – untranslated region

W

WB – western blot

Wnt – wingless-related integration site

WHO – World Health Organization

List of Figures

Figure 1 – TME cellular components.
Figure 2 – Macrophage inflammatory spectrum consists in a multiphenotype plastic landscape.
Figure 3 – Distribution of pro-inflammatory macrophages and anti-inflammatory macrophage populations on several human diseases.
Figure 4 – Location of gene regulation steps.
Figure 5 – Transcription and co-transcriptional processes involve many layers of regulation.
Figure 6 – Schematization of protein domains in the SRSF12 linear protein structure.
Figure 7 – 3' end process is a tightly regulated nuclear process with multiprotein complexes functioning synergistically, whence *cis*-acting sequences are recognized by *trans*-acting complexes working in connection with RNA Polymerase II.
Figure 8 – Alternative Polyadenylation (APA) affects both the coding region and the 3' UTR (3' UTR-APA, down) of mRNAs.
Figure 9 – Polyadenylation signal hexamer sequence efficiency in ascending order recognized by the cleavage and polyadenylation machinery.
Figure 10 - Specific 3' UTR mRNA isoforms are associated to distinct cell states and disease.

Subchapter 3.1
Figure 1 – Macrophage differentiation, polarization, and co-culture.
Figure 2 – Experimental setup and workflow of siRNA knockdown in primary human macrophages.
Figure 3 – RNA fractionation and RNA-Seq library construction from primary human macrophages.
Figure 4 – *MALAT1* expression levels in fractionated RNA.
Figure 5 – Bioinformatic RNA-Seq analyses pipelines.
Figure 6 – Heatmaps of Pearson correlation coefficients for 3' mRNA-Seq.
Figure 7 – Representative donor heatmap showing DEGs in M0, M1 and M1 co-cultured macrophages.
Figure 8 – IGV gene profiles and transcript counts of PAPOLA in ChrRNA-Seq, NpRNA-Seq and 3' mRNA-Seq of M0 macrophages, M1 and co-cultured macrophages.
Figure 9 – IGV gene profiles, transcript counts and qPCR validation of RAC1.

Subchapter 3.2
Figure 1 – Gene expression profiles, differentially expressed genes and *in vivo* patient data in M0, M1 and co-cultured macrophages.
Figure 2 – APA isoform profiles**,** differential APA genes and *in vivo* patient data in M0, M1 and co-cultured macrophages.
Figure 3 – SRSF12 modulates gene expression in M1-like macrophages.
Figure 4 – SRSF12 upregulates shorter APA isoforms and contributes to isoform diversity**.**

Supplementary Figure 1 – Inflammatory profile characterization of M1, normalized to M0. GSEA analyses of M0, M1 and co-cultured macrophages. Validation of DEGs in *in vivo* databases and qPCR.
Supplementary Figure 2 – APA profile characterization. Validation of genes with differential APA in *in* vivo databases and qPCR.
Supplementary Figure 3 – siSRSF12 characterization in M1 macrophages. Gene counts of DEGs.
Supplementary Figure 4 – GSEA analyses in SRSF12. Characterization of genes undergoing APA in siSRSF12.
Supplementary Table 3 – PAS sequences of DEGs in co-cultured macrophages.
Supplementary Table 4 – PAS sequences of DEGs not undergoing APA in co-cultured macrophages.
Supplementary Table 5 – PAS sequence study in mRNA isoforms with upregulated short 3' UTRs in M1 macrophages vs. M0, as identified by DEXSeq.
Supplementary Table 6 – PAS sequence study in mRNA isoforms with upregulated long 3' UTRs in M1 macrophages vs. M0, as identified by DEXSeq.

Supplementary Table 7 – Primer pairs used for RT-qPCR validation.
Supplementary Table 8 – Percentage of reads passing filters after pre-processing, respective input read and uniquely mapped reads in 3' RNA-Seq of si*SRSF12* data.

Subchapter 3.3
Figure 1 – Housekeeping and RBP gene study by RT-qPCR.
Figure 2 – Fold change gene expression study of individual genes in primary human macrophages, measuring the coding, and distal polyadenylation signal.
Figure 3 – IGV gene profile and transcript counts of *RAC1* (A), *MCL1* (C), IL*1B* (D) and *CD47* (E), and protein levels of YBX1 and Rac1.
Figure 4 – *RAC1* 3'RACE.
Figure 5 – RAC1-YBX1 binding study.
Figure 6 – Immunofluorescence images of unpolarized macrophage Rac1, actin and nuclei staining.
Figure 7 – Fold change gene expression study of individual genes in hypoxic RKO.
Figure 8 – Fold change expression of RBPs and RAC1 in hypoxic RKO. RIP of YBX1 in the 3' UTR of MCL1, RAC1 and CD47 of hypoxic RKO.
Figure 9 – RAC1 study and validation of chemically hypoxic RKO.

Supplementary Figure 1 – Scheme of the macrophage polarization experiment workflow.

Supplementary Figure 2 – THP-1 characterization.

List of Tables

Table 1 – Prognosis relation of TAMs infiltration and cancer progression in each tissue.

Subchapter 3.2

Supplementary Table 1 – Percentage of reads passing filters after pre-processing, respective input read and uniquely mapped reads in ChrRNA-Seq data.
Supplementary Table 2 – Percentage of reads passing filters after pre-processing, respective input read and uniquely mapped reads in 3' RNA-Seq data.
Supplementary Table 3 – Primer pairs used for RT-qPCR validation.
Supplementary Table 4 – Percentage of reads passing filters after pre-processing, respective input read and uniquely mapped reads in 3' RNA-Seq of si*SRSF12* data.

Subchapter 3.3
Table 1 – *In silico* analyses of RBP binding sites in the 3' UTRs of the selected mRNAs surveyed in the single gene studies in RKO and primary macrophages, and their connection to the inflammatory profile of macrophages.

Chapter I – General Introduction

Chapter I – General Introduction

1. Hallmarks of cancer

1.1 Colorectal cancer

Recent epidemiological data highlights the increased incidence and mortality associated to colorectal cancer (CRC), the third most incident, and the second deadliest cancer worldwide, in both sexes (Globocan., 2020c, 2020a). In Portugal, this disease gains even more relevance, constituting the most incident and the second deadliest cancer (Globocan., 2020b; Globocan Observatory, 2019), immediately after lung cancer.

Along carcinogenesis, tumor cells acquire several mutations, frequently on oncogenes or on tumor suppressor genes. Notably, CRC stands as one of the few tissues for which the mutational map during the tumorigenic process has been extensively described (Armaghany *et al.*, 2012; Fearon & Vogelstein, 1990; Lengauer *et al.*, 1997), and hence stands as a very good model to investigate mechanisms of gene regulation. Notably, only 20% of CRC cases have reported to be of familial origin, namely Lynch Syndrome and Familial Adenomatosis Polyposis, and the remaining 80% sporadic cases are divided into chromosomal instability and serrated phenotype (microsatellite stable (MSS, 84 %) or unstable (MSI, 16 %) (Müller *et al.*, 2016).

Healthy colon cells need several consecutive tumorigenic mutations to transform into avid highly dividing non-dormant primary tumors (Lengauer *et al.*, 1997; Vogelstein *et al.*, 1988). Briefly, the earliest mutation is recurrently on the *APC* gene (adenomatous polyposis coli), which shifts pre-neoplastic cells to an intermediate aberrant crypt stage through hyperactivation of the Wnt pathway. After the occurrence of the *APC* mutation, subsequent driver mutations differ among patients, including the following alterations (Jones *et al.*, 2008): in K-ras, correlating with transition to intermediate adenoma; in, PIK3, PTEN, BMP, MAPK, MMR pathways, correlating with CRC progression; finally, in TGFBR2, p53, SMAD4, correlating with transition to carcinoma.

Accumulation of mutations will increase colon cancer cell stem-like properties, alter their immunogenicity and immune cell recognition, and stimulate invasion into the underlying tissues, enhancing their ability to form distant liver and lung metastasis

(Yoshida *et al.*, 2012). During the tumorigenic process, transcription factors such as NF-kB, HIF1-α and STAT3 are frequently activated. Notably, NF-kB was shown to be the master tumor cell regulator with the ability to modulate tumor proliferation, angiogenesis, metastasis, inflammation and immune surveillance (Wang *et al.*, 2014).

This tumorigenic switch affects multiple cell functions and modulate their interaction with the neighboring tumor microenvironment (Hui & Chen, 2015). In most cases, the immune system recognizes and attacks tumor cells, but the few cells that escape may favor angiogenesis, invade the underlying tissues and metastasize to receptive novel microenvironments. Recolonization and stable metastasis formation occur after successful cancer cell adaptation to the new metastatic microenvironment (Wurth & Gebauer, 2015).

Increased anti-tumor therapeutic success has been achieved through screening, patient genetic profiling and treatment design, even with the observed increase in cancer rates proportionally with human lifespan (American Cancer Society, 2018b, 2018a; Capocaccia *et al.*, 2015). The role of the tumor microenvironment, in particular of immune cells, in CRC is an ever-evolving research field (Giannakis *et al.*, 2016). Nevertheless, current immunotherapeutic solutions are limited, requiring further research to understand the mechanisms that regulate the immune response to cancer cells.

1.2 The tumor microenvironment

Knowledge about solid tumors evolved from being considered an exclusively genetic disease to a multi-component process. Twenty years ago, Hanahan and Weinberg characterized cancer cells as having limitless replicative potential, self-sufficiency in growth signals and insensitivity to growth inhibition, their ability to evade apoptosis, exhibit sustained angiogenesis, tissue invasion and metastasis (Hanahan & Weinberg, 2000). A decade later, authors improved their definition by extending these abilities beyond the cancer cells to their surrounding microenvironment, adding other parameters as immune evasion, tumor-promoting inflammation, deregulating cellular energy management and genome instability and mutation (Hanahan &

Weinberg, 2011), that ultimately changed the view on cancer to an intricate multistep process involving many cell types and interconnected pathways.

The tumorigenic process begins with the occurrence of gene mutations in epithelia, stroma or germline cells. Multiple mutations escaping the Mismatch repair (MMR), Base excision repair (BER) and Nucleotide excision repair (NER) mechanisms may grant cells a selective advantage to resist destruction brought about by multiple checkpoints (Liu *et al.*, 2017). However, these processes are asynchronous: multiple cells in the tissue may be at different steps of the tumorigenic progression, with several clones with different degrees of tumorigenicity existing simultaneously, a phenomenon observed originally by Virchow (Virchow, 1863) and coined “intratumor heterogeneity”. Cancer cell heterogeneity has been observed in most solid tumors (González-García *et al.*, 2002; Shipitsin *et al.*, 2007) and leukemias, with important consequences to cancer therapy response (Lim & Ma, 2019; Wang *et al.*, 2017).

All tissues have a specific microenvironment. Upon tumorigenic transformation, microenvironments change drastically in cell composition and tissue architecture, among others, due to the communications established between neighbor cell types activating proliferative, avidity metabolic pathways and cytokine production (Amend & Pienta, 2015; Devaud *et al.*, 2014; Hirayama *et al.*, 2009; Thomas *et al.*, 2015). The tumor microenvironment (TME) is usually composed by acellular elements, such as extracellular matrix components (e.g., collagen, fibronectin, vimentin, elastin) and arrested secreted factors, by cellular elements as tumor and healthy cells, and by their cellular neighbors as fibroblasts, osteoclasts/osteoblasts, adipocytes, endothelial and immune cells (Figure 1).

1.2.1 Tumor Microenvironment: cellular components

The cellular TME is mainly composed by epithelial, stromal cells and immune cells. The focus of this thesis are the macrophages and CRC cells, and the other microenvironmental elements are briefly described.

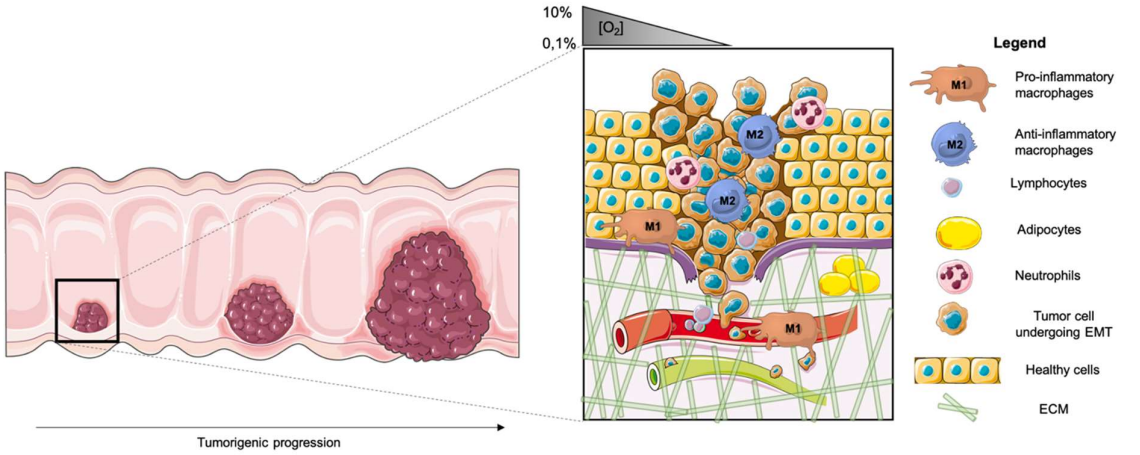


Figure 1 – Illustration of major TME cellular components: left, during the tumorigenic process, the colorectal tumor grows (left) and its microenvironment changes accordingly during the transformation of healthy into tumor cells. Right, changes occurring in cell populations –immune cells (macrophages (**red** and **blue**), lymphocytes (**light blue**), neutrophils (**pink**), adipocytes (**yellow**), – and non-cellular components – extracellular matrix (ECM, **light green**), O_2 levels (**grey**) and epithelial to mesenchymal transition (EMT, **center**). For simplicity, fibroblasts and endothelial cells are not shown (described in the text). Compiled with copyright-free images from Smart Servier Art.

1.2.1.1 Stromal Cells

Adipocytes are focused on energy storage and have endocrine roles. They regulate energy homeostasis through lipid absorption and hydrolysis, while producing inflammatory cytokines via autocrine or paracrine pathways. In tumors, adipocytes and associated clinical parameters, such as body-mass index, are positively associated with tumor development through interaction with macrophages and consequent establishment of a tumor-permissive microenvironment (Corrêa *et al.*, 2017) via activation of STAT3 and IL-6 signaling (Bochet *et al.*, 2011; Endo *et al.*, 2011).

Endothelial cells coating the surface of blood vessels are crucial for tumor progression, through angiogenesis (Lee *et al.*, 2015). Increased vascularization in tumors enables access to nutrients and oxygen, stimulating growth and metastasis through intravasation. In turn, tumor cells produce pro-angiogenic factors such as VEGF, galectin-1, or Notch activation, all of which cause endothelial cell proliferation and branching, and stimulate cancer cell invasion and metastasis (Thijssen *et al.*, 2010; Zeng *et al.*, 2005).

Fibroblasts are the main ECM producers during wound healing and tissue repair (LeBleu & Neilson, 2020). In CRC, cancer-associated fibroblasts crosstalk with other

TME components through HGF and tenascin-C signaling (De Wever *et al.,* 2004), increasing primary tumor size and promoting invasion and metastasis *(*Hwang *et al.*, 2008).

1.2.1.2 Macrophages

Discovery and brief historical perspective

In 1882, the zoologist Élia Metchnikoff described macrophages for the first time as "phagocytes" (Metschnikoff, 1892), with the pictorial meaning of "large glutton". Decades later, Cohn and others described other macrophage properties, such as secretion of immune mediators, antimicrobial resistance and endocytosis (Gordon & Cohn, 1973; van Furth & Cohn, 1968), while the discovery of growth factors such as Macrophage Colony Stimulating Factor (M-CSF) enabled *in vitro* macrophage culture and differentiation (Monteleone *et al.*, 2018). This facilitated the study of macrophages as infection effectors, responders to interferon-gamma (IFN-γ) produced endogenously or by T cells (Le Page *et al.*, 2000), and producers of reactive oxygen (ROS) and nitrogen (RNS) species (Dedon & Tannenbaum, 2004).

As myeloid antigen-presenting cells (APC), macrophages phagocyte pathogens and damaged host cells, them, exposing digested pathogenic proteins on their cell surface. This antigen processing and presentation activates T lymphocytes that are recruited to the macrophage vicinity in response to infection, cell damage or macrophage cytokines secretion (Owen *et al.*, 2013). Indeed, macrophages are decisive for an effective host response to pathogens (Mackaness, 1964).

In the past 30 years, numerous regulatory macrophage markers were identified, such as complement (Von Furth, 1985), mannose receptor (CD206) *(*Taylor *et al.*, 2005), lysozyme (Ibrahim et al., 2017), tumor necrosis factor alpha (TNF-α) (Klostergaard, 1987), and the co-stimulator receptors (CD80 and CD86) (Woldai, 2014), among others. Despite this growth in the knowledge about macrophages, its importance as an antigen-presenting cell was controversial until the 1990s. However, the discovery of the Toll pathway in *Drosophila* (Lemaitre *et al*., 1996) reignited the interest in the importance of innate immunity in mammals, unveiling its links to antiviral resistance (Victoria et al., 2013) and cancer-related actions (Valanne et al., 2011), among others.

Since then, the origin, specificity, and diversity of macrophage functions have been deeply investigated.

Origin

Macrophages' first appearance was in teleosts around 300 Million years ago (Lu & Chen, 2019). They are highly plastic, ubiquitous cells from the hematopoietic system, which play crucial roles in homeostasis, inflammatory response, tolerance, development, and tissue repair (Wynn *et al.*, 2013).

After hematopoiesis, mature monocytes may stay in the bone marrow microenvironment, where they direct production, differentiation, and turnover of hematopoietic cells. On the other hand, tissue macrophages, adapted to separate, local microenvironments, originate from several populations, which have been extensively characterized. Previously, it was accepted that circulating blood monocytes derived from bone marrow precursor cells continuously replenished tissue macrophages in all body organs. As the field advanced, numerous intermediate myeloid precursors were discovered contributing to the characterization of macrophage development. In humans, identified precursors are elusive, but some have been identified, such as the hMDP (human monocyte-dendritic progenitor, which gives rise to monocytes, macrophages and DCs), characterized by $CD34^{+}CD45RA^{+}CD123^{int}CD115^{+}$ expression, and cMoP (common monocyte progenitor, lineage restricted to macrophages), characterized by $CLEC12A^{hi}CD64^{hi}$ expression (Kawamura *et al.*, 2017; Lee *et al.*, 2015).

Simultaneously, other research showed that tissue macrophage origin was not exclusively from the bone-marrow. Indeed, self-maintained macrophages derived from embryonic precursors exist being originally derived from the yolk sac (microglia in the brain, Kupffer cells in the liver), the fetal liver (alveolar macrophages in lung) or an unknown fetal cell type (Langerhans cells in the spleen) (Ginhoux et al., 2010; Hashimoto et al., 2013; P. Li et al., 2017; Wynn et al., 2013). In contrast, in organs with high cell turnover such as the colon and the skin, it is accepted that self-renewing tissue macrophage populations are supplemented by bone-marrow derived circulating macrophages (Bain et al., 2014; De Schepper et al., 2018; Malissen et al., 2014). Notably, both organs have increased need of innate immune cells, due to persistent microbiome colonization, with positive consequences for the host (Quail & Joyce,

2017). Additionally, stress conditions such as inflammation and infection will produce recruiting signals for circulating monocytes that stem from the bone marrow (Davies *et al.*, 2014; Gordon & Plüddemann, 2017; Wynn *et al.*, 2013). Therefore, even in the same tissue, macrophage profile and hence functional phenotype differ depending on ontogeny.

Nevertheless, macrophages have innate immune functions in each tissue niche, through heterogenous expression of membrane receptors and secreted products, which aid in the regulation of effector cells.

Differentiation and Inflammatory profile

Macrophages are plastic, modulator sentinel cells existing in a diverse inflammatory spectrum, varying in phenotype and lifespan. As professional phagocytes, they have key functions in development, homeostasis, angiogenesis and inflammation, which are particularly important during infection, cancer and inflammatory diseases, as they quickly react to their microenvironment. After exposure to an activation stimulus, monocytes are recruited to the peripheric tissue, reacting to the local microenvironment and producing a specific pattern of surface receptors and secretory proteins.

After pro-inflammatory stimuli, such as Lipopolysaccharide (LPS) – a pathogen-associated molecular pattern (PAMP) present in Gram-negative bacteria –, pro-inflammatory macrophages (M1) secrete inflammatory and cytotoxic mediators. This secretion in turn activates T helper 1 cells (Th1), in a positive feedback mechanism mediated by Pattern Recognition Receptors (PRRs) (Owen *et al.*, 2013) such as CD14. Afterwards, adaptive immune response is triggered through pathogen phagocytosis, via Toll-like Receptors and secretion of inflammatory mediators (IL-1, TNF-alpha, IL-6, IL-8, IL-12, IL-23) (Hoshino *et al.*, 1999; Kawai & Akira, 2011; Mackaness, 1964). These macrophages, also known as “classically activated” (Celada *et al.*, 1984), phagocyte infected, mutated or dead cells, creating an oxidative microenvironment that increases the recruitment of T cells, monocytes and neutrophils to further eliminate the threat to the host (Duque & Descoteaux, 2014). This pro-inflammatory response is tightly controlled, to avoid widespread inflammation that could cause tissue damage, and ultimately give rise to autoimmune disorders.

After the threat is eliminated, macrophages switch their polarization and cytokine profile toward an anti-inflammatory phenotype (M2). This phenotype is responsible for phagocyting infected, senescent or apoptotic cells, cell debris, and oxidized lipoproteins. The recognition of these molecules occurs due to the absence of expression of "self" receptors such as CD47 (Barclay & Brown, 2006) and does not lead to an inflammatory response, via STAT3,5 and 6 activation, which is promoter respectively by IL-10, IL-4 and IL4/IL-13 (Locati *et al*., 2013). These anti-inflammatory phagocytes are recruited by T helper 2 cells (Mantovani *et al.*, 2002) and are also known as "alternatively activated macrophages" (Gordon & Martinez, 2010).
In vitro, macrophages differentiate in the presence of growth factors (e.g., macrophage-colony stimulating factor, M-CSF), adopting different phenotypes depending on cytokine modulation. The *in vivo* phenotype of macrophages is modulated by cytokines such as IL-1β, IL-12, IL-18 (pro-inflammatory), IL-10 and TGFß (anti-inflammatory) (Paul, 2008). Other metabolites such as TNF-α are induced by LPS and CD14, and contribute to infection resistance, but prolonged activation can cause local and systemic inflammatory diseases, while IL-6 and IL-10 contribute to acute inflammation resolution, through stimulation of CD163 (scavenger receptor for the hemoglobin-haptoglobin complex) and CD206 (the mannose receptor) (Roszer, 2015).

The inflammatory spectrum of macrophages is very dynamic (Stout & Suttles, 2012), exhibiting a continuum of differentiation. This allows each tissue to have more than one inflammatory population, with varying ratios during homeostasis and disease (Pinto *et al.*, 2019). Building on the original classification of M1/M2 macrophages, and mirroring the Th1/Th2 T cell subtype with which each macrophage subpopulation interacts (Mills *et al.*, 2000), Alberto Mantovani and collaborators suggested further stratification of M2 macrophages into three different subpopulations, induced by different polarization stimuli and characterized by the expression of distinct cell surface receptors and cytokines (Mantovani *et al.*, 2004) (Figure 2): M2a, resulting from IL-4/IL-13 stimulation, involved in Th2 inflammatory processes and helminth elimination through production of IL-10, IL-1ra and MHC II complex; M2b, consistent with immune complex and TLR/IL1R agonists stimulation, participating in immunoregulatory processes through expression of TNFα, IL-1, IL-6 IL-10 and CD86; M2c, induced by

IL-10 stimulation or glucocorticoids, contribute to matrix deposition and tissue remodeling, and inhibitor of cytotoxic, pro-inflammatory responses due to expression of IL-10 and TGFβ.

More recently, another subtype of M2 macrophages have been described (M2d, also termed TAMs by some authors (Patel *et al.*, 2017)), which are elicited by stimulation with adenosine receptor agonists and TLR2, 4, 7, or 9 agonists. M2d are associated with high expression of VEGF, adenosine receptors and IL-10, and low IL12 and TNFα secretion (Ferrante *et al.*, 2013).

Furthermore, Mox macrophages (detoxifying macrophages) have been also described and characterized by rebalancing redox homeostasis (Serbulea et al., 2017). Mox macrophages were previously found in pro-tumoral microenvironments such as gastric adenocarcinoma and ulcerative colitis, and are induced by both pro-inflammatory (oxidized phospholipids) and anti-inflammatory stimuli (sulforaphane and HMOX) (Eren *et al.*, 2018; Kadl *et al.*, 2010; Lai *et al.*, 2019).

It is also worth to mention the colored-wheel nomenclature created by Mosser and Edwards, in which macrophages are grouped functionally into three groups: host defense, wound healing, and immune regulation (Mosser & Edwards, 2008). Ultimately, the field concedes the complexity, specificity and simultaneous occurrence of multiple macrophage populations.

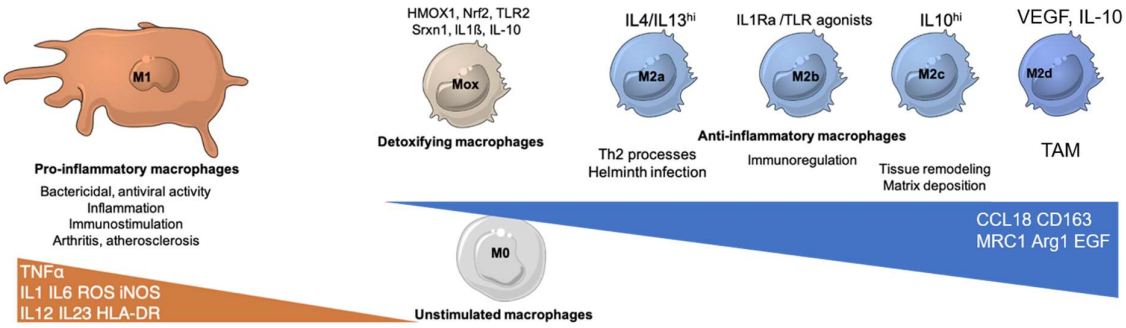


Figure 2 – **Macrophage inflammatory spectrum consists in a multiphenotype plastic landscape.** According to Mantovani and colleagues(Mantovani *et al.*, 2004), M0 (unstimulated macrophages, **light grey**, down) can be polarized into distinct cell states in response to the microenvironment. M1 (pro-inflammatory macrophages, **red**) are characterized by high expression of TNF-α, IL-1β, IL-6 and others, while M2 (anti-inflammatory macrophages, **blue**) are further divided in M2a – M2d, each with specific stimuli, functions and expression of receptors and cytokines, and Mox (detoxifying macrophages). Compiled with copyright-free images from Smart Servier Art.

In conclusion, as both homeostasis regulators and immune effectors, macrophages are intimately linked to many inflammatory diseases, such as rheumatoid arthritis, atherosclerosis, and cancer (Sica & Mantovani, 2012).

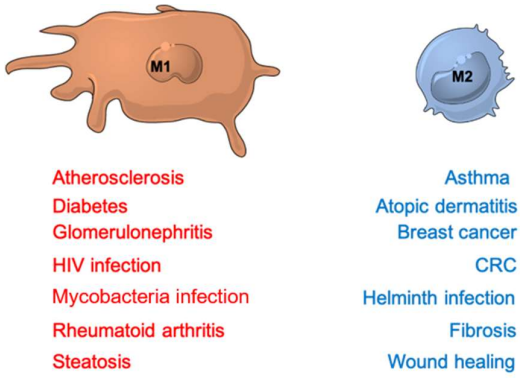


Figure 3 – Distribution of pro-inflammatory macrophages (M1, left) and anti-inflammatory macrophages (M2, right) populations according to their predominance in several human diseases. Compiled with copyright-free images from Smart Servier Art.

Functional roles in cancer

Macrophages display relevant roles at the tumor microenvironment: as APCs for T cells, namely regulatory T cells (Treg) and Th17 cells (Wang & Vella, 2016); and as ECM producers (Tsukamoto *et al.*, 1981), stimulating complex spectra of inflammation, from pro- to anti-inflammatory (Khan & Falcone, 1997; Stahl *et al.*, 2013). They play different roles throughout the tumorigenic process, acting during tumor growth, invasion, and metastasis (Condeelis & Pollard, 2006).

As the most abundant immune cells in the TME (van Ravenswaay Claasen *et al.*, 1992), macrophages are frequently found in the tumor invasive region or in the tumor core. Herein, they are called tumor-associated macrophages (TAMs). As their homeostatic counterparts, TAMs ontogeny is heterogenous: they may derive from circulating monocytes (Franklin & Li, 2017; Mantovani *et al.*, 1992), or resident macrophages, whether from embryonic progenitors or, in the case of CRC, also from repopulating monocytes from blood circulation (De Schepper *et al.*, 2018; Zigmond & Jung, 2013). TAMs recruitment is performed by chemotactic factors released by the TME, such as M-CSF (Tang *et al.*, 1992), chemokine (C-C motif) ligand 2 (CCL2 or

monocyte chemoattractant chemotaxis protein, MCP-1 (Sica, Saccani, Bottazzi, Bernasconi, *et al.*, 2000)), and angiogenic factors as vascular endothelial growth factor (VEGF). Moreover, *in situ* TAMs proliferation has been found in breast tumors, regulated by CSF1 via STAT1 promoter and associated with CD163 signaling and worst prognosis (Tymoszuk *et al.*, 2014; Yu Zhu *et al.*, 2017). However, further research is needed to understand the outcome of in situ TAM proliferation and the mechanisms in more tissues.

It is hypothesized that at the beginning of the tumorigenic process, macrophage recruitment will contribute to tumor eradication through the activation of pro-inflammatory molecular pathways. Yet, TAMs are predominantly characterized by their anti-inflammatory M2 polarization profile (Mantovani *et al.*, 2002) and are associated with worse prognosis (Table 1). These TAMs upregulate immunosuppressive, pro-tumoral and wound healing factors such as IL-10 and TGFß, involved in suppressing T cell activation, EGFR, and also CXCL8 and other angiogenic factors, and downregulating IL-12 and iNOS (Bingle *et al.*, 2006; DiNapoli *et al.*, 1996; Jetten *et al.*, 2014; Lewis *et al.*, 2000; Sica, Saccani, Bottazzi, Polentarutti, *et al.*, 2000).

High TAMs infiltration is associated with lower survival in several tumors, such as breast, ovarian and skin cancer. Results for TAMs studies and clinical prognosis are summarized on Table 1.

Table 1 – Prognosis relation of TAMs infiltration and cancer progression in each tissue.

Bad prognosis	Conflicting reports	Good prognosis
Breast (Tiainen *et al.*, 2015)	CRC (Kang *et al.*, 2010; Kwak *et al.*, 2016)	M1 TAMs in CRC (Pinto *et al.*, 2019)
Bladder (Hanada *et al.*, 2000)	Lung (Ma *et al.*, 2010; Welsh *et al.*, 2005)	
Esophagus (Yagi *et al.*, 2019)		
Head and neck (Kumar *et al.*, 2019)		
Hodgkin's Lymphoma (Steidl *et al.*, 2009)		
Leiomyosarcoma (Lee *et al.*, 2008)		
Liver (Ding *et al.*, 2009)		
Ovary (Yuan *et al.*, 2017)		
Skin (Falleni *et al.*, 2017)		
Stomach (Yan *et al.*, 2016)		
Thyroid (Ryder *et al.*, 2008)		

In CRC, several studies reported distinct associations between TAMs infiltration and patient overall survival. While some works revealed that high macrophage presence was related to reduced liver metastases and improved patient survival, others showed worst prognosis and advanced clinical states (Kang et al., 2010; Kwak et al., 2016; Marta L. Pinto et al., 2019). In the past, TAMs were frequently identified solely by the CD68 marker, but recent advances allowed for inflammatory and geographical stratification of TAMs population in tumors. For instance, TAMs may be stratified according to total (CD68), M1 (e.g., CD80) and M2 (e.g., CD163) populations and to their location in regards to the intratumoral region and normal adjacent tissue. Although this approach relies on the use of biomarkers that are not entirely specific of a given macrophage population, it revealed that macrophages expressing CD80 recruitment is upregulated in the intratumor regions when compared to normal mucosa, and that macrophages expressing CD163 are a major inflammatory population in CRC tumor invasive front (Pinto *et al.*, 2019).

In CRC, $CD163^+$ TAMs are generally recruited by CCL2 signaling, increasing cancer cell migration and metastasis through IL-1 and IL-6 secretion and concomitant activation of the JAK2/STAT3 pathway (Kaler *et al.*, 2009; Larionova *et al.*, 2020; Schneider *et al.*, 2000; Wei *et al.*, 2019). Macrophages are differentially associated with CRC patient prognosis. Most cohort studies centered on $CD68^+$ macrophages, as determinant for patient prognosis. Some studies indicate TAMs as a marker of better patient prognosis (Larionova *et al.*, 2020; Ye *et al.*, 2019), while other works show low numbers of $CD68^+$ macrophages were correlated with metastasis. Interestingly, when stratifying macrophages for simultaneous $CD163^+CD68^+$ expression, researchers found a correlation with tumor TNM stage and negative patient prognosis. Simultaneous CD206/MRC^+CD68^+ expression correlated with secondary tissue invasion and poor patient survival. Pro-inflammatory $CD80^+$ macrophages were associated with less invasive tumors (Larionova *et al.*, 2020). Therefore, macrophage polarization status and precise localization in the TME appear to be both more informative and more predictive of patient survival (Mola *et al.*, 2020). As macrophages are inherently plastic and their inflammatory profiles occur on a spectrum, further research is needed to expand the repertoire of TAMs biomarkers in CRC and other tumors, and hence increase the knowledge on the phenotype of these

cells. This will in turn make the design for immunomodulating therapies in TAMs more feasible.

It must be mentioned that patient cohorts studied show high disparity in patient number, tumor MSS/MSI status, and therapy strategies used, while not correcting for the $CD68^+$ presence in CRC tumors depending on position in the organ (ascending, transverse or descending colon, which have different expression profiles). Other studies have stratified the inflammatory profile of TAMs as a potential factor for this difference in clinical prognosis (Kang *et al.*, 2010; Kwak *et al.*, 2016; Pinto *et al.*, 2019). Therefore, more research is needed to understand the role of macrophages and, specifically, TAMs in CRC and its consequences to patients.

Achieving macrophage repolarization for cancer treatment is still somewhat restricted, but several strategies have been developed to increase therapy success.

In particular, nanoparticles (NPs)-centered antitumor modulation has been intensively explored in the last decades. This strategy is considered very versatile and effective for TAMs, due to their inherent phagocytic ability, tissue ubiquity and plasticity, and the technology benefits of surface functionalization, pH sensitivity or adjuvant addition.

Indeed, NPs will cause modulation of the macrophage inflammatory profile, depending on surface composition – cation polymers and gold NPs induce a pro-inflammatory profile, while iron oxide NPs, originally used to treat iron deficiency, induce a strong immunostimulatory action due to pro-inflammatory macrophage polarization, and consequently inducing Th1 responses (Castro *et al.*, 2019; Nath *et al.*, 2018; Zanganeh *et al.*, 2016). NPs surface may be coated with agents which explore tumor properties to patient benefit, such as integrin, VEGF, and VCAM, ROS generators or even oxygen carriers (Dai *et al.*, 2017). These strategies may be customized to the tumor type, used synergistically and at the lowest possible dose to reduced undesirable side effects, and optimize patient response. However, as most delivery studies have been performed in mice xenograft models, more research is needed to deeply understand *in vivo* human TME pathology and swiftly overcome its challenges.

Other therapeutic strategies involve the addition of pro-inflammatory molecules to modulate the inflammatory profile of TAMs, to decrease their pro-tumorigenic role and

reverse their M2-like to an M1-like phenotype. Examples include anti-STAT3,6 inhibitors such as Sorafenib, a STAT3 inhibitor which suppresses IL-10 production and restores IL-12 to its M1 level, and Fenretinide, which represses STAT6 phosphorylation in CRC, and hence downregulates the M2 population and inhibits angiogenesis (Genard *et al.*, 2017). In more advanced cases, FDA-approved zoledronic acid liposomes in metastatic bone cancer may be used, which works by downregulating VEGF, IL-10, and MMP9 and upregulating iNOS in TAMs (Lin *et al.*, 2019). Nanoparticles and synthetic polymers containing IFN-γ can modulate IL-10-polarized macrophages towards a more pro-inflammatory phenotype, inhibiting cancer cell invasion (Cardoso, Gonçalves, et al., 2015). Conversely, nanoparticle delivery of anti-inflammatory drugs to pro-inflammatory macrophages in the context of rheumatoid arthritis, achieve some phenotype reversion towards an anti-inflammatory profile (Freitas *et al.,* in preparation).

We believe that in the future TAMs manipulation strategies can be used alone or in combination with other therapies to improve patient survival and care. As the TME contains immunosuppressive TAMs, combination therapy strategies to counteract the action of these cells with immunotherapy agents may improve patient prognosis, lower therapy resistance and activate adaptive immunity. For instance, IFNγ combinatorial therapy has mixed responses depending on the strategy and the tumor: while a combination trial using IFNγ and chemotherapeutic agents carboplatin and paclitaxel in advanced ovarian cancer caused increased hematological toxicity in patients, another trial using IFNγ and epirubicin/cisplatin/5-fluorouracil in patients with advanced liver cancer induced complete response although with bone marrow suppression (Alberts *et al.*, 2008; Kim *et al.*, 2011).

On the other hand, M-CSF receptor CSF1R inhibitors in combination with paclitaxel downregulated macrophage infiltration in breast tumors. Another approach using CSF1E and adoptive cell therapy in melanoma showed downregulation of TAMs and shifting of their inflammatory profile to pro-inflammatory macrophages (DeNardo *et al*., 2011; Mok *et al.*, 2014).

Therefore, when attempting combinatorial therapies, individual patient response to current therapy and additional inflammatory modulator molecules should be constantly

and extensively evaluated to increase therapy efficacy, avoid serious side effects and include appropriate immunotherapeutic co-adjuvants.

In conclusion, macrophage populations act as a barometer of cancer dormancy or invasion and metastasis (Locati *et al.*, 2013; Mantovani *et al.*, 2002; Mantovani & Locati, 2013) and the development of immunomodulatory therapies that modulate this important element of the tumor microenvironment may in turn improve patient outcome.

1.2.1.3 Other immune cells

The TME has immune cells to detect and eliminate early developing cancer cells, as a second line of defense after collapse of intrinsic cell anti-tumoral checkpoints. Although macrophages are one of the most prevalent immune cell populations in the gut, current immunotherapy focuses on T cells through the concept of cancer immunoediting.

T lymphocytes are adaptive immune cells, which respond to an antigen specifically presented by an APC (Owen *et al.*, 2013) through the immunological synapse. T cells are divided into several lineages, most of which are important in the tumorigenic processes. Briefly, $CD4^+$ differentiate into helper T cells (Th) that secrete several cytokines when primed: Th1 cells produce IFN-γ and lymphotoxin and boost macrophage microbicidal action; Th2 produce IL-4, IL-13, IL-6 and IL-10 and focus on B cell development; finally, Th17 produce IL-17 and recruit granulocytes. CD8+ develop into cytotoxic T lymphocytes that focus on lysing target APCs, among which the cancer cells. Finally, Tregs are CD4+ cells that have differentiated after FoxP3 stimulus and contribute to an immunosuppressive microenvironment.
T cells are crucial in colon cancer: in contrast with other tissues, CRC-associated T cells are less proliferative, and upregulate IL-17 and PD-1 and downregulate anticancer IFNγ and IL-2 production in comparison to their non-tumor matched tissue (Taylor *et al.*, 2016). Notably, in CRC, Jerôme Galon and colleagues have developed Immunoscore to assess T lymphocyte infiltration in the tumor center and invasive margin, particularly $CD3^+$, $CD8^+$ and CD45RO, which is more predictive of patient

clinical outcome than the classical Tumor/Node/Metastasis (TNM) classification (Galon *et al.*, 2013; Pagès *et al.*, 2018). Recent cancer immunotherapy approaches are precisely centered on targeting T cells, either using Tumor-Infiltrating Lymphocytes (TILs) or *ex vivo*-developed Chimeric Antigen Receptor (CAR)-T cells, in a process called adoptive immune therapy that has been successfully adapted for several tumors, namely leukemia and lymphoma (Rosenberg *et al.*, 2008).

Immunoediting describes the selective pressure, actions of the immune system to either prevent or stimulate the tumorigenic process. It is divided in three stages: elimination, equilibrium, and escape. Immune elimination is mainly done through surveillance done by innate and adaptive immune cells: neutrophils and macrophages will phagocyte tumor cells and produce pro-inflammatory cytokines, chemokines, complement and prostaglandins. This secretion paraphernalia will recruit and activate T cells, to which macrophages and dendritic cells will present antigens. The final outcome is the coordination of both arms of the immune system to purge tumor cells through pro-inflammatory IFN-gamma pathways and activation of transcription factors in several immune populations, such as IRF, NF-kB and FOXP3 (Alexander *et al.*, 2020; Shankaran *et al.*, 2001; Whiteside, 2018).

Equilibrium is achieved through immune selection: some tumor cells survive in a dormant state. They experience several mutations due to immune cells acting through continuous selective pressure, originating several heterogenous tumor variants capable to escape immune cell action due to upregulation of cell surface proteins (e.g. PD-L1) (Quezada *et al.*, 2011). During this *quasi* dormancy, cancer cells might still stimulate and be attacked by immune cells, but the number of eliminated tumor cells is replenished by the proliferating tumor cells.

Immune escape is the later stage of immune surveillance, wherein immune-resistant cancer cell clones in the TME proliferate (Mittal *et al.*, 2014) through several mechanisms, such as upregulation of TRAIL (which induces immune cell apoptosis) and immunomodulatory cytokines such as IL-6, IL-10, and TGFβ (increasing the recruitment of Treg and MDSC cells, that perform immunosuppressive functions, and inhibiting the presence of NK, CD8 and DC), and downregulation of MHC I (which decreases detection by cytotoxic CD8 cells) (Chabanon *et al.*, 2016). These strategies ultimately enable tumor cells to invade and metastasize to secondary organs.

Interestingly, intratumor heterogeneity, which is prevalent in CRC, also contributes to the rise of immune escape in patients, due to the coexistence of many clones and the inherent Darwinian pressure for the fittest survivor.

Understanding the involvement of all immune cells in the TME will enable us to design personalized therapeutic strategies, in combination with classical radio- or chemotherapy. These strategies are achieved with recourse to high-throughput transcriptomic studies, and research is quite advanced in cancers such as lung and skin (Rizvi *et al.*, 2015; Zaretsky *et al.*, 2016).

Dendritic cells (DCs) are myeloid APCs that serve as mediators of the innate immune response. This occurs through recognition of foreign antigens, maturation and MHC, CD80 and CD86 synthesis, which are instrumental in presenting the antigens to naïve T cells (Chistiakov *et al.*, 2019). However, tumor-associated DCs are immunosuppressed due to cytokine expression and physicochemical properties. Therefore, their cross-presentation abilities may be impaired. In CRC, however, a small subset of DCs remain activated and are also a positive prognostic factor (Veglia & Gabrilovich, 2017).

Neutrophils are circulating, short-lived innate immune cells that secrete ROS, NOS and granules in response to cytokines and chemokines produced by macrophages (such as IL-8) and other immune cells (Paul, 2008). Similarly to macrophages, researchers have also proposed neutrophil inflammation profiles connected to cancer prognosis: N1 (pro-tumoral) and N2 (anti-tumoral). In CRC, increased neutrophil recruitment is connected to bad prognosis due to the generation of neutrophil extracellular traps. However, this phenotypic characterization of functional heterogeneity lacks the establishment of clear transcriptomic profile signatures (Gonzalez *et al.*, 2018).

1.2.2 Physico-chemical properties of the Tumor Microenvironment

1.2.2.1 Oxygen content: hypoxia and angiogenesis

Most factors present in the TME may be stored in the body for later use – e.g. iron in storage or serum proteins, acidic particles in lysosomes, glucose as glycogen

deposits in hepatocytes (Cao *et al.*, 2016; Lane *et al.*, 2015; Nocito *et al.*, 2015). One notable exception is oxygen, which cannot be stored in its gaseous form. Animal tissues are slightly hypoxic, ranging from 1,1 % (skin) to 9,5 % (kidney) and 10 % (colon) oxygen concentrations (Carreau *et al.*, 2011; Graboń *et al.*, 2016); therefore, oxygen availability is tightly controlled. The tumor microenvironment is highly hypoxic, when compared to healthy cells from the same tissue (Bussink *et al.*, 2003) (Figure 1). Upon hypoxia, healthy cells immediately react with conserved stress responses, including metabolic alterations; but cancer cells are quicker to react, due to their faster proliferative ability, sustained angiogenesis and abnormal metabolic pathways (Hanahan & Weinberg, 2000, 2011; McKeown, 2014; Nakazawa *et al.*, 2016).

Immediate cytotoxic consequences of hypoxia include production of Reactive Oxygen Species (ROS), immune evasion, increasing resistance or increasing efficiency of chemotherapy, tumor regrowth and metastasis (Barsoum et al., 2014; D'Ignazio *et al.*, 2016; Schioppa *et al.*, 2003; Shah & Xie, 2015; Strese *et al.*, 2013). Notably, macrophages are recruited to tumor hypoxic areas (Murdoch *et al.*, 2004) and are consequently primed towards a pro-angiogenic M2 phenotype with upregulation of HIF-1 and HIF-2 (Talks *et al.*, 2000; Tripathi *et al.*, 2014). Other transcription factors such as NF-kB are also known to be upregulated upon hypoxic exposure, in immune cells, healthy intestinal tissue and cancer (D'Ignazio & Rocha, 2016; Schioppa *et al.*, 2003; Shah, 2016; Sivridis *et al.*, 2005).

Recently, Martins and colleagues (Martins *et al.*, 2020) established a beneficial link between hypoxia (measured by HIF1A) and TAMs (measured by CD68), due to the development of a pro-inflammatory microenvironment, increasing levels of IL1B secretion by macrophages and upregulating tumor cytotoxic T cells.

The growing field of gene expression regulation in cancer cells upon hypoxic challenge still lacks works about the interaction of tumor tissue, the immune system and their shared microenvironment. Therefore, we sought to understand how hypoxic conditions affect gene expression and alternative 3' UTRs of macrophages.

1.2.2.2 Epithelial to mesenchymal transition

There are three types of epithelial-to-mesenchymal transition (EMT), arising during development, fibrosis and, finally, the tumorigenic process (Kalluri & Weinberg, 2009). The latter type will be described in this section.

Solid tumors arise from epithelial cells; to intravasate into blood circulation and metastasize at a secondary site, tumor cells need to overcome their connection to the remaining epithelia and the basement membrane, through EMT (Quail & Joyce, 2013). Briefly, tumor cells, particularly at the invasive front, gain mesenchymal properties such as motility, migration, invasion, resistance to apoptosis, and disruption of cell polarity, cytoskeleton reorganization and elimination of tight junctions. EMT is regulated by the previously described microenvironmental stimuli (cytokines, growth factors) and is associated with upregulation of stemness, vimentin, the ZEB, SNAIL and TWIST transcription factors family, due to induction by TGFß (Medici *et al.*, 2008). The activation of oncogenes induces cell senescence, but EMT prevents it to facilitate cancer cell dissemination (Weinberg, 2008).

For instance, E-cadherin expression is inversely correlated with patient survival and is lost during EMT, due to repression by ZEB1 and ZEB2 (Kalluri & Weinberg, 2009). It also involves the loss of other proteins, such as ß-catenin (Kim *et al.*, 2002). Importantly, EMT affects cancer clones differently and contributes to tumor heterogeneity (Kalluri & Weinberg, 2009).

In CRC, the EMT phenotype correlates with increased invasion and metastasis and is associated with increased expression of IL1ß, TNFα, TGFß, and HIF1α, as well as the other TFs mentioned above (Ieda *et al.*, 2019; Vu & Datta, 2017). Notably, all these molecules are associated with roles in transmission of extracellular signaling, contributing to the enhancement of EMT in the rest of the tumor cell community, even if their autologous EMT signals are weaker.

When tumor cells reach an adequate metastasis site, they undergo the inverse transformation (MET – mesenchymal to epithelial transition) to create micro metastases and ultimately colonize the secondary organ (Zeisberg *et al.*, 2005).

1.2.2.3 Extracellular matrix: cellular architecture

The extracellular matrix (ECM) is a tissue-specific macromolecule network responsible for maintaining structural tri-dimensional (3D) integrity, flexibility and adhesion. It is composed by proteins and polysaccharides, and it is also crucial to sustain signaling, as a biomolecules reservoir, through arresting of cytokines, chemokines and growth factors, modulating cell survival, differentiation, polarization, polarity, migration and invasion (Naba *et al.*, 2012).

The role of ECM on determining cellular behavior is performed through reciprocal gene expression regulation, affecting not only the target cell type but all the interconnected cell types in the tissue (Streuli & Bissell, 1990). Moreover, the ECM has also been connected to inflammatory regulation: after inflammatory stimuli, the ECM is deposited or remodeled by macrophages performing wound healing; in chronic inflammation and cancer, excessive fibrotic ECM deposits is akin to a never-healing wound (Dvorak, 1986).

Tumor ECM is organized differently: increased tissue stiffness (Levental *et al.*, 2009) due to increased protein deposition inarguably changes the ECM composition and biomechanics, actively promoting tumor growth in CRC (Hilska *et al.*, 1998) through modulation of cancer hallmarks (Hanahan & Weinberg, 2011). Additionally, ECM remodeling enzymes are dysregulated in cancer, instigating new, cryptic fragments that recruit monocytes (Houghton *et al.*, 2006) and releasing pro-tumoral cytokines to the surrounding environment that further influence this crosstalk. In CRC, abnormal ECM dynamics are associated with increased angiogenesis, EMT and metastasis (Kechagia *et al.*, 2019; Vu & Datta, 2017).

1.3 Mimetizing the Tumor Microenvironment: Co-cultures

Communication between macrophages and cancer cells inarguably imposes alterations in gene expression, which may dictate the success of cancer progression. In this work, we performed indirect transwell co-cultures with macrophages and cancer cells.

Immune cell involvement in colorectal cancer is an area with increasing interest due to tumor heterogeneity and regulation of therapy escape (Giannakis *et al.*, 2016) and tumor-microenvironment interactions (Cardoso, Pinto, *et al.*, 2015; Pinto *et al.*, 2016; Pinto *et al.*, 2017). Macrophages, one of the most abundant immune components at the tumor microenvironment, may either cooperate or abrogate cancer cells, depending on their inflammatory phenotype (Mantovani & Locati, 2013), as previously discussed.

Cancer cells and macrophages work together in a paracrine mechanism loop – cancer cells stimulate macrophages through CSF-1 production, while macrophages produce pro-angiogenic factors that allow for tumor growth (Hardbower *et al.*, 2017).

When choosing co-cultures as model systems, one must optimize each cell population density in order to obtain a cellular monolayer capable of eliciting measurable responses, and to include controls from all conditions and biological replicates including each monocultured cell population.

The establishment of transwell co-cultures with CRC cell lines and polarized macrophages allows the study of the different cell populations in biomimetic microenvironments. Co-cultures may be used to pinpoint transcriptomic alterations imposed by the microenvironment, and correlate them to the macrophage inflammatory state, and also to identify new immune APA and gene expression modulators.

Furthermore, the indirect contact of macrophages with cancer cells allows the sharing of soluble factors, enabling the study of the communication between the two cell types, while still permitting easy separation of the different cell types for downstream studies, such as transcriptomics (Goers *et al.*, 2014).

Past work from the Tumor and Microenvironment Interactions (TMI) group has uncovered mechanisms in the crosstalk between CRC cells and unpolarized macrophages, stimulating tumor cell invasion, migration and motility through action of matrix metalloproteases and EGFR, which is a phenotype more efficiently achieved by IL-10 polarized macrophages (Cardoso, Pinto, *et al.*, 2015).

2. Transcription and alternative 3' UTR regulation

Regulation of gene expression is crucial for all cells maintenance and function (Jacob & Monod, 1961). In eukaryotes, it defines cell type, fate and function by complex co- and post-transcriptional mechanisms, during differentiation, development and other cell stages. Some of the regulation layers include chromatin modification, alternative splicing and alternative polyadenylation (APA). This thesis aims to study APA in macrophages, during polarization and upon exposure to colorectal cancer cells.

2.1 Transcription: initiation, elongation and termination

For the majority of the eukaryotic genes, transcription is the most important step of gene expression regulation, determining the fates of mRNA and protein (Nick J. Proudfoot, 2016). It consists on the synthesis of a RNA molecule from a template strand of DNA, culminating in a nucleotide sequence complementary to the initial coding strand. Transcription may be divided into sequential stages with specific regulatory mechanisms: initiation, elongation and termination. For the scope of this thesis, we will only introduce and discuss transcription of mRNAs that code for protein-coding genes. Any other RNAs will be mentioned whenever relevant.

Protein-coding genes are transcribed by RNA Polymerase II (RNAPII), a highly conserved enzyme consisting of 12 subunits encoded by genes *RPB1-12*, which code for the catalytic site, a stalked structure, and the disordered Carboxy Terminal Domain (CTD) (Werner & Grohmann, 2011). The CTD is exclusive to RNAPII and crucial for its function, consisting of 52 tandem repeats of the consensus Tyr-Ser-Pro-Thr-Ser-Pro-Ser sequence (Chapman *et al.*, 2008). Several residues of the CTD repeats are modified during transcription, by phosphorylation, acetylation and methylation, among others (Schlackow *et al.*, 2017; Schröder *et al.*, 2013; Sims *et al.*, 2011). The CTD also tethers capping, splicing and cleavage and polyadenylation factors, in particular CPSF and CstF, depending on its phosphorylation status (McCracken *et al.*, 1997). Therefore, the CTD can adopt different conformations during transcription initiation, elongation and termination, wherein specific proteins assemble on the CTD to perform their functions (Egloff & Murphy, 2008; Portz *et al.*, 2017).

Akin to a train traveling on its tracks, RNAPII transcription needs several conditions for successful mRNA expression: accessibility of the corresponding gene on the DNA, and surpassing the checkpoint on the transcription cycle.

A mature mRNA is produced after intron excision and exon ligation, and subsequent pre-mRNA processing, cleavage and polyadenylation. The mRNA molecule is then exported to the cytoplasm and eventually translated into a protein. The three transcription stages, initiation, elongation and termination, are intimately linked to enhance efficiency of all the enzymatic reactions occurring on the nascent RNA (Proudfoot & Maniatis, 1980).

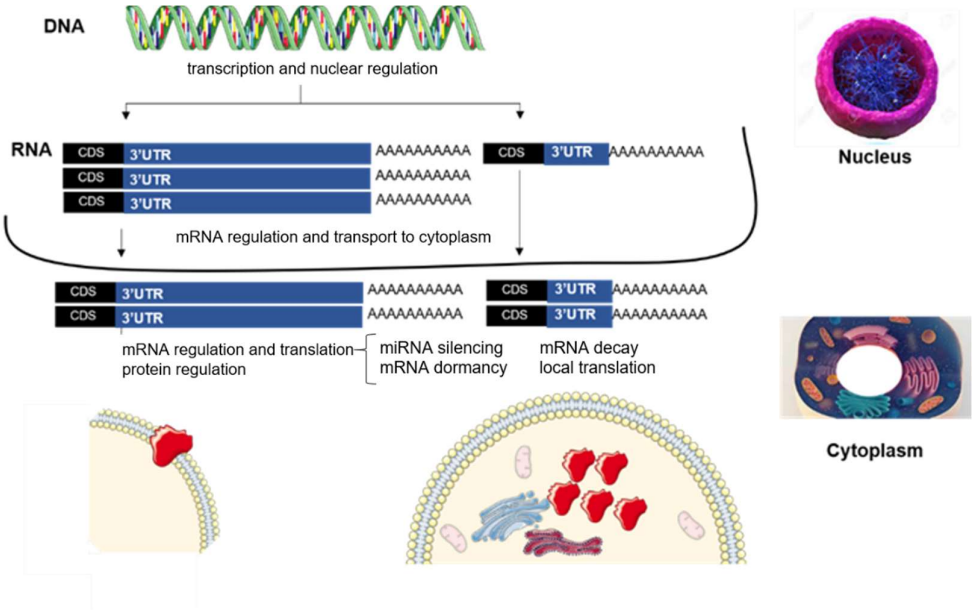


Figure 4 – Location of gene expression regulation steps: the DNA double helix (up) is unwound to prepare for transcription into mRNA by RNA Polymerase II, which occurs in the nucleus. mRNA (blue) is transported into the cytoplasm, where it is translated into a protein (red). Post-transcription and translation, the protein may be allocated to the membrane or stay in the cytoplasm with cell organelles (endoplasmic reticulum in **blue**, Golgi apparatus in **purple**, mitochondria in pink).

In the next sections, the transcription cycle and co-transcriptional processes will be described, with an emphasis on mRNA 3' end formation.

The transcription cycle begins by initiation, through binding of general transcription factors (TF) to specific regions in the promoter, and concomitant binding of RNAPII, which in turn stimulates the assembly of the pre-initiation complex (Fuda *et al.*, 2009). The Mediator complex recruits a helicase that separates both DNA

strands and the RNAPII synthesizes the first ~20 nucleotides (nt) of the pre-mRNA, which is almost instantaneously capped at its 5' end, preventing 5' exonuclease action (Grünberg & Hahn, 2014; Guo & Price, 2013; Krumm *et al.*, 1992; McCracken *et al.*, 1997; Muse *et al.*, 2007; Singh *et al.*, 2015) (Figure 5A).

The transcript is challenged by promoter-proximal pausing (Gilchrist *et al.*, 2010), which pauses RNAPII on the promoter of 75 % of human protein-coding genes (Guenther *et al.*, 2007) in an inactive state and inhibits elongation, causing premature termination (Guo & Price, 2013). The promoter-proximal pausing checkpoint is important for the transcript to be bound by the appropriate RNA binding proteins (RBPs) (Adelman & Lis, 2012; Sims *et al.*, 2004). The pre-initiation complex fully disassembles once RNAPII disengages from the promoter, continuing to the transcription elongation phase (Adelman & Lis, 2012).

Successful transcription elongation occurs through recruitment of elongation factors that phosphorylate the CTD and the promoter-pausing effectors NELF and DSIF (Cheung *et al.*, 2011; Marshall *et al.*, 1996; Palangat *et al.*, 2005; Peterlin & Price, 2006). These effectors stimulate RNAPII escape, release of the pre-initiation complex and subsequent elongation, chromatin remodeling and pre-mRNA processing (Ahn *et al.*, 2004; Bentley, 2005; Gu *et al.*, 2013; Hirose & Manley, 1998; Komarnitsky *et al.*, 2000; Peterlin & Price, 2006). After initiation and during elongation, RNAPII CTD phosphorylated residues gradually change from Ser5P and Ser7P to Ser2P through action of the phosphatase Ssu72 and the kinases CDK9, CDK12 and CDK13 (Bösken *et al.*, 2014; Devaiah *et al.*, 2012; Itzen *et al.*, 2014; Marshall *et al.*, 1996; Rosado-Lugo & Hampsey, 2014)(Bösken et al., 2014; Devaiah et al., 2012; Itzen et al., 2014)(Bösken et al., 2014; Devaiah et al., 2012; Itzen et al., 2014) among others, as the polymerase moves through the gene (Figure 5B).

RNAPII moves from the 5' to the 3' of the DNA as it polymerizes RNA, but it can occasionally backtrack in certain DNA sequences, often causing transcription arrest (Izban & Luse, 1991; Kireeva *et al.*, 2005). TFIIS, a general transcription factor, can resume elongation through realignment of the polymerase active site (Cheung *et al.*, 2011; Nechaev *et al.*, 2010; Sheridan *et al.*, 2019).

Transcription termination is a finely-tuned, quality-control failsafe mechanism. Along this process, RNAPII transcribing the gene must correctly interpret the termination signals - enrichment of Ser2P and Thr4P of the CTD (Davidson *et al.*, 2014; Glover-Cutter *et al.*, 2008; Schlackow *et al.*, 2013) and transcription of a polyadenylation signal – to produce a mRNA and to disengage from the DNA template (Figure 5C).

Although it is an area of increasing interest, especially the survey of the active site of RNAPII through NET-Seq (Churchman & Weissman, 2012; Nojima *et al.*, 2015), in high eukaryotes, transcription termination is still not completely understood. Two termination models have been proposed, as occurring alone or in combination (Rosonina *et al.*, 2006; West & Proudfoot, 2008).

The allosteric model of transcription termination is centered on conformational changes occurring on the elongation complex of RNAPII due to release of elongation factors and binding of termination factors. These actions lead to untethering of RNAPII to the template DNA (Calvo & Manley, 2005; Greenblatt *et al.*, 1993). The torpedo model (Luo *et al.*, 2006; Proudfoot, 2016) implies that the RNAPII continues elongating beyond the polyadenylation signal (PAS) (Laitem *et al.*, 2015). Although the 3' end of the pre-mRNA is correctly processed, as RNAPII continues to transcribe, the 5' end of this uncapped transcript is targeted for degradation by the Xrn2 exonuclease (Proudfoot, 2011; West *et al.*, 2004). As Xrn2 degrades the transcript, it meets RNAPII, and causes conformational changes that induce RNAPII disengagement, inducing transcription termination (Fong *et al.*, 2015).

Capping, termination and 3' end processing factors act as regulators of transcription termination, as these factors follow RNAPII to areas downstream of PAS to instigate pausing, enhancing termination efficiency through exonuclease degradation (Davidson *et al.*, 2014; Glover-Cutter *et al.*, 2008; Gromak *et al.*, 2006; Nojima *et al.*, 2015; Zhang *et al.*, 2015). Conversely, correct termination has consequences for gene expression. For instance, RNAPII occupancy at promoters and functional polyadenylation signals correlates with higher levels of mRNA expression (Core & Lis, 2008; Fusby *et al.*, 2015; Grosso *et al.*, 2012; Ji *et al.*, 2011) and protein expression (West & Proudfoot, 2009), in which erythropoietin pre-mRNA termination is vital for protein expression

The advent of electron microscopy and transcriptomic analyses shed some light on the mechanisms of co-transcriptional pre-mRNA processing. For instance, most introns are excised on pre-mRNA transcripts as they are transcribed by RNAPII (Bentley, 2014). Repression of premature 3' end is achieved by the binding of the spliceosomal U1 small nuclear ribonucleoprotein particle (snRNP) along the nascent pre-mRNA inhibiting the binding of the cleavage and polyadenylation machinery (Kaida et al., 2010). It is also known that transcription termination driven by XRN2 is dependent upon poly(A) site recognition and that pre-mRNA cleavage facilitates detethering of RNAPII from the DNA template (Connelly & Manley, 1988; Whitelaw & Proudfoot, 1986). Studies have also emphasized the successive interactions of splicing factors and polyadenylation factors that occur on the nascent pre-mRNA, contributing to correct processing (Glover-Cutter *et al.*, 2008). Importantly, a negative feedback between transcription termination and initiation has been described, as a mutation on the PAS mutation hampers transcription initiation (Mapendano *et al.*, 2010).

The integration of pre-mRNA processing with transcription co-evolved to ensure that the pre-mRNA is efficiently and accurately processed to maturation, and increases the number of regulation layers in gene expression. Indeed, integration actually goes beyond co-transcriptional processes, as transcription initiation and elongation factors affect mRNA 3' end formation, and *vice versa* (Andersen *et al.*, 2012; Nagaike *et al.*, 2012; Schroeder *et al.*, 2004).

Termination marks the end of the transcription cycle. As another cycle begins, the CTD of the RNAPII must be fully dephosphorylated for re-initiation (Sims *et al.*, 2004). Indeed, malfunctioning transcription termination is extremely deleterious for the cell. Notably, aberrant transcription termination has been found to have downstream effects in CRC (Ueda *et al.*, 2015).

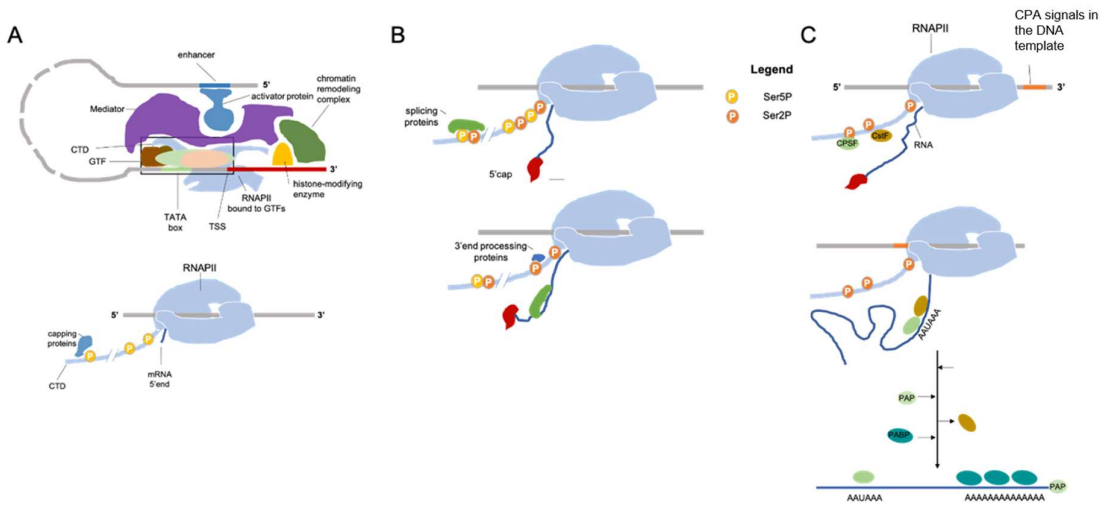


Figure 5 – Transcription and co-transcriptional pre-mRNA processing involve many layers of regulation. For all images, DNA is shown in grey, RNA in **dark blue**. **A.** Successful transcription initiation requires chromatin remodeling complexes (**green**) and histone-modifying enzymes (**yellow**). Transcription initiation needs activator proteins (**blue**) binding distant enhancers to stimulate assembly of the initiation complex, consisting of specific and general transcription factors (GTF, **brown**), RNA polymerase II (RNAPII, light blue) and its C-terminal domain (CTD), and the Mediator complex (**purple**), at the promoter. **B.** RNAPII elongation and 5' RNA capping occurs through binding of RNA-processing proteins to the CTD, either at Ser5 (for capping, shown in **red**) or Ser2 (splicing and 3' end processing) positions. **C.** Pre-mRNA 3' end processing consists of binding of the pre-mRNA by CPSF and **CstF**, cleavage of the pre-mRNA and polymerization of a polyadenylated tail by PolyA Polymerase (**PAP**). The polyA tail is covered by PolyA Binding Protein (**PABP**) Adapted from (B. Alberts et al., 2008).

2.2 Pre-mRNA 5' capping and splicing

Throughout evolution, several regulation layers have arisen that actively contribute for increased mRNA diversity while saving genome space. The transcription cycle described above is coupled with pre-mRNA capping and splicing, which will be briefly described below, along with cleavage and polyadenylation, described in detail in section 2.3.

Capping consists on the co-transcriptional addition of a methylguanosine cap to the 5' end of all eukaryotic pre-mRNAs (Rasmussen & Lis, 1993; Shatkin, 1976), which both stabilizes the pre-mRNA, increases splicing efficiency (Inoue *et al.*, 1989) and is necessary for efficient mRNA nuclear export and translation into protein (Ramanathan *et al.*, 2016). Capping is coupled to transcription initiation-to-elongation through the CTD in actively transcribing RNAPII (Moteki & Price, 2002).

A typical mammalian gene has 7-8 short protein-coding exons with 100-200 base pairs (bp) separated by long non-coding but important regulatory introns with more than 1kb (kilobase)(Lewin, 2008). The spliceosome coordinates the removal of

introns after recognition of donor and acceptor sites on the pre-mRNA, the formation of a lariat, and ligation of the exons (Konarska *et al.*, 1985). Notably, splicing occurs concurrently with transcription elongation, but also actively promotes it through kinetic competition: competing splicing sites in a given pre-mRNA may be accessed by splicing factors differentially, depending on RNAPII elongation speed (Bentley, 2014). A slow elongation rates favor weaker upstream 3' splice sites in comparison to stronger 3' splice sites downstream, as the former has the spliceosome complex formed before the latter is transcribed and recognized.

Serine/Arginine (SR)-enriched proteins are regulatory splicing factors that act synergistically by identifying and binding to RNA regulatory motifs in the nascent pre-mRNA. SRSF12 (*aka* SRrp35, SFRS13B, SFRS19), the protein identified in this thesis as a modulator of alternative polyadenylation, contains an RNA Recognition Motif (RRM) and an arginine and serine (SR) domain, as shown in Figure 6. An important characteristic of SR proteins is their ability to auto-regulate and to cross-regulate the expression of other RNA binding proteins. SRSF12 represses alternative splicing by binding to SRSF1, SRSF2 and SRSF6 (Chandler *et al.*, 1997; Cowper *et al.*, 2001; Roca *et al.*, 2013), and is upregulated in M1 macrophages (H. Liu *et al.*, 2018) and testis (*GTex Analysis for SRSF12*, 2021). SRSF12 was shown to be present at stoichiometric levels to exon-junction complex core factors during splicing (Singh *et al.*, 2013), and was found to be at higher concentration than SRSF2 and SRSF6, two its repressed SR proteins. Therefore, one can hypothesize that SRSF12 repression may impede SR proteins SRSF2 and SRSF6 function.



Figure 6 – Schematization of protein domains in the SRSF12 linear protein structure. SRSF12 is a protein consisting of 261 amino acids. Residues 11 to 99 comprise an RNA Recognition Motif, while residues 111 to 256 comprise serine and arginine-rich sequences (RS domains) characteristic of SR proteins.

SR proteins are frequently recruited to active transcription sites, and several studies have highlighted that SR protein functions are not fully interchangeable between all

the members (Long & Caceres, 2009). Furthermore, many SR proteins have non-nuclear functions such as NMD, translation and shuttling. Fittingly, SRSF12 may have non-canonical nuclear functions (Long & Caceres, 2009). SRSF12 is phosphorylated by CDK6, a non-canonical transcriptional regulator involved in NF-kB recruitment that elicits inflammatory gene responses such as IL-8 production, after IL-1 stimulation (Anders *et al.*, 2012; Tigan *et al.*, 2016). As phosphorylation of SR proteins affects their subcellular localization and function (Misteli *et al.*, 1998), it is possible that SRSF12 phosphorylation by CDK6 will affect its function in immune cells.

2.3 Pre-mRNA 3' end processing – cleavage and polyadenylation

Pre-mRNA 3' end processing is a highly regulated co-transcriptional step. It consists in the cleavage of the pre-mRNA after recognition of a polyadenylation signal (PAS) in the coding region or in the 3' UTR (3' untranslated region), and on the polymerization of a poly-adenosine (polyA) tail at the 3' end (Tian & Manley, 2013). This two-step reaction modulates gene expression and occurs in all pre-mRNAs transcribed by RNAPII, except canonical histone mRNAs (Danckwardt et al., 2008; Marzluff et al., 2013).

PAS recognition and usage is modulated by auxiliary *cis*-acting RNA elements, or *trans*-acting proteins factors, that work together to produce a mature mRNA molecule (Millevoi & Vagner, 2009; Pereira-Castro & Moreira, 2021). *Cis*-acting elements and *trans*-acting proteins elicit a fine-tuned modulation of APA.

Pre-mRNA 3' end processing is crucial for cell physiology. Defective 3' end processing is the cause of several diseases, such as thrombophilia, muscular dystrophy, neurodegenerative diseases, and cancer (Curinha *et al.*, 2014; Danckwardt *et al.*, 2008).

The polyadenylation signal (PAS) is the most important sequence for mRNA 3' end formation, consisting of a hexameric sequence necessary for the binding of the cleavage and polyadenylation complex. There are several validated PASs (Beaudoing *et al.*, 2000), but the most efficient one is the AAUAAA, a highly conserved hexamer occurring in 53 % human genes, followed by AUUAAA (15 %) (Tian *et al.*, 2005). As different hexamers have variable efficiencies (Wickens, 1990), this will arguably impact mRNA 3' end formation for each specific gene, with a possible consequence on protein expression levels. Indeed, mRNA 3' end formation influences protein levels.

Steven West demonstrated that transcription termination of the erythropoietin pre-mRNA, which also contains a very weak PAS sequence (AAGAAC) was crucial for erythropoietin protein expression (West & Proudfoot, 2009). Consequences of substitutions or mutations in the PAS cause several diseases, such as β-thalassemia (α2-globin PAS: AATAAA → AATAAG), immune dysfunction (AATAAA → AATGAA) and several types of cancer (p53 PAS: AATAAA → AATACA, affecting up to 2% European populations) (Bennett *et al.*, 2001; Higgs *et al.*, 1983; Stacey *et al.*, 2011). Therefore, the correct recognition of this deceptively simple non-coding hexamer, in combination with the other sequences and protein factors described below, is tantamount to correct mRNA 3' end formation and protein expression.

Other crucial sequences in the 3' UTR are the cleavage site (pA), consisting of a CA/TA dinucleotide located 10-30 nt downstream of the PAS, and the downstream sequence element (DSE), consisting of several G/U or U residues in a non-consensus sequence located up to 30 nt downstream of the pA site. DSEs function as a platform to tether the 3' end processing machinery, in particular CstF (described below), to accurately define the 3' end of the mRNA, influencing PAS efficiency, usage and recognition (Di Giammartino *et al.*, 2011; Legendre & Gautheret, 2003; Millevoi & Vagner, 2009; Neve *et al.*, 2017).

Cleavage and polyadenylation (CPA) occur at the pA. Briefly, CPA begins upon transcription termination by RNAPII and by binding of the newly transcribed pre-mRNA to three core *trans*-acting factors - Cleavage and Polyadenylation Stimulating Factor (CPSF) and WDR33, Cleavage stimulating factor (CstF), Cleavage Factor I (CFIm). This binding then triggers the recruitment of Cleavage Factor II (CFIIm), Symplekin and Poly A Polymerase (PAP) (**Figure 7**). CFIm binds to UGUA sequences upstream of the pA, which results in promotion of PAP-CPSF interaction with CFIm via CPSF30 and WDR33 to the pA and via CPSF160 to (Brown & Gilmartin, 2003; Chan *et al.*, 2014; Schönemann *et al.*, 2014). CPSF73 cleaves the pre-mRNA preferentially at the CA dinucleotide that characterizes the pA, and FIP1L1 stimulates the addition of adenosines by (Bienroth *et al.*, 1993; Kaufmann *et al.*, 2004; Murthy & Manley, 1992; Ryan *et al.*, 2004; Takagaki *et al.*, 1989). In turn, the CstF complex stimulates 3' end formation by binding of its subunit CstF64 to the DSE. Symplekin acts as a scaffold protein to the CTD itself (MacDonald *et al.*, 1994; McCracken *et al.*, 1997; Murthy & Manley, 1995; Proudfoot, 2011; Takagaki & Manley, 2000).

This multiprotein complex stabilizes itself synergistically with each interactor, allowing for efficient CPA (Proudfoot, 2011; Zhao *et al.*, 1999). As the RNA molecule is now capped, spliced and polyadenylated, it is now referred to as mRNA and transported into the cytoplasm for translation (B. Alberts et al., 2008).

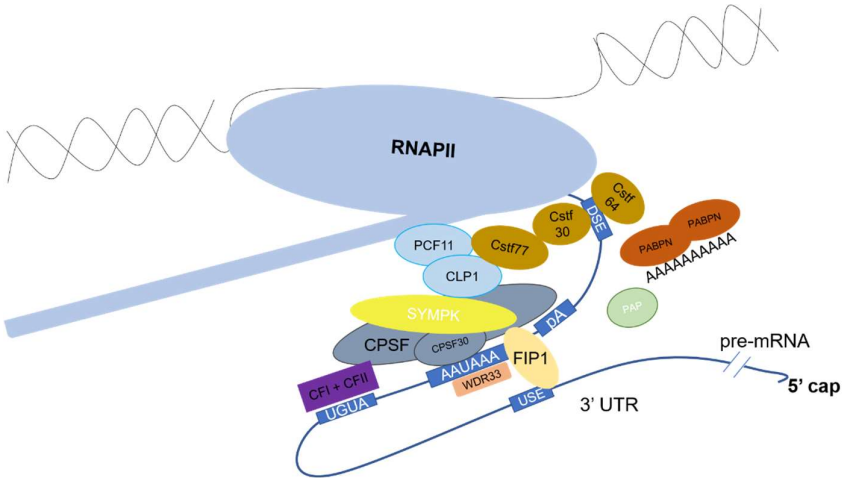


Figure 7 – 3' end process is a tightly controlled nuclear process with multiprotein complexes functioning synergistically, whence *cis*-acting sequences are recognized by *trans*-acting proteins working in connection with RNA Polymerase II. Specifically, the CFIm recognizes sequences at the USE, while CPSF complex and associated factor SYMPK bind to the PAS and the CstF complex recognizes the DSE. These protein-RNA interactions then favor protein-protein interactions between CPSF, SYMPK, CstF and CFIm, which further increase the stability of the protein-RNA interactions. Next, cleavage and polyadenylation occur through recruitment of CFII, PAP and PABP(N) proteins. RNA sequence: 3' UTR (dark blue line); USE – Upstream Sequence Element; AAUAAA – polyadenylation signal; pA – polyadenylation site; DSE – Downstream Sequence Element. Proteins: CF – Cleavage Factor (**purple square**); CPSF – Cleavage and Polyadenylation Element (**grey circles**); CstF – Cleavage stimulation Factor (**brown circles**); SYMPK – Symplekin (**yellow circle**); PABPN – Poly A Binding Protein (**orange circles**); PAP – Poly A Polymerase (**light green circle**); RNAPII – RNA Polymerase II (right, **light blue multidomain protein**). PCF11 – Pre-MRNA Cleavage Complex II Protein (**blue circle**, left); CLP1 – Cleavage Factor Polyribonucleotide Kinase Subunit 1 (**blue circle**, right). Modified from (Pereira-Castro & Moreira, 2021)

2.3.2 Auxiliary regulatory elements:

Cis-acting sequences

The auxiliary *cis*-acting sequences include upstream sequence elements (USE), named thus due to their localization in regards to the PAS. USEs contain binding sites for *trans*-acting protein factors such as RBPs, and core 3' end processing factors such as CstF, and are present in a plethora of genes with varying functions (Danckwardt *et al*., 2007; Lutz & Moreira, 2011; Moreira *et al.*, 1998; Newnham *et al.*,

2010; Oliveira *et al.*, 2019), indicating their post-transcriptional relevance for 3' UTR fine-tuned modulation in diverse cellular processes.

Trans-acting factors

Trans-acting protein factors ensure correct mRNA 3' end processing through competition or synergistic action (Millevoi & Vagner, 2009; Proudfoot, 2011; Tian & Manley, 2013; Zhao *et al.*, 1999). RNA binding proteins (RBPs) bind competitively and transiently to consensus motifs on the pre-mRNA – e.g., *PTBP1* binds to low-complexity, (C)U-rich short binding *cis* motifs on RNA (Castelo-Branco *et al.*, 2004; Dominguez *et al.*, 2018), or in a structure- and expression-dependent mechanism, and via 3' end processing factors or RBP post-translational modifications (Brown & Gilmartin, 2003; Dominguez *et al.*, 2018; Ryan & Bauer, 2008; Wu & Bartel, 2017). Regardless of function, RBPs dynamically bind RNA to form ribonucleoprotein complexes (RNPs).

Classic RBP examples are ELAVL1 (Embryonic Lethal Abnormal Vision Like 1) and PTBP1 (Polypyrimidine Tract Binding Protein 1), that play roles in splicing, translation and 3' end processing (Berkovits & Mayr, 2015; Castelo-Branco *et al.*, 2004; Danckwardt *et al.*, 2011; Hall-Pogar *et al.*, 2007; Kafasla *et al.*, 2012; Millevoi & Vagner, 2009; Valcárcel & Gebauer, 1997). ELAVL1 is also related to mRNA stability through synergism with other RBPs such as RBM38 (Cho *et al.*, 2010). PTBP1 is a classic splicing factor that is also involved in 3' end processing through activation or inhibition of pre-mRNA cleavage, as in the case of immune gene *C2* complement (Castelo-Branco *et al.*, 2004; Moreira *et al.*, 1998) and others (Valcárcel & Gebauer, 1997).

2.3.3 Alternative Polyadenylation (APA) and alternative 3' UTRs

The total estimated number of highly conserved PAS in the human genome exceeds 569,000 (Herrmann *et al.*, 2020). Yet, there are frequently more than one PAS in a gene, that may be recognized alternatively by a process termed Alternative Polyadenylation (APA), which occurs in all eukaryotes (Edge & Macrae, 2017; Sandberg *et al.*, 2008; Shi, 2012; Tian & Manley, 2013). The existence of more than one PAS in a given gene decreases the chances of stopping mRNA expression due to PAS mutation, while allowing for another layer of gene regulation (Graber *et al.*,

1999) There are alternative 3' UTRs in 74 % of human genes expressed in healthy and disease conditions (Derti *et al.*, 2012; Hoque *et al.*, 2016; Lee *et al.*, 2018; Shi, 2012; Tian *et al.*, 2005; Wang *et al.*, 2008), effectively leading to many mRNA isoforms due to differential usage of PAS sites.

There are two types of APA: if one PAS located in the coding region is used, we have coding region-APA (CR-APA); if a PAS in the 3' UTR is selected, we have 3' UTR-APA (Figure 8 below). In CR-APA, transcripts will most likely be translated into different proteins, contributing to increasing proteomic diversity, similarly to what happens by alternative splicing (Ben-Dov *et al.*, 2008). In 3' UTR-APA, transcripts will give rise to the same protein, but the mRNAs may have different functional properties. Different *cis*-regulatory elements, and *trans*-acting elements that bind to them, will increase post-transcription regulation, and ultimately, protein expression. For example, the differential binding of RBPs to AREs present in alternative 3' UTRs affect mRNA stability and protein translation (Diaz-Muñoz et al., 2015; Guo *et al.*, 2021; Mazan-Mamczarz & Gartenhaus, 2007; Soni *et al.*, 2019). Moreover, long 3' UTRs are frequently more subject to regulation, both by increased number of RBPs or miRNA binding sites (Gruber *et al.*, 2016; Theil *et al.*, 2018).

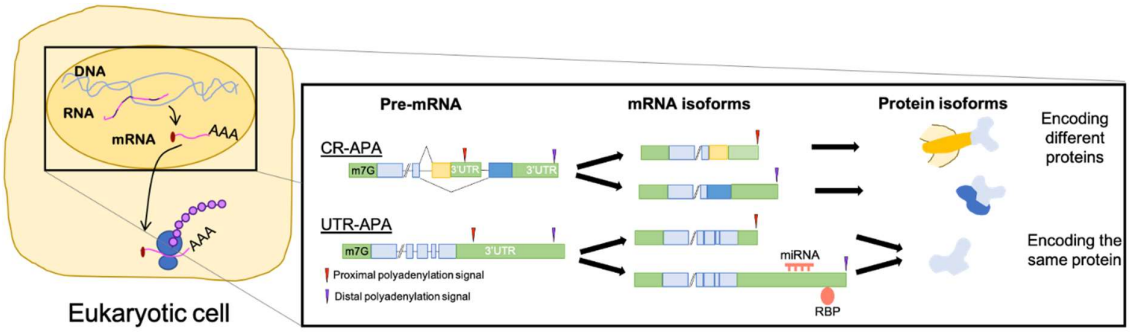


Figure 8 – Alternative Polyadenylation (APA) affects both the coding region and the 3' UTR (3' UTR-APA, down) of mRNAs. Coding region APA (CR-APA, top) occurs when PAS within the coding region are recognized, producing mRNA isoforms with distinct C-terminal coding regions, and hence coding for different protein isoforms. UTR-APA (down) occurs when mRNA isoforms have the same coding region, hence coding for the same protein, but differ in their 3' UTR length due to the use of different PAS in the 3'UTR. Pre-mRNA sequence – introns as black lines, coding regions in **light blue**, **yellow**, and **dark blue**, non-coding regions (5'UTR and 3' UTR) in **green**, PAS sequences as triangles. Adapted from Khan Academy,(Braz *et al.*, 2017; Elkon *et al.*, 2013; Lee *et al.*, 2018; Lutz & Moreira, 2011; Mayr, 2017; Pai *et al.*, 2016; Shi, 2012; Tian & Manley, 2013, 2016).

But how is one PAS chosen in detriment of another? There are several mechanisms under discussion, including the "first come, first served" model. Briefly, proximal PAS are chosen instead of distal PAS as the 3' end processing machineries recognize the

proximal PAS first as the nascent pre-mRNA exits the RNAPII channel, and hence assemble there (Proudfoot, 2011). This model implies that transcription elongation rate is the main driver for 3' end processing. However, this is not the only player in APA, as the strength of the PAS sequence, as well as additional auxiliary sequences and the presence of regulators all play important roles in APA (Berkovits & Mayr, 2015; Hoque *et al.*, 2016; Pinto *et al.*, 2011), and it has been described that alternative polyadenylation is a gene-specific mechanism (Braz *et al.*, 2017). In this model, the context of the individual 3'UTR controls PAS usage. This model highlights the large selective pressure exerted in regulatory sequences in the 3' UTR, which then has a strong impact on APA and mRNA production.

Literature search revealed that distal PAS tend to be more frequently composed of the canonical, more efficient AAUAAA sequence (Beaudoing *et al.*, 2000; Shi, 2012). This may occur as a failsafe mechanism to ensure mRNA 3' end formation and transcription termination at the end of the gene (Shi, 2012). Furthermore, the less efficient proximal PAS may be compensated by the increasing frequency of auxiliary *cis*-acting elements (Graber *et al.*, 1999; Oliveira *et al.*, 2019). Figure 9 illustrates the signal strength of different PAS hexamer sequences.

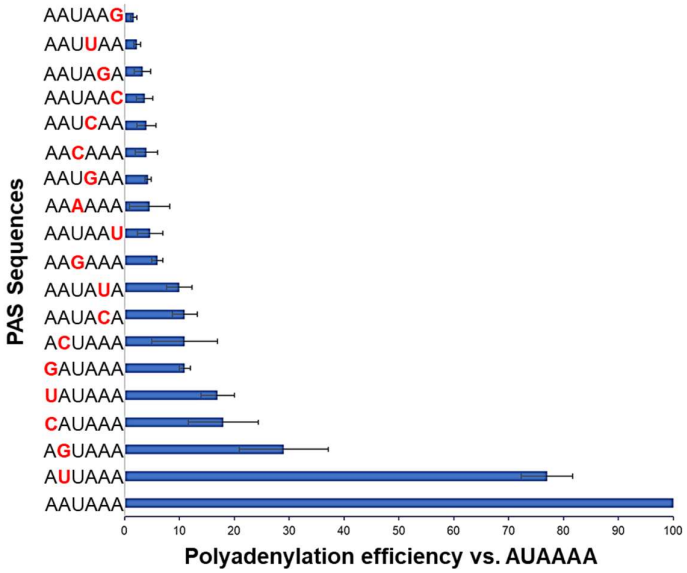


Figure 9 – PAS hexamer sequence efficiency in ascending order recognized by the cleavage and polyadenylation machinery. Shown in blue is the base change from the canonical AAUAAA PAS sequence. The experiment that gave origin to these data was done by generating point mutations in the AATAAA sequence by site-directed mutagenesis, which were subsequently *in vitro* transcribed containing ^{32}P nucleoside triphosphates. Quantification was performed by scanning densitometry, always normalizing the cleaved and polyadenylated mRNA product obtained transcription of sequences containing each point mutation PAS to the canonical AATAAA-containing RNA efficiency. Adapted from (Sheets *et al.*, 1990).

Notably, proximal and distal PASs can have different usage efficiencies, depending on the tissue or cell type (Liu, Freitas, *et al.*, 2017; Mayr & Bartel, 2009; Sandberg *et al.*, 2008). mRNAs with short 3' UTRs are more prevalent in cancer cells, proliferative cells and in activated immune cells, compared to healthy and resting cells (Castello *et al.*, 2012; Elkon *et al.*, 2013; Lutz & Moreira, 2011; Mayr & Bartel, 2009; Pai *et al.*, 2016; Sandberg *et al.*, 2008; Tian & Manley, 2016). In turn, longer 3' UTRs, generated by distal PAS selection, are more common in differentiated cells such as neurons and also during organism (Derti *et al.*, 2012; Ji et al., 2009; Miura *et al.*, 2013) (Figure 10).

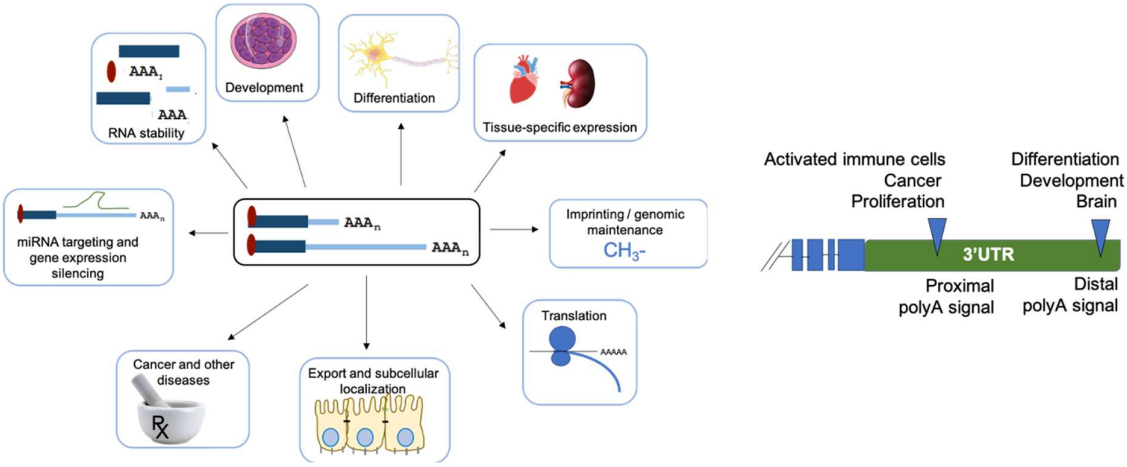


Figure 10 - Specific 3' UTR mRNA isoforms are associated to distinct cell states and disease. Middle circle, choice of mRNA isoform that only differ in the 3' UTR has many consequences for mRNA stability and miRNA targeting, and is specific for several cell types and cell states. Surrounding panels, summary of genome-wide PAS selection: short 3' UTRs tend to be more prevalent in activated immune cells, cancer cells, and proliferative cells; long 3' UTR are more frequently used during embryonic development, cell senescence processes and brain tissue. Image adapted from (Lutz & Moreira, 2011).

Alternative 3' UTRs may affect protein expression levels and subcellular location with relevant consequences for the cell, such as proliferation, differentiation and in the cell cycle (Berkovits & Mayr, 2015; W. Ma & Mayr, 2018). For instance, the IgM heavy chain protein is either bound to the cell membrane or secreted, depending on CstF64 levels that control IgM APA in pre-B and plasma cells (Takagaki *et al.*, 1996). On the other hand, Gruber and colleagues found limited effects of differential 3' UTR expression on protein levels (Gruber *et al.*, 2014).

Additionally, alternative 3' UTRs were also recently found to mediate protein-protein interactions (PPIs) determining protein localization (Berkovits & Mayr, 2015): CD47 is a cell surface protein that functions as an anti-phagocytosis "don't eat me" signal, frequently found on tumor cells (Willingham *et al.*, 2012). The proximal and distal PAS of *CD47*, produced by APA, stimulate distinct PPIs: the longer 3' UTR isoform of *CD47* serves as a scaffold to promotes interaction between the HuR/Elav and SET1. CD47 protein translated from the mRNA with the long 3'UTR interacts with SET1 and is translocated to the plasma membrane via interaction with Rac1 (Berkovits & Mayr, 2015). Therefore, the CD47 protein translated from the long 3'UTR mRNA isoform is mainly localized at the cell surface. Conversely, CD47 protein produced by the mRNA isoform with the short 3'UTR does not contain the binding site for interact with HuR/Elav, does not interact with SET1 and is found in the cytoplasm (Berkovits & Mayr, 2015). Other examples include *RAC1*, a Rho-family GTPase that regulates many processes (including cell adhesion, motility, migration and invasion (Carr & Frost, 2013; Gopal *et al.*, 2016; Ishii *et al.*, 2017)) and produces two 3' UTR mRNA isoforms. The Gene Regulation group has shown that the mRNA isoform with the longer 3' UTR of *RAC1* is predominantly found in the neurites, while the short 3' UTR isoform is found in the soma (Braz *et al.*, 2017). These examples are illustrative of the biological relevance of APA.

As each cell-type and state has its own levels of RBPs and effectors, the outcome for the mRNA molecule will depend upon those interactions. It is important to note that the binding of the *trans*-acting factor to the *cis*-acting sequences depends not only on the RNA sequence *per se*, but also on its context in the 3' UTR. For instance, the presence of activating and repressing sequences, the existence of post-translation modifications in specific RBPs or other RBP interactors, as well as steric hindrance due to 3' UTR secondary structure, changes the overall binding probability in each case (Wissink *et al.*, 2016). Therefore, even if there is a predictive binding of a given RBP on the short and long 3' UTR of a mRNA, it may actually only bind one 3' UTR. Importantly, RBP binding to alternative 3' UTRs may confer different translation efficiencies hence up- or downregulating its protein production in a 3' UTR-dependent fashion. For instance, neuronal BDNF alternative 3' UTR mRNA isoforms are differentially associated with polyribosomes in the brain: the short 3' UTR mRNA is

basally activated, while the longer 3' UTR mRNA, in the absence of neuronal stimuli is kept dormant in RNP particles, but readily made available for ribosomes upon neurotrophic stimuli, increasing BDNF levels when they are most needed (Di Giammartino *et al.*, 2011)

3. Alternative 3' UTR mRNA isoforms produced by Alternative Polyadenylation

The advances in RNA sequencing methodologies allowed extensive genome-wide studies in alternative polyadenylation, permitting the characterization of thousands of mRNA APA isoforms in different cells and tissues (Gruber *et al.*, 2014; Singh *et al.*, 2018; Zheng *et al.*, 2018). As APA is a cell-type- and cell-state-specific mechanism the state-of-the-art knowledge regarding Alternative Polyadenylation is described for the two cell populations analyzed in this thesis – macrophages and cancer cells.

3.1 Alternative 3' UTR mRNA isoforms in macrophages

Although genome-wide studies in macrophages are rare, due to the technical challenges imposed by the plastic nature of primary human macrophages and also by their inherent heterogeneity, the interest in this field is increasing. Albeit macrophage gene expression was shown to be regulated by transcription factors such as Nuclear factor-kB (NF-kB), Interferon-regulatory factors (IRF) and Erythroblast transformation specific (ETS) transcription factor families (Antonczyk *et al.*, 2019), alternative polyadenylation studies in macrophages are scarce. The main works in this field were performed by Pai and colleagues (Pai *et al.*, 2016) who reported extensive genome-wide 3' UTR isoform shortening in pro-inflammatory mice macrophages after *Salmonella* and *Listeria* infection, and by Shell and colleagues (Shell *et al.*, 2005) who described upregulated proximal polyA site selection occurring after *Cstf64* overexpression due to M1-like stimulation.

Alasoo and colleagues (Alasoo *et al.*, 2015) studied gene expression in monocyte-derived macrophages (MDMs) and iPS-derived macrophages, finding that much of the transcript expression variation differences stem from the 3' UTR-APA, with activation of proximal PAS upon LPS activation.

Liepelt and colleagues (Liepelt *et al.*, 2016) created an atlas of RBPs in RAW macrophages through interactome capture and LC-MS/MS, using LPS treatment for 2 hours as a differential stimulus. While ELAVL1 and hnRNP K were upregulated in both control and LPS-stimulated RAW cells, RNA-binding proteins TTP, JUNB and RRP1 were exclusive to LPS-stimulated RAW cells. Jia and colleagues (Jia *et al.*, 2017) studied monocyte-derived macrophages (MDM) infected with vesicular stomatitis virus. They showed that during the infection process, there was an overall initial trend of upregulation in the expression of short 3' UTR mRNAs (from 0 to 8 hours post infection (hpi)), while the expression of long 3' UTR mRNAs was upregulated later, at 16 hpi. The authors did not observe a correlation between gene expression levels and APA, but they showed that genes that expressed APA mRNA isoforms had varying functional roles depending on the infection time: gene ontology terms for 2-4 hpi in upregulated genes were related to inflammatory response, while those expressed at 8-16 hpi were related to adaptive immunity and protein transport, and later, to apoptosis-related processes.

Single gene studies also deserve a highlight in this section. For instance, Huang et al studied the regulation of the 3' UTR of IL-16 by mir-145 in THP-1 macrophages, promoting M2 macrophage polarization (Huang *et al.*, 2019). Cok *et al.* identified a murine LPS-responsive AU-rich sequence, consisting of several copies of the AUUUA pentamer in the 3' UTR of the *COX2* gene. The AUUUA sequence was repeated seven times in the first 60 nucleotides of the 3' UTR of *COX2* of mice RAW264.7 macrophages, part of the short 3' UTR isoform upregulated upon LPS stimulation. Indeed, the first 60 nucleotides alone are enough for LPS-mediated COX2 expression, and removal of the ARE sequences caused total loss of LPS-mediated COX2 induction. Several RBPs were shown to bind to the several copies of the identified AU-rich element present in the short 3' UTR of COX2 upon M1 polarization, except for hnRNP A0, a specialized, low-abundance hnRNP that exclusively bound to the distal mRNA isoform (Myer & Steitz, 1995). RBPs binding to the short 3' UTR of *COX2* regulate mRNA stability (HuR, AUF1, CPF-A), protein translation (TIA-1, TIAR) and cytoplasmic trafficking (hnRNP A2/B1, A3) of the *COX2* mRNA (Cok *et al.*, 2004).

3.2 Alternative 3' UTR mRNA isoforms in cancer

As cancer cells are differentially regulated in comparison to healthy cells (He *et al.*, 2016; Kazemian *et al.*, 2015; Lutz & Moreira, 2011; Sandberg *et al.*, 2008; Tian & Manley, 2013), a correlation between differential 3' UTR expression and oncogene activation or metastasis shows a growing interest in the CRC field (Bilanges & Stokoe, 2007; Hatchi *et al.*, 2015; Lai *et al.*, 2015; Mayr & Bartel, 2009). Additionally, multi-UTRs are abundant in genes such as transcription factors, RBPs, kinases/phosphatases, RNA and protein transport mechanisms (Mayr, 2016), which are also frequently altered in cancer, but their use as specific biomarkers is still elusive.

Literature centered in aberrant 3' UTR–APA involvement in cancer is growing, focusing on breast, ovary and lung cancers (Akdeli *et al.*, 2014; Hatchi *et al.*, 2015; He *et al.*, 2016; Mayr & Bartel, 2009; Yang *et al.*, 2012). Remarkably, there is a global increase in proximal PAS usage in rapidly dividing cells and cancer cells, suggesting a link between proliferation and proximal PAS choice, leading to the production of mRNAs containing shorter 3' UTRs (Ji *et al.*, 2011). Alterations in 3' UTR-APA and transcription termination mechanisms may therefore have downstream cellular events relevant to cancer progression. Consequently, studying these mechanisms is of utmost importance to fully understand the crosstalk between the tumor and its microenvironment.

In CRC, the Agami group (Morris *et al.*, 2012) highlighted the relevance of APA changes, by analyzing biopsies from colorectal tumor resections through RNA-Seq. They found that when studying differential alternative polyadenylation in these samples, 75% genes undergoing differential mRNA isoform expression had 3'UTR-APA and only 25% had CR-APA. Therefore, in cancer cells, the coding sequence of the APA mRNA isoforms was frequently unaltered. By matching sets of tumor and normal tissue samples from the same patient, they uncovered a shift towards the usage of proximal PAS in the colorectal tumor tissue, particularly when comparing adenocarcinoma to carcinoma, and hypothesized that this APA shift was due to upregulation of CPA factors. However, they highlighted the high heterogeneity of colon cancer patients, and its potential drawbacks for biomarker research and broader APA regulation studies.

Fischl and colleagues (Fischl *et al.*, 2019) compared three cell lines – nonmalignant 1CT, primary adenocarcinoma CRC cell line SW480 and metastatic cell line SW620 (derived from the same donor as SW480). In order to infer a connection between APA changes and increased tumorigenicity, they established early and late APA profiles. They defined early APA changes comparing APA profiles occurring in non-tumorigenic cell lines to the ones occurring in adenoma cell lines, and late APA changes comparing APA profiles occurring in adenoma cell lines to the ones occurring in carcinoma cell lines. They found that the subcellular fractionated RNA isolated from nuclear fractions, largely nascent RNA, showed an increase in proximal PAS usage in both CRC cell lines, when comparing to 1CT. The establishment of similar APA profiles in early and late cancer cell lines indicates causality and consistency in the choice to upregulate a single mRNA isoform in detriment to the other. Interestingly, these genes were involved in proliferative functions, which stands as one of the most important hallmarks of cancer. Curiously, CR-APA profiles in the cytoplasmic and nuclear fractions differed, and varied depending on tumorigenic progression: use of the internal (proximal) PAS was preferred in both cell lines, whereas the full-length mRNA isoform was overrepresented in the metastatic cell line. Finally, they found and characterized hnRNPC as crucial for distal PAS regulation in the cytoplasm of metastatic CRC cells, as mRNA isoforms containing binding sites for this RBP and hnRNPC itself were upregulated in SW620 cells. Elegantly, hnRNPC depletion reverted SW620 APA profile to the one similar in 1CT cells. Therefore, not only is hnRNPC crucial for defining the APA profile in CRC cell lines, but CR-APA events are connected to increased tumorigenic capability, which increases proteomic diversity and hence contributes to clonal heterogeneity in cancer.

In disagreement with the literature listed above, Begik and colleagues (Begik *et al.*, 2017) found a shift towards the distal PAS selection in colon cancer patients, as well as in lung and ovary tumors. Interestingly, this shift was also disproportionally associated for gene ontology terms related to RNA metabolism or proliferation, which are beneficial for tumor growth. While these differences may be explained with the MSI/MSS status of the tumors assayed, or on the algorithm approach applied in each study, all these studies highlight the importance of APA in CRC progression, and call attention to the need for further research.

In conclusion, if genes with downstream tumorigenic effects show APA alterations or aberrant transcription termination, it is plausible that these alterations occur before any deleterious effects to the cell, or to the adjacent tissue, are observed. Mutations in the 3' UTR may be as important for gene expression as in the coding region, but will be silent to exome-sequencing approaches. Therefore, studying cancer from the perspective of non-coding regions will undoubtedly enrich our fundamental knowledge in the field, increase the spectrum of known alterations in cancer cells, and possibly shed light on cancer mechanisms in which the causative coding mutation is unknown.

Chapter II – Thesis Aims

Chapter II – Thesis Aims

Alterations in the 3' UTRs of the transcripts driven by the intercellular macrophage-colorectal cancer cell communication are still poorly investigated and constitute blind spots to the identification of possible new targets for anti-cancer therapeutic approaches.

This PhD thesis aimed to investigate gene expression and APA events triggered by the communication between colorectal cancer cells with immune cells, in particular macrophages, and to identify the molecular mechanisms involved.

Specifically, our research addressed the following aims:

1. Establishment of a new methodology for simultaneous analyses of gene expression and alternative polyadenylation in primary human macrophages

Current tools to investigate mRNAs in different subcellular fractions and gene expression in primary human immune cells analyses are still lacking. Transcriptomic studies in primary macrophages are notoriously challenging due to the high cell plasticity and population heterogeneity. Consequently, methodologies to obtain sufficient amounts of homogenously polarized macrophages suitable are needed. We described an approach to identify new APA mRNA isoforms and quantify gene expression levels by 3'RNA-Seq and ChrRNA-Seq, in primary human macrophages that were differentiated and polarized *ex-vivo* and co-cultured with CRC cells. This methodology allowed us to identify robust macrophage APA mRNA signatures driven by the cancer cells, which alter the macrophage inflammatory profile, with consequences for macrophage physiology and tumor evasion.

This methodology was published in *Methods of Enzymology* (Wilton *et al.*, 2021) and are presented in subchapter 3.1.

2. Investigate how macrophage polarization and CRC cells modify macrophage gene expression and APA and identify the molecular mechanisms involved

Tumor-associated macrophages (TAMs) are associated with invasive cancer negative prognosis in several tissues, but it remained to be investigated how CRC affects macrophage gene expression and APA. We mimetized the *in vivo* environment

in the beginning of the tumorigenic process by exposing macrophages to CRC cell lines. We found that co-cultured macrophages showed a reversal of the pro-inflammatory macrophage phenotype, simultaneously with a decrease in APA.

Furthermore, we found that SRSF12 is involved in APA modulation in macrophage-relevant and RNA processing genes, a new function for this protein. We also found that SRSF12 is involved in the upregulation of Csf64, RBPs and chromatin organization genes.

Results obtained are presented in subchapter 3.2 as a manuscript recently submitted to *Cell Reports*:

Joana Wilton, Michael Tellier, Takayuki Nojima, Isabel Pereira-Castro, Angela M Costa, Jaime Freitas, Ricardo Pinto, Luísa Pereira, Shona Murphy, Maria Jose Oliveira, Nicholas J Proudfoot, Alexandra Moreira, *Proximity to colorectal cancer cells modulates macrophage alternative polyadenylation, in revision.*

3. **Quantifying individual gene expression and alternative 3'UTR in hypoxic CRC cells and polarized macrophages**

The effect of hypoxia on gene expression regulation is widely studied (Claffey *et al.*, 1998; Uniacke *et al.*, 2012), but little is known how hypoxia modifies APA. Similarly, APA studies in macrophages upon infection have been described (Jia *et al.*, 2017; Pai *et al*., 2016), but how APA is modified in each macrophage inflammatory population has not been determined. Here we aim to unveil the importance of the hypoxic tumor microenvironment in APA in CRC cells and primary human macrophages. To achieve this goal, we analyzed a selection of individual genes with alternative 3' UTR mRNA isoforms in macrophages under normoxia, and in cancer cells under normoxia and hypoxia. We show that, in M1 macrophages, the short 3' UTRs of most genes is upregulated, with the exception of *RAC1*, which shows upregulation of the long 3' UTR, which is consistent with upregulation in protein levels and subcellular delocalization. In hypoxic RKO, upregulation of the short 3'UTR of RAC1 was correlated with increased transcription (ChIP), Rac1 protein downregulation, and found that YBX1 binds the *Rac1* mRNA.
Results pertaining to this study are presented on subchapter 3.3.

Chapter III – Results

Chapter III – Results

This Results chapter is divided in three subchapters:

- 1 corresponds to the article published recently in *Methods in Enzymology* (Wilton et al., 2021), wherein the macrophage-CRC cells co-culture and subsequent RNA-Seq strategies are described.
- 2 corresponds to a revised research article recently submitted to Cell Reports, describing the results obtained with the aforementioned experimental strategy.
- 3 corresponds to a paper in preparation on the study of APA in individual genes in the macrophage and CRC cancer cell line populations before co-culture.

3.1 *Simultaneous studies of gene expression and alternative polyadenylation in primary human immune cells*

Published book chapter:

Wilton, J, Tellier, M, Nojima, T, Costa, AM, Oliveira, MJ and Moreira A (2021) “Chapter sixteen: Simultaneous studies of gene expression and alternative polyadenylation in primary human immune cells”, *in* Bin Tian (Ed) “mRNA 3’ End Processing and Metabolism”, Methods in Enzymology, Elsevier, 655: (pp. 349-399), DOI:10.1016/bs.mie.2021.04.004”

CHAPTER SIXTEEN

Simultaneous studies of gene expression and alternative polyadenylation in primary human immune cells

Joana Wilton[a,b,c], Michael Tellier[d], Takayuki Nojima[d,e], Angela M. Costa[f,g], Maria Jose Oliveira[f,g,h], and Alexandra Moreira[b,c,i,*]

[a]Graduate Program in Areas of Basic and Applied Biology (GABBA) PhD Program, ICBAS-Instituto de Ciências Biomédicas Abel Salazar, Universidade do Porto, Porto, Portugal
[b]Gene Regulation, i3S—Instituto de Investigação e Inovação em Saúde, Universidade do Porto, Porto, Portugal
[c]IBMC-Instituto de Biologia Molecular e Celular, Porto, Portugal
[d]Sir William Dunn School of Pathology, University of Oxford, Oxford, United Kingdom
[e]Medical Institute of Bioregulation, Kyushu University, Fukuoka, Japan
[f]Tumor and Microenvironment Interactions Group—i3S—Instituto de Investigação e Inovação em Saude, Universidade do Porto, Porto, Portugal
[g]INEB-Instituto Nacional de Engenharia Biomédica, Porto, Portugal
[h]Faculdade de Medicina, Universidade do Porto, Porto, Portugal
[i]ICBAS-Instituto de Ciências Biomédicas Abel Salazar, Universidade do Porto, Porto, Portugal
*Corresponding author: e-mail address: alexandra.moreira@i3s.up.pt

Contents

1. Introduction 350
2. Overview of the method 352
3. Detailed protocol 355
   3.1 Before you begin 355
4. Key resources table 357
5. Materials, reagents and equipment 360
   5.1 Materials 360
   5.2 Alternative materials and reagents 361
   5.3 Equipment 361
6. Step-by-step method details 361
   6.1 Preparation of primary human macrophages for co-cultures/transfection 361
   6.2 RNA isolation 367
   6.3 Library construction, RNA sequencing and QC 373
   6.4 Bioinformatics pipeline 385
   6.5 Gene expression analyses of the RNA-Seq results 388
7. Concluding remarks 391
8. Safety considerations 392
9. Expected outcomes 392

Methods in Enzymology, Volume 655
ISSN 0076-6879
https://doi.org/10.1016/bs.mie.2021.04.004

Copyright © 2021 Elsevier Inc.
All rights reserved.

10. Quantification and statistical analysis 393
11. Advantages 394
12. Limitations 395
13. Optimization and troubleshooting 395
13.1 Problem and solution 395
Ethical statement 396
Acknowledgments 396
Author contributions 396
References 396

Abstract

Transcription termination in eukaryotic cells involves the recognition of polyadenylation signals (PAS) that signal the site of pre-mRNA cleavage and polyadenylation. Most eukaryotic genes contain multiple PAS that are used by alternative polyadenylation (APA), a co-transcriptional process that increases transcriptomic diversity and modulates the fate of the mRNA and protein produced. However, current tools to pinpoint the relationship between mRNAs in different subcellular fractions and the gene expression outcome are lacking, particularly in primary human immune cells, which, due to their nature, are challenging to study. Here, we describe an integrative approach using subcellular fractionation and RNA isolation, chromatin-bound and nucleoplasmic RNA-Sequencing, 3′ RNA-Sequencing and bioinformatics, to identify accurate APA mRNA isoforms and to quantify gene expression in primary human macrophages. Our protocol includes macrophage differentiation and polarization, co-culture with cancer cells, and gene silencing by siRNA. This method allows the simultaneous identification of macrophage APA mRNA isoforms integrated with the characterization of nuclear APA events, the identification of the molecular mechanisms involved, as well as the gene expression alterations caused by the cancer-macrophage crosstalk. With this methodology we identified macrophage APA mRNA signatures driven by the cancer cells that alter the macrophage inflammatory and transcriptomic profiles, with consequences for macrophage physiology and tumor evasion.

1. Introduction

All human protein-coding genes with the exception of histones contain polyadenylation signals (PAS), pointing the 3′ end of the pre-mRNA and where a polyadenylation tail is added for correct mRNA 3′ end formation. Seventy-four percent of all human genes contain more than one PAS (Derti, Garrett-Engele, MacIsaac, et al., 2012; Lee et al., 2018; Shi, 2012; Tian, Hu, Zhang, & Lutz, 2005; Wang, Sandberg, Luo, et al., 2008) that may be used by alternative polyadenylation (APA) increasing transcriptomic diversity. APA produces several mRNA isoforms transcribed from the one single gene that may have different mRNA stabilities, result in diverse

protein expression levels, distinct mRNA and protein subcellular locations. This is due to the regulatory properties of the alternative 3′ UTRs conferred by the differential binding of RNA Binding Proteins (RBPs) and miRNAs (Berkovits & Mayr, 2015; Ma & Mayr, 2018; Mitra, Johnson, & Coller, 2016; Wurth & Gebauer, 2015).

The total estimated number of highly conserved PAS in the human genome exceeds 569,000 (Herrmann et al., 2020), and recent advances in the transcriptomic field highlighted the contribution of APA to the establishment of gene- and cell-specific programs such as cell activation and differentiation (Castello, Fischer, Eichelbaum, et al., 2012; Mayr, 2017; Pai, Baharian, Pagé Sabourin, et al., 2016; Sandberg, Neilson, Sarma, Sharp, & Burge, 2008; Tian & Manley, 2016). In particular, there are genome-wide trends consisting of proximal PAS selection in cancer cells and activated immune cells (Jia, Yuan, Wang, et al., 2017; Mayr & Bartel, 2009; Pai et al., 2016; Sandberg et al., 2008), and distal PAS selection in more differentiated cells such as neurons and during organism development (Braz, Cruz, Lobo, et al., 2017; Ji, Lee, Pan, Jiang, & Tian, 2009). These APA profiles have been established by powerful transcriptomic methodologies, including dedicated RNA-sequencing and bioinformatic protocols.

Cleavage and polyadenylation are mostly co-transcriptional events (Dye & Proudfoot, 1999) occurring in the nucleus, but the expression of APA mRNA isoforms containing alternative 3′ UTRs is also modulated by microRNAs, which occurs in the cytoplasm. Thus, it is often difficult to identify APA mRNA isoforms correctly by simple RNA-Sequencing methodologies without the use of subcellular fractionation procedures or bioinformatic algorithms. Nevertheless, it is possible to accurately pinpoint APA mRNA isoforms as they are transcribed by RNAPII by dedicated RNA sequencing methodologies such as chromatin RNA-Seq (Nojima, Gomes, Carmo-Fonseca, & Proudfoot, 2016) combined with 3′ mRNA-Sequencing, allowing to quantify and distinguish mRNA isoform levels produced by APA or other post-transcriptional events.

The use of primary human immune cells in transcriptomic studies has been hampered by the plastic nature of those cells and the different protocols for differentiation and polarization in use that may result in diverse transcriptomic data. Macrophages are plastic immune cells that depending on their inflammatory profile, function as phagocytes to infectious pathogens (named M1, or pro-inflammatory) and in tissue healing (named M2, or anti-inflammatory). They are also abundant cells of the tumor

microenvironment where they may either cooperate with or abrogate the progression of cancer (Locati, Mantovani, & Sica, 2013; Mantovani & Locati, 2013).

Here we describe an integrative approach using chromatin bound and nucleoplasm RNA-Seq, 3′ mRNA-Seq and bioinformatics, to understand how cancer cells affect the transcriptome of primary human macrophages. We describe a robust protocol for macrophage differentiation and polarization and how to co-culture M1 polarized macrophages with CRC cells in a transwell chamber. This model system allows a proper communication between the two different cell types while permits an efficient separation of the two cellular populations for the transcriptomic studies. Comparing the RNA profiles and data obtained by the different RNA-Seq methods using RNA isolated from the same donor allow us to ascertain whether changes in gene expression are due to APA, or if they are due to post-transcriptional regulation. We also describe a successful method for siRNA transfection in difficult to transfect primary human macrophages. Functional studies in physiologically-relevant macrophage and cancer cellular populations can then be easily be performed to explore the molecular mechanisms that regulate gene expression and APA.

2. Overview of the method

Here, we describe in detail how to perform transcriptomic studies in primary human macrophages in co-culture with CRC cells, which can be extended to other immune cells or organotypic cultures. An overview and workflow of the full protocol is presented on Figs. 1A, 2 and 3A. This strategy allows the analyses of steady-state, chromatin-bound (ChrRNA-Seq) and nucleoplasmic RNA (NpRNA-seq), as well as 3′ RNA-Seq by QuantSeq, and the bioinformatic processing needed to obtain simultaneous differential gene and mRNA isoform expression data.

The cell culture protocol lasts for 9 days, starting with primary human monocyte isolation from healthy blood donors, and macrophage differentiation and polarization into M1 macrophages which are subsequently co-cultured with CRC cells in a transwell chamber (workflow in Fig. 1A). Subsequently, total RNA is extracted from total, nuclear or cytoplasmic fractions, libraries are constructed and chromatin-bound RNA-Seq and 3′ RNA-Seq is performed and the data is analyzed bioinformatically (Fig. 3).

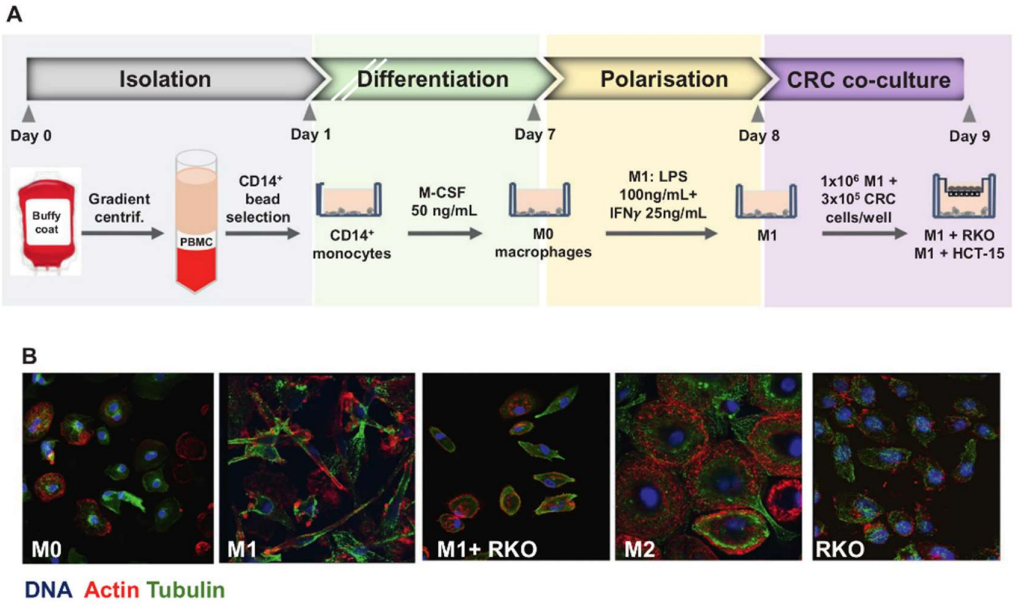


Fig. 1 (A) Workflow and experimental setup: buffy coats are subject to gradient centrifugation to obtain PBMCs, which are then exposed to $CD14^+$ beads to select $CD14^+$ monocytes. Monocytes are differentiated for 7 days in presence of M-CSF, obtaining M0 macrophages which are then polarized to M1 or M2 macrophages for 24 h. M1 macrophages are put into contact with CRC cell lines RKO or HCT-15 for 24 h. (B) Confocal microscopy images of unpolarized macrophages (M0) showing actin-tubulin cytoskeleton of pro-inflammatory macrophages (M1), M1 macrophages after RKO co-culture (M1 + RKO), anti-inflammatory macrophages (M2) and RKO cells for reference (RKO). Actin shown in red, tubulin shown in green, DNA shown in blue.

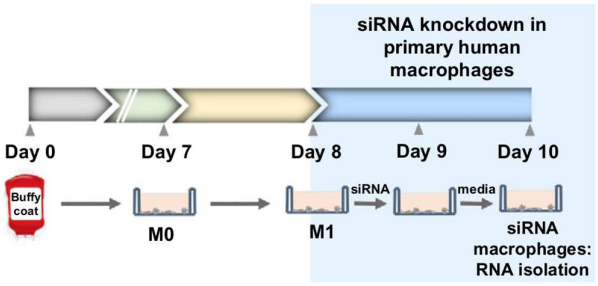


Fig. 2 Experimental setup and workflow of siRNA knockdown in primary human macrophages.

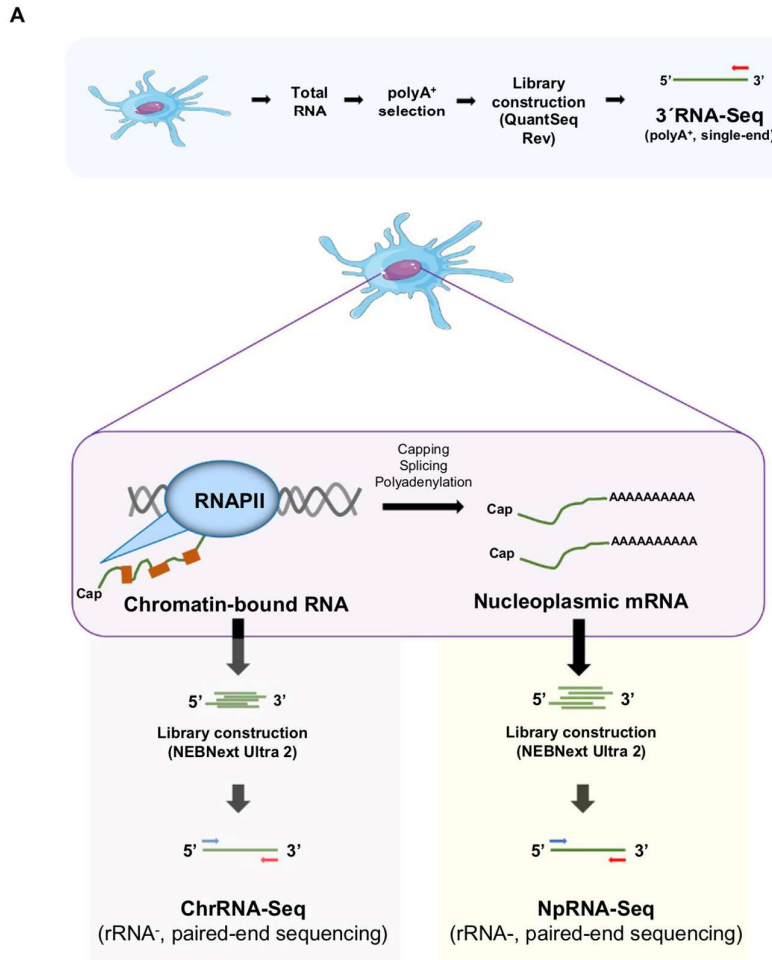


Fig. 3 (A) Workflow and setup of RNA fractionation and library construction of RNA samples from primary human macrophages. Top, conversion of total RNA into single-end 3′ mRNA-Seq libraries. Left, chromatin-bound RNA is converted into rRNA-depleted paired-end RNA-Seq libraries. Right, nucleoplasmic RNA is converted into rRNA-depleted paired-end RNA-Seq libraries. (B) Scheme of chromatin-bound and nucleoplasmic RNA fractionation. *Panel B adapted from Nojima T., Gomes T., Grosso A. R. F, et al. (2015) Mammalian NET-seq reveals genome-wide nascent transcription coupled to RNA processing.* Cell, 161*(3), 526–540. doi:10.1016/j.cell.2015.03.027.*

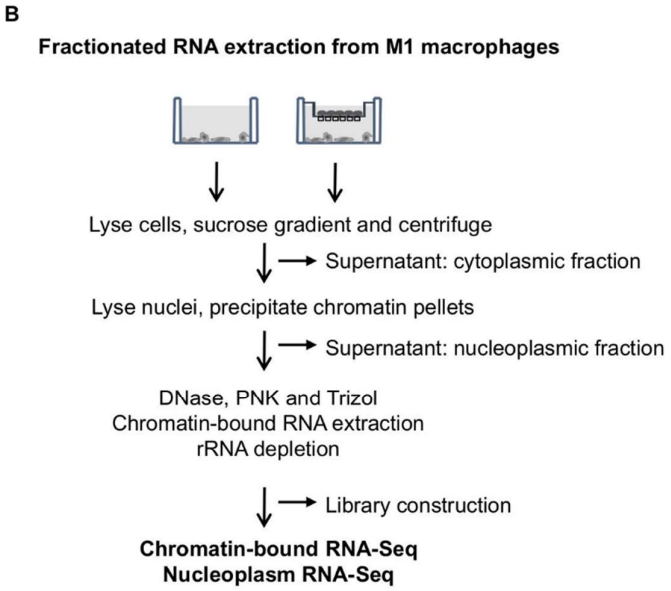


Fig.3—Cont'd

3. Detailed protocol

3.1 Before you begin

Timing: 4 h

1. When manipulating RNA, work in an RNase-free workstation: clean pipettes, benches, tip boxes, centrifuge, thermocycler, thermomixer, etc., with RNase Xterminator. Preventive measures such as not sharing reagents to avoid RNA degradation and cross-contamination are mandatory
2. Keep macrophage cell number consistent between conditions and biological replicates to isolate similar amounts of RNA
3. Maintain colorectal cancer (CRC) cell lines and primary human macrophages in a humified atmosphere at 37 °C and 5% CO_2, in complete RPMI medium with 10% FBS and 1× penicillin/streptomycin. When polarized to pro-inflammatory conditions, macrophages are kept for 24 h in RPMI medium with 2% FBS.
4. Prepare cell culture solutions and buffers:

(a) CD14 beads buffer to isolate $CD14^+$ monocytes: PBS pH 7.2/5% FBS/2 mM EDTA. For each PBMC sample, a total of 15 mL are needed

(b) Red blood cell lysis buffer: 0.15 M NH_4Cl/0.01 M $NaHCO_3$/1.3 mM EDTA. For each PBMC sample, a total of 5 mL are needed

(c) RPMI Complete: RPMI/10% FBS/1 × penicillin/streptomycin

(d) RPMI polarization media: RPMI/2% FBS

5. Prepare subcellular fractionation solutions for chromatin-bound, nucleoplasm and cytoplasmic RNA isolation

Critical: Always use RNase-free water. For the buffers used in RNA isolation add protease inhibitors (cOmplete Mini), phosphatase winhibitors (PhosStop) and RNase inhibitors (Ribolock) just before use, according to manufacturer's instructions. For Ribolock, use a final concentration of 2 U/μL.

(a) HLB/NP40 lysis buffer: 10 mM Tris-HCl pH 7.5/10 mM NaCl/2.5 mM $MgCl_2$/0.5% (v/v) NP-40. For each macrophage sample, 4 mL of HLB/NP40 lysis buffer are used, therefore we recommend to prepare 30 mL, adding in the following order: 28.02 mL RNase-free H_2O + 300 μL 1 M Tris-HCl pH 7.5 + 30 μL 5 M NaCl + 75 μL 1 M $MgCl_2$ + 1.5 mL 10% NP-40

(b) HLB/NP40/Sucrose buffer: 10 mM Tris-HCl pH 7.5/10 mM NaCl/2.5 mM MgCl2/0.5% (v/v) NP-40/10% (w/v) sucrose. For each macrophage sample, 1 mL of HLB/NP40/Sucrose buffer is used, therefore we recommend to prepare 10 mL, adding in the following order: 7.355 mL RNase-free H_2O + 100 μL 1 M Tris-HCl pH 7.5 + 20 μL 5 M NaCl + 25 μL 1 M $MgCl_2$ + 0.5 mL 10% NP-40 + 2 mL 50% (w/v) sucrose

(c) NUN1 buffer: 20 mM Tris-HCl pH 7.9/75 mM NaCl/0.5 mM EDTA/50% (v/v) glycerol. For each macrophage sample, 125 μL of NUN1 buffer are used, therefore we recommend to prepare 10 mL, adding in the following order: 4.625 mL RNase-free H_2O + 200 μL 1 M Tris-HCl pH 7.9 + 150 μL 5 M NaCl + 25 μL 0.2 M EDTA + 5 mL 100% (v/v) glycerol. Add protease and phosphatase inhibitors and Ribolock

(d) NUN2 buffer: 20 mM HEPES-KOH pH 7.6/300 mM NaCl/0.2 mM EDTA/7.5 mM $MgCl_2$/1% (v/v) NP-40/1 M urea. For each macrophage sample, 1.2 mL of NUN2 buffer is used, therefore we recommend to prepare 30 mL, adding in the following order: 24.345 mL RNase-free H_2O + 0.6 mL 1 M HEPES-KOH

pH 7.6 + 1.8 mL 5 M NaCl + 30 µL 0.2 M EDTA + 225 µL 1 M $MgCl_2$ + 3 mL 10% (v/v) NP-40 + 1.8 g urea. Add protease and phosphatase inhibitors and Ribolock

(e) HSB buffer: 10 mM Tris-HCl pH 7.5/500 mM NaCl/10 mM $MgCl_2$/0.25 U/µL TURBO DNase. For each macrophage sample, 50 µL of HSB buffer is used, therefore we recommend to prepare 500 µL, adding in the following order: 382.5 µL RNase-free H_2O + 5 µL 1 M Tris-HCl pH 7.5 + 50 µL 5 M NaCl + 62.5 µL 2 U/µL TURBO DNase

6. Before starting the library construction

(a) Always centrifuge microtubes before and after thermocycler incubation steps

(b) Prepare mastermixes of reagents for library construction (steps 50–55 and 63–68) and include an extra 10% of volume surplus per reaction

(c) Thermocycler lid must be maintained at 99 °C except where indicated otherwise

(d) Resuspend and equilibrate magnetic beads at RT 30 min before using. They must have a uniformly brown color, without clumps

4. Key resources table

Reagent or resource	Source	Identifier
Antibodies		
AlexaFluor488 conjugated secondary antibody	Life Technologies	Cat # A32723
DAPI-Vectashield	Vector Laboratories	Cat # H1200-10
Monoclonal anti-α-tubulin antibody	Sigma-Aldrich	Cat # T9026
AlexaFluor 647 Phalloidin	Life Technologies	Cat # A22287
Biological Samples		
Buffy coats from anonymized blood donors	Centro Hospitalar Universitário *São João, Porto, Portugal*	–

Continued

—cont'd

Reagent or resource	Source	Identifier
Chemicals, Peptides, and Recombinant Proteins		
CD14 Microbeads	Miltenyi Biotec	Cat # 130-050-201
Chloroform	Merck	Cat # R49352845737
CompleteMINI protease inhibitors	Sigma	Cat # 11836153001
Recombinant DNase I	Roche	Cat # EN0521
GenMute transfection reagent for Primary Human Macrophages	SignaGen	Cat # SL100568-PMG
Interferon-gamma (IFNγ)	Peprotech	Cat # 300-02
Interleukin-4 (rhIL-4)	Peprotech	Cat # 200-04
Interleukin-10 (rhIL-10)	Peprotech	Cat # 200-10
Lipopolysaccharide (LPS from *Escherichia coli* subtype O55:B5)	Sigma-Aldrich	Cat # L4005
Lymphoprep	Axis-Shield	Cat # 1114547
Macrophage Colony Stimulating Factor (M-CSF)	Peprotech	Cat # 300-25
NP-40 Igepal	Sigma-Aldrich	Cat # 18896
SuperScript IV reverse transcriptase	ThermoFisher Scientific	Cat # 18090050
Sybr Green I for qPCR detection	ThermoFisher	Cat # S7563
Trizol reagent	Ambion	Cat # 15596018
TURBO DNase 0.25 U/μL	ThermoFisher Scientific	Cat # AM2238
Critical Commercial Assays		
AMPure XP beads	Beckman Coulter	Cat # A63880
DynaBeads mRNA Purification kit	Invitrogen	Cat # 61006
High Sensitivity DNA kit	Agilent	Cat # 5067-4626, 5067-4627
KAPA Library Quantification kit	Roche	Cat # 07960140001

—cont'd

Reagent or resource	Source	Identifier
NextSeq High-Output kit for 75 cycles	Illumina	Cat # FC-404-2005
NEBNext Ultra II directional library prep kit for Illumina	New England Biolabs	Cat # E7760
Qubit RNA HS Assay Kit	ThermoFisher	Cat # Q32852
QuantSeq REV kit	Lexogen	Cat # 016.24
QuantSeq 3′ mRNA-Seq PCR Add-on kit for Illumina	Lexogen	Cat # 020.96
Ribo-Zero Gold rRNA removal kit for Human/Mouse/Rat	Illumina	Cat # MRZG12324
Experimental Models: Cell Lines		
HCT-15 cell line	ATCC	CCL-225
RKO cell line	ATCC	CRL-2577
Oligonucleotides		
Non-targeting siRNA control (ONTARGETplus SMARTpool siNTC)	Dharmacon	Cat # D-001810-10-05: 5′-UGGUUUACAUGUCGACUAA-3′ 5′-UGGUUUACAUGUUGUGUGA-3′ 5′-UGGUUUACAUGUUUUCUGA 3′ 5′-UGGUUUACAUGUUUUCCUA-3′

Software and Algorithms

Name	Source
7500 v2.0.6 software	https://www.thermofisher.com/pt/en/home/technical-resources/software-downloads/applied-biosystems-7500-real-time-pcr-system.html
Bedtools	https://bedtools.readthedocs.io/en/latest/
Bowtie	http://bowtie-bio.sourceforge.net/bowtie2/index.shtml

Continued

—cont'd
Software and Algorithms

Name	Source
Cutadapt	https://cutadapt.readthedocs.org/en/stable
DESeq2	https://bioconductor.org/packages/release/bioc/html/DESeq2.html
DEXSeq	https://bioconductor.org/packages/devel/bioc/vignettes/DEXSeq/inst/doc/DEXSeq.html
FastQC	http://www.bioinformatics.babraham.ac.uk/projects/fastqc
FIJI package for ImageJ	https://fiji.sc/
Galaxy	https://usegalaxy.org/
Human genome release hg38	https://www.gencodegenes.org/human/
GraphPad Prism Software version 7	https://www.graphpad.com/scientific-software/prism/
htseq-count	https://htseq.readthedocs.io/en/master/
ImageLab Software (Bio-Rad)	https://www.bio-rad.com/en-pt/product/image-lab-software?ID=KRE6P5E8Z
Python v. 2.7	https://www.python.org/
RStudio	https://rstudio.com/products/rstudio/download/
SAMtools	http://samtools.sourceforge.net/
STAR aligner	https://github.com/alexdobin/STAR
TopHat	http://ccb.jhu.edu/software/tophat/index.shtml

5. Materials, reagents and equipment

5.1 Materials

- 6 multi-well plates made of plasma-treated tissue culture polystyrene (TCPS) (Ref. 657,160, Greiner Bio-One)
- 6 multi-well plate permeable transwell insert (Corning, Ref 353,102) with 1.0 μm pore size

- 24 multi-well plates (Ref. 4,430,400, Frilabo) for immunofluorescence
- LS column (Ref. 130-042-401, Miltenyi Biotec)
- Nuclease-free microcentrifuge tubes, 1.5 mL (Ref. 616,201, Greiner bio-one)
- Nuclease-free PCR tubes 0.2 mL (72,991,002, Sarstedt)
- Nuclease-free 15 mL Falcon tubes (Ref. 430,055, Corning)
- Nuclease-free 50 mL Falcon tubes (Ref. 430,828, Corning)
- T-flasks for cell culture (Corning)

5.2 Alternative materials and reagents

- Commercial alternatives to RNase Xterminator may be used, or it may be substituted by 3% H_2O_2 and 0.5% SDS, followed by 70% ethanol
- Equivalent equipment and consumables may be used, except for TCPS plastic cell culture plates for macrophage cultures and co-cultures with CRC cells

5.3 Equipment

- 48-well Thermocycler (Biometra)
- 7500 Fast Real-Time PCR System (Applied Biosystems)
- Bioanalyzer 2100 (G2939BA, Agilent)
- Cell culture CO_2 incubator (CO_2 at 5%, humidified, 37 °C, Binder)
- Cell culture laminar flow hood (Thermo MSC ADV 1.2)
- Centrifuges (Eppendorf 5415R and 5810R)
- DynaMag2 magnetic rack for microcentrifuge tubes (Ref. 12321D, ThermoFisher)
- Inverted light microscope (Zeiss Axiovert 25)
- Minispinner (Elmi DOS-20L)
- Nanodrop ND-1000 (Thermo Scientific)
- Qubit fluorometer (ThermoFisher, cat. no. Q33216)
- TCS-SP5 laser confocal microscope (Leica Microsystems, Germany)
- Thermomixer (Eppendorf)
- Vortex (ZX3, VELP Scientifica)

6. Step-by-step method details

6.1 Preparation of primary human macrophages for co-cultures/transfection

See Fig. 1A for workflow.

6.1.1 Isolation of PBMCs from human peripheral blood and CD14$^+$ enrichment (adapted from Ohradanova-Repic, Machacek, Fischer, & Stockinger, 2016)

Timing: 8 h (day 1).

Critical

- As this method is designed for primary human macrophages, special attention should be taken to design your experiment to use PBMCs from as many donors (3–4) as possible in each experiment
- Work as quickly as possible at RT to avoid macrophage cell death
- Cell culture plastic materials as well as all the reagents should be selected from the Key Resources Table and the Materials and Methods section. In particular, we recommend TCPS 6-multiwell plates to increase macrophage adhesion and prevent macrophage polarization (Lerman, Lembong, Muramoto, Gillen, & Fisher, 2018; Rostam, Singh, Salazar, et al., 2016)
- All reagents must be sterile; on steps 1–2, reagents must be at room temperature (RT).

1. Separate the PBMC ring from the other buffy coat sections by density gradient centrifugation using Lymphoprep Ficoll reagent
2. Red Blood Cell (RBC) removal and PBMC counting:
   (a) Add 5 mL RBC lysis buffer to PBMCs. Incubate at 37 °C for 5 min, add 25 mL PBS and centrifuge at 300 g for 10 min at 4 °C
   (b) Resuspend pellet in RPMI medium (10% FBS, 1 × streptomycin/penicillin) and count cells, using the trypan blue exclusion test
   (c) Determine cell number and centrifuge the appropriate number of cells at 300 g for 10 min, at 4 °C

Critical

- From this point on, the protocol should be performed as quickly as possible until cells are plated, keeping the cells at 4 °C whenever possible to prevent cell mortality.
- PBMCs contain 10–20% macrophage content, therefore you should multiply the amount of macrophages you need by 5 to determine the amount of PBMCs to be centrifuged in this step.
  (a) CD14$^+$ monocytes were purified from PBMCs by magnetic-activated cell sorting using CD14 microbeads as follows: resuspend pellet in 47.5 µL CD14$^+$ beads buffer and 5 µL CD14 microbeads per each 10×10^6 cells. Mix and incubate for 20 min at 4 °C, mixing every 5 min

(b) Wash cells in 2–3 mL of CD14 beads buffer and centrifuge at 300 g for 10 min at 4 °C

(c) Remove the supernatant completely and resuspend in 500 µL $CD14^+$ beads buffer, for a maximum of 100×10^6 PBMCs
Critical: ensure that the PBMC suspension is clump-free.

3. $CD14^+$ positive selection (adapted from Ohradanova-Repic et al., 2016):

(a) In the flow hood, equilibrate each column by adding 500 µL $CD14^+$ beads buffer

(b) For each donor used, load PBMC suspension on the column. Add 500 µL in the Falcon tube containing the remaining PBMCs, resuspend and load in the column

(c) Wash the column three times with 3 mL $CD14^+$ beads buffer

4. $CD14^+$ cell elution:

(a) Load column with 5 mL $CD14^+$ beads buffer and immediately insert the plunger, eluting the $CD14^+$ cells into the Falcon tube

(b) Centrifuge cells at 300 g for 10 min at 4 °C, resuspend in complete RPMI

(c) Count cells using the trypan blue exclusion test

6.1.2 Macrophage differentiation and M1 polarization

Timing: 2 h + 6 days incubation (days 1–7)

Critical

- Plate cells in a cell density of 1×10^6/well (for co-culture with CRC cells) or 1.5×10^6/well (for transfection).
- If performing immunofluorescence, seed macrophages on 6-wells containing 4 glass coverslips each

1. $CD14^+$ cell plating:

(a) Resuspend $CD14^+$ cells in complete RPMI medium

(b) Add recombinant human macrophage colony stimulating factor (M-CSF) to a final concentration of 50 ng/mL, to improve differentiation and adhesion

(c) Seed cells into 6-well plates, 2 mL in each well

(d) Incubate in a CO_2 incubator at 37 °C for 7 days

(e) Add M-CSF-containing RPMI at day 4
Critical: On day 7, check if macrophages have adhered to the well surface. If so, macrophages may be efficiently polarized. If not, wait until day 7.

Note: This differentiation protocol yields ~93% $CD14^+$ cells (Ohradanova-Repic et al., 2016).

2. Macrophage polarization:
   (a) Take out media and slowly add 2 mL polarization medium (RPMI/2% FBS, no antibiotics) containing polarization agents: M1—lipopolysaccharide (LPS) 100 ng/mL and interferon-gamma (IFNγ) 25 ng/mL. Incubate for 24 h at 37 °C
   (b) Keep unpolarized macrophages as controls, adding the same volume of RPMI polarization media without polarization agents

Critical

- Add the polarization media drop by drop, to avoid macrophage detachment
- LPS and IFNγ concentrations are critical to proper macrophage polarization, as different concentration combinations will give rise to distinct transcriptional profiles
- The lack of antibiotics in the media is purposefully done to avoid immunomodulatory effects that could hinder proper polarization (Brooks, Hart, & Coleman, 2005)
- The decreased amount of FBS is used to increase attachment and phagocytosis, and lower local TGFβ concentrations, which diverts macrophage polarization toward anti-inflammatory conditions (Oida & Weiner, 2010; Suganuma, Fahey, Bryan, Healy, & Talalay, 2011; Zhang, Wang, Wang, et al., 2016)

Note: If desired, one can also polarize macrophages toward anti-inflammatory conditions (M2) through addition of RPMI 2% FBS without antibiotics containing 10 ng/mL recombinant human IL-10 (Ref. 200-10, Peprotech) or 20 ng/L IL-4 (Ref. 200-04, Peprotech).

6.1.3 Macrophage and colorectal cancer co-cultures

Timing: 3 + 24 h incubation (days 7–8)

1. Prepare cell lines for co-culture:
   (a) Trypsinize RKO and HCT-15 cells, resuspend separately in 5 mL RPMI and count cells via trypan blue exclusion test
   (b) Resuspend in a cell density of 3.75×10^5 cells/mL

Critical

- Ensure initial cell confluency is equal in both cell lines
- For a typical sequencing run, using 6×10^6 macrophages and 3 biological replicates, we recommend to use two T75 flasks with at least 80% confluency of CRC cell line, to obtain sufficient cells for co-culture

Note: We used RKO and HCT-15 CRC cell lines for co-culture with macrophages. Optimize co-culture conditions by titrating cell confluency in the transwells, using different timepoints and initial seeding cell densities.

2. Prepare macrophages for co-culture:
   a. Remove macrophage polarization media from wells
   b. Add 1.2 mL complete RPMI per 6-multiwell that will have co-cultured CRC cells, and 2 mL complete RPMI in control wells
   Note: As macrophage polarization has been successfully achieved, macrophages can be exposed again to antibiotic-containing media without detrimental polarization effects.
3. Perform co-cultures:
   a. Carefully add co-culture 1.0 μm inserts to each respective well
   Critical: The porosity level of the co-culture insert filter stops cancer cells from crossing to the lower compartment while still allowing soluble factor exchange between the upper and lower compartment cell populations.
   b. Add 800 μL RKO or HCT-15 cells in the insert, making sure that its surface is fully covered
   c. Incubate co-cultures for 24 h

6.1.4 Macrophage and CRC immunofluorescence

Timing: 6 h (staining) + ~2 h (imaging) (day 9)

1. Transfer glass coverslips containing macrophages to 24-well plates after mono- or co-culture
2. Prepare the samples at room temperature:
   a. Fix macrophages by adding 4% PFA for 10 min
   Pause point: at this point, PFA-fixed cells may be kept at 4 °C protected from light for a maximum of 3 weeks.
   b. Wash cells with PBS 3 × 5 min each, under gentle agitation
   c. Quench cells by adding 50 mM NH_4Cl for 10 min
   d. Repeat step (b).
   e. Permeabilize cells by adding 0.2% Triton X-100 for 10 min
   f. Repeat step (b).
   g. Block cells by adding 5% BSA for 1 h
3. Sample incubation, protected from light:
   a. First incubate with monoclonal alpha-tubulin antibody (1:4000 dilution) for 1 h
   b. Secondly, incubate with AlexaFluor 488 conjugated secondary antibody (1:1000 dilution) for 45 min

c. Lastly, stain actin by incubating with AlexaFluor 647 Phalloidin (1:40 dilution) for 20 min

4. Mount coverslips using DAPI-Vectashield and sealing with polish
   Pause point: coverslips may be kept at −20 °C for a maximum of 6 weeks, away from light.
5. Image cells on a confocal microscope (e.g., Leica TCS-SP5), using the 40× oil objective
6. Perform image analysis on appropriate software (e.g., FIJI)

Fig. 1B shows macrophage and CRC cell images obtained through this protocol.

6.1.5 Macrophage siRNA transfection

Timing: 2 + 48 h incubation.

Fig. 2 shows the workflow for macrophage siRNA transfection.

1. Take out co-culture or polarization media and add 1 mL complete RPMI media 30 min to 1 h before transfection.
2. Prepare GenMute Transfection Buffer working solution.
   Note: This 1 x working solution is shelf-stable for 24 months, but we recommend to prepare it fresh with RNase-free water before every use, keeping it at RT until needed.
3. For transfection of 6-wells, dilute 50 pmol siRNA in 100 µL GenMute Transfection Buffer working solution. Add 4 µL GenMute Transfection Reagent and incubate for 15 min at RT.
   - Never incubate the transfection complex containing the transfection reagent and the siRNA for longer than 30 min, as transfection complexes increase in size proportionally to the incubation time. If the transfection complex incubation is too long, transfection efficiency will decrease.
4. Add the transfection mix to the cells drop-by-drop, on the center of the well.
5. Gently rock the 6-multiwell plate back and forth, and incubate at 37 °C overnight.

Critical

- Macrophages must be plated at a cell density of 1.5×10^6/well on Day 1, to obtain at least 50% confluency on transfection day.
- Primary human macrophages are notoriously hard to transfect, due to their inherent ability to detect non-self molecules. Therefore, we recommend using GenMute.

6. Take out the transfection media and add complete RPMI to macrophages and incubate for 48 h.
7. Isolate RNA (Section 6.2).

Note: Knockdown levels can be assessed by RT-qPCR.

6.2 RNA isolation

RNA is extracted from macrophages after 24 h of co-culture and monoculture, and after transfection with siRNA.

Critical

- In order to obtain intact RNA samples, keep the bench, all materials and reagents RNase-free by wiping with RNase Xterminator or similar
- Similarly, avoid RNases by changing gloves frequently during the protocol
- Labcoats should also be frequently changed
- It is also useful to create a dedicated RNA-only work space to reduce cross-contamination
- We recommend to use commercially available RNase-free water, and to avoid DEPC-treated water due to its reactivity to extracted RNA and incompatibility with many of the solutions used for RNA subcellular fractionation (e.g., Tris).

6.2.1 Total RNA extraction

Timing: 4 + 16 h incubation at −80 °C.

Total RNA extraction for 3′-mRNA-Seq is shown on the upper panel of Fig. 3A.

1. Cell lysis
   - **(a)** Remove RPMI from the macrophage culture
   - **(b)** Wash with ice-cold PBS
   - **(c)** Add 250 µL Trizol per 6-multiwell and pipet up and down to homogenize

     Note: Trizol contains acidic phenol to separate RNA from the remaining fractions, and guanidinium thiocyanate to inactivate endogenous RNases.
   - **a.** Transfer to RNase-free microcentrifuge tube
   - **b.** Incubate samples at RT for 2 min to dissociate the nucleoprotein complex
   - **c.** Add 200 µL of chloroform per each mL Trizol reagent
   - **d.** Mix them thoroughly by inverting the tube
   - **e.** Incubate at RT for 1 min

f. Centrifuge at 4 °C for 15 min at 12000 g
g. Transfer the upper aqueous phase to a new 1.5 mL RNase-free microcentrifuge tube

Critical: avoid taking out the organic layer and lower phase containing contaminants (phenol from Trizol, DNA, and protein).

2. RNA precipitation
h. Add an equal volume of isopropanol to the samples. Add 1 µL of glycogen to act as co-precipitant
i. Vortex briefly
j. Incubate at −80 °C for 16 h, to maximize RNA yield
k. Centrifuge at 4 °C for 20 min at 12000 g
l. Remove the supernatant carefully
m. Wash with 1 mL of 70% Ethanol, flick the tube to release the pellet from the bottom of the tube
n. Centrifuge at 4 °C for 5 min at 7500 g
o. Discard the supernatant and air dry the RNA pellet

Critical

- After isopropanol precipitation, macrophage RNA needs to be incubated at −80 °C for a minimum of 4 h, but the optimum time is 16 h
- Avoid to dry the RNA completely to facilitate resuspension

Notes

- RNA can optionally be resuspended at 55 °C for 5 min before quantification
- RNase inhibitors (e.g., Ribolock) can be added at a 1:20 dilution to prevent RNA degradation

3. Quantify RNA concentration with a fluorescent dye-based method such as the Qubit RNA HS Assay Kit. Briefly, dilute 1 µL resuspended RNA in a solution containing RNA HS reagent in a 1:200 dilution with Qubit RNA HS Buffer, incubate at RT for 2 min and quantify the RNA in a Qubit fluorometer. Calculate the RNA concentration taking into account the previously made dilution.

Pause point: RNA can be kept at −80 °C for 2 weeks before proceeding with library construction; if samples are kept any further, we recommend to check RNA quality on a electrophoretic chip such as RNA 6000 Pico Kit (Agilent), or to run an RNase-free 0.8% agarose gel to confirm RNA integrity, visualizing the gel on a UV trans illuminator such as GelDoc or similar imaging system. Total RNA should appear as two sharp rRNA bands (28S and 18S) in a 2:1 ratio, while degraded RNA should appear as a smear.

6.2.2 RNA extraction from nuclei and cytoplasm fractions

Timing: 8 + 16 h precipitation time.

The protocol is an adaptation of Nojima, Gomes, Grosso, et al. (2015) (Fig. 3A and B).

Critical

- For one RNA-sequencing experiment, 6×10^6 macrophage cells were used as input material, at a cell density of 1×10^6/well
- Prepare HLB/NP40, HLB/NP40/sucrose, NUN1, NUN2, and HSB buffers beforehand, adding protease, phosphatase and RNase inhibitors just before use as shown in the initial Before you Begin section
- If possible, work in the cold room on the Nuclei and Cytoplasm Fractionation and Chromatin and Nucleoplasm Fractionation steps
- Continuously renew the ice inside the icebox to ensure RNA samples are kept at 4 °C at all times

1. Wash cells in 2 mL of ice-cold PBS twice, keeping the multiwell chambers on ice
   Critical: ensure PBS is added slowly as to avoid removing or disrupting macrophages.
2. Lyse cells in 4 mL of HLB/NP40 buffer and incubate on ice for 5 min
3. Transfer to a 15 mL Falcon tube
4. Underlay slowly 1 mL ice-cold HLB/NP40/sucrose buffer and centrifuge at 300 g for 5 min at 4 °C
5. Collect the pellet
   Note: The supernatant can be kept at −80 °C for up to a month if cytoplasmic fraction needs to be analyzed.

6.2.3 RNA extraction from chromatin and nucleoplasm fractions

1. Resuspend completely the isolated nuclei with 125 μL NUN1 buffer
2. Add ice-cold 1.2 mL NUN2 buffer
3. Mix thoroughly by vortex with max speed
4. Note: NUN2 buffer includes 1 M urea which improves chromatin isolation.
5. Incubate on ice for 15 min
6. Mix thoroughly by vortex with max speed every 5 min
7. Centrifuge at 15680 g for 10 min at 4 °C
8. Keep both fractions: the supernatant is nucleoplasmic RNA, the pellet is chromatin-bound RNA
9. Isolate chromatin-bound RNA:
   a. Resuspend the chromatin pellet in 50 μL HSB (containing DNase)

b. Incubate at 37 °C for 10 min, 1400 rpm on a Thermomixer
c. Add 50 µL Proteinase K/SDS solution
d. Incubate at 37 °C for 10 min, 1400 rpm on a Thermomixer
e. Extract RNA with acid phenol-chloroform to remove TURBO DNase:
  i. Add 100 µL acid phenol: chloroform: isoamyl alcohol and shake for 15 s
  ii. Centrifuge at 10000 g at 4 °C for 2 min
  iii. Transfer upper aqueous phase to a new tube
  iv. Add 0.1 volumes of 3 M sodium acetate, 2 µL glycogen and 250 µL of 100% ethanol. Vortex for 5 s
  v. Incubate at −80 °C overnight for increased yield and centrifuge at 16000 g for 20 min at 4 °C
  Critical: After isopropanol precipitation, macrophage RNA needs to be incubated at −80 °C for a minimum of 4 h, but the optimum time is 16 h.
  vi. Remove ethanol carefully and dry RNA pellet
  vii. Resuspend in 50 µL RNase-free water

10. Isolate RNA with Trizol:
a. Add 500 µL Trizol
b. Vortex until RNA pellet disappears
c. Incubate samples at RT for 2 min to dissociate the nucleoprotein complex
d. Add 100 µL chloroform
e. Mix them thoroughly by inverting the tube
f. Incubate at RT for 10 min
g. Centrifuge for 10 min at 12000 g at 4 °C
h. Transfer the upper aqueous phase (~100 µL) containing RNA to a new 1.5 mL RNase-free microcentrifuge tube

Critical: avoid taking out the organic layer and lower phase containing contaminants (phenol from Trizol, DNA, and proteins).

11. RNA precipitation:
a. Add an equal volume (~100 µL) of isopropanol to the samples
b. Add 1 µL of glycogen to act as co-precipitant
c. Mix them by vortex briefly and incubate at −80 °C for 16 h, to maximize RNA yield
d. Centrifuge at 12000 g for 20 min at 4 °C
e. Remove the supernatant. Keep the pellet
f. Wash the pellet with 500 µL of 70% Ethanol

g. Centrifuge at 7500 g for 5 min at 4 °C
h. Remove carefully the supernatant. Keep the pellet
i. Air dry the pellet
j. Critical: Avoid complete dry to facilitate resuspension.
k. Resuspend the pellet with 10 μL of nuclease-free water

Notes

- Resuspended RNA can optionally be heated at 55 °C for 5 min before quantification
- RNase inhibitors (e.g., Ribolock) may be added at a 1:20 dilution to prevent RNA degradation

12. Quantify RNA concentration with a fluorescent dye-based method such as the Qubit RNA HS Assay Kit

13. Before proceeding, analyze subcellular fractionated RNA by RT-qPCR: *MALAT1*, a highly expressed nuclear lncRNA (Zhang, Hamblin, & Yin, 2017) is recommended to check successful subcellular fractionation. *MALAT1* should only be detected in the chromatin-bound and nucleoplasmic fractions
Critical: This is a quality control step in the protocol, to ensure correct subcellular fractionation. An example of expected results is shown on Fig. 4A.

14. Prior to library construction, check for potential bacterial contamination
Critical: Cross-contamination of cell culture samples due to manipulation or donor nosocomial infection can ruin the experiment. Therefore, it is essential to rule out the presence of microbes before library construction.

(a) Convert 100 ng RNA to cDNA using a reverse transcriptase such as SuperScript IV (SSIV), according to manufacturer's instructions. Briefly, to 100 ng RNA, add RNase-free water up to 12 μL, 1 μL of 50 μM random hexamers and 1 μL of 10 mM dNTPs, to a final concentration of 2.5 μM and 0.5 mM respectively. Incubate at 65 °C for 5 min. 4 μL SSIV buffer, 1 μL DTT, 0.5 μL Ribolock, and 0.5 μL SSIV

(b) Perform the following PCR program:
i. 23 °C for 10 min
ii. 55 °C for 10 min
iii. 80 °C for 10 min

(c) Analyze the cDNA with PCR using primers for the bacterial 16S gene (27F: 5′-AGAGTTTGATCCTGGCTCAG-3′ and 1492R:

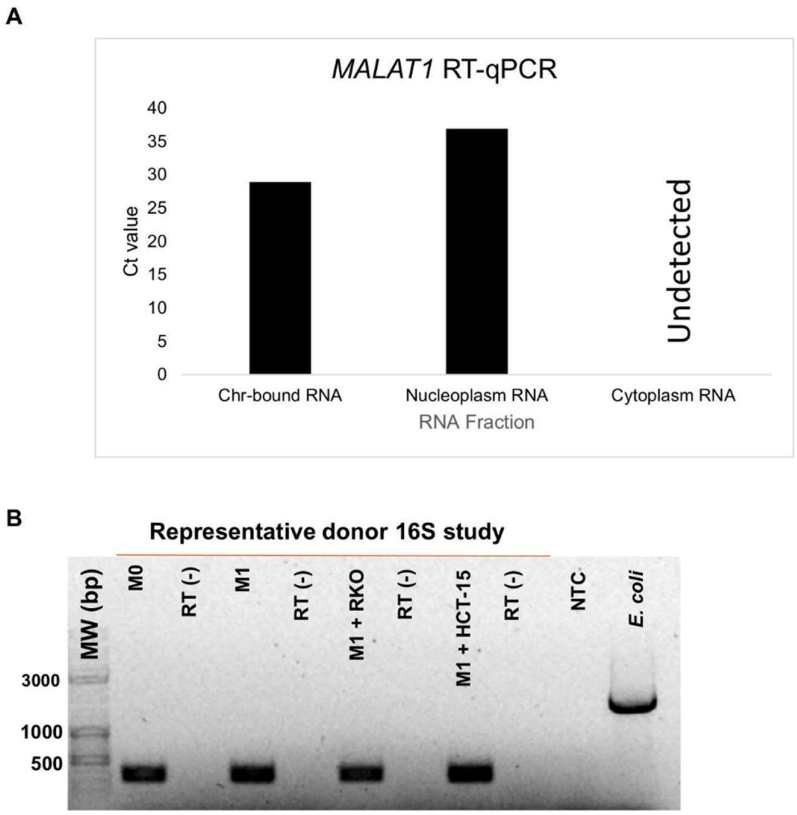


Fig. 4 (A) *MALAT1* expression levels in fractionated RNA. *MALAT1* is detected in ChrRNA and nucleoplasm RNA fraction but not detected in the cytoplasmic RNA fraction. (B) Assessment of bacterial contamination in macrophage samples by PCR of 16S (0.8% agarose gel, GeneRuler DNA Ladder mix (Invitrogen) as molecular weight (MW) marker). RT—no reverse transcriptase added; NTC—non-target control. Bands in macrophage lanes were subject to Sanger sequencing and correspond to human precursor 45S pre-rRNA.

5′-CGGTTACCTTGTTACGACTT-3′). Use bacterial genomic DNA (e.g., *E. coli* DH5α) as a positive control. Perform the following PCR program:

i. 95 °C for 5 min
ii. 30 cycles of 30 s at 94 °C, 90 s at 48 °C, and 2 min at 72 °C
iii. final extension for 10 min at 72 °C

Subsequently, run samples on a 0.8% agarose gel. A representative example is shown in Fig. 4B.

6.3 Library construction, RNA sequencing and QC

Workflows on Figs. 3A and B, 5A.

Critical

- Use the compatible DynaMag2 magnetic stand for accurate and quick nucleic acid separation

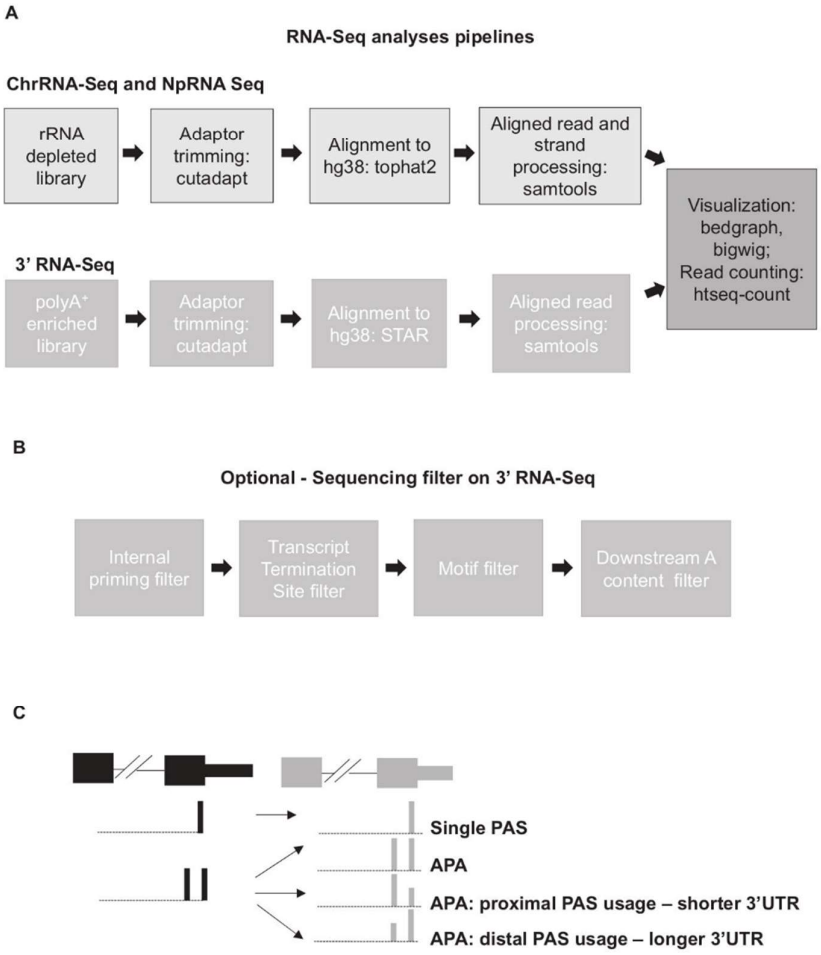


Fig. 5 (A) Pipelines of the bioinformatic RNA-Seq analyses. Top, pipeline used on the chromatin-bound (ChrRNA-Seq) and nucleoplasmic RNA-Seq (NpRNA-Seq) data. Bottom, pipeline used on the total 3′ mRNA-Seq data. (B) Scheme showing the consecutive sequencing filters on 3′ mRNA-Seq for identification of true PAS. (C) Scheme showing possible outcomes on PAS choice after stimuli on cells.

- Do not change position of the tube containing beads, or take it out while it sits on the magnetic stand, since it might disrupt both beads and RNA

6.3.1 Total RNA

Timing: 5.5 + 2 h qPCR.

Total RNA libraries for 3′ mRNA-Seq are prepared by first performing mRNA enrichment using oligo (dT)25 Dynabeads. Libraries are prepared using the QuantSeq REV kit, according to manufacturer's instructions. Both protocols are briefly described below.

6.3.2 mRNA enrichment

1. Prepare total RNA for mRNA enrichment:
   a. Use up to 1 μg total RNA as a starting material in 100 μL
      Critical: This kit has a maximum of 75 μg starting total RNA. While the recommended cell quantities will not exceed this amount, it is important to consider it as excess RNA quantities will inhibit final mRNA yield.
   b. Incubate at 65 °C for 2 min
   c. Place the tube immediately on ice
2. Prepare oligo (dT)25 Dynabeads:
   a. Completely resuspend the Dynabeads
   b. Transfer 200 μL of resuspended oligo (dT)25 Dynabeads to a 1.5 mL RNase-free microcentrifuge tube
   c. Place the tube in the magnetic stand for 30 s
   d. Wash beads once with 100 μL of the binding buffer
   e. Keep the tube on the magnetic stand
3. Incubate RNA with oligo (dT)25 Dynabeads:
   a. Add immediately 100 μL of the binding buffer to the oligo (dT)25 Dynabeads
   b. Add denatured RNA to the oligo (dT)25 Dynabead suspension
   c. Mix by pipetting
   d. Rotate at RT for 5 min to allow for annealing of RNA to the oligo (dT) on the Dynabeads
4. Wash and elute pA^+ mRNA:
   a. Place the tube on the magnetic stand
   b. Wait for 30 s until the solution becomes clear
   c. Remove the supernatant
   d. Remove the tube from the magnetic strand
   e. Wash the Dynabeads with 200 μL of washing buffer

f. Place the tube on the magnetic stand
g. Repeat the steps (b–f) once more
Critical: Remove all the supernatant before adding the next buffer (either wash or elution). If needed, tilt the whole system (magnetic stand + tube) at an angle to remove all the liquid phase.
h. Add 10 µL of 10 mM Tris-HCl pH 7.5 to each tube
Critical: mRNA must be eluted through addition of a low-salt buffer.
i. Incubate at 65 °C for 2 min
j. Place the tube on the magnetic stand until the solution becomes clear
k. Transfer the eluted mRNA to a new RNase-free tube
l. Quantify polyA$^+$ mRNA using the Qubit RNA HS kit

Pause point: We recommend not to pause once mRNA is enriched, as the first pause point of the library construction is fairly soon after (see below). As freeze-thaw cycles damage RNA, it is best to pause after RNA conversion to cDNA during the library construction.

6.3.3 Library construction—Enriched mRNA from total RNA using the QuantSeq REV kit from Lexogen

5. First Strand (FS) Synthesis:
a. Add 10–500 ng RNA with 5 µL of FS1 buffer in 0.2 mL microcentrifuge tube. If needed, add RNase-free water up to 10 µL
b. Mix by pipetting

Critical

- Use as much RNA as you can as input (maximum 500 ng), provided the amounts do not vary considerably between samples—e.g., do not synthesize RNA from 10 ng from one sample and 100 ng from the other
- If sample input is 10 ng, consult the manufacturer's instructions to adapt the protocol for low input
- All master mixes should be performed with a 10% surplus to account for pipetting errors

Note: Input RNA must be in a volume lower than 5 µL.

c. Pre-warm a mixture containing 9.5 µL of FS2 and 0.5 µL of E1 at 42 °C
Note: This mixture should be pre-warmed in a thermomixer.
d. Incubate RNA sample tube (step b) at 85 °C for 3 min on the thermocycler
e. Cool down to 42 °C
f. Centrifuge the tube briefly
g. Place the tube on the thermocycler

h. Add 10 µL of pre-warmed FS2 + E1 mixture (step c) into the sample tube (step g).
i. Mix by pipetting
Critical: It is imperative that the temperature of the sample does not lower from 42 °C at this stage, to prevent mishybridization. Therefore, both RNA + FS1 and FS2 + E1 mixes have to be kept at 42 °C at all times.
j. Centrifuge the tube briefly
k. Place the tube on the thermocycler
l. Incubate at 42 °C for 15 min

6. RNA Removal:
a. Centrifuge the tube briefly
b. Add 5 µL of RS solution into the sample tube (step a).
c. Mix well with a pipette set for 15 µL
d. Centrifuge the tube briefly
e. Incubate at 95 °C for 10 min
f. Cool down to 25 °C
g. Centrifuge the tube briefly

7. Second Strand (SS) Synthesis:
Note: The second strand synthesis occurs through binding of Illumina-compatible random primers at the 5′ end of the cDNA sequence.
a. If not pausing, place the beads and purification solution at RT to re-equilibrate, to use at step 8
b. Add 10 µL of SS1 solution to the sample
c. Mix with a pipette set for 30 µL
d. Incubate at 98 °C for 1 min
e. Cool down slowly to 25 °C, setting ramp speed to 0.5 °C/second
Critical: Test your thermocycler for the ramp speed, using a timer if necessary to ensure correct ramp speed at this stage.
f. Incubate at 25 °C for 30 min
g. Prepare a pool containing 4 µL of SS2 and 1 µL of E2 per sample
h. Add 5 µL of the pool to each tube
i. Mix with a pipette set for 30 µL
j. Incubate at 25 °C for 15 min
k. Transfer to a 1.5 mL microcentrifuge tube
Pause point: Unpurified, unamplified dsDNA libraries may be kept at −20 °C overnight or up to a week.

8. First Purification

Critical

- Do not open 1.5 mL microcentrifuge tubes while on the magnetic stand to avoid accidental spillage
- Place a paper tissue over the tubes whenever they are on the magnetic stand, to prevent aerosol contamination
- Prepare 80% EtOH and use it for up to a week to prevent evaporation bringing changes to the protocol

a. Ensure all components are at RT
b. Resuspend purification beads (PB)
c. Spin down sample PCR tube
d. Add 16 µL of resuspended PB to each sample
e. Mix by pipetting
f. Incubate at RT for 5 min
g. Place tubes on the magnetic stand until the solution becomes completely clear
Critical: The manufacturer's protocol mentions this step as taking 2–5 min, but as time depends on the strength of your magnetic stand, this period may vary.
h. Remove and discard supernatant, not disturbing the bead suspension
i. Add 40 µL of EB buffer
j. Remove the tube from the magnetic stand
k. Resuspend beads
l. Incubate at RT for 2 min
m. Add 56 µL of PS solution to the beads and EB mix to reprecipitate library
n. Mix by pipetting
o. Incubate at RT for 5 min
p. Repeat steps (g) and (h).
q. Add 120 µL of freshly made 80% EtOH, and incubate for 30 s to wash
r. Remove and discard supernatant
Critical: Leave tubes in contact with the magnetic stand to avoid resuspending beads, which would lower library yield.
s. Repeat step (q).
t. Remove the supernatant completely
Critical: EtOH traces can inhibit subsequent PCR reactions.
u. Let beads dry at RT until all EtOH is evaporated

Critical: Environmental conditions of your laboratory affect the drying time of beads. While the manufacturer's instructions mention 5–10 min, if your laboratory is particularly dry, this time may be shortened.

v. Add 20 µL of EB buffer into the tube
w. Remove the tube from magnetic stand
x. Resuspend beads
y. Incubate at RT for 2 min
z. Place tube on the magnetic stand
aa. Leave the tube until the solution becomes clear
bb. Transfer 17 µL of clear solution into a new 0.2 mL PCR tube

Pause point: store libraries at −20 °C overnight or up to a week.

9. Calculate exact PCR cycle number

Critical: Differences in cell types, sample conditions and RNA integrity may cause different outcomes. Therefore, optimizing the precise endpoint PCR number of cycles for each sample is mandatory for library construction. For this optimization, the QuantSeq 3′ mRNA-Seq PCR Add-on kit for Illumina kit in the Key Resources Table is required.

a. Add 2 µL EB buffer to the previous 17 µL purified library
b. Dilute Sybr Green I 1:4000 using DMSO. This will be the 2.5 × stock concentration

Critical: Sigma is the only supplier for Sybr Green I recommended by the manufacturer.

c. For each sample, mix 1.7 µL of diluted library + 7 µL PCR + 5 µL 7000 primer + 1 E + 1.2 µL Sybr Green I 2.5 × + 14.1 µL EB buffer. All these reagents, except for Sybr Green I, are included in the PCR Add-on Kit. Add one extra reaction tube for non-template control, substituting the diluted library for EB buffer
d. Perform the following qPCR program:
  i. 98 °C for 30 s
  ii. 35 cycles of 98 °C for 10 s, 65 °C for 20 min, 72 °C for 30 s
  iii. Final extension 72 °C for 1 min
  iv. Hold at 10 °C

Critical: Adjust the emission maximum at 520 nm (Sybr Green I) on the RT-qPCR apparatus if needed.

e. Calculate the number of cycles for the subsequent endpoint PCR, according to the Annex E on manufacturer's protocol (Lexogen QuantSeq Rev). Briefly, obtain the Ct at half of the maximum fluorescence. From the Ct value obtained, subtract 3 Ct values,

as one-tenth of the library has been used. The final Ct value will be the number of cycles needed to amplify each library sample by endpoint PCR (step 10 below).

10. Library amplification:
In this section, libraries are amplified by endpoint PCR to generate enough material for sequencing, after adding complete adapters required for cluster generation and unique indices to each sample to enable multiplexing.
Note: This section will only describe single-indexed libraries (i7). To perform amplification of dual-indexed libraries (i5 and i7), please consult the manufacturer's instructions.
   a. Place the beads and purification solution at RT to re-equilibrate, to use at step 11
   b. Pool 7 µL of PCR and 1 µL of E3 per sample
   c. Add 8 µL of the pool to each of the purified library
   d. Spin down the i7 index plate before opening. Pierce the sealing foil of each desired index with a needle. Add 5 µL of each respective index to each sample. Mix well by pipetting. Seal the opened wells of each i7 index with two layers of parafilm
   Critical: Change needles every time, discarding safely to avoid cross-contamination.
   e. Spin down the tubes. Perform x number of PCR cycles (11 to 22, as determined by step 54), using the following PCR program:
      i. 98 °C for 30 s
      ii. 35 cycles of 98 °C for 10 s, 65 °C for 20 min, 72 °C for 30 s
      iii. Final extension 72 °C for 1 min
      iv. Hold at 10 °C

11. Second Purification: repeat step 8, using 30 µL instead of the recommended volumes of EB and PS, but maintain 20 µL as the final EB addition

6.3.4 Library quality control

After construction, libraries must go through a quality control step. This can be performed at the sequencing facility, but we recommend it is done beforehand, in order not to send unsuitable, under- or overamplified libraries.

We recommend the use of two independent quality control methods: KAPA quantification (via qPCR), to infer library concentration, and a DNA quality chip (e.g., TapeStation), to infer library size.

Libraries are subsequently sequenced with NextSeq500 using Single-End 75-nucleotide reads, a read length needed to precisely map the mRNA 3′ ends. In order to obtain enough reads per sample to identify statistically significant differences in mRNA isoforms between conditions, special attention should be taken not to overmultiplex each library sequencing lane. It is recommended not to go beyond 6 samples of human macrophage RNA-Seq per lane, which allows to achieve at least 42 M reads per sample.

Critical: It is extremely important not to overamplify the libraries, to avoid sequence bias. Therefore, researchers should keep to the number of cycles quantified in the add-on protocol.

6.3.5 Fractionated RNA (nucleoplasmic and chromatin-bound RNA)

Timing: 6 + 2 h at −80 °C.

Fractionated RNA are rRNA-depleted using the Ribo-Zero Gold rRNA removal kit for Human/Mouse/Rat. Sequencing libraries are constructed using the NEBNext Ultra II directional library prep kit for Illumina, according to manufacturer's instructions. Both protocols are briefly described below.

6.3.6 rRNA removal

Ribosomal RNA consists of ~80% of total RNA (Westermann, Gorski, & Vogel, 2012). If left on the RNA sample to be sequenced, most of the sequencing reads will reflect this portion to the detriment of other RNAs.

Critical: Pre-treat your RNA with DNase, according to the manufacturer's protocol.

1. Wash magnetic beads
   a. Leave all required components (beads, RNase-free water, bead resuspension solution) at RT for 30 min
   b. Add 225 µL of beads in a 1.5 mL microcentrifuge tube
   c. Place the tube on magnetic stand and leave for 1 min or until the solution becomes clear
      Critical: As in 3′ mRNA-Seq, the strength of your magnetic stand may alter the incubation times.
   d. Discard the supernatant
   e. Remove the tube from magnetic stand
   f. Add the beads with 225 µL of RNase-free water to wash the beads
   g. Resuspend by vortex

h. Place the tube on magnetic stand and leave for 1 min or until the solution becomes clear
i. Repeat steps (d–h) once
j. Discard the supernatant
k. Remove tube from magnetic stand
l. Add 65 µL of bead resuspension solution
m. Resuspend by vortex
n. Optional step: Add 1 µL of Ribolock RNase inhibitor and mix by pipetting

2. Hybridize probes:
a. Thaw all necessary ingredients on ice
b. Mix up to 2.5 µg RNA with 4 µL of RB buffer, 8 µL of RS solution, and RNase-free water up to 40 µL in total
c. Incubate at 68 °C for 10 min
d. Centrifuge the tube briefly
e. Incubate the reaction mixture at RT for 5 min

3. rRNA removal:
f. Add sample to the washed magnetic beads (65 µL, prepared in 14).
g. Mix thoroughly by vortex for 10 s
h. Incubate the mixture at RT for 5 min
i. Transfer the tube to another heat block and incubate at 50 °C for 5 min
j. Place the tube on the magnetic stand
k. Leave the tube for 1 min or until the solution becomes clear
l. Transfer 90 µL of the supernatant (rRNA-depleted RNA fraction) to a new 1.5 mL microcentrifuge tube

Pause point: samples may be kept overnight at −20 °C or at −80 °C up to a month.

4. rRNA Purification:
m. Add 90 µL of RNase-free water to each sample
n. Add 18 µL $NaCH_3COO$ 3 M and 2 µL glycogen
o. Mix thoroughly by vortex
p. Incubate for 2 h at −80 °C
q. Centrifuge at 4 °C for 20 min at 10000 g
r. Discard the supernatant
s. Wash the pellet with 200 µL of freshly made 70% EtOH
t. Centrifuge the tube at 4 °C for 5 min at 10000 g
u. Discard the supernatant

v. Repeat steps (g)–(i) once
w. Discard the supernatant
x. Air dry at RT for 5 min
y. Dissolve the pellet in 10 μL
z. Quantify the rRNA-depleted RNA using the Qubit RNA HS kit

Pause point: samples may be kept overnight at −80 °C or up to a month.

6.3.7 Library construction—rRNA-depleted fractionated RNA—Using the NEB Next Ultra 2 directional library prep for Illumina

1. RNA Fragmentation and Priming
   Note: Maximum input for this kit is 100 ng rRNA-depleted RNA in a maximum of 5 μL.
   a. Add 5 μL of rRNA-depleted RNA (>100 ng) to 4 μL of FSSB and 1 μL of RP
   b. Mix by pipetting
   c. Spin down the mixture briefly
   d. Incubate for at 94 °C 15 min
   e. Transfer the tube on ice
2. cDNA Synthesis
   a. Add the first strand synthesis mixture, 8 μL of SSR and 2 μL of FSSE
   b. Mix by pipetting
   c. Spin down the reaction mixture briefly
   d. Incubate for 10 min at 25 °C, 15 min at 42 °C and 15 min at 70 °C, hold at 4 °C. Keep lid temperature at 99 °C
   e. Transfer the tube to ice
   f. Add the second strand synthesis mixture, 48 μL of RNase-free water, 8 μL of SSSB, and 4 μL of SSSE
   g. Mix by pipetting
   h. Keep the tube on ice
   Critical: SSSB contains dUTP, which confers strand-specificity to this protocol.
   i. Centrifuge the tube briefly
   j. Incubate for 1 h at 16 °C
3. First purification
   a. Ensure all components of the purification module are completely thawed before start the following steps
   b. Resuspend magnetic beads by vortex

c. Transfer libraries to 1.5 mL microcentrifuge tubes and add 144 µL of the magnetic beads
d. Mix them thoroughly by vortex
e. Incubate for 5 min at RT
f. Centrifuge the tube briefly
g. Place tube on the magnetic stand
h. Incubate for 1 min or until the solution becomes clear
i. Carefully discard the supernatant without disturbing the beads
j. Add 200 µL of freshly made 80% EtOH at RT
k. Leave for 30 s
l. Discard supernatant
Critical: always leave tubes in contact with the magnet to avoid resuspending beads, which would lower library yield.
m. Repeat steps (j)–(l) once
n. Air dry beads at RT for 5 min on the magnetic stand
o. Remove tube from magnetic stand
p. Elute DNA by adding 53 µL of RNase-free water
q. Mix them by vortex
r. Centrifuge the tube briefly
s. Incubate for 2 min at RT
t. Place the tube on magnetic stand and leave until the solution becomes clear
u. Transfer 50 µL of the supernatant to a new 0.2 mL microcentrifuge tube

4. End prep and adaptor ligation:
a. Keep RNA sample on ice
b. Add 7 µL of EPB and 3 µL of EPE to the sample
c. Mix them with a pipette set to 50 µL
d. Centrifuge the tube briefly
e. Incubate for 30 min at 20 °C and 30 min at 65 °C, hold at 4 °C. Keep lid temperature at 99 °C on the thermal cycler
f. Dilute sequencing adaptor in ice-cold dilution buffer (5-fold dilution for high input, 25-fold for 1–10 ng initial RNA). Keep on ice
g. Add 2.5 µL diluted adaptor, 1 µL of LE and 30 µL of LMM
h. Mix them with a pipette set to 80 µL
i. Centrifuge the tube briefly
j. Incubate at 20 °C for 15 min
k. Add 3 µL of USER enzyme to the ligation mixture
l. Mix them with a pipette set to 80 µL

m. Incubate the reaction mixture at 37 °C for 15 min. Keep lid temperature at 99 °C on the thermal cycler

5. Second library purification: repeat step 20. Use 87 μL of magnetic beads and incubate for 10 min. Elute RNA sample with 32 μL of RNase-free water. Transfer 30 μL of eluted sample to a new 0.2 mL microcentrifuge tube for the following PCR amplification
6. Library PCR amplification:
   Note: as with 3′ mRNA-Seq, we will describe single-indexed library prep.
   a. Divide the 30 μL library into two fractions. Keep the remaining half at −20 °C in case of mishandling such as over amplification
   b. Mix 15 μL of the RNA sample, 25 μL of Q5 MM, 5 μL of universal i5 primer, and 5 μL index i7 primer
   c. Mix them by pipetting
   d. Perform the following PCR program, keeping lid temperature set to 105 °C on the thermal cycler:
      1. °C for 30 s (Initial denaturation)
      2. 7 cycles (for 100 ng input RNA) of 98 °C for 10 s, 65 °C for 75 s
      3. 65 °C for 5 min (Final extension)
      4. Hold at 4 °C
7. Third library purification: repeat step 20. Use 45 μL of magnetic beads. Elute libraries with 23 μL of RNase-free water. Transfer 20 μL of the PCR sample to a new 0.2 mL microcentrifuge tube

6.3.8 Library quality control

Libraries *should* be subject to a quality control step before proceeding. This can be performed at the sequencing facility, but we recommend it is done beforehand in order not to send unsuitable, under- or overamplified libraries.

We recommend the use of two independent quality control methods: KAPA quantification (via qPCR), to infer library concentration, and a DNA quality chip (e.g., TapeStation and Bioanalyzer), to infer library size.

Sequence the libraries in a HiSeq2000 using Paired-End 42 base pairs, a read length needed to determine sense and antisense RNA from fractionated samples. In order to obtain enough reads per sample to identify statistically significant differences in gene expression in subcellular fractionated RNA in several macrophage conditions, special attention should be taken not to overmultiplex each library sequencing lane. It is recommended not to go

beyond 6 samples of human macrophage RNA-Seq per lane, which allows for obtaining at least 66 M paired-end reads per sample.

Critical: It is extremely important not to overamplify the libraries, to avoid sequence bias. Therefore, keep to the number of cycles recommended on the manufacturer's instructions (NEBNext Ultra 2 directional kit for Illumina). If libraries are overamplified, you need to repeat the protocol starting from step 23.

It is crucial to mention that changes to the polarization stimuli of macrophages may give rise to dramatically different RNA-Seq results.

6.4 Bioinformatics pipeline

Timing: 28 h for preliminary analysis, but variable depending on number of samples and computational power.

Pipelines are shown on Fig. 5A and B.

As in library construction, bioinformatics pipeline for sequencing data analyses differs between total and fractionated RNA samples. However, some steps are common and hence will only be described once. This pipeline is mostly performed on the command line, but it is also possible to perform the same steps in platforms such as Galaxy of Bioconductor. For ease of explanation, code excerpts will be used to exemplify some steps.

Critical

- You must use the same human genome version and release as reference for the whole sequencing project
- Any changes made to the following pipelines or to software versions may generate distinct data

6.4.1 Chromatin-bound and nucleoplasm RNA-Seq (paired-end)

1. Sequencing QC was performed using FastQC
   Note: Pay attention to the per base sequence quality and adapter dimer contamination. High levels of the former (score >30) and low levels of the latter (adaptor content <2%) are indicative of high-quality reads.
2. Remaining adapters were trimmed with Cutadapt, removing low-quality reads under 10 bases, using the following code:
   ```
   cutadapt -minimum-length 10 -q 15,10 -a adaptersequence_Fwd -A
   adaptersequence_Rev -o rawfile_read1_trimmed.fastq.gz -p rawfile_
   read2_trimmed.fastq.gz rawfile_read1.fastq.gz rawfile_read2.fastq.gz
   ```
3. Trimmed data were aligned to the reference human genome using TopHat2, with Bowtie2 indexes

Notes

- In this step, we recommend to allow for read pairs to be separated by up to 3 kb (chromatin-bound) and up to 200 bp (nucleoplasm) and only one alignment to the reference genome for each read
- Aligned read mapping rate should be high at this stage (~90%).

```
tophat2 -r 3000 -g 1 -a 5 -library-type fr-firststrand --no-coverage-search -o/path/to/index rawfile_read1_trimmed.fastq.gz rawfile_read2_trimmed.fastq.gz
```

(for Chromatin-bound)

```
tophat2 -r 200 -g 1 -a 5 -library-type fr-firststrand --no-coverage-search -o/path/to/index rawfile_read1_trimmed.fastq.gz rawfile_read2_trimmed.fastq.gz
```

(for Nucleoplasm)

4. Process aligned read pairs with SAMtools (Li, Handsaker, Wysoker, et al., 2009). Index the bam files with SAMtools index. Call the total number of mapped reads using SAMtools idxstats. Every sample was normalized by dividing by 100×10^6 reads

   Critical: Samples were mapped in proper orientation and strand-specific.

5. Sort samples with SAMtools sort and create bedgraph using Bedtools with the following code:

```
bedtools genomecov -ibam mappedfile_read1_strand+.sorted.bam -bg -scale #readsby100M -split > mappedfile_read1_strand+.bedGraph
```

Bigwig files can be created from the bedgraph files with the bedGraphToBigWig tool and a file containing the chromosome sizes of the genome version used (both accessible from the UCSC genome browser):

```
bedGraphToBigWig mappedfile_read1_strand+.bedGraph hg3b.chrom.sizes mappedfile_strand+.bw
```

6. Count reads with htseq-count using the following code:

```
htseq-count -f bam -s yes -r name -t exon mappedfile_read1_strand+.sorted.bam Homo_sapiens.GRCh38.90.chr+.gtf > mappedfile_read1_strand+_ht.txt
```

After obtaining gene counts, all sample replicates must be compared through a correlation matrix, to ensure reproducibility. A representative example is shown on Fig. 6A and B. Alternatively, a Principal Component Analysis (PCA) graph may instead be produced. Subsequently, gene expression studies are performed in the fractionated samples (see Section 6.5.1).

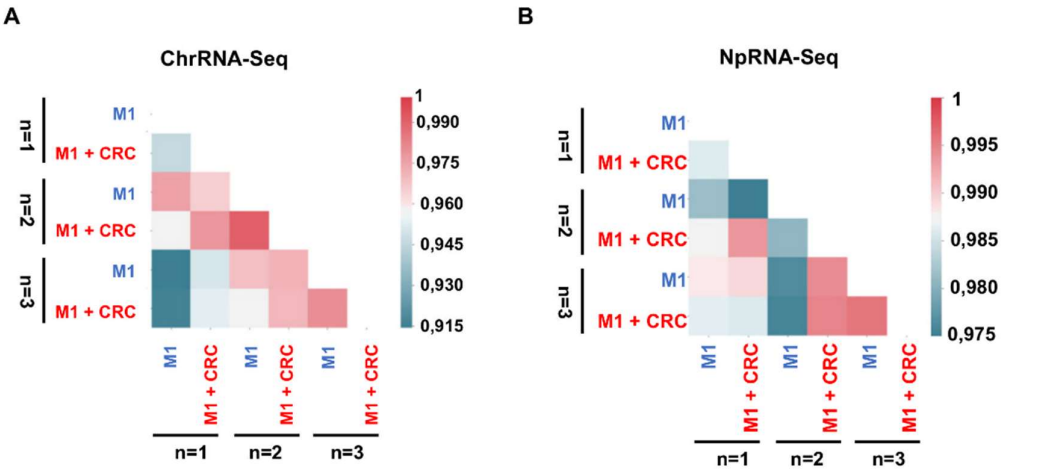


Fig. 6 (A and B) Heatmap of Pearson correlation coefficients for 3′ RNA-Seq, using transcript counts per million (CPM) on chromatin-bound RNA-Seq data (A) or nucleoplasmic RNA-Seq data (B) performed with three different blood donors; 0 means total lack of correlation, while 1 means total correlation.

Joana Wilton | PhD thesis

6.4.2 3′ mRNA-Seq (single read)

The first optional step to analyze 3′ mRNA-Seq data is to identify the true used PAS, which is performed sequentially. Due to possible leakiness in PAS detection, 3′ mRNA-Seq results were filtered by the sequencing company.

Briefly, the input fastq file was mapped to the reference and 3 filters were applied in sequence in the pipeline shown on Fig. 5B:

(1) a Transcript Termination Site (TTS) filter, taking out transcripts not lying within ~10 nt of an annotated transcript end site;

(2) a Motif filter removed all sequencing peaks whose read start contained a subset of hexamer sequences upstream (Livak & Schmittgen, 2001);

(3) a downstream A content filter checked the amount of As in a window downstream of the read start. If a given peak passed the validated threshold, the read was considered internal priming and was removed.

All reads passing the three consecutive filters were retained as non-internal priming and put into subsequent differential expression and alternative mRNA isoform analyses.

7. The sequencing QC is performed similarly to the paired-end data, as is cutadapt, with the following adaptations due to the single read format:

```
cutadapt -minimum-length 10 -q 10 -a adaptersequence -o rawfile_
trimmed.fastq.gz rawfile.fastq.gz
```

8. Trimmed data were aligned using STAR aligner using the same genome build as for chromatin and nucleoplasm RNA-Seq. Aligned read mapping rate is lower due to the library used, but should exceed 75%.

```
STAR -runThreadN 8 -genomeDir/path/to/index -readFilesIn/path/to/
sample/rawfile_trimmed.fastq.gz -readFilesCommand zcat -outFile
NamePrefix/path/to/sample/mappedfile.bam
```

9. Aligned reads were also processed using SAMtools, and reads were counted with htseq-count:

```
htseq-count -f bam -r name -s reverse -r mappedfile_read1_strand.
sorted.bam Homo_sapiens.chr.gtf > mappedfile_read1_strand_ht.txt
```

Subsequently, gene expression and mRNA APA isoform analyses are performed.

6.5 Gene expression analyses of the RNA-Seq results

6.5.1 Differential gene expression

Differences in gene expression were calculated using DESeq2. To detect true gene expression, differentially expressed genes were followed up if their

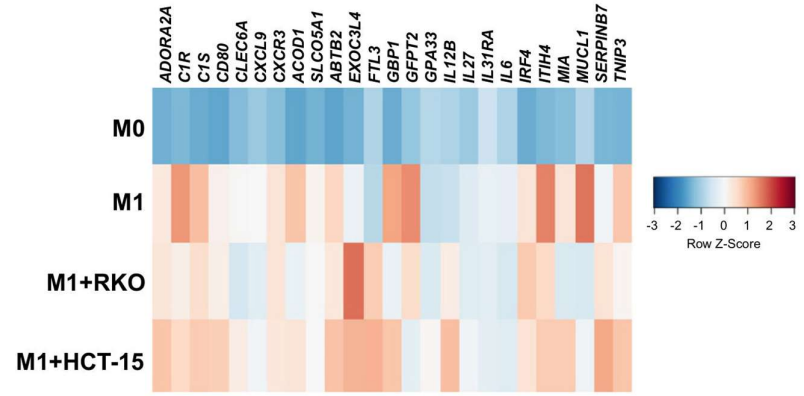


Fig. 7 Heatmap of a representative donor, showing differentially expressed genes (DEGs) in M0, M1 and M1 macrophages co-cultured with RKO or HCT-15 cell lines.

transcripts per million (TPM) are >5 mean TPM, Log2Fold Changes greater than 1 or smaller than −1, and adjusted *p*-value <0,05, calculated by DESeq2 (Love, Huber, & Anders, 2014).

A representative example of results is represented in Fig. 7, showing a heatmap of statistically significant differentially expressed genes in M0, M1, and M1 macrophages co-cultured with two different CRC cell lines (RKO and HCT-15).

6.5.2 Differential expression of APA mRNA isoforms

Differences in the expression of mRNA isoforms due to APA were calculated using DEXSeq (Love et al., 2014) in the 3′ mRNA-Seq data, with the Galaxy pipeline. Firstly, sorted bam files were subjected to DEXSeq-count, to count the sequencing reads associated with each PAS—and hence each mRNA isoform. Afterwards, DEXSeq-Count files were compared between each condition, and the resulting table was organized by corrected p-value, to identify genes in which at least one mRNA isoform varied with statistical significance.

Alternative polyadenylation was considered to be present when two or more alternative 3′ UTRs (depicted in Fig. 5C) were expressed, and when the second highest mRNA isoform level was at least 10% of the highest isoform in at least two replicates.

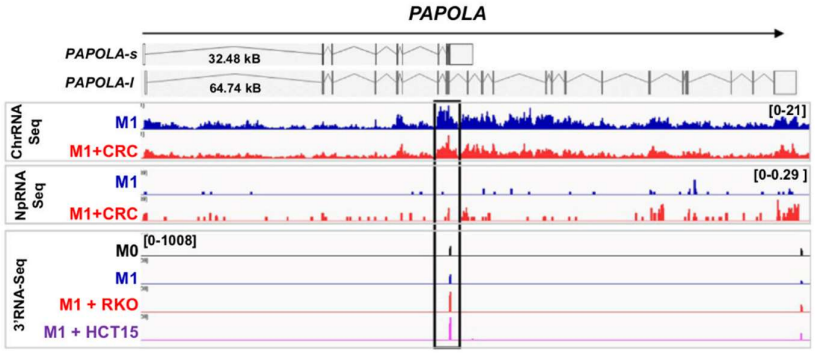


Fig. 8 IGV gene profiles and transcript counts of *PAPOLA*. Data obtained through ChrRNA-Seq (top), NpRNA-Seq (middle) and 3′ mRNA-Seq (bottom) of macrophages, M1 macrophages cultured alone and co-cultured with the CRC cell lines RKO or HCT-15.

A representative example of results is represented in Fig. 8, showing *PAPOLA* (Poly(A) Polymerase gene) gene counts and mRNA isoform differences between macrophage conditions.

6.5.3 RT-qPCR validation of the RNA sequencing data

Total RNA was digested with DNase I (Ref. EN0521, Roche) for 25 min at 37 °C, inactivating the enzyme for 10 min at 80 °C. RNA was reverse transcribed using SuperScript IV (Ref. 18,090,010, ThermoFisher) and random hexamers, according to manufacturer's instructions and above. RT-qPCR reactions were performed in triplicate using SYBR Select Master Mix (Ref. 4,472,908, Applied Biosystems) and 0.125 µM of primers, using the following protocol:

(a) Hold 20 s at 20 °C
(b) Incubate 10 min at 95 °C
(c) 40 cycles of 15 s at 95 °C and 1 min at 60 °C
(d) Perform melt curve by incubating for 15 s at 95 °C, 1 min at 60 °C and until 95 °C with a slope of 1%, 20 s each

A representative example of results is represented in Fig. 9, showing *RAC1* (Ras-related C3 botulinum toxin substrate 1 gene) gene counts and mRNA isoforms (Fig. 9A) and validation by RT-qPCR (Fig. 9B and C) in M1 macrophages.

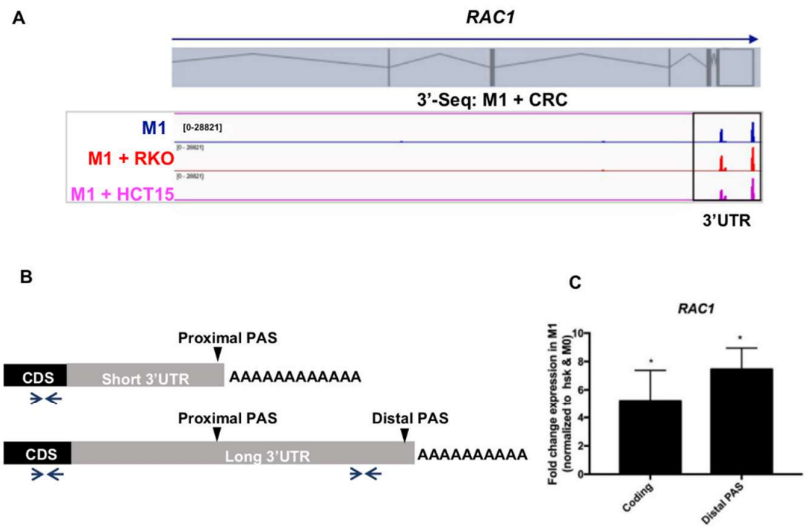


Fig. 9 (A) IGV gene profiles and transcript counts of *RAC1*. Data obtained through ChrRNA-Seq (top), NpRNA-Seq (middle) and 3′ mRNA-Seq (bottom) of M0 macrophages, M1 macrophages cultured alone and co-cultured with the CRC cell lines RKO or HCT-15. (B) Schematic representation of the primers used in RT-qPCR validation of 3′ RNA-Seq data. (C) Fold change of the coding region and the long 3′ UTR isoform (distal PAS) of the *RAC1* gene in M1 vs. M0 macrophages.

7. Concluding remarks

Studying the transcriptome of macrophages interacting with cancer cells and other components of the tumor microenvironment is crucial to better understand immune evasion. RNA-Seq data on primary human macrophages co-cultured with CRC thus allows for the development of more efficient diagnostic and therapeutic tools. Isolating macrophages from healthy donors, exposing them to inflammatory stimuli conditions and co-culturing them indirectly with cancer cells mimics the macrophage-cancer cell crosstalk that occurs in the colon. This model system is ideal for transcriptomic studies, bypassing the difficulty of isolating primary immune cells from the stroma of colorectal tumors. Importantly, our primary human macrophages closely mimic the microenvironment to which the macrophages are subject, which would not be the case if monocytic cell lines such as THP-1 were used, which do not share embryonic progenitors nor transcriptomic profiles (Tedesco, De Majo, Kim, et al., 2018).

With the co-cultures with cancer cells and human primary macrophages homogenously polarized to M1 inflammatory populations, and the use of Chromatin-bound RNA-Seq, Nucleoplasm RNA-Seq and 3′ mRNA-Seq methodologies and dedicated bioinformatics, we are able to characterize precisely APA mRNA isoform profiles and quantify gene expression changes in a highly plastic immune cell population from the same human donor. By quantifying the statistical significance of the mRNA isoform changes between conditions, we observed that different genes display different APA profiles and that CRC cells modulate macrophage APA.

The described protocol is a low-cost, big data approach for transcriptomic studies adapted to the need and budget of research laboratories, and particularly in the macrophage—CRC model system. This protocol requires low quantities of primary macrophages to obtain simultaneously nuclear and total RNA for sequencing and analyse differential gene expression, as well as identify novel APA mRNA isoforms, in Illumina-compatible systems. Using this methodology a thorough, unbiased transcriptomic characterization of plastic immune cells in a relevant pathophysiologic context is achieved. Furthermore, with this method we can identify genome-wide APA mRNA signatures with important roles in immune responses that may serve as potential diagnostic and therapeutic targets, using relatively few macrophage cells. With subsequent siRNA depletion of genes with functions in gene expression regulation may lead to the identification of the molecular mechanisms involved.

In conclusion, our method provides a basis for a comprehensive transcriptomic analyses using co-cultures of primary human macrophages with cancer cells (Supplementary Fig. S1 in the online version at https://doi.org/10.1016/bs.mie.2021.04.004).

8. Safety considerations

Chloroform, HCl, Isopropanol, PFA, and TRIzol reagent are dangerous. Manipulate them in the chemical hood using gloves and eyeglasses. If exposed, thoroughly wash skin in running water.

9. Expected outcomes

This protocol presents an integrated approach to study gene expression and alternative polyadenylation events. It accurately determines true APA isoforms, due to comparison of subcellular fractionated RNA-Seq

(chromatin-bound RNA and nucleoplasm RNA) and whole-cell 3′ mRNA-Seq. Therefore, researchers are able to distinguish accurate APA mRNA isoforms produced in the nucleus, from the cytoplasmic mRNA isoforms, which may be subjected to modulation by miRNAs and RNA binding proteins.

Raw sequencing data by 3′ mRNA-Seq, chromatin-bound RNA-Seq and nucleoplasm RNA-Seq can be converted into differential gene expression in macrophage populations. Chromatin-bound and nucleoplasm RNA-Seq approaches further inform researchers of regulatory RNAs such as long non-coding RNA and antisense transcripts genome-wide.

Globally, the RNA sequencing data obtained using this protocol reveals transcriptomic profiles relevant for the innate immune system and for anti-tumoral therapy studies, as it pinpoints gene expression alterations occurring in primary human macrophages.

Timing: full protocol

Isolation of PBMCs from human peripheral blood and $CD14^+$ enrichment: 8 h.

Differentiation of macrophages from $CD14^+$ cells and inflammatory polarization: 2 h + 6 days incubation.

Macrophage and Colorectal cancer co-cultures: 3 + 24 h incubation.

Macrophage and CRC Immunofluorescence: 6 h (staining) + ∼2 h (imaging).

Macrophage siRNA transfection: 2 + 48 h incubation.

Total RNA isolation: 4 + 16 h incubation at −80 °C.

Fractionated RNA isolation: 8 + 16 h precipitation time.

Total RNA library construction: 5.5 + 2 h qPCR.

Fractionated RNA library construction: 6 + 2 h at −80 °C.

Bioinformatics: 28 h.

10. Quantification and statistical analysis

Statistical analyses for bioinformatics were performed using the following tests:

- DESeq2: *p*-value calculated with the Wald test, adjusted using Benjamini-Hochberg False Discovery Rate (FDR), selecting for padj <0.05
- DEXSeq: *p*-value calculated with the LRT test, adjusted using Benjamini-Hochberg False Discovery Rate (FDR), selecting for padj <0.05

Differentially expressed genes selected for validation by RT-qPCR should have a large differential gene expression fold differences (>2 Fold Change (FC)) between mono and co-culture in all donors. This criteria is applied to identify non-random transcriptomic changes with potential physiological consequences.

For APA analysis, mRNA isoforms with differential expression between conditions were validated by RT-qPCR using two sets of primer pairs as described, one pair for the coding region and another for the distal PAS. Relative expression was calculated using the reference gene *18S* (Fwd: 5′-GCAGAATCCACGCCAGTACAAGA-3′; Rev.: 5′-CCCTCTAT GGGCCCGAATCTT-3′) and results were analyzed applying the ΔΔCt method.

Statistical analyses for qPCR were performed using GraphPad Prism Software version 7. Presented data is shown as mean ± standard deviation (SD). Comparison between two independent groups was performed with the Student's *t*-test. *P*-values below 0.05 were considered statistically significant ($* = p < 0.05$).

11. Advantages

This approach allows for the simultaneous study of fractionated and total RNA of primary human macrophages. Moreover, true APA mRNA isoforms identification and differential gene expression results are obtained in the same human donor due to this integrative protocol.

Primary human macrophages are successfully polarized to the extremes of the inflammatory spectrum (M1, M2), and researchers will obtain homogenous populations able to survive ex-vivo for up to 10 days.

The establishment of the co-culture system allows for the sequencing of both cell populations—macrophages and cancer cells—if desired, allowing researchers to obtain reciprocal transcriptomic signatures and to further characterize their model system.

The use of RNA molecules present in different cellular compartments for each sequencing method (ChrRNA-Seq, NpRNA-Seq, cytoplasmic RNA-Seq) is achieved by subcellular fractionation, which is validated by independent techniques (*MALAT1* expression by RT-qPCR). Ribosomal RNA removal and mRNA enrichment ensures that the libraries are made with the RNA fractions of interest.

Additionally, the whole protocol is easily scaled-up to include more inflammatory conditions, increased input for sequencing, and includes crucial quality control stages at each step to ensure robust and high-quality data.

12. Limitations

This approach does not enable the identification of ribosomal RNAs from primary human macrophages. Therefore, transcriptomic studies to identify protein translation regulators, which are relevant for inflammation (Poddar et al., 2013), should follow a different approach when selecting macrophage rRNA for sequencing libraries.

This protocol recommends avoiding excessive multiplexing of samples. We favor increasing the number of sequencing runs if possible to avoid the risk of lowering sequencing read per sample. But if many macrophage replicates and conditions are needed, the cost of sequencing will increase.

We recommend the selection of blood donors below 40 years old, due to a decreased risk of hematological malignancies or chronic anti-inflammatory utilization by the donor, which may interfere with the results.

13. Optimization and troubleshooting

13.1 Problem and solution

$CD14^+$ cells are non-adherent—Use fresh M-CSF for macrophage isolation.

Heterogeneous macrophage polarization—control LPS, IFNγ, and IL-10 lots. Additionally, add these regents when macrophages are adherent and sufficiently differentiated with M-CSF, and keep the polarization RPMI media 2% FBS without antibiotics.

Low amounts of RNA are present by the end of RNA isolation—This may be due to RNA degradation or low amount of RNA due to a small number of macrophages. Therefore, use RNase-free reagents on the whole procedure or use more cells as starting material.

No PCR product is obtained at the end of library construction—PCR products are underamplified, hence we suggest to use higher PCR cycle numbers, or higher RNA input for the library.

PCR products are longer than expected (450 bp on QuantSeq Rev. 300 bp on NEB Next)—PCR products are overamplified, therefore we suggest to reduce PCR cycle number and to restart library construction.

Matrix correlation data or heatmap showing differences between replicates and/or gene expression results and APA mRNA isoforms are too variable—This indicates intrinsic donor variability. Therefore, the number of biological replicates should be increased.

Ethical statement

Buffy coats isolated in accordance with the Ethics Committee protocol of Centro Hospitalar Universitário São João (CHUJ) (90/19) consist of waste products of healthy anonymized blood donations containing high amounts of leukocytes. Donors filled informed consent prior to each donation, and their identity was archived exclusively at CHUJ.

Acknowledgments

We thank members of the Gene Regulation, Cell Activation and Gene Expression, and Tumor and Microenvironment Interactions laboratories at i3S, and Nick Proudfoot and Shona Murphy laboratories at the Sir William Dunn School of Pathology, University of Oxford, for critical and fruitful discussions of this work. This work was supported by the Fundação para a Ciência e Tecnologia (FCT) by funding to AM (FEDER—Fundo Europeu de Desenvolvimento Regional funds through the COMPETE 2020—POCI/Portugal 2020 and POCI-01-0145-FEDER-007274 projects), by Norte-01-0145-FEDER-000051—"Cancer Research on Therapy Resistance: From Basic Mechanisms to Novel Targets," supported by Norte Portugal Regional Operational Programme (NORTE 2020), under the PORTUGAL 2020 Partnership Agreement, through the European Regional Development Fund (FEDER) and by PhasAge. This project has received funding from European Union's Horizon 2020 research and innovation program under grant agreement No 952334. J.W. was supported by studentships from FCT (PD/BD/114168/2016) and (H2020-NMP-PILOTS-2015-683356-FOLSMART). The authors acknowledge Centro Hospitalar Universitário São João—Immunohemotherapy Department for their kind buffy coats donations, and the i3S Bioimaging (María Lázaro, PPBI-POCI-01-0145-FEDER-022122), and Scientific Genomics Platforms (Mafalda Rocha and Rob Mensink).

Author contributions

J.W., M.J.O., and A.M. designed the project; J.W., A.M.C., M.T., T.N., M.J.O. and A.M. wrote the paper.

References

Berkovits, B. D., & Mayr, C. (2015). Alternative 3′ UTRs act as scaffolds to regulate membrane protein localization. *Nature*, *522*(7556), 363–367. https://doi.org/10.1038/nature14321.

Braz, S. O., Cruz, A., Lobo, A., et al. (2017). Expression of Rac1 alternative 3′ UTRs is a cell specific mechanism with a function in dendrite outgrowth in cortical neurons. *Biochimica et Biophysica Acta, Gene Regulatory Mechanisms*, *1860*(6), 685–694. https://doi.org/10.1016/j.bbagrm.2017.03.002.

Brooks, B. M., Hart, C. A., & Coleman, J. W. (2005). Differential effects of β-lactams on human IFN-γ activity. *The Journal of Antimicrobial Chemotherapy*, *56*(6), 1122–1125. https://doi.org/10.1093/jac/dki373.

Castello, A., Fischer, B., Eichelbaum, K., et al. (2012). Insights into RNA biology from an atlas of mammalian mRNA-binding proteins. *Cell*, *149*(6), 1393–1406. https://doi.org/10.1016/j.cell.2012.04.031.

Derti, A., Garrett-Engele, P., MacIsaac, K. D., et al. (2012). A quantitative atlas of polyadenylation in five mammals. *Genome Research*, *22*(6), 1173–1183. https://doi.org/10.1101/gr.132563.111.

Dye, M. J., & Proudfoot, N. J. (1999). Terminal exon definition occurs cotranscriptionally and promotes termination of RNA polymerase II. *Molecular Cell*, *3*(3), 371–378. https://doi.org/10.1016/S1097-2765(00)80464-5.

Herrmann, C. J., Schmidt, R., Kanitz, A., Artimo, P., Gruber, A. J., & Zavolan, M. (2020). PolyASite 2.0: A consolidated atlas of polyadenylation sites from 3′ end sequencing. *Nucleic Acids Research*, *48*(D1), D174–D179. https://doi.org/10.1093/nar/gkz918.

Ji, Z., Lee, J. Y., Pan, Z., Jiang, B., & Tian, B. (2009). Progressive lengthening of 3′ untranslated regions of mRNAs by alternative polyadenylation during mouse embryonic development. *Proceedings of the National Academy of Sciences of the United States of America*, *106*(17), 7028. https://doi.org/10.1073/pnas.0905246106.

Jia, X., Yuan, S., Wang, Y., et al. (2017). The role of alternative polyadenylation in the antiviral innate immune response. *Nature Communications*, *8*, 14605. https://doi.org/10.1038/ncomms14605.

Lee, S. H., Singh, I., Tisdale, S., Abdel-Wahab, O., Leslie, C. S., & Mayr, C. (2018). Widespread intronic polyadenylation inactivates tumour suppressor genes in leukaemia. *Nature*, *561*(7721), 127–131. https://doi.org/10.1038/s41586-018-0465-8.

Lerman, M. J., Lembong, J., Muramoto, S., Gillen, G., & Fisher, J. P. (2018). The evolution of polystyrene as a cell culture material. *Tissue Engineering. Part B, Reviews*, *24*(5), 359–372. https://doi.org/10.1089/ten.teb.2018.0056.

Li, H., Handsaker, B., Wysoker, A., et al. (2009). The sequence alignment/map format and SAMtools. *Bioinformatics*, *25*(16), 2078–2079. https://doi.org/10.1093/bioinformatics/btp352.

Livak, K. J., & Schmittgen, T. D. (2001). Analysis of relative gene expression data using real-time quantitative PCR and the 2-ΔΔCT method. *Methods*, *25*(4), 402–408. https://doi.org/10.1006/meth.2001.1262.

Locati, M., Mantovani, A., & Sica, A. (2013). Macrophage activation and polarization as an adaptive component of innate immunity. *Advances in Immunology*, *120*, 163–184. https://doi.org/10.1016/B978-0-12-417028-5.00006-5.

Love, M. I., Huber, W., & Anders, S. (2014). Moderated estimation of fold change and dispersion for RNA-seq data with DESeq2. *Genome Biology*, *15*(12), 1–21. https://doi.org/10.1186/s13059-014-0550-8.

Ma, W., & Mayr, C. (2018). A membraneless organelle associated with the endoplasmic reticulum enables 3′UTR-mediated protein-protein interactions. *Cell*, *175*(6), 1492–1506. e19. https://doi.org/10.1016/j.cell.2018.10.007.

Mantovani, A., & Locati, M. (2013). Tumor-associated macrophages as a paradigm of macrophage plasticity, diversity, and polarization lessons and open questions. *Arteriosclerosis, Thrombosis, and Vascular Biology*, *33*(7), 1478–1483. https://doi.org/10.1161/ATVBAHA.113.300168.

Mayr, C. (2017). Regulation by 3′–untranslated regions. *Annual Review of Genetics*, *51*(1), 171–194. annurev-genet-120116-024704 https://doi.org/10.1146/annurev-genet-120116-024704.

Mayr, C., & Bartel, D. P. (2009). Widespread shortening of 3′UTRs by alternative cleavage and polyadenylation activates oncogenes in cancer cells. *Cell*, *138*(4), 673–684. https://doi.org/10.1016/j.cell.2009.06.016.

Mitra, M., Johnson, E. L., & Coller, H. A. (2016). Alternative polyadenylation can regulate post-translational membrane localization. *Trends in Cell & Molecular Biology*, *10*, 37–47.

Nojima, T., Gomes, T. T., Carmo-Fonseca, M., & Proudfoot, N. J. (2016). Mammalian NET-seq analysis defines nascent RNA profiles and associated RNA processing genome-wide. *Nature Protocols*, *11*(3), 413–428. https://doi.org/10.1038/nprot.2016.012.

Nojima, T., Gomes, T., Grosso, A. R. F., et al. (2015). Mammalian NET-seq reveals genome-wide nascent transcription coupled to RNA processing. *Cell*, *161*(3), 526–540. https://doi.org/10.1016/j.cell.2015.03.027.

Ohradanova-Repic, A., Machacek, C., Fischer, M. B., & Stockinger, H. (2016). Differentiation of human monocytes and derived subsets of macrophages and dendritic cells by the HLDA10 monoclonal antibody panel. *Clinical & Translational Immunology*, *5*(1). https://doi.org/10.1038/cti.2015.39, e55.

Oida, T., & Weiner, H. L. (2010). Depletion of TGF-β from fetal bovine serum. *Journal of Immunological Methods*, *362*(1–2), 195–198. https://doi.org/10.1016/j.jim.2010.09.008.

Pai, A. A., Baharian, G., Pagé Sabourin, A., et al. (2016). Widespread shortening of 3′ untranslated regions and increased exon inclusion are evolutionarily conserved features of innate immune responses to infection. *PLoS Genetics*, *12*(9), 1–24. https://doi.org/10.1371/journal.pgen.1006338.

Poddar, D., Basu, A., Baldwin, W. M., Kondratov, R. V., Barik, S., & Mazumder, B. (2013). An Extraribosomal function of ribosomal protein L13a in macrophages resolves inflammation. *Journal of Immunology*, *190*(7), 3600–3612. https://doi.org/10.4049/jimmunol.1201933.

Rostam, H. M., Singh, S., Salazar, F., et al. (2016). The impact of surface chemistry modification on macrophage polarisation. *Immunobiology*, *221*(11), 1237–1246. https://doi.org/10.1016/j.imbio.2016.06.010.

Sandberg, R., Neilson, J. R., Sarma, A., Sharp, P. A., & Burge, C. B. (2008). Proliferating cells express mRNAs with shortened 3′ UTRs and fewer microRNA target sites. *Science*, *320*(5883), 1643–1647. https://doi.org/10.1126/science.1155390.Proliferating.

Shi, Y. (2012). Alternative polyadenylation: New insights from global analyses. *RNA*, *18*(12), 2105–2117. https://doi.org/10.1261/rna.035899.112.

Suganuma, H., Fahey, J. W., Bryan, K. E., Healy, Z. R., & Talalay, P. (2011). Stimulation of phagocytosis by sulforaphane. *Biochemical and Biophysical Research Communications*, *405*(1), 146–151. https://doi.org/10.1016/j.bbrc.2011.01.025.

Tedesco, S., De Majo, F., Kim, J., et al. (2018). Convenience versus biological significance: Are PMA-differentiated THP-1 cells a reliable substitute for blood-derived macrophages when studying in vitro polarization? *Frontiers in Pharmacology*, *9*(FEB), 1–13. https://doi.org/10.3389/fphar.2018.00071.

Tian, B., Hu, J., Zhang, H., & Lutz, C. S. (2005). A large-scale analysis of mRNA polyadenylation of human and mouse genes. *Nucleic Acids Research*, *33*(1), 201–212. https://doi.org/10.1093/nar/gki158.

Tian, B., & Manley, J. L. (2016). Alternative polyadenylation of mRNA precursors. *Nature Reviews. Molecular Cell Biology*, *18*(1), 18–30. https://doi.org/10.1038/nrm.2016.116.

Wang, E. T., Sandberg, R., Luo, S., et al. (2008). Alternative isoform regulation in human tissue transcriptomes. *Nature*, *456*(7221), 470–476. https://doi.org/10.1038/nature07509.

Westermann, A. J., Gorski, S. A., & Vogel, J. (2012). Dual RNA-seq of pathogen and host. *Nature Reviews. Microbiology*, *10*(9), 618–630. https://doi.org/10.1038/nrmicro2852.

Wurth, L., & Gebauer, F. (2015). RNA-binding proteins, multifaceted translational regulators in cancer. *Biochimica et Biophysica Acta, Gene Regulatory Mechanisms*, *1849*(7), 881–886. https://doi.org/10.1016/j.bbagrm.2014.10.001.

Zhang, X., Hamblin, M. H., & Yin, K. J. (2017). The long noncoding RNA Malat1: Its physiological and pathophysiological functions. *RNA Biology*, *14*(12), 1705–1714. https://doi.org/10.1080/15476286.2017.1358347.

Zhang, F., Wang, H., Wang, X., et al. (2016). TGF-β induces M2-like macrophage polarization via SNAILmediated suppression of a pro-inflammatory phenotype. *Oncotarget*, 7(32), 52294–52306. https://doi.org/10.18632/oncotarget.10561.

3.2 *Proximity to colorectal cancer cells modulates macrophage alternative polyadenylation*

Paper in revision.

Joana Wilton[1-3], Michael Tellier[4], Takayuki Nojima[4, *], Isabel Pereira-Castro[2,3], Angela M Costa[5,6], Jaime Freitas[6,&], Ricardo Pinto[7], Luísa Pereira[7], Shona Murphy[4], Maria Jose Oliveira[5,6,8], Nicholas J Proudfoot[4], Alexandra Moreira[2,3,9 #]

[1] Graduate Program in Areas of Basic and Applied Biology (GABBA) PhD Program, ICBAS-Instituto de Ciências Biomédicas Abel Salazar, Universidade do Porto, Portugal, [2] Gene Regulation - Instituto de Investigação e Inovação em Saúde, Universidade do Porto, Portugal, [3] IBMC-Instituto de Biologia Molecular e Celular, Portugal, [4]Sir William Dunn School of Pathology, University of Oxford, United Kingdom, [5]Tumor and Microenvironment Interactions Group – Instituto de Investigacao e Inovacao em Saude, Universidade do Porto, Portugal, [6]INEB-Instituto Nacional de Engenharia Biomédica, Portugal, [7]Instituto de Patologia e Imunologia Molecular, Universidade do Porto, Portugal, [8]Faculdade de Medicina, Universidade do Porto, Portugal, [9]ICBAS-Instituto de Ciências Biomédicas Abel Salazar, Universidade do Porto, Portugal

* Current address: Medical Institute of Bioregulation, Kyushu University, Fukuoka, Japan

[&] Current address: INEB-Instituto Nacional de Engenharia Biomédica, Portugal

Corresponding author: alexandra.moreira@i3s.up.pt

Summary

Macrophages are known to restrict cancer growth. Using ChrRNA-Seq and 3'RNA-Seq, we show that differentiation of macrophages from naïve to pro-inflammatory alters gene expression and alternative polyadenylation (APA) profiles, producing mRNAs with long 3'UTRs. In addition, colorectal cancer (CRC) cells co-culture causes a switch in macrophage gene expression from a pro-inflammatory to an anti-inflammatory profile, and decreases the number of APA mRNA isoforms expressed. Depletion of the splicing factor *SRSF12* by siRNA*,* which is highly upregulated in pro-

inflammatory macrophages, leads to a decrease in the expression of genes involved in innate immune response regulation and RNA metabolism. Notably, *SRSF12* depletion reduces APA in pro-inflammatory macrophages, especially in genes related to macrophage-related functions and to RNA binding. Overall, our results indicate that pro-inflammatory polarization and CRC co-culture modify macrophage gene expression and APA profiles, and suggest that *SRSF12* is involved in these events. Our results also show that SRSF12 acts as a novel immune modulator by favoring proximal polyA signals in macrophages, impacting the expression of genes involved in macrophage-associated inflammation and anti-tumor activity.

Introduction

Communication between adjacent cell types often alters gene expression. This is especially relevant for immune cells recruited to sites of colorectal cancer (CRC). CRC is the worldwide second and deadliest form of cancer (WHO, 2018), and is influenced by tumor heterogeneity (Giannakis *et al.*, 2016) and the microenvironment interactions (Pinto *et al.*, 2016; Pinto *et al*., 2017; Pinto *et al.*, 2019). CRC was the first cancer type for which a mutational map has been extensively described during the tumorigenic process (Armaghany *et al*., 2012; Fearon & Vogelstein, 1990; Lengauer *et al.*, 1997). However, the mechanisms regulating changes in gene expression that arise upon interactions between cancer cells, the immune system and their shared microenvironment are still poorly understood.

Macrophages are abundant immune cells of the tumor microenvironment that depending on their inflammatory profile, may either cooperate with or abrogate cancer progression (Locati *et al.*, 2013; Mantovani & Locati, 2013). Naïve (hereby referred as M0) macrophages may be polarized towards pro-inflammatory (M1-like, hereby referred as M1), detoxifying (Mox) or anti-inflammatory (M2-like, hereby referred as M2). Concomitantly, they can be involved in immune evasion, a hallmark of tumorigenic progression (Hanahan, Weinberg, 2000; Hanahan and Weinberg, 2011). Importantly, macrophages present transcriptional programs that affect both pro- and anti-inflammatory cellular responses, enabling a spectrum of phenotypes to respond to each stimulus (Németh *et al*., 2005).

Colonic macrophages are typically pro-inflammatory to maintain a tight gut microbiome control (De Schepper *et al.*, 2018; Zigmond & Jung, 2013) and at the onset

of CRC progression, macrophages recognize and attack tumor cells (Bögels *et al.*, 2012). Yet, the few cancer cells that escape have increased invasive and metastatic properties, creating a microenvironment within which macrophages develop an anti-inflammatory, tumor-permissive phenotype (Cardoso, Pinto, *et al.*, 2015; Lawrence & Natoli, 2011; Locati *et al.*, 2013; Quail & Joyce, 2017). Macrophages may also acquire a detoxifying (Mox) phenotype when exposed to CRC (Lai *et al.*, 2019). Mox phenotype is characterized by pro- and anti-inflammatory characteristics (Eren *et al.*, 2018; Kadl *et al.*, 2010), which rebalances redox homeostasis (Serbulea *et al.*, 2017). Transcriptomic studies have highlighted the commonality of mRNA isoforms with alternative 3' Untranslated Regions (3’ UTRs) formed by alternative polyadenylation (APA; 3’UTR-APA), occurring in more than 74% of human genes (Derti *et al.*, 2012; Lee *et al.*, 2018; Shi, 2012; Tian *et al*., 2005; Wang *et al.*, 2008). APA contributes to a wide range of gene- and cell-specific regulatory mechanisms (Berkovits & Mayr, 2015; Braz *et al.*, 2017; Pai *et al.*, 2016) with consequences for cell proliferation, differentiation, and cell cycle progression (Castello *et al.*, 2012; Elkon *et al.*, 2013; Mayr, 2017; Sandberg *et al.*, 2008; Tian & Manley, 2016). Thus, mRNA isoforms generated by APA determine mRNA half-life, subcellular location and protein expression levels (Ma & Mayr, 2018; Mitra *et al.*, 2016), partly due to the selective binding of RNA-binding proteins (RBP) (Berkovits & Mayr, 2015; Wurth & Gebauer, 2015). In cancer and activated immune cells, mRNAs with short 3’ UTRs are more prevalent than those with long 3’ UTRs (Jia *et al.*, 2017; Mayr & Bartel, 2009; Pai *et al.*, 2016; Sandberg *et al.*, 2008) and this is also the case for cells under stress (Zheng et al., 2018).

Cleavage and polyadenylation is a co-transcriptional event (Dye & Proudfoot, 1999), with RBPs having an integrative role (Xiao *et al.*, 2019). Many APA regulators have been identified that work competitively or synergistically to ensure correct mRNA 3’ end processing (Pereira-Castro & Moreira, 2021), including Pcf11 (Kamieniarz-Gdula *et al.*, 2019; Wang *et al.*, 2019), CFI (Hardy and Norbury, 2016;Gruber *et al.*, 2018) and especially its CFIm25 subunit (Turner *et al.*, 2020; Zhu *et al.*, 2017), Elav (Berkovits & Mayr, 2015; Diaz-Muñoz et al., 2015), PTBP1 (Castelo-Branco *et al*., 2004; Domingues *et al.*, 2016; Fischl *et al.*, 2019; West *et al.*, 2019), and SR proteins such as SRSF3 and SRSF7 (Schwich *et al.*, 2021)

Here, we show that CRC cells affect fundamental processes such as primary human macrophage gene expression and APA, modulating the macrophage inflammatory phenotype. We used an experimental system designed to dissect the macrophage-cancer cell crosstalk (Wilton *et al.*, 2021) that consists in isolating monocytes from healthy donors, exposing them to pro-inflammatory conditions and performing indirect co-cultures. By chromatin RNA-seq (*ChrRNA-Seq)* analysis we show that macrophages co-cultured with CRC cells have generally higher transcription levels than macrophages alone. By 3'RNA-Seq we identified a robust 35-gene signature of differentially-expressed genes (DEGs) in co-cultured macrophages, consisting of anti-inflammatory and immune-related genes, with particular alterations in the expression of Wingless and Int-1 (Wnt), Nuclear Factor-kB (NF-kB) and Mitogen-activated protein kinase (MAPK) pathways. We found that there is an upregulation in the expression of genes involved in some of these pathways, and also in the expression of mRNAs with long 3' UTRs. Curiously, co-culture with CRC leads to a decrease in the number of APA mRNA isoforms for each gene in macrophages and to the identification of a 45-gene signature consisting of 3 'UTR-APA mRNAs.

The top upregulated RNA processing gene in pro-inflammatory macrophages is *SRSF12*, which encodes a protein involved in alternative splicing, also known as SRrp35 (SRSF12) (Cowper *et al.*, 2001). Notably, *SRSF12* siRNA depletion in primary human M1 macrophages causes a decrease in the number of APA mRNA isoforms and an upregulation of mRNAs with long 3' UTRs, in particular in genes involved with innate immunity. Taken together, our results uncover a non-canonical role for SRSF12 in proximal polyadenylation signal (PAS) selection of immune-related genes in pro-inflammatory macrophages, which may allow an adaptation of the macrophages to their surrounding microenvironment.

Results

Polarization and CRC co-culture induce alterations in the macrophage transcription profile and inflammatory state

Macrophages can be experimentally differentiated from quasi naïve M0 cells into a spectrum of inflammatory phenotypes (Figure 1A), ranging from pro-inflammatory and anti-tumoral M1 to anti-inflammatory and pro-tumoral M2 macrophages (Yang *et al.*, 2018). We therefore obtained primary human $CD14^+$ monocytes isolated from healthy

blood donor buffy coats, differentiated into macrophages in the presence of M-CSF and polarized them towards a pro-inflammatory phenotype (M1) by incubation with LPS and IFNγ for 24 hours, following a well-established methodology (Machacek *et al.*, 2016; Ohradanova-Repic *et al.*, 2018; Wilton *et al.*, 2021) as depicted in Figure 1B. Unpolarized naïve M0 macrophages are predominantly round and amoeboid-like, while M1 macrophages have an elongated fibroblast-like morphology. Characterization of the inflammatory profile shows that M1 macrophages maintained the lineage marker CD14 as compared to M0 (Figure S1A). In addition, they showed upregulation of the pro-inflammatory markers CD86, CCR7 and IL1ß and downregulation of anti-inflammatory markers CD163 and TGFβ (Figures S1B-S1D), indicating that they are polarized into a pro-inflammatory phenotype.

We next performed an indirect co-culture of these polarized M1 macrophages with the colorectal cancer (CRC) cell line RKO (Cardoso, Pinto, *et al.*, 2015; Pinto *et al*., 2016). Using this method, the different cell populations are spatially separated, but as the media is the same, they exchange secreted molecules, such as growth factors and cytokines. Following co-culture of M1 macrophages with CRC cells, macrophage morphology reverts to an amoeboid-like phenotype, similar to M0 (Figure 1B, Figure S1E).

To understand the effect of CRC co-culture in APA in primary human M1 macrophages we performed ChrRNA-seq (Figure 1C) (Nojima et al., 2016). Metaprofiles of M1 macrophages cultured alone or co-cultured with RKO show that co-cultured macrophages present slightly higher RPKM levels across coding regions and after transcription end sites (TES), indicating a mild global increase in transcription (Figure 1D). Differential gene expression and Gene Ontology (GO) terms determined by Gene Set Enrichment Analysis (GSEA) indicate that the upregulated genes are related to anti-inflammatory conditions and stress (Figure S1G). In agreement with the cell morphology alterations observed, several anti-inflammatory genes – such as *LRP5*, *SEMA6B*, *THBS1* – were upregulated (Figure 1E), indicating a reversion of the macrophage pro-inflammatory M1 phenotype towards an anti-inflammatory phenotype.

Figure 1

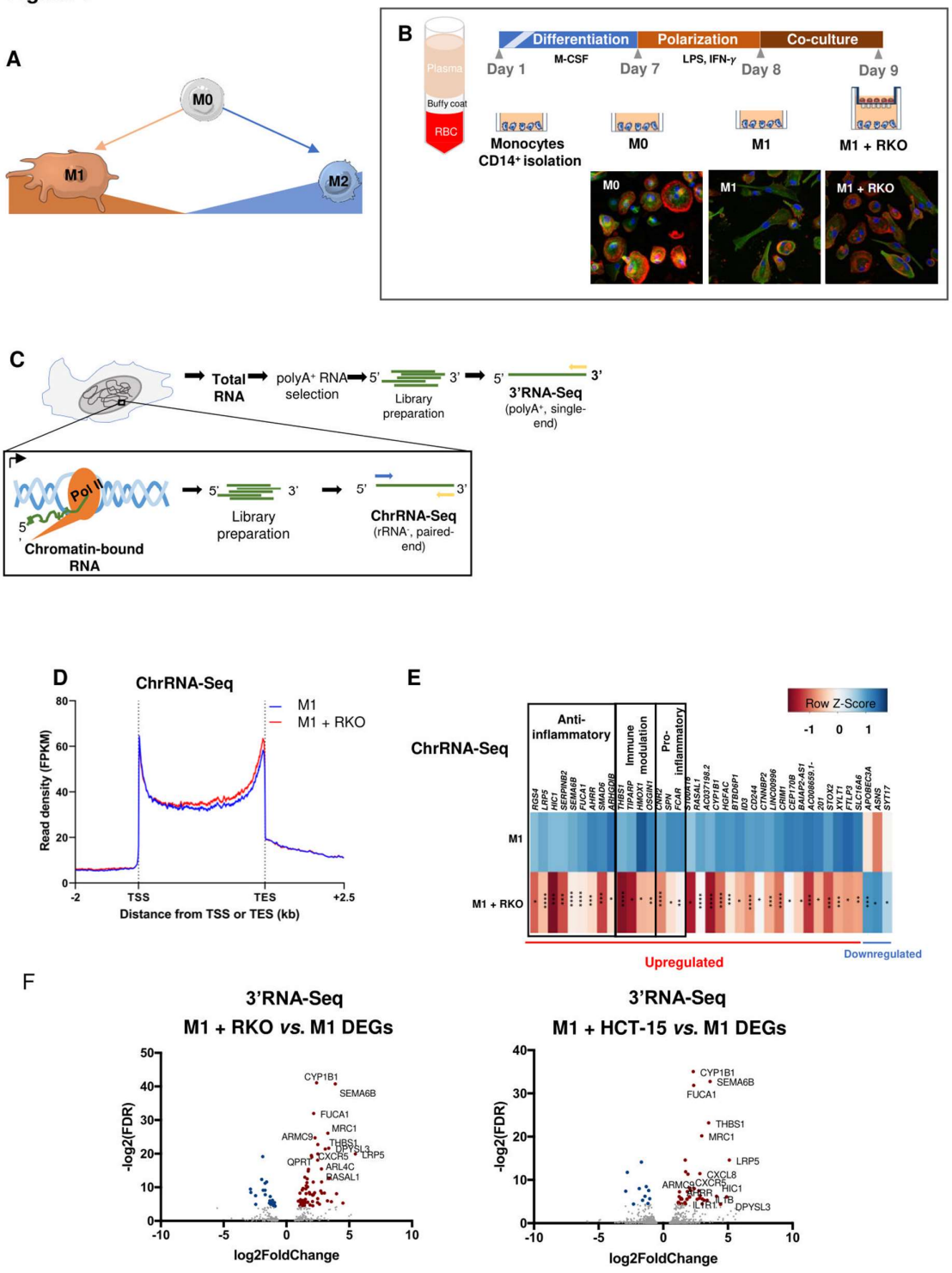


Figure 1 – Co-culture with colorectal cancer cells drives pro-inflammatory M1 macrophages into an anti-inflammatory polarization profile. A. Polarization spectrum of primary human macrophages: unpolarized M0 macrophages, pro-inflammatory M1 macrophages and anti-inflammatory Mox (detoxifying macrophages) and M2 macrophages. **B.** Top, experimental setup: CD14+ cell isolation from PBMCs contained in Buffy coats, macrophage differentiation, polarization and CRC co-cultures.

3'RNA-Seq reveals a 35-gene expression macrophage signature driven by co-culture with CRC cells

To determine whether the macrophage co-transcriptional events detected by ChrRNA-Seq correlate with alterations in APA and differential gene expression, we next performed 3' RNA-Seq analysis (Figure 1C, Table S2). This methodology provides both a quantification of gene expression based on RNA levels at 3' ends of the genes, and APA profiles for each gene (Del Valle Morales *et al.*, 2020; Wilton *et al.*, 2021). We extended our analysis to M0, M1 and co-cultured macrophages, and included HCT-15 as an additional CRC cell line in the co-culture assays (Figure S1F). RKO and HCT-15 cell lines differ from one another in several important markers such as *APC*, *K-ras*, *B-raf*, *TGFBR2* and *MLH1*, which affect important tumorigenic pathways (Ahmed et al., 2013). Mutations in these genes, occurring in RKO (*BRAF*, *MLH1*) or HCT-15 (*APC*, *KRAS*, *TGFBR2*), affect common pathways such as PI3K, MAPK and Rho GTPase. As the aforementioned pathways are interconnected, mutations occurring in one cell line but not the other may act on distinct molecular targets on the same pathway, such as cell division (*APC*, *BRAF*, *TGFBR2*), motility (*TGFBR2*), invasion (*KRAS*), adhesion (*APC*), DNA repair (*BRAF*, *MLH1*) and apoptosis (*KRAS*, *BRAF*, *TGFBR2*) (Aghabozorgi *et al.*, 2019; Caputo *et al.*, 2019; Steele *et al.*, 2019; Vander Ark *et al.*, 2018; Yamamoto & Imai, 2019). Consequently, the effect of each cell line on the macrophages upon co-culture will be similar, but different. The use of the two CRC cell lines will determine whether the effect on the macrophage reflects a general mechanism of response to CRC – shown by a common transcriptomic signature – or if it was due to intrinsic characteristics of each cell line – shown by individual transcriptomic signatures arising after exposure to each cell line.

Figure 1 (cont.) – Bottom, confocal microscopy images show actin-tubulin cytoskeleton of unpolarized naïve macrophages (**M0**), LPS+IFNγ stimulated pro-inflammatory (**M1-like**) polarized macrophages, and LPS+IFNγ stimulated macrophages co-cultured with CRC cell line RKO (**M1 + RKO**). DNA stained in blue, actin stained in red, tubulin stained in green. **C.** Setup of extraction and library preparation for RNA-Seq of fractionated RNA samples of primary human macrophages. rRNA-depleted chromatin-bound RNA were converted into paired-read libraries for ChrRNA-Seq, and polyA$^+$-enriched total RNA were converted into single-end libraries for 3'Seq. **D.** Representative donor gene metaprofile of the ChrRNA-Seq in M1 (**blue**) and M1 + RKO (**red**). TSS=transcription start site, TES=transcription end site). **E.** Representative donor heatmap of DEGs on ChrRNA-Seq of a representative donor in M1 + RKO, ordered by inflammatory profile function and fold change. **F**. Volcano plot of 3' RNA-Seq data comparing differentially expressed genes (DEGs) in in M1-like macrophages co-cultured with RKO cells (M1+ RKO) or HCT-15 cells (M1 + HCT15) *vs*. M1-like macrophages in monocultures (M1). Red and blue dots represent statistically significant genes with log2(Fold Change) >1 or <-1.

3' RNA-Seq results reveal that 3513 genes show a significantly altered expression in M1 macrophages in comparison to M0. As expected, upregulated genes include pro-inflammatory markers such as *CCR7, CCL19, SYNPO1-2, IDO1, IL7R* and the immune checkpoint *PD-L1* (Figure S1H). Upregulated genes were significantly enriched in GO terms related to response to stress, innate immunity, TNF-alpha and interferon-gamma response, and regulation of cytokine production (Figure S1I, left), typical of pro-inflammatory responses. In agreement with a pro-inflammatory phenotype, anti-inflammatory markers such as *MRC1*, *MRC2*, *CD163* and *ACE* are downregulated. Furthermore, GO terms related to extracellular matrix, secretory vesicles and endocytosis, lipid binding, and reduced GPCR and trimeric G proteins (Figure S1I, right), which are GO terms classically associated with anti-inflammatory macrophages (Martinez *et al.*, 2006) and to the cancer-immune cell crosstalk (DeNardo & Ruffell, 2019; Goossens *et al.*, 2019; Pathria *et al.*, 2019), are downregulated. Our results thus indicate that M1 polarization results in a robust pro-inflammatory transcriptomic profile.

Upon co-culture with CRC cells, there is a partial reversion of M1 macrophages to an anti-inflammatory phenotype revealed by a robust signature of 35 differentially-expressed genes (DEGs) that includes a subset of 15 anti-inflammatory, pro-tumorigenic genes (*LRP5, MRC1, EREG* and *SEMA6B*) and genes related to immune modulation and inflammation (*THBS1, CXCL8)* (Figures 1F and 1G). Curiously, 29 upregulated genes in this signature have GO terms associated to vesicle-mediated transport and endocytosis, response to IL-1-mediated signaling pathways, leukocyte chemotaxis and migration (Figure S1J, left). As these GO terms are associated with macrophage recruitment to tumors and are indicative of tumor progression (Kahles *et al.*, 2018; Larionova *et al.*, 2020; Ruiz-López *et al.*, 2018), our results indicate that co-cultured macrophages adopt increased anti-inflammatory and tumorigenic characteristics.

One of these genes is *LRP5*, presenting a >2-fold increase in LRP5 protein levels, induced by CRC co-culture (Figure 1H). To study this in a physiologically-relevant context, we analyzed CRC patient RNA-Seq data from The Cancer Genome Atlas (TCGA) database. In the TCGA RNA-Seq dataset of CRC patients, *LRP5* RNA upregulation was found *in vivo* in macrophages associated with colorectal tumor

(identified as the $CD68^{High}$ population) in patients diagnosed with colorectal tumor stages III and IV. Notably, *LRP5* mRNA upregulation seen in TCGA data is also associated with increased patient survival (Figure 1I, center and right, Figure S1K).
Of note, some of the most upregulated genes found in co-cultured macrophages – *LRP5*, *EREG*, *DPYSL3*, *CXCL8*, *IL1ß* and *THBS1* – are all related to the Wnt pathway (Figure S1L) (Abdelwahab *et al*., 2019; Kaler *et al*., 2009; Kim *et al.*, 2018; Logan & Nusse, 2004; Masckauchán *et al.*, 2005; Sutherland, 2011). This suggests that CRC co-culture activates the Wnt pathway and may lead to a transition in the macrophage phenotype into M2 (Yang *et al*., 2018), which was observed to occur in CRC patients (Lee *et al.*, 2020; Pinto *et al.*, 2019; Xiong *et al.*, 2018; Yahaya *et al.*, 2019).
Other upregulated genes are *SEMA6B* and *THBS1*. Of note, *SEMA6B* upregulation is associated with increased macrophage infiltration in tumors of CRC patients (Figure 1J) and with a slight protective effect on patient survival (Figure S1K). *THBS1* upregulation is also associated with increased macrophage infiltration in the tumor, but does not affect patient survival (Figure S1M). Our results indicate that these gene expression alterations in co-cultured macrophages are physiologically relevant for CRC patients.
3'RNA-Seq results were validated for some genes, by western blot, RT-qPCR and ELISA (Figure 1H, S1N and S1O, Table S7). LRP5 protein levels increase when macrophages are co-cultured with CRC, indicating that the increase in gene expression quantified by 3'RNA-Seq correlates to an augment of the protein levels produced (Figure 1H, 1I). Notably, upon co-culture, *SEMA6B* expression levels recover to those in unpolarized macrophages (M0) (Figure 1J), suggesting a reversal of the co-cultured macrophage profile to an anti-inflammatory state. Similarly, THBS1 protein thrombospondin secretion decreases upon pro-inflammatory polarization and increases again upon co-culture, again indicating that macrophages are less pro-inflammatory after CRC stimuli. EREG protein epiregulin secretion response is similar but milder to that of thrombospondin (Figure S1O). Moreover, most (19) of the 35-element signature genes produce at least two APA isoforms. In two-thirds of these 19 genes, the sequences of the primary PAS used was A(A/T)TAAA (Tables S3 and S4).

3' RNA-Seq data also revealed specific DEGs for each CRC cell line co-cultured with macrophages: 72 genes were differentially expressed at $p<0,05$ in M1 + RKO but not

in M1 + HCT-15 and conversely 14 genes were differentially expressed exclusively in M1 + HCT-15 (Figures S1P).

Figure 1

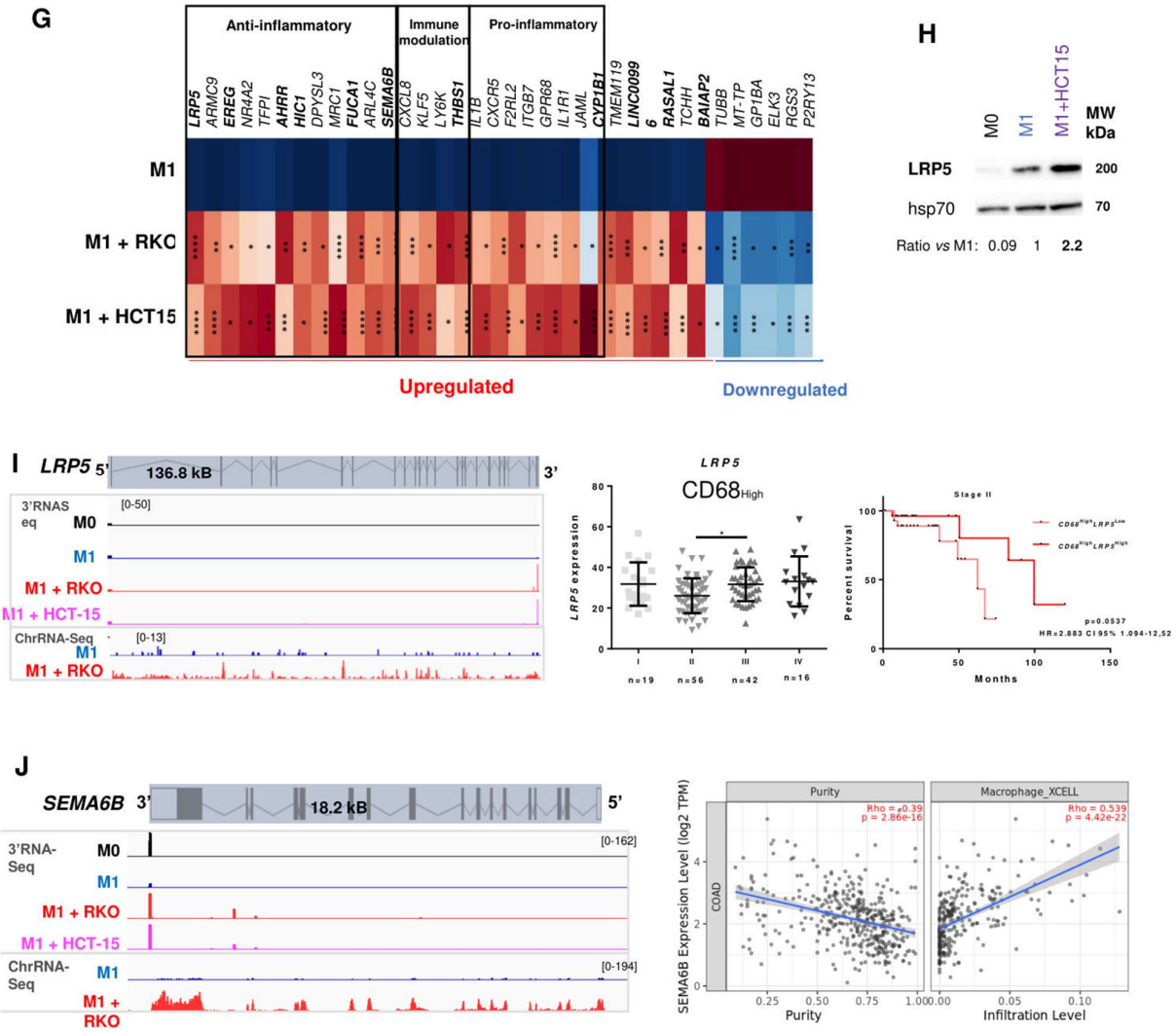


Figure 1 (continued) – **G**. Representative donor heatmap of common 3' RNA-Seq DEGs in macrophages co-cultured with RKO (M1 + RKO) or HCT15 (M1 + HCT15) *vs.* M1-like macrophages in monocultures, ordered by inflammatory profile function and fold change. Highlighted in bold text are DEGs from chromatin-bound RNA-seq data from Fig 1E. **H.** western blot showing protein levels (H) of DEG LRP5. **I.** Differentially expressed gene *LRP5* profile and transcript counts obtained by 3' RNA-Seq (top) and ChrRNA-Seq (down) visualized in IGV (left), and TCGA database patient data: microarray and RNA-Seq gene expression of *LRP5* in $CD68^{High}$ population stratified by stages (middle) and Kaplan-Meier survival curves of $CD68^{High}LRP5^{Low/High}$ patients in stage II (right). **J**: Differentially expressed gene *SEMA6B* profile and transcript counts obtained by 3' RNA-Seq (top) and ChrRNA-Seq (down) visualized in IGV (left), and macrophage infiltration and abundance in CRC patients measured in TIMER (right). **D-G**: n=3 independent experiments, p-value calculated using DESeq2 test through the Benjamini-Hochberg method: * = p < 0,05; ** = p < 0,01; *** = p < 0,005; **** = p<0,0001. **I,J**: Data obtained by 3' RNA-Seq (top), ChrRNA-Seq (bottom) of M0 macrophages (**black**), M1 macrophages

cultured alone (**blue**) and M1 macrophages co-cultured with the CRC cell lines RKO (**red**) or HCT-15 (**lilac**) visualized in IGV.

Additionally, co-culture causes an upregulation of anti-oxidative detoxifying macrophage markers (Mox), *CXCL8*, *IL1ß* (RKO and HCT15), *SRXN1* and *HMOX1* (RKO). This indicates an additional alteration from their original M1 profile caused by the CRC co-culture.

Altogether, our 3' RNA-Seq results indicate a loss of pro-inflammatory activity of the macrophages after exposure to CRC, and the acquisition of an anti-inflammatory and pro-tumorigenic potential.

CRC co-culture triggers distal PAS usage of key macrophage genes

Cell stimuli such as M1 polarization or cell-cell communication may cause changes in mRNA 3'end formation (Pai et al., 2016). We quantified the number of APA mRNA isoforms in M0, M1 and M1 macrophages co-cultured with CRC by analyzing the 3'RNA-Seq data. We built an alternative 3'UTR expression atlas as in (Singh et al., 2018) analyzing the 3'RNA-Seq data using DEX-Seq Count and quantifying of the number of APA mRNA isoforms produced in M0, M1 and M1 macrophages co-cultured with CRC. We selected every gene with at least two alternative 3' UTR mRNA isoforms in at least two out of the three biological replicates, and considered the levels of the most expressed mRNA isoform as 100% for a given gene. We also considered that the second most expressed mRNA isoform must be at least 10% to be included in an alternative 3' UTR usage atlas in primary human macrophages (Singh et al., 2018).
We found that approximately 50% of M0 and M1 genes undergo APA use at least two PAS (Figure 2A). However, CRC co-culture causes a ~50% reduction in the number of macrophage APA mRNA isoforms, with 75% genes using only one PAS (Figure 2A). Intriguingly, these genes are connected to GO terms related to RNA binding and transcription (Figures S2A and S2B), suggesting that upon co-culture with cancer cells, macrophages undergo broad transcriptomic alterations. Of note, most macrophage genes expressing only one PAS are the same in co-culture with either RKO or HCT-15 cells (1761 genes) indicating that this is a CRC feature and does not depend on the CRC cell line used (Figure S2C).

Notably, we found that the distal PAS is preferentially chosen, leading to the production of mRNAs with long 3'UTRs (Figure 2B). These results indicate that exposure to CRC cells affect macrophages 3'UTR-APA.

Figure 2

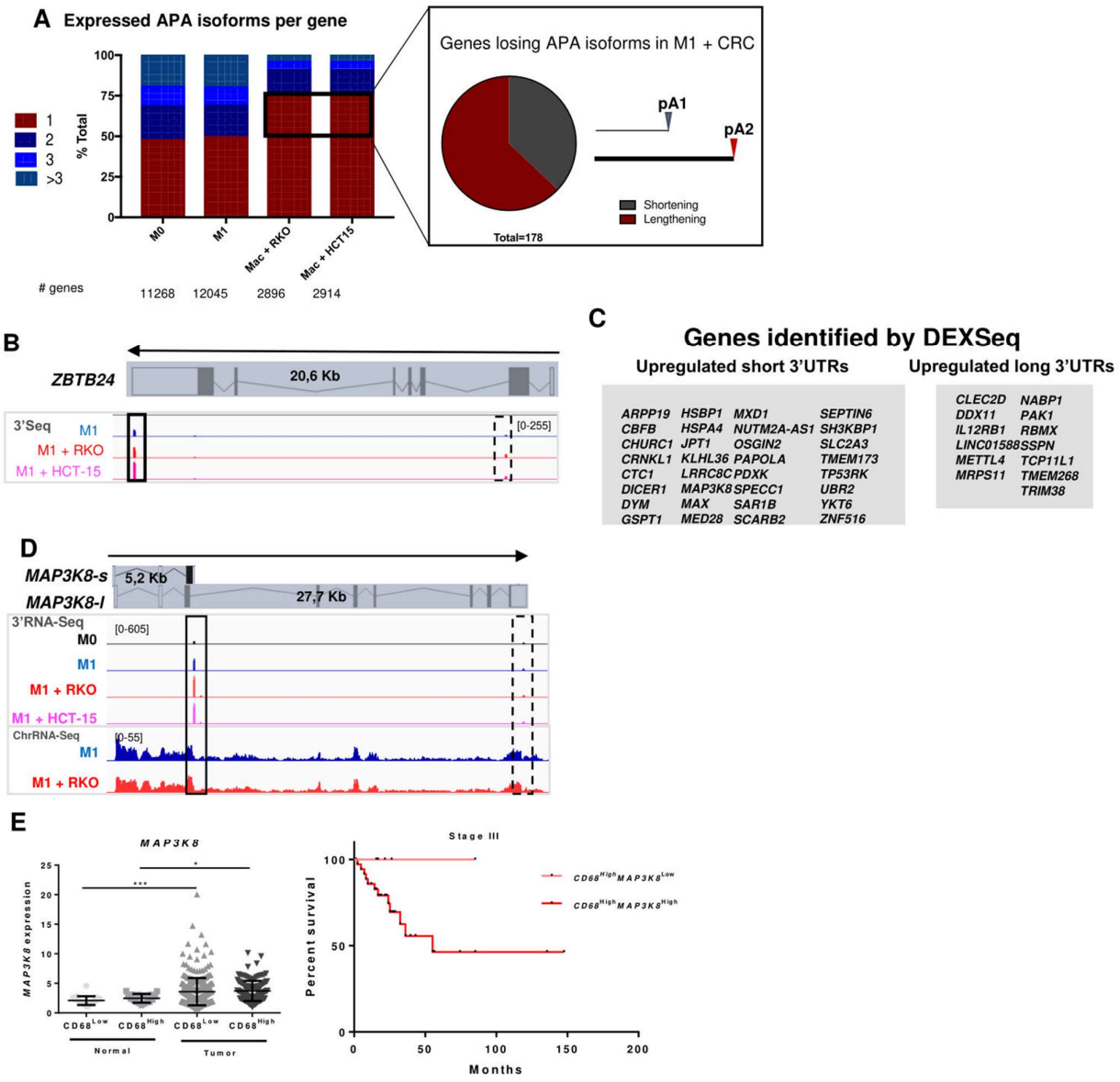


Figure 2 – CRC co-culture decreases macrophage transcriptomic diversity and increases distal PAS selection. A. Left, percentage of differentially expressed APA isoforms per gene in M0 and M1-like (M1) macrophages. Right, pie chart showing 3' UTR isoform outcome of genes losing APA in co-cultured macrophages. Grey shows shortening 3' UTR, red shows lengthening 3' UTR. **B.** IGV gene

profiles and transcript counts of genes losing APA *ZBTB24* (**B**) in M1 macrophages cultured alone (**blue**) and co-cultured with the CRC cell lines RKO (**red**) or HCT-15 (**lilac**), visualized in IGV **C**. Gene lists identified by DEXSeq, divided in upregulated short 3'UTRs (left) and long 3'UTRs (right). **D, E**: IGV gene profiles and transcript counts of *MAP3K8* (**D**), patient data from TCGA database: microarray and RNA-Seq gene expression of *MAP3K8* and *MXD1* in $CD68^{Low/High}$ populations in normal and tumor mucosas and Kaplan-Meier survival curves of $CD68^{High}$, $MAP3K8^{Low/High}$ (**E**). **A:** n=3 independent experiments, p-value calculated by DEXSeq. **B**,**D**: Data obtained through 3'Seq (**top**), ChrRNA-Seq (**bottom**) of M0 macrophages (**black**), M1 macrophages cultured alone (**blue**) and co-cultured with the CRC cell lines RKO (**red**) or HCT-15 (**lilac**), visualized in IGV.

During M1 polarization we observe a significant upregulation of mRNAs with short 3' UTRs determined by DEXSeq: 33 genes show proximal PAS selection and 13 show distal PAS choice (Figures 2C), but no correlation to mRNA expression is observed (Figure S2C). Of note, independently of the PAS selected, distal PAS is the canonical in all 46 genes identified, following the literature paradigm (Tables S5 and S6). While both gene sets had GO terms connected to transcription and the immune system regulation, short 3' UTRs are specifically associated with regulation of gene expression and transcription while long 3' UTRs include stress response and signal transduction (Figures S2D). These trends towards short or long 3' UTRs in M1 macrophages are even more pronounced after co-culture with CRC cells. Upregulated mRNAs with short 3' UTRs include *MAP3K8* (Figure 2D and 2H) and *MXD1*/*MAD1* (Figures 2F and 2H). Strikingly, upregulation of *MAP3K8* short 3'UTR is associated with *in vivo* RNA overexpression in CRC-associated macrophages and to a protective role for patient survival (Figure 2D and 2E). For *MAP3K8* we observe an increase in protein production in M1, milder after CRC co-culture, (Figures 2D,2E and 2H). The shorter protein isoform of MAP3K8 is predicted in the Uniprot database (Q5T854) but the corresponding protein band was undetected in macrophages by western blot. In turn, *MXD1*/*MAD1* is downregulated *in vivo* in CRC-associated macrophages and this is associated to decreased patient survival (Figure 2F and 2G). However, lower MW MAD protein levels are downregulated upon M1 polarization and upregulated again in co-culture indicating that other mechanisms are necessary to control MAD1 protein levels (Figure 2H). *MAP3K8* and *MXD1 in vivo* RNA levels do not vary significantly upon cancer progression (Figure S2E).

In M1 and M1 co-cultured macrophages, *IL12RB1* long 3' UTR mRNA is upregulated (Figure 2I) and the protein expression of the IL12RB1 ligand, IL12p70, is also upregulated (Figure S2F). *IL12RB1* is part of the IL-12 and IL-23 transmembrane receptor complexes (in conjunction with IL12RB2 and IL23R respectively).

Interestingly, the long 3' UTR mRNA isoform of IL12RB1 identified in this work corresponds to the previously identified IL12RB1 isoform 2, and contains a completely independent alternative 3' UTR on exon 9b. IL12RB1 isoform 2 is the predominant isoform in PBMCs, does not have transmembrane domains, and localizes to the cytoplasm due to its C-terminal sequence. Isoform 2 may be oligomerized with IL12RB1 and restrict IL12 signaling to sustain immune cell survival (Ray *et al.*, 2015).

Although *IL12RB1* levels do not vary *in vivo* in CRC-associated macrophages, there is a striking significant hazardous effect of upregulated *IL12RB1* in patient survival (Figure 2J center and right), particularly in cancer Stages III and IV (Figure S2G).
In conclusion, CRC co-culture induces a decrease in macrophage APA mRNA isoforms in a gene set involved in transcription and macrophage-related functions.

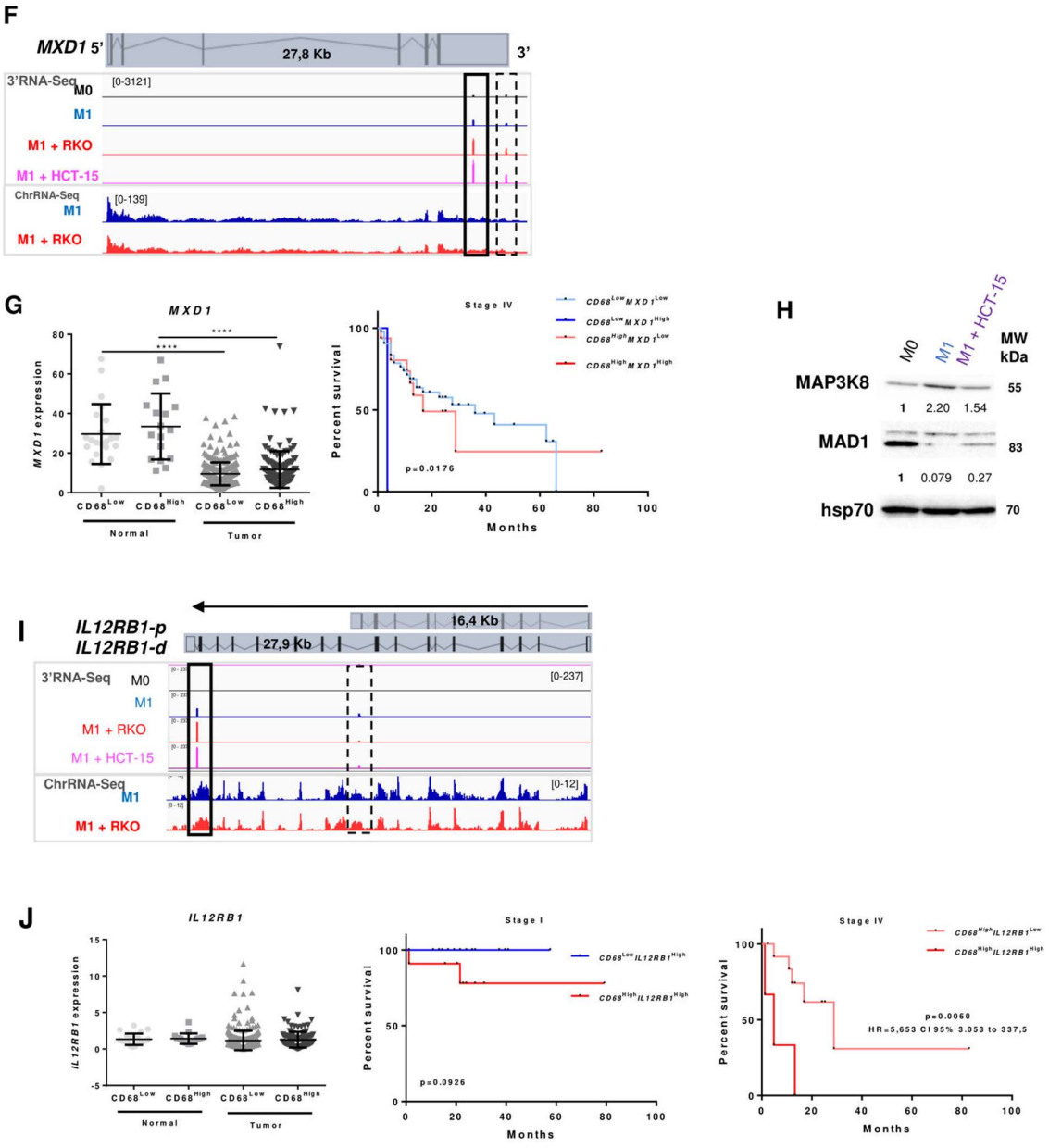


Figure 2 (continued) – F. IGV gene profiles and transcript counts of *MXD1*. **G**. Patient data from TCGA database: microarray and RNA-Seq gene expression of *MXD1* in CD68$^{Low/High}$ populations in normal and tumor mucosas (left) and Kaplan-Meier survival curves of CD68^{High}, *MXD1*$^{Low/High}$ in Stage IV (right). **H**. *MAP3K8* and *MXD1* protein quantification by western blot using heat-shock protein hsp-70 as loading control. **I**. IGV gene profiles and transcript counts of *IL12RB1*. **J.** Patient data from TCGA database: microarray and RNA-Seq gene expression of *IL12RB1* in CD68$^{Low/High}$ populations in normal and tumor mucosas (left) and Kaplan-Meier survival curves of CD68^{High}, *IL12RB1*$^{Low/High}$ in Stages I and IV (right). **F, I:** Data obtained through 3'Seq (**top**), ChrRNA-Seq (**bottom**) of M0 macrophages (**black**), M1 macrophages cultured alone (**blue**) and co-cultured with the CRC cell lines RKO (**red**) or HCT-15 (**lilac**), visualized in IGV.

.

SRSF12 modulates APA in macrophages

To understand the underlying mechanisms behind our observed APA alterations in macrophages following their polarization and CRC co-culture, we analyzed expression levels of RNA metabolism factors, including cleavage and polyadenylation and transcription termination factors. The most upregulated gene in M1 macrophages is the splicing repressor *SRSF12/SRrp35* (Figure 3A and S3B), in agreement with the previous literature (Liu *et al*., 2018). SRSF12 has been previously described as a splicing repressor (Cowper *et al.*, 2001). Indeed, its mRNA depletion caused a downregulation of the *SRSF2* full-length spliced mRNA isoform and an upregulation of the shorter spliced mRNA isoform (Figure S3D). Interestingly, the *SRSF12* expression *in vivo* is slightly downregulated in tumor macrophages, but it has a protective role in patient survival (Figure 3B).

To investigate a possible function for SRSF12 in the gene expression alterations observed, we depleted *SRSF12* mRNA in macrophages by siRNA transfection following M1 polarization (Figures 3C, 3D, S3C, S3E, Table S8). Interestingly, *SRSF12*-depleted macrophages show a marked gene expression downregulation (Figure 3E) in genes related to gene expression regulation (Figure 3F). Of note, genes involved in macrophage-relevant functions, such as regulation of the immune response and leukocyte proliferation were also downregulated, indicating that SRSF12 is required for their expression. Notably, CstF2/CstF64, which has a key role in cleavage/polyadenylation, and SR proteins SRSF2 and SRSF3 are all downregulated in the si*SRSF12* dataset (Figure 3G), while the chromatin regulator *SUPT7L* is downregulated in the si*SRSF12* data (Figure 3H).

Figure 3

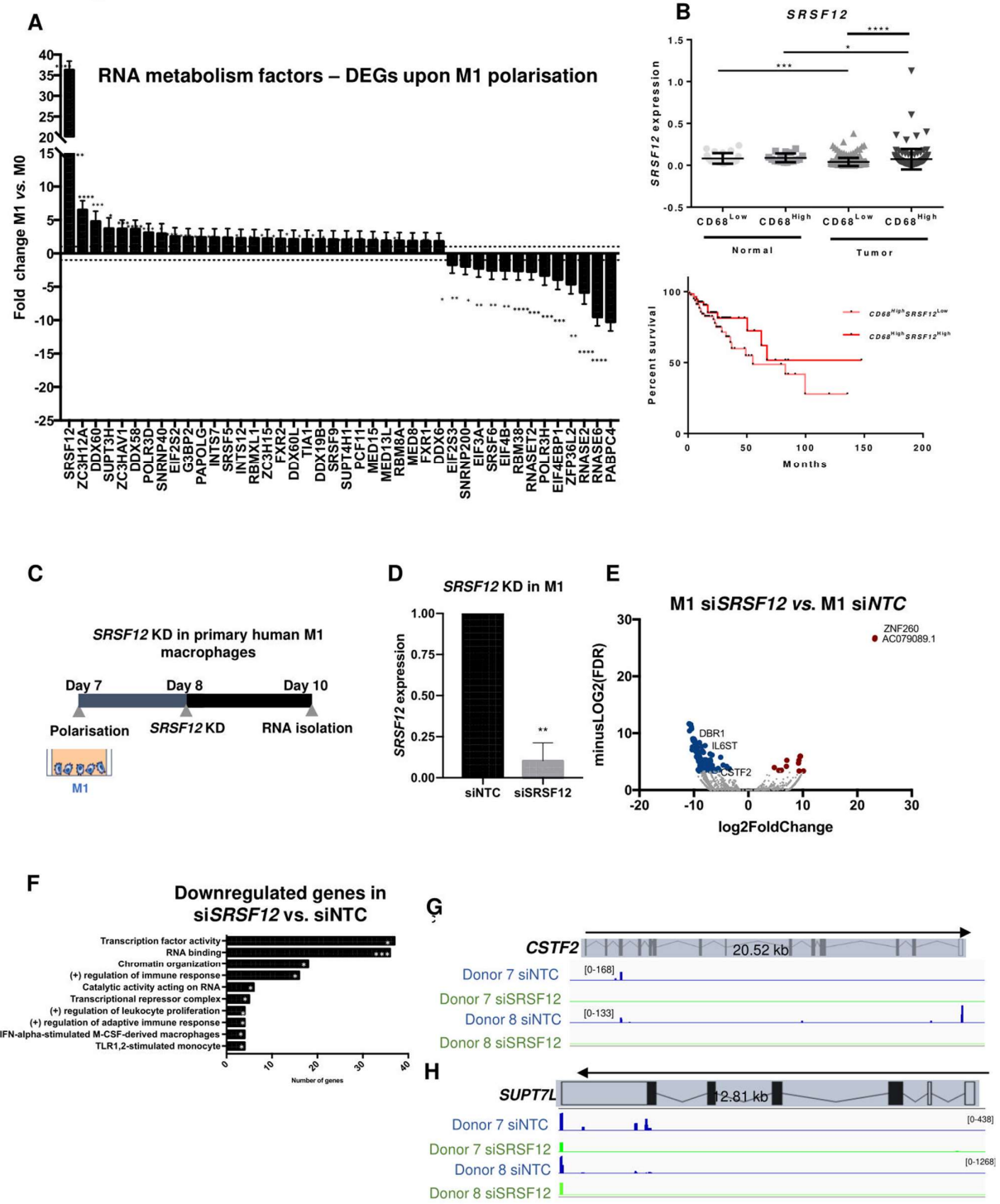


Figure 3 – SRSF12 modulates gene expression in M1-like macrophages. A. Fold change distribution of CPA and transcription regulation DEGs upon M1 polarization, ordered by fold change. **B.** Patient data from TCGA database: microarray and RNA-Seq gene expression of SRSF12 in $CD68^{Low/High}$ populations in normal and tumor mucosas (top) and Kaplan-Meier survival curves of $CD68^{High}$ $SRSF12^{Low/High}$. **C.** Experimental setup of *SRSF12* knockdown in primary human macrophages. **D.** KD levels of si*SRSF12* validated through RT-qPCR. **E.** Volcano plot of DEGs in si*SRSF12* vs si*NTC* M1-like macrophages. Red dots represent genes with log2(Fold Change) >1 or <-

We next studied if SRSF12 was involved in alternative 3' UTR mRNA expression. We analyzed the number of APA isoforms for each gene in siNTC and siSRSF12 with the same approach as in Figure 2, and then divided our analysis depending on the number of APA mRNA isoforms observed upon SRSF12 depletion, comparing to siNTC controls. We found that when the same number of APA mRNA isoforms was produced in siSRSF12, these do not show a preference for the expression of short or long 3' UTRs (Figure 4A). However, a subset of genes is transcribed into more APA mRNA isoforms upon siSRSF12, and in this set there was a slight correlation towards the expression of shorter 3'UTRs (11 genes) (Figure 4B). Strikingly, in the subset of genes that express less APA mRNA isoforms, there was a clear tendency towards the expression of longer 3' UTRs. This was the case for the majority of genes consistently affected (Figure 4C), suggesting that SRSF12 activates proximal PAS selection.

Subsequently, we analyzed the number of genes undergoing APA in siNTC and siSRSF12. If ~20,000 genes are expressed in a given cell, we expect that 50% to 70% of them will undergo APA (Derti *et al*., 2012; Hoque *et al*., 2016), i.e. ~14,000. Surprisingly, we show that in SRSF12-depleted cells, 3373 genes do not undergo APA and that only 4231 genes undergo APA (Figures 4D-E). Of these, only 348 genes undergo APA, representing 8% of total genes with APA in siSRSF12, indicating the importance of SRSF12 for the expression of alternative 3' UTRs. Interestingly, genes losing APA isoforms are connected to RNA processing and innate immune regulation (Figure 4F).

Figure 3 (cont.) – 1 and p < 0,1, grey dots represent non-significantly expressed genes. **F.** GSEA terms of downregulated DEGs in *siSRSF12 vs siNTC*. **G-H:** IGV gene profile and transcript counts of downregulated genes CSTF2 (H), and *SUPT7L* (**H**) in *siNTC* (blue) and *siSRSF12* (green) on M1-like macrophages derived from two donors. **A**: n=3 independent experiments; p-value calculated using DESeq2: * = p < 0,05; ** = p < 0,01; *** = p < 0,005; **** = p < 0,0001. **D**: n=3 independent experiments, p-value calculated using Student's t test: ** = p < 0.01. **E**. n=2 independent experiments. p-value calculated using DESeq2, using the Benjamini-Hochberg method: p < 0,1 shown in red. **F**: p-value calculated using GSEA: * = p < 0,05; *** = p < 0,005.

Figure 4

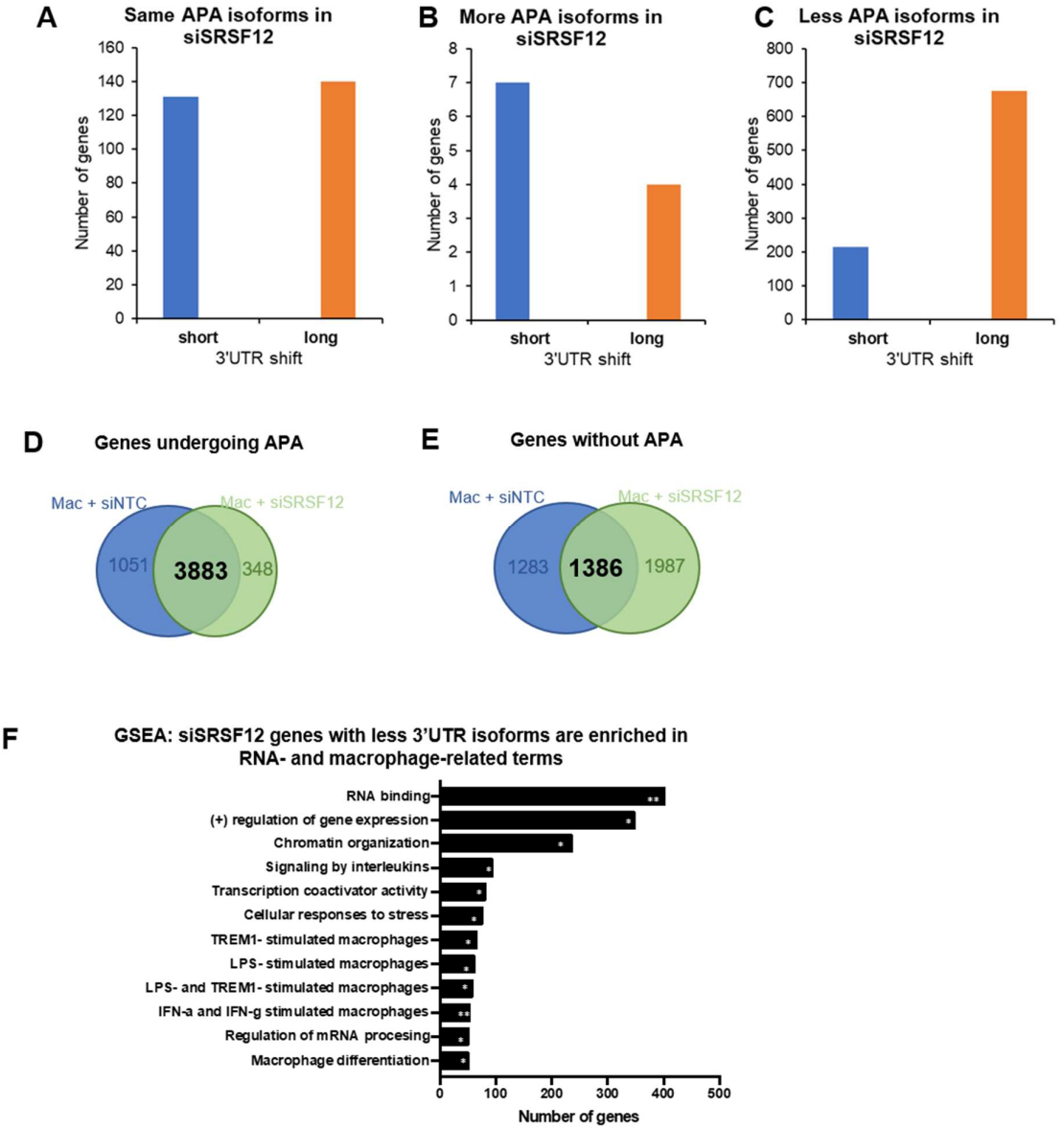


Figure 4 – SRSF12 upregulates short APA mRNA isoforms and contributes to mRNA diversity. A-C. Stratification of genes with short and long 3' UTR shifts in genes with APA, divided by subsets of genes that had, upon SRSF12 depletion and in comparison to siNTC controls, the same number of APA isoforms (**A**), increased number of APA isoforms (**B**) and decreased number of APA isoforms (**C**). **D-E.** Venn diagram representing number of genes undergoing APA (**D**) and without APA (**E**) in *siNTC* (**blue**) and *siSRSF12* (**green**). **F.** GSEA terms of genes with less APA isoforms in Mac + *siSRSF12*. p-value calculated using GSEA: * = p < 0,05, ** = p < 0,01.

GO terms of these genes are connected to RNA metabolism and macrophage-related functions (Figure 4D), in particular the response to inflammatory stimuli such as LPS, IFNα or IFNγ, in comparison to GO terms related to general functions presented by genes that show no difference in APA (Figure S4A). These results suggest an involvement of SRSF12 in APA specifically in genes relevant to macrophage functions. These genes include those previously found to be differentially-expressed from M0 to M1 polarization, as well as those found after CRC co-culture. One such gene is *IL12RB1*, which shows an upregulation of a short 3' UTR mRNA isoform upon *SRSF12* depletion (Figure S4B), indicating that SRSF12 is necessary for full-length *IL12RB1* mRNA production.

Taken together our results indicate that *SRSF12* is involved in APA of macrophage genes related to response to an inflammatory stimulus.

Discussion

Understanding the mechanisms regulating gene expression in innate immune cells, such as macrophages that are key players in the tumor microenvironment and modulators of cancer cells, will provide new insights into the mechanisms of immune evasion and cancer progression. Several studies have shown that the macrophage microenvironmental-driven polarization profile is predictive of CRC patient survival (Bögels *et al.*, 2012). In CRC, M2-like macrophages tend to be closer to the intratumor region and to the invasive front, and M1-like macrophages are closer to the tumor periphery and healthy mucosa (Pinto *et al*., 2019). This stratification in macrophage localization may favor tumor cell proliferation, angiogenesis and tumor growth (Hao *et al.*, 2012; Liu *et al*., 2014). To our knowledge it is the first time that a transcriptomic signature has been obtained after only 24 hours of co-culture with CRC cancer cells. Our results clarify the role of CRC in macrophage transcriptomic modulation and may lead to the identification of new diagnostic and therapeutic tools.

Primary human macrophages undergo CRC-driven APA modifications

APA is a regulatory mechanism of gene expression that has been widely described in eukaryotes, although it is less well characterized in primary human cells (Jia *et al.*, 2017; Pai *et al.*, 2016). We performed an unbiased genome-wide transcriptomic study using primary human macrophages polarized to pro-inflammatory and co-cultured with two different CRC cell lines. Our 3' RNA-Seq data report the biggest known catalog of

alternative 3' UTRs primary human macrophages following M1 polarization (56331 total APA events), including APA shifts in inflammatory-related genes, indicating a correlation between APA and macrophage inflammatory functions. After polarization, macrophages present significant differential expression of 18,1% genes, greater than the 5% differential expression previously reported in this population by microarray (Martinez *et al.*, 2006). Furthermore, after 24 hours of co-culture only, pro-inflammatory M1 macrophages convert into an anti-inflammatory M2/Mox population, decrease the number of APA isoforms produced per each gene and produce mRNAs with longer 3' UTRs. Fifty-four percent of DEGs underwent APA, mostly producing the short alternative 3' UTR isoform (Tables S3 and S4).

CRC co-cultures drive two main transcriptomic changes in pro-inflammatory macrophages: firstly, it induces a robust 35-gene "signature" in macrophages, which consists of upregulated genes involved in immune-related altered pathways, including LRP5, an integral part of the Wnt pathway (Logan & Nusse, 2004), which is associated to macrophage M2 polarization and immune evasion (Cai *et al.*, 2018; Feng *et al.*, 2018; Gong *et al.*, 2017). The most upregulated genes were connected to the anti-inflammatory macrophage profile in agreement with the remarkable phenotypic changes observed by confocal microscopy from ramified, elongated macrophage monocultures to amoeboid co-cultured macrophages. As macrophage morphology is very sensitive to microenvironmental cues (Ploeger *et al.*, 2013), these morphological alterations reveal a reversion of the pro-inflammatory to an anti-inflammatory phenotype driven by a dynamic transcriptomic response to the molecular factors secreted by the CRC cells. Notably, upregulated genes display functions related to immune evasion and extracellular matrix assembly, consistent with the M1 to M2 transition observed *in vivo* in CRC patients, and thus this signature may be of diagnostic and therapeutic value.

Secondly, we identified a striking downregulation in APA transcriptome diversity in CRC co-cultured macrophages and a tendency to produce longer 3'UTRs. Genomic studies show that CRC cells preferentially use distal polyadenylation signals, whereas activated T cells and pro-inflammatory macrophages use proximal polyadenylation signals (Gruber *et al.*, 2014; Pai *et al.*, 2016; Yang *et al.*, 2018). Here, we report that CRC cells induce a decrease in primary human macrophage APA and drives distal PAS usage. Interestingly, genes belonging to this APA signature follow the paradigm

established in the literature that distal PAS sequences are stronger, regardless of the alternative mRNA isoform produced (Tables S5 and S6).

Although pro-inflammatory macrophages are the main *in vivo* population in the colonic microenvironment at the beginning of a tumorigenic process and before immune evasion (Bohlson *et al.*, 2014; Cardoso, Pinto, *et al.*, 2015), it is suggested that along disease progression, macrophage profile might change towards a more anti-inflammatory and permissive microenvironment. Notably, the gene "signatures" identified correlate with the macrophage inflammatory phenotype and anti-tumor activity.

SRSF12 as an APA modulator

SRSF12 is an SR protein involved in splicing (Chandler *et al.*, 1997; Cowper *et al.*, 2001; Roca *et al*., 2013). As some splicing factors also affect polyadenylation and SRSF12 is the top upregulated gene with functions in RNA metabolism in M1 macrophages, we asked SRSF12 could be involved in APA. We found that a subset of the gene expression "signature" found in macrophages co-cultured with CRC cells that are related to the anti-inflammatory phenotype (e.g., *ARMC9*, *SEMA6B*, *MRC1*) loses APA mRNA isoforms upon si*SRSF12* in M1 macrophages and that si*SRSF12* leads to the production of mRNAs with long 3'UTRs. This may be a mechanism of bypassing the regulation imposed by RBPs and miRNAs that bind to long 3'UTRs, as macrophages need to react quickly to their surroundings and hence hasten mRNA and protein production.

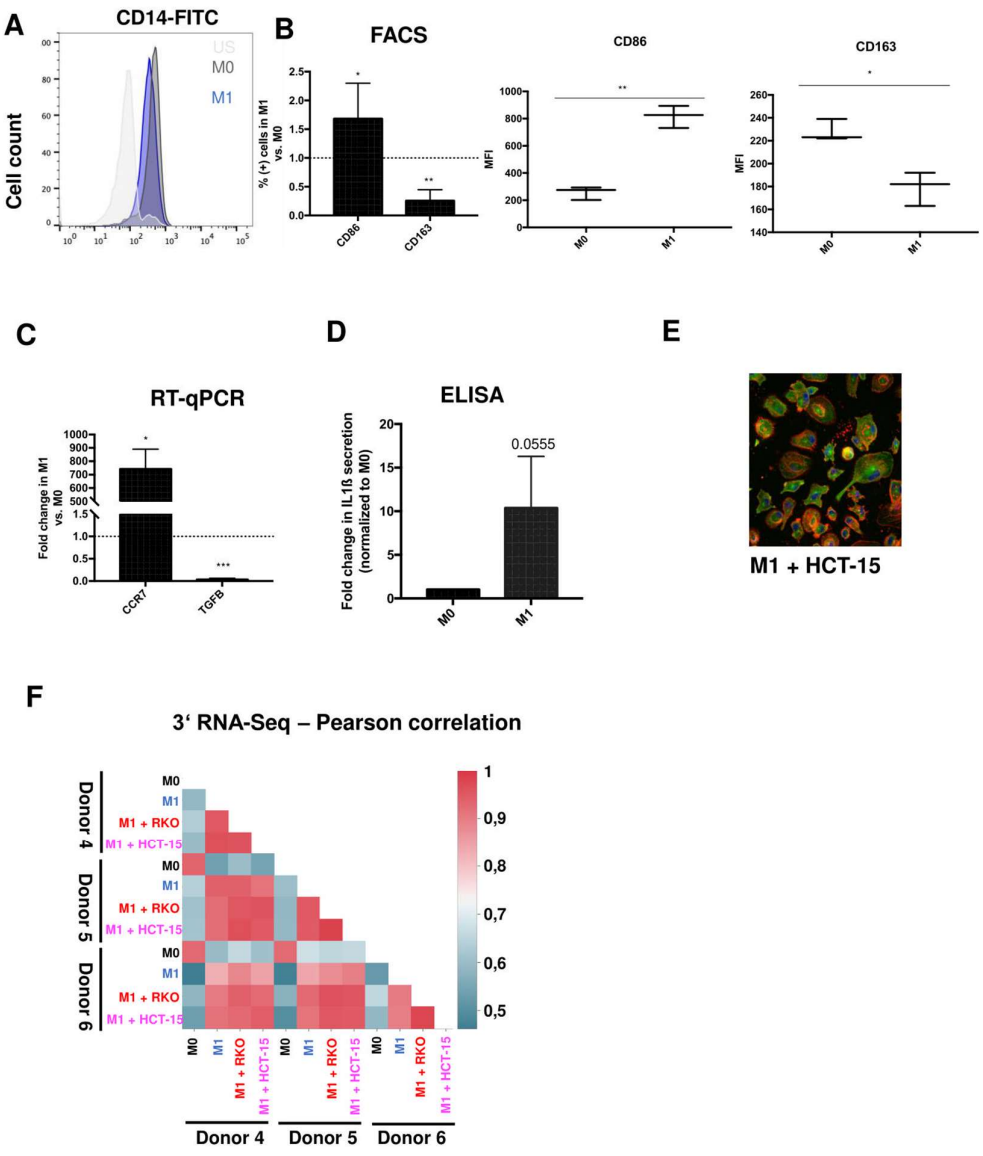
We also observed that si*SRSF12* depletion caused a marked downregulation of *CSTF2*, a core cleavage and polyadenylation factor, suggesting that the APA alterations we observe may be due to a decrease in CstF2. It is attractive to envisage that SRSF12 cooperates with other *trans*-acting factors by increasing their levels, such as CSTF2, to activate proximal polyadenylation signals. Accordingly, it has been shown that high levels of CSTF2 activates the selection of proximal polyadenylation signals of the IgM heavy chain pre-mRNA, leading to the switch from membrane-bound to secreted-form IgM that occurs during differentiation of B lymphocytes (Takagaki *et al.*, 1996). Furthermore, other SR proteins, such as SRSF3 – also downregulated in siSRSF12 (Figure S3G), work in conjunction with CPA factors to increase proximal PAS selection in a splicing-independent fashion, suggesting that a

similar mechanism may be at play here (Schwich *et al.*, 2021). However, further studies are needed to prove this hypothesis.

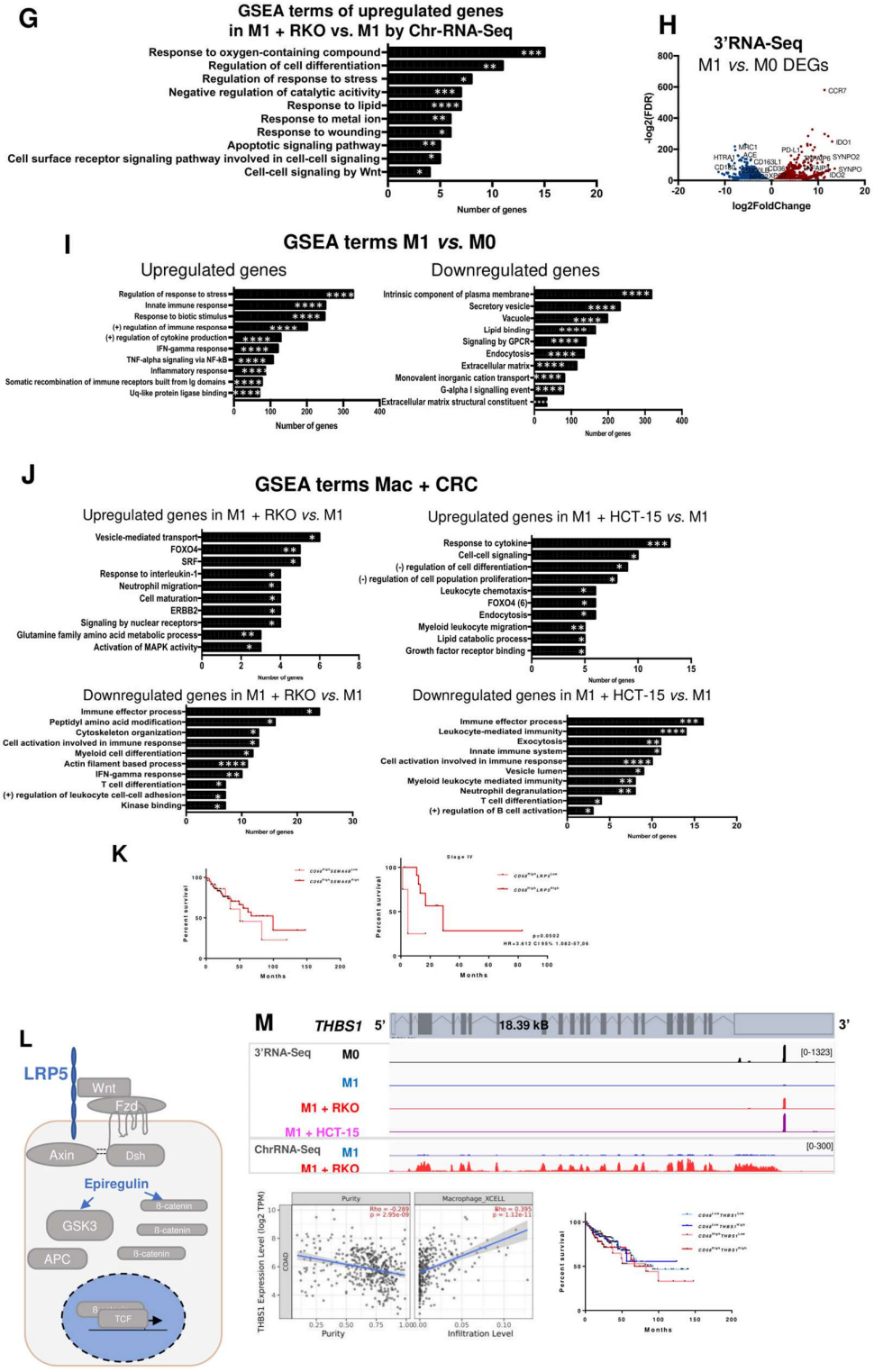
Taken together our results show that CRC cells modify fundamental processes in primary human polarized macrophages, in particular their gene expression and transcriptomic profiles, with consequences for their inflammatory phenotype. We reveal a new role for SRSF12 and hypothesize that SRSF12 controls the macrophage inflammatory profile.

Supplementary Figures

Supplemental Figure 1

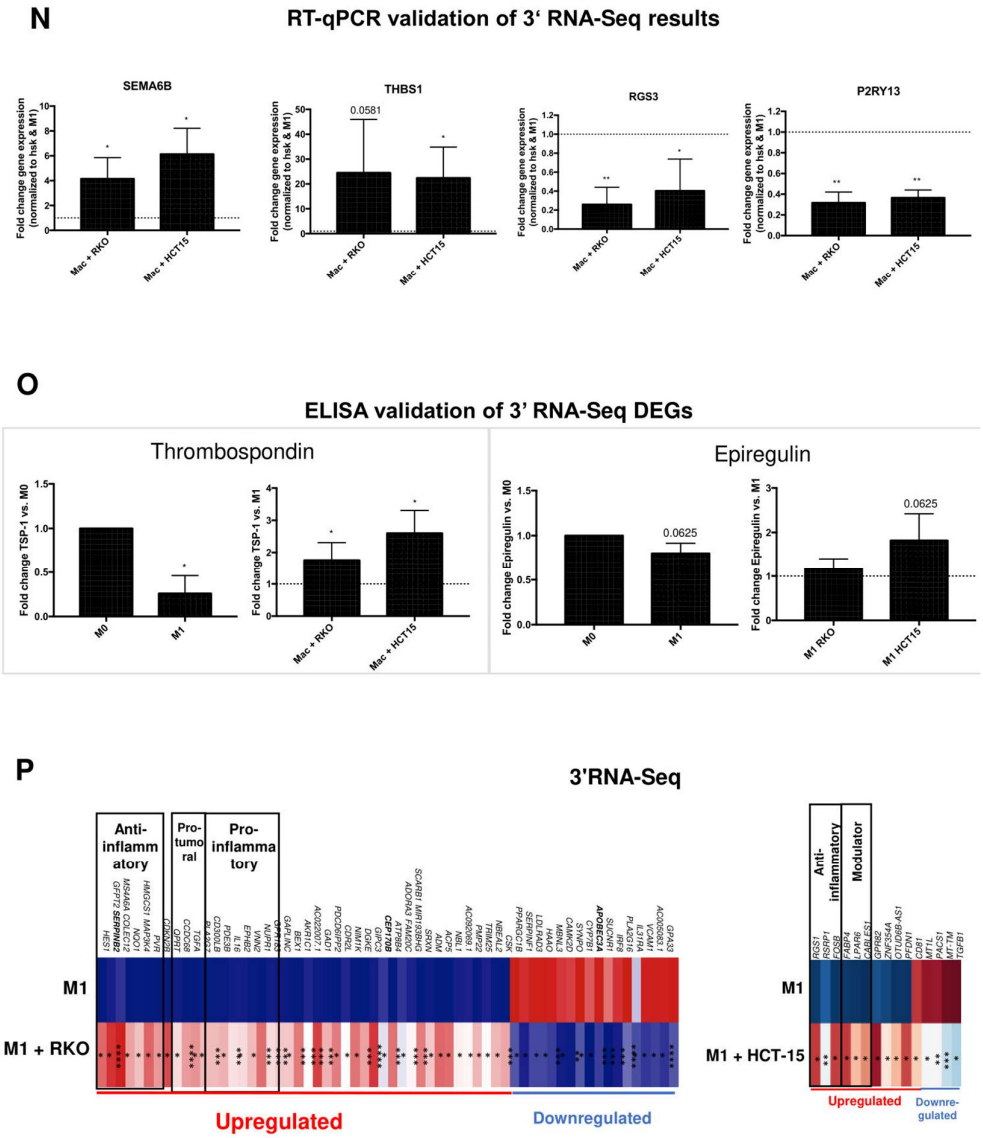


Supplementary Figure 1 (relative to Figure 1) – **A-D**. Inflammatory profile characterization of M1 (pro-inflammatory macrophages), normalized to M0 (unpolarized macrophages). **A**. Percentage of positive cells for CD14 marker measured by flow cytometry; unstained controls shown in light grey, M0 in dark grey, M1 in blue. **B**. Inflammatory markers measured by flow cytometry: left, percentage of cells positive for CD86-APC (pro-inflammatory) and CD163-PE (anti-inflammatory) macrophage markers in M1 *vs*. M0; MFI of CD86-APC (center) and CD163-PE (right) in M0 and M1. **C**. Pro-inflammatory marker *CCR7* and anti-inflammatory marker *TGFB* measured by RT-qPCR. **D**. IL1ß secretion in M1 *vs*. M0 macrophages, measured by ELISA. **E**. Confocal image of macrophages co-cultured with CRC cell line HCT-15 for 24 hours as shown in Figure 1B (M1 + HCT-15). DNA stained in blue, actin stained in red, tubulin stained in green. **F**. Heatmap of Pearson correlation coefficients for 3' mRNA-Seq samples, using transcript counts per million (CPM); 0 means total lack of correlation, while 1 means total linear correlation. **A-D**: independent experiments; **A, B** (CD86): n=5 healthy donors. **B** (CD163), **C, D, G**: n=3 healthy donors. **A-D**: Bars represent mean ± SD, Student's t-test: * = $p < 0,05$; ** = $p < 0,01$.



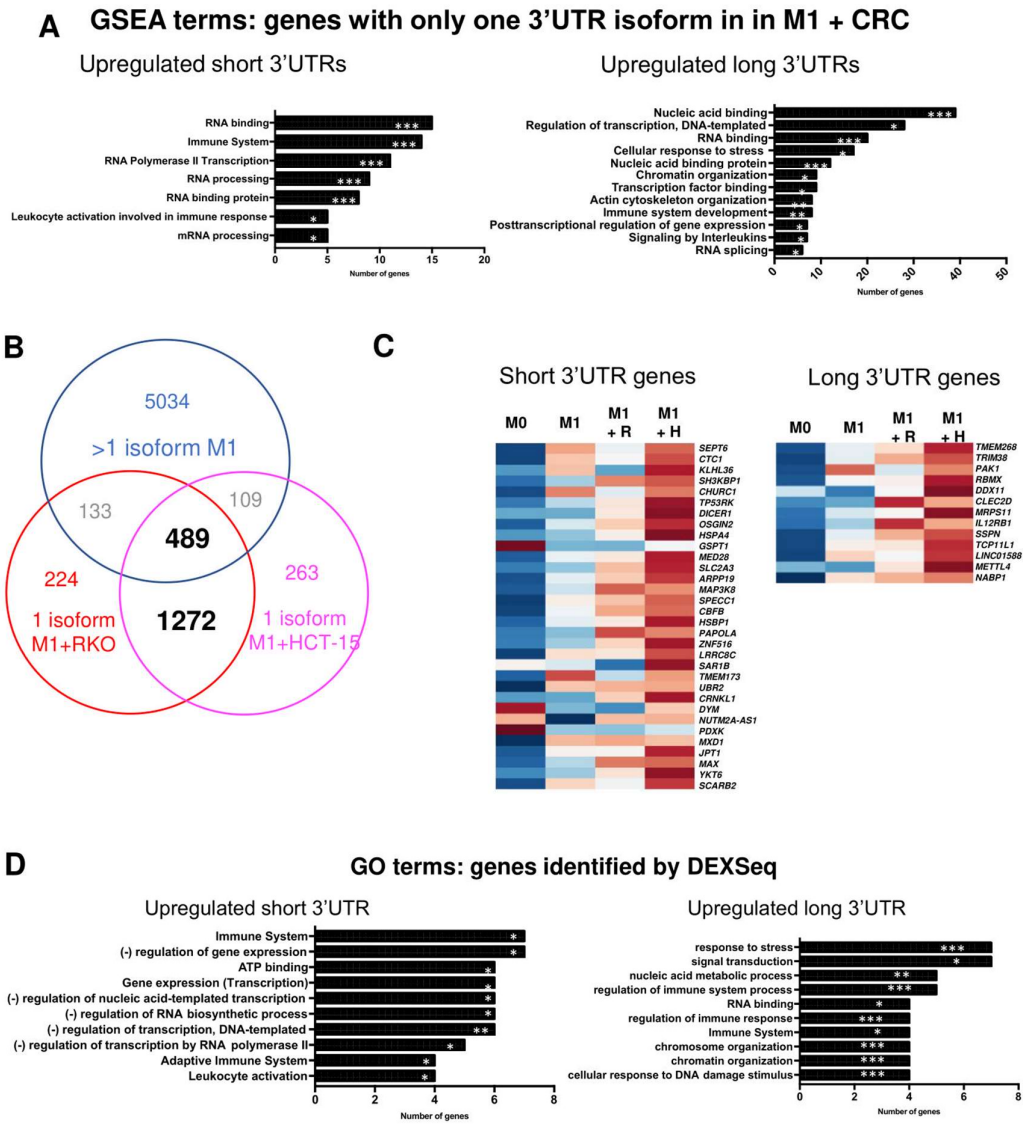
Supplementary Figure 1 (continued) – **G**. GSEA terms of genes upregulated in ChrRNA-Seq data. **H**. Volcano plot of 3' Seq data comparing differentially expressed genes (DEGs) in M1-like vs. M0. Red and blue dots represent statistically significant genes with log2(Fold Change) >1 or <-1. **I**. GSEA terms of genes upregulated (left) and downregulated (right) in M1 *vs.* M0. **J**. GSEA terms of upregulated genes and downregulated genes in M1 + RKO *vs.* M1 (left) and M1 + HCT-15 *vs.* M1 (right). **K**. CD68^{High}SEMA6B^{High} and CD68^{High}LRP5^{High} CRC patients have better survival. The Bittner Oncomine CRC cohort Kaplan-Meier curves made comparing patient populations CD68^{High}SEMA6B^{High} and CD68^{High}SEMA6B^{Low} (left) and CD68^{High}LRP5^{High} and CD68^{High}LRP5^{Low} (right),

measuring patient survival. The definition of high/low expression data was made according to the median normal expression of the selected genes. **L**. Scheme of the Wnt pathway. Upregulated DEGs are in blue. **M**. Representative gene profiles and transcript counts of *THBS1* (top), THBS1 macrophage infiltration and abundance in CRC patients measured in TIMER (bottom left) and Kaplan-Meier curves comparing $CD68^{Low/High}THBS1^{Low/High}$ populations in CRC (bottom right). Top: RNA-Seq data obtained through 3' Seq, ChrRNA-Seq of M0 macrophages (black), M1 macrophages cultured alone (blue) and M1 macrophages co-cultured with the CRC cell lines RKO (red) or HCT-15 (lilac) visualized in IGV. **H, M**: n=3 healthy donors, independent experiments, p-value calculated using DESeq2 test through the Benjamini-Hochberg method: * = p < 0,05; ** = p < 0,01; *** = p < 0,005; **** = p<0,0001. **I-J**: n= 3 healthy donors, independent experiments, representing number of enriched genes, p-value calculated using GSEA: * = p < 0,05; ** = p < 0,01; *** = p < 0,005; **** = p<0,0001.



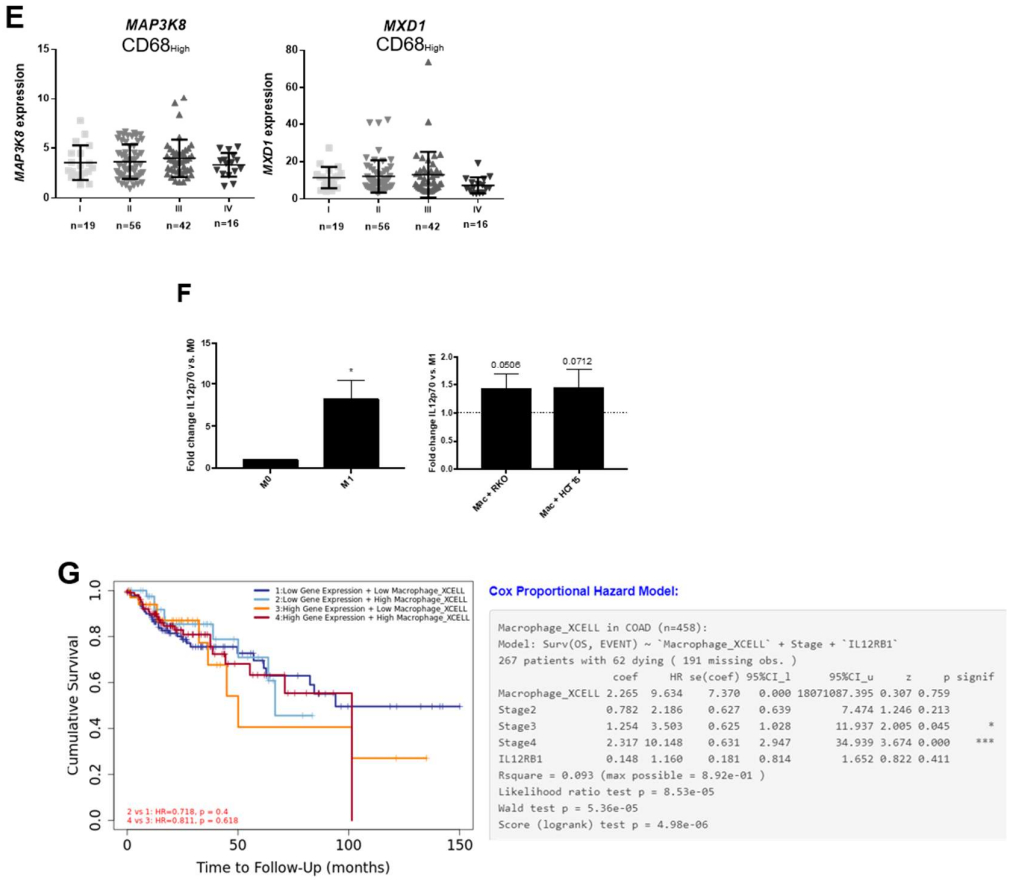
Supplementary Figure 1 (continued) – **N.** RT-qPCR validation of common 3' RNA-Seq DEGs in co-cultured macrophages *SEMA6B*, *THBS1* (upregulated genes, top), *RGS3* and *P2RY13* (downregulated genes, bottom). **O.** Fold change production of thrombospondin and epiregulin in M0 and M1 (left) and co-cultured macrophages (right). **P.** Representative donor heatmap of genes exclusively upregulated in M1 + RKO *vs*. M1 (left) M1 + HCT-15 *vs.* M1 (right), ordered by inflammatory profile function and fold change. Independent experiments. **N**. *SEMA6B*, *P2RY13*: n=3; *THBS1*, *RGS3*: n=4 healthy donors, p-value calculated using Student's t-test * = p < 0,05; ** = p < 0,01; *** = p < 0,005. **O**. Thrombospondin: n=6; Epiregulin: n=5 healthy donors, p-value calculated using Wilcoxon test, * = p < 0,05. **P**. n=3 healthy donors, p-value calculated using DESeq2 test through the Benjamini-Hochberg method: * = p < 0,05; ** = p < 0,01; *** = p < 0,005; **** = p<0,0001.

Supplemental Figure 2



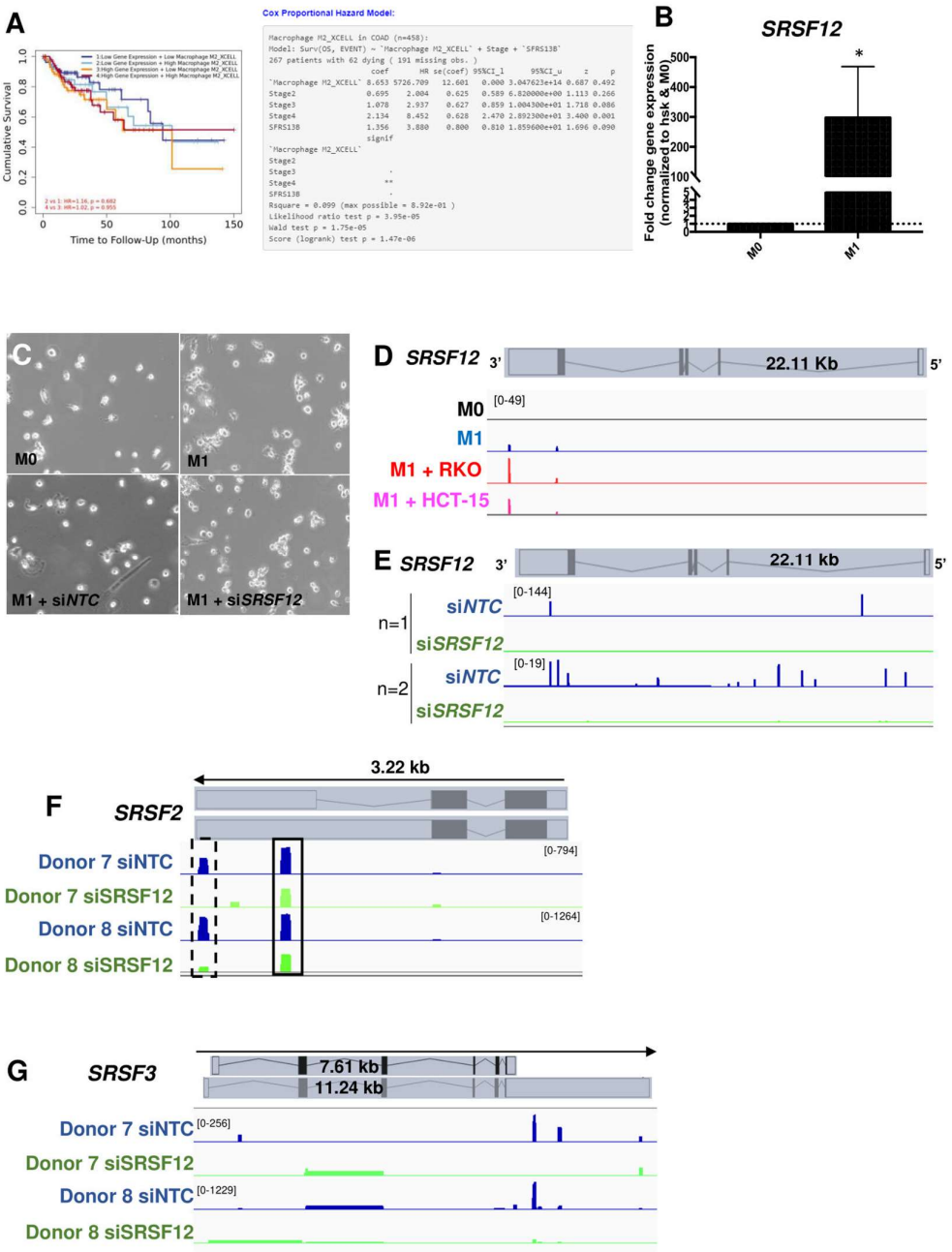
Supplementary Figure 2 (relative to Figure 2) – **A:** Common GO terms in genes losing APA isoforms (from figure 3A, right) producing shortened (left) and lengthened (right) 3'UTRs. **B.** Venn diagram showing genes losing APA isoforms upon CRC co-culture. **C**. Gene expression levels are unrelated to PAS choice in genes with upregulated short (left) and long (right) 3'UTRs upon M1 polarization. **D.** Genes that undergo APA changes and respective Gene Ontology terms in pro-inflammatory and co-cultured macrophages, shown by shifting towards shorter 3' UTRs (left) or longer 3' UTRs (right). **A**-**D**: n=3 independent experiments. **A:** p-value calculated using Fisher's test: * = p < 0,05; ** = p < 0,01; *** = p < 0,005; **** = p < 0,0001. **C:** n=3 healthy donors, data obtained through DEXSeq. **D**. Gene Ontology p-value calculated using Fisher's test (Panther). * = p < 0,05; ** = p < 0,01; *** = p < 0,005.

Supplemental Figure 2 (continued)



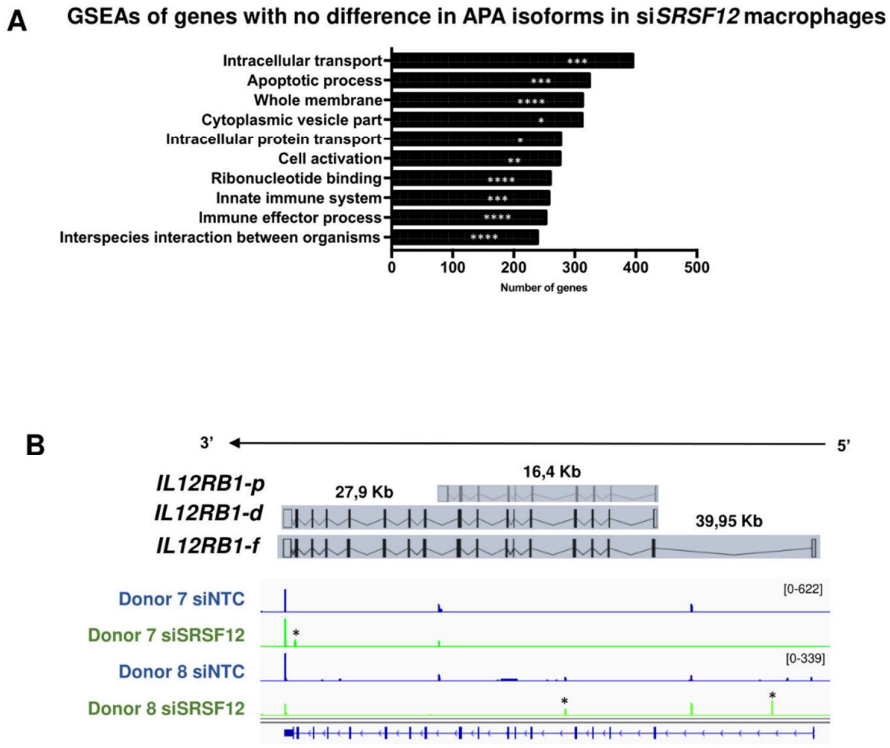
Supplementary Figure 2 (continued) – **E**. Upregulated shorter 3'UTR gene expression data in CD68^{High} CRC patients, stratified by cancer stages – *MAP3K8* (left) and *MXD1* (right), using TCGA microarray and RNA-Seq data . **F**. Fold change in IL12p70 secretion in M0, M1-like in monoculture (left) and co-cultured macrophages (right), concurrently with *IL12RB1* distal selection: n=3 healthy donors and independent experiments; p-value calculated using Student's t-test: * = p < 0,05. **G**. Kaplan-Meier curve measuring IL12RB1 and macrophage abundance in CRC patients measured in TIMER, showing a negative correlation of IL12RB1 with patient survival in stages 2 and 3, including an increase on IL12RB1 Hazard Ratio on Stage 3.

Supplementary Figure 3



Supplementary Figure 3 (relative to Figure 3) – **A**. Kaplan-Meier curve measuring SRSF12 and macrophage abundance in CRC patients measured in TIMER, showing a negative correlation of *SRSF12* expression in macrophages with patient survival and Hazard Ratio on Stage 4. **B**. Fold change in *SRSF12* production in M1 vs. M0 macrophages by RT-qPCR. **C**. Brightfield microscopy images of a representative donor through the experimental setup shown in Fig 4C. **D-E**. 3' RNA-Seq: IGV gene profile and transcript counts of *SRSF12* in M0 (black), M1 (blue) and co-cultured macrophages (red and lilac) (**D**) and in M1 + si*NTC* (blue) and M1 + si*SRSF12* (green) (**E**). **F-G**. 3' RNA-Seq: Gene profile and transcript counts of *SRSF2* (**F**) and SRSF3 (**G**) in M1 + si*NTC* (blue) and M1 + si*SRSF12* (green), visualized in IGV. **B-G**: independent experiments. **B.** n=4 healthy donors; p-value calculated using Student's t-test: * = $p < 0,05$. D-G: n=2 healthy donors

Supplemental Figure 4



Supplementary Figure 4 (relative to Figure 4) – **A**. GSEA terms of genes without any isoform number difference in M1 + si*SRSF12*. **B**. Gene profile and transcript count of genes undergoing 3' UTR shifts *IL12RB1* in M1 + si*NTC* (blue) and M1 + si*SRSF12* (green), visualized in IGV. A: GSEA: * = p < 0,05, ** = p < 0,01; *** = p < 0,005; **** = p < 0,0001.

Supplemental Table 1 - Percentage of reads passing filters after pre-processing, respective input read and uniquely mapped reads in ChrRNA-Seq data.

Sample	Input reads	Uniquely mapped reads	Aligned pairs
D1_M1	132,282,932	118,810,242	57,235,826 (89,8%)
D1_Mac + RKO	156,488,832	142,596,491	67,403,267 (91,1%)
D2_M1	147,426,396	131,189,998	62,318,634 (89%)
D2_Mac + RKO	120,061,720	109,392,734	51,800,326 (91,1%)
D3_M1	196,644,824	176,867,389	83,826,939 (89,9%)
D3_Mac + RKO	167,811,172	153,049,138	72,376,906 (91,2%)

Supplemental Table 2 - Percentage of reads passing filters after pre-processing, respective input read and uniquely mapped reads in 3' RNA-Seq of M0, M1 and co-cultured macrophages data.

Sample	Pre-processed reads passing filter (%)	Input reads	Uniquely mapped reads
D4_M0	65.218	28,035,543	23,288,888 (83,1%)
D4_M1	69.5065	25,491,051	19,264,000 (75,6%)
D4_Mac + RKO	66.0313	31,733,385	24,728,890 (77,9%)
D4_Mac + HCT15	68.1757	25,414,996	19,811,079 (77,9%)
D5_M0	50.0446	21175635	18,085,441 (85,4%)
D5_M1	70.3475	27,450,875	20,864,609 (76%)
D5_Mac + RKO	65.8951	28,013,142	21,991,907 (78,5%)
D5_Mac + HCT15	65.7408	34,958,610	27,044,240 (77,4%)
D6_M0	59.2683	22,766,165	19,026,324 (83,6%)
D6_M1	47.4429	25,282,986	19,794,383 (78,3%)
D6_Mac + RKO	59.8334	27,686,265	21,470,620 (77,5%)
D6_Mac + HCT15	64.9537	29,334,724	22,526,156 (76,8%)

Supplementary Table 3 – PAS sequences of DEGs in co-cultured macrophages. The primary PAS sequence is the main upregulated mRNA isoform. Other expressed alternative 3' UTR isoforms and localization in relation to the primary alternative 3' UTR mRNA isoform are shown.

Long 3'UTR mRNA	Primary PAS sequence	Other PAS (sequence and localization in relation to primary PAS)
LRP5	TATAAA	AATAAA (upstream, intron)
ARMC9	AATAAA	AATAAA (upstream, intron)
EREG	AATAAA	AATAAA, ATTAAA (upstream, 3'UTR)
NR4A2	AAAAGA	AATAAA (upstream, 3'UTR)
AHRR	AATACA	ATTAAA (upstream, 3'UTR)
DPYSL3	ATTAAA	ATTAAA (upstream, 3'UTR)
MRC1	AATAAA	CATAAA (upstream, 3'UTR)
ARL4C	AATAAA	AGTAAA, 2xAATAAA (upstream, 3'UTR)
CXCL8	TATAAA	AATAAA (upstream, 3'UTR)
THBS1	AATAAA	AATAAG, AATACA, AGTAAA (upstream, 3'UTR) 4xAATAAA (downstream, 3'UTR)
IL1R1	AATAAA	ATTAAA (upstream, intron)
JAML	GATAAA	AATAAA (upstream, intron)
CYP1B1	AATAAA	AATAAA, ATTAAA (upstream, 3'UTR)
LINC00996	AATAAA	AAGAAA (upstream, 3'UTR)
RASAL1	ACTAAA	2xATTAAA (upstream, intron) TATAAA (downstream, 3'UTR)
TCHH	AATAAA	TATAAA (upstream, 3'UTR)
BAIAP2	AAGAAA	AATAAA (upstream, 3'UTR) AATAAA,AAGAAA (downstream, 3'UTR)
TUBB	AATAAA	AATAAA (downstream, 3'UTR)
RGS3	AATAAA	2xAATAAA, ATTAAA (upstream, intron)

Supplementary Table 4 – PAS sequences of DEGs not undergoing APA in co-cultured macrophages.

Gene	PAS sequence
HIC1	AATAAA
TFPI	ATTAAA
FUCA1	AATAAA
KLF5	AATAAA
LY6K	ATTAAA
IL1B	AATAAA
CXCR5	TATAAA
F2RL2	AATAAA
ITGB7	AATAAA
GPR68	AATAAA
SEMA6B	AATAAA
TMEM119	AATAAA
GP1BA	AATAAA
ELK3	AATAAA
P2RY13	AATAAA

Supplementary Table 5 – PAS sequence study in mRNA isoforms with upregulated short 3' UTRs in M1 macrophages vs. M0, as identified by DEXSeq. Short and long isoform PAS sequence hexamers strength are compared and the strongest sequences is noted, using the efficiency data on Sheets et al. 1990

Upregulated short 3' UTR mRNA isoform	Type of APA	Proximal PAS sequence	Distal PAS sequence	Strongest PAS hexamer
MAP3K8	CR-APA	ATTAAA	AATAAA	L
NUTM2A-AS1	CR-APA	AATAAA	AATAAA	L
PAPOLA	CR-APA	AATAAA	AATAAA	Both AATAAA
ARPP19	UTR-APA	AATACA	AATAAA	L
CBFB	UTR-APA	ATTAAA	AATAAA	L
CHURC1	UTR-APA	AATACA	AATAAA	L
CRNKL1	UTR-APA	TATAAA	CATAAA	L
CTC1	UTR-APA	AATGAA	AATAAA	L
DICER1	UTR-APA	AATAAA	AATAAA	L
DYM	UTR-APA	AATAAA	GATAAA	S
GSPT1	UTR-APA	AATAAA	AATAAA	Both AATAAA
HSBP1	UTR-APA	ATTAAA	AATAAA	L
HSPA4	UTR-APA	ATTAAA	AATAAA / AAAAAA	L
JPT1	UTR-APA	ATTAAA	AGTAAA	S
KLHL36	UTR-APA	ATTAAA	ATTAAA	Both ATTAAA
LRRC8C	UTR-APA	AATAAA	AATAAA	Both AATAAA
MAX	UTR-APA	CATAAA	AATAAA	L
MED28	UTR-APA	AATACA	ATTAAA	L
MXD1	UTR-APA	TATAAA	AATAAA / ATTAAA	L
OSGIN2	UTR-APA	ATTAAA	AATAAA	L
PDXK	UTR-APA	AATAAC/AACAAA	AATAAA	L
SAR1B	UTR-APA	AATAAA	AATAAA	Both AATAAA
SCARB2	UTR-APA	AATAAA	AATAAA	Both AATAAA
SEPT6	UTR-APA	AATAAA	ATTAAA	S
SH3KBP1	UTR-APA	ATTAAA	ATTAAA	Both ATTAAA
SLC2A3	UTR-APA	AATAAA	AATAAA	Both AATAAA
SPECC1	UTR-APA	AATAAA	AATAAA	Both AATAAA
TMEM173	UTR-APA	CATAAA	AAAAAA	S
TP53RK	UTR-APA	AGTAAA	ATTAAA	L
UBR2	UTR-APA	AATAAA	AATAAA	Both AATAAA
YKT6	UTR-APA	CATAAA	GATAAA	S
ZNF516	UTR-APA	AATAAA	AATAAA / ATTAAA	Both AATAAA

Supplementary Table 6 – PAS sequence study in mRNA isoforms with upregulated long 3' UTRs in M1 macrophages vs. M0, as identified by DEXSeq. Short and long isoform PAS sequence hexamers strength are compared and the strongest sequences is noted, using the efficiency data on Sheets et al. 1990

Upregulated long 3'UTR mRNA isoform	Type of APA	Proximal PAS sequence	Distal PAS sequence	Strongest PAS hexamer
DDX11	CR-APA	(NMD)	AATAAA	L
IL12RB1	CR-APA	AATAAA	AAAACA	S
LINC01588	CR-APA	AATAAA	AATAAA	Both AATAAA
METTL4	CR-APA	ATTAAA	ATTAAA	Both ATTAAA
MRPS11	CR-APA	AATAAA	AATAAA	Both AATAAA
PAK1	CR-APA	AAGAAA	AATAAA	L
RBMX	CR-APA	AATAAA	AATAAA	Both AATAAA
CLEC2D	UTR-APA	AATAAA	GATAAA	S
NABP1	UTR-APA	AAAAAA/AATAAC	AATAAA	L
SSPN	UTR-APA	AAAAAA	AATAAA	L
TCP11L1	UTR-APA	ATTAAA /AAGAAT	ATTAAA	Both ATTAAA
TMEM268	UTR-APA	AATAAA	AATAAA	L
TRIM38	UTR-APA	TATAAA	AGTAAA	L

Supplementary Table 7 - Primer pairs used for RT-qPCR validation.

Primer name	5'-3' sequence
*LRP5*_fwd	AACATCAAGCGAGCCAAGGA
*LRP5*_rev	CGGCTGTAGATGTCGATGCT
*SEMA6B*_fwd	TACTCGGGGTGTATGAAGAACTG
*SEMA6B*_rev	GGACACGTCCTGCTCAAAGG
*THBS1*_fwd	AGTCGTCTGCAACAACCC
*THBS1*_rev	ACAGGCATCCATCAATTGGACA
*RGS3*_fwd	CAGGCATGCAAGGAGGTCAA
*RGS3*_rev	GCGAGGGTACGAGTCCTTTT
*P2RY13*_fwd	TCCCAAAGGTGACACTGGAAG
*P2RY13*_rev	GGATGCCGGTCAAGAAAACC
*SRSF12*_fwd	CAAGGTGATCGCAAAACACCA
*SRSF12*_rev	TTCTTTGGCTGGGGCTTCTT

Supplementary Table 8 – Percentage of reads passing filters after pre-processing, respective input read and uniquely mapped reads in 3' RNA-Seq of si*SRSF12* data.

Sample	Input reads	Uniquely mapped reads (%)
D7_M1_si*NTC*	54335347	48.71
D7_M1_si*SRSF12*	46393540	38.84
D8_M1_si*NTC*	58517422	57.79
D8_M1_si*SRSF12*	44565423	45.27

STAR Methods

Key Resources Table

REAGENT or RESOURCE	SOURCE	IDENTIFIER
Antibodies		
Mouse monoclonal CD14-FITC (clone M5E2, used for flow cytometry)	BD	Cat# 555397; RRID: AB_395798
Mouse monoclonal CD86-APC (clone BU63, used for flow cytometry)	Exbio	Cat# 1A-531-T100; RRID: AB_10734084
Mouse monoclonal CD163-PE (clone GHI/61, used for flow cytometry)	BD	Cat# 556018; RRID: AB_396296
DAPI-Vectashield (for immunofluorescence)	Vector Laboratories	Cat H-1200-10
Mouse monoclonal anti-α-tubulin	Sigma-Aldrich	Cat# T9026
Anti-mouse AlexaFluor 488 conjugated secondary antibody	Life Technologies	Cat # A32723
Alexa Fluor 647 Phalloidin	Life Technologies	Cat # A22287
Mouse monoclonal anti-Cstf64	Kind gift from James Manley	
Mouse anti-tubulin	Sigma	B-5-1-2
Mouse anti-hsc70	SCBT	sc-7298
Rabbit anti-LRP5	Cell Signaling	5731S
Rabbit anti-MAP3K8	Abcam	ab137589
Rabbit anti-MAD1	Abcam	ab175245
Chemicals, Peptides, and Recombinant Proteins		
TURBO DNase	ThermoFisher Scientific	Cat# AM2238
M-CSF	Peprotech	Cat# 300-25
LPS	Sigma-Aldrich	Cat# L4005
IFN-γ	Peprotech	Cat# 300-02
IL-10	Immunotech	Cat# 11340105
Experimental Model: Cell Lines		
RKO (human)	Oliveira Lab	CRL-2577
HCT15 (human)	Oliveira Lab	CRL-225
Experimental Model: Primary Cells		
Primary human macrophages	Immunohemotherapy Service, Centro Hospitalar Universitário São João	
Critical Commercial Assays		
NEBNext Ultra II Directional RNA Library Prep Kit for Illumina	NEB	Cat# E7760
NextSeq High-Output v2 Kit, 75 cycles	Illumina	Cat# FC-404-2005
Superscript IV Reverse Transcriptase	ThermoFisher	Cat# 18090050
Ribo-Zero Gold rRNA removal kit (Human/Mouse/Rat)	Illumina	Cat# MRZG12324
QuantSeq 3'mRNA-Seq library prep kit REV for Illumina	Lexogen	Cat# 016.24

QuantSeq 3'mRNA-Seq PCR Add-on Kit for Illumina	Lexogen	Cat # 020.96
Sybr Green I	ThermoFisher	Cat # S7563
ELISA Kits	Biolegend ThermoFisher Abcam	Cat # 430504 (Human IL-12p70) Cat # 88-7261-88 (Human IL-1ß) ab213775 (Human epiregulin), ab193716 (Human thrombospondin)
Deposited Data		
Raw and processed NGS data (chromatin RNA-Seq and 3' RNA-Seq)		
Oligonucleotides		
siNTC ON-TARGETplus Non-targeting Pool	Dharmacon D-001810-10-05	Sequence (5'-3'), Target sequences: UGGUUUACAUGUCGACUAA UGGUUUACAUGUUGUGUGA UGGUUUACAUGUUUUCUGA UGGUUUACAUGUUUUCCUA
si*SRSF12* ON-TARGETplus SMARTpool siRNA	Dharmacon J-016381-17 J-016381-18 J-016381-19 J-016381-20	Sequence (5'-3'), Target sequences: CUUAAAGAGUCUCGACACA UCUCGAAGUUAUCGUCAUA GCACAAGGUGAUCGCAAAA CCGUGAGUUUGGUCGAUAU
Software and Algorithms		
GENCODE release 38	-	https://www.gencodegenes.org/
FastQC	-	http://www.bioinformatics.babraham.ac.uk/projects/fastqc/
Cutadapt (v.1.13)	(Martin, 2011)	https://cutadapt.readthedocs.io/en/stable/installation.html
Bowtie2 (v.2)	(Langmead *et al.*, 2009)	http://bowtie-bio.sourceforge.net/bowtie2/index.shtml
Tophat (v. 2.0.13)	(Trapnell *et al.*, 2009)	https://ccb.jhu.edu/software/tophat/index.shtml
STAR	(Dobin, 2014; Dobin *et al.*, 2016)	https://github.com/alexdobin/STAR
Samtools (v. 1.6)	(Li *et al.*, 2009)	http://www.htslib.org/doc/samtools.html
htseq-count	-	https://htseq.readthedocs.io/en/release_0.11.1/count.html
DESeq2	(Anders *et al.*, 2015)	http://bioconductor.org/packages/devel/bioc/vignettes/DESeq2/inst/doc/DESeq2.html
DEXSeq	(Love *et al.*, 2014)	https://bioconductor.org/packages/release/bioc/html/DEXSeq.html
Ggplot2	-	https://ggplot2.tidyverse.org/
Heatmap	-	R Studio, v. 3.4.2
Volcano plot	-	GraphPad Prism, v. 7
Deeptools2	-	https://deeptools.readthedocs.io/en/develop/
Seaborn library	-	Python, v.2.7

For ChrRNA-Seq, rRNAs were removed using Ribo-Zero Gold rRNA removal Kit (Human/Mouse/Rat) (Illumina) according to manufacturer's protocol. Chromatin-

bound RNA libraries from three biological replicates were generated using NEBNext Ultra II Directional Prep Kit for Illumina (New England Biolabs), according to the manufacturer's protocol, and sequenced with Illumina NextSeq High-Output Kit, 75 cycles, using paired-end 42-nucleotide reads (Table S1).

For 3' mRNASeq (3' Seq), polyA$^+$ mRNA was obtained from total RNA using Dynabeads mRNA purification kit (ThermoFisher), according to manufacturer's protocol. QuantSeq Rev (Lexogen) mRNA libraries were generated at i3S, Porto, Portugal, using the manufacturer's protocol, quantified using Agilent TapeStation and KAPA Library Quantification Kit (KAPA Biosystems), and sequenced with NextSeq500 using single-end 75-nucleotide reads in the Lexogen Sequencing Facility (Vienna).

For si*NTC* and si*SRSF12*, QuantSeq Rev mRNA libraries were generated from total RNA, using the manufacturer's protocol, quantified using Agilent TapeStation and KAPA Library Quantification Kit and sequenced with NextSeq500 using single-end 75-nucleotide reads in the Lexogen Sequencing Facility.

Data pre-processing | In all datasets, quality control was performed using FastQC and adapters were trimmed with Cutadapt (v1.13), discarding reads under 10 bases.

For ChrRNA-Seq, data were aligned to the reference human genome (hg38) using TopHat (v.2.1) (Kim et al. 2013), allowing read pairs to be separated by 3 kb and only one alignment to the reference genome for each read. Aligned data had 89%-91.2% overall read mapping rate (Supp Table 1).

For 3'Seq gene counts for donors 4 to 6, sequencing data were filtered to detect accurate poly(A) signals, since this sequencing technique may have intrinsic leakiness in polyadenylation signal discovery. Briefly, the input fastq file was mapped to the hg38 reference and three filters were applied in sequence: 1) a Transcript Termination Site (TTS) filter, removing transcripts not lying within ~10 nt of an annotated transcript end site; 2) a Motif filter removed all sequencing peaks whose read start contained a subset of hexamer sequences upstream (Nojima *et al.*, 2015) and 3) a downstream A content filter checked the amount of As in a window downstream of the read start; if a given peak passes the validated threshold, the read is considered internal priming and is removed. All reads passing the three filters are retained as non-internal priming. Total fragments passing all filters ranged from 47.4-70.7% (Suppl Table 2). Data were aligned to the reference human genome (hg38) using STAR (Derti *et al.*, 2012; Gruber

et al., 2016; Liu, Hoque, *et al.*, 2017). Aligned data had 75.6%-85.4% overall read mapping rate (Suppl Table 2).

For 3'Seq for donors 7 and 8, the bioinformatic pipeline was equal, with the exception that the initial filtering algorithm was not applied, to include unproductive transcripts in the analysis.

In all datasets, aligned reads were processed with SAMtools (Dobin *et al*., 2016) and counted with htseq-count (Li *et al.*, 2009) and gene expression differences were calculated using DESeq2 (Anders *et al.*, 2015). Sequencing read distribution through the genome was visualized in IGV, v 7.0, using BedGraphToBigWig.

To increase statistical robustness to our analysis, we only considered genes with >5 mean TPM, Log2Fold Changes ≥ 1 or ≤ -1, and adjusted p-value < 0,05, calculated by DESeq2 (Love *et al.*, 2014). Additionally, to establish data set reproducibility, we used, used 3 independent experiments with macrophages from three donors and analyzed the Pearson correlation values. R values exceeded 0.9 for each condition, exceeded 0.8 between pro-inflammatory and co-cultured macrophages, and exceeded 0.5 between M0 and M1 (Figure S1G).

mRNA isoform expression differences were calculated in the 3'Seq data using DEXSeq (Love *et al.*, 2014). Alternative polyadenylation was considered when and if two or more alternative 3' UTRs were expressed and the second highest mRNA isoform level was at least 10% of the highest isoform, in at least two replicates. For downstream analyses, we focused on isoforms of protein-coding genes, excluding out-of-scope isoforms such as NMD.

To clarify the identity of each mRNA isoform being produced in each condition, mRNA isoforms detected by 3' RNA-Seq were compared to Chr-bound RNA-Seq data from M1 and M1 + RKO macrophages and to transcripts deposited in the ENSEMBL database.

Human primary macrophages | Human monocytes were isolated from anonymized buffy coats kindly provided by the Immunohemotherapy Service at Centro Hospitalar Universitário São João, Porto, Portugal. All experiments using human cells were conducted according to Portuguese and European guidelines for human research and approved by the institutional ethics committee (Protocol 90/19). Blood donors signed

informed consent forms as part of the Ethics Committee guidelines. Healthy blood donors aged below 40 years old were selected for isolation.

Methods Details

Reagents | Macrophage colony stimulating factor (M-CSF, 300-25, Peprotech), lipopolysaccharide (LPS, L4005, Sigma-Aldrich), interferon-gamma (IFNγ, 300-02, Peprotech) and IL-10 (11340105, Immunotech) were prepared as in the manufacturers' instructions. RPMI 1640 medium, streptomycin, penicillin, trypan blue and heat-inactivated fetal bovine serum (FBS) were obtained from Gibco. Bovine Serum Albumin (BSA) was obtained from nzytech.

Cell lines | RKO and HCT-15 cells, both from American Type Culture Collection (ATCC) were maintained in complete Roswell Park Memorial Institute 1640 medium (RPMI) with GlutaMAX and supplemented with 10% FBS, 100 U/mL penicillin and 100 µg/mL streptomycin antibiotic solution. Cells were kept at 37ºC, 5% CO_2 in a humidified incubator, and subcultured every 3 to 5 days to maintain subconfluency. Trypan blue dye (Gibco) exclusion test was used to assess cell viability.

Human monocyte isolation | Briefly, peripheral blood mononuclear cells (PBMCs) were isolated from buffy coats using Ficoll gradient centrifugation, followed by enrichment of $CD14^+$ cells using $CD14^+$ magnetic beads (Miltenyi Biotech, 130-050-201), according to the manufacturer instructions.

Macrophage differentiation and activation | $1x10^6$ human $CD14^+$ cells were plated on 6-multiwell plates and maintained in RPMI 1640 medium supplemented with 10% FBS (Gibco), 100 U/mL penicillin (Invitrogen), 100 µg/mL streptomycin (Invitrogen) and 50 ng/mL M-CSF (Peprotech), and differentiated for 7 days. On day 7, media was refreshed and cells were polarized using 100 ng/mL LPS (Sigma-Aldrich) and 25 ng/mL IFNγ (Peprotech) (for pro-inflammatory M1 macrophages) or 10 ng/mL IL-10 (for anti-inflammatory M2 macrophages) in RPMI 1640 medium supplemented with 2% FBS without antibiotics for additional 24 h. Non-polarized M0 macrophages were maintained in RPMI 2% FBS without antibiotics. At the end of the experiment, spent culture media were collected for ELISA.

Macrophage-cancer cell indirect co-cultures | 24 hours after macrophage polarization, $3x10^5$ RKO or HCT-15 cells were Millenia seeded into transwell inserts with 1.0 µm pore size membrane (Corning 353102) and put on top of $1x10^6$ M1 macrophages. Co-cultures were maintained in complete RPMI 1640 medium for 24 h at 37º C and 5% CO2 in a humidified atmosphere, after which both cell populations and cell culture media were collected for downstream assays.

Immunofluorescence | Macrophages grown on coverslips were fixed using 4% paraformaldehyde in 1X PBS for 15 min. Cells were quenched in 50 mM ammonium chloride for 10 min, permeabilized in 0.2 % Triton X-100 in 1x PBS for 5 min and incubated in 5% BSA blocking solution for 30 min, all at room temperature, before incubating for 1 h with mouse anti-ß-tubulin and for 45 min with anti-mouse AlexaFluor 488 secondary antibody, protecting from light. Coverslips were then incubated with Phalloidin-FITC for 15 min at room temperature, and mounted with DAPI-Vectashield. Confocal images were acquired in a Leica Spectral Confocal TCS-SP5 AOBS (Wetzlar, Germany) microscope, using the 40x or 63x oil objective. All experimental conditions were surveyed using the same microscope conditions. Images were analyzed and processed using the FIJI package for Image J (Schindelin *et al.*, 2012).

Flow cytometry | Macrophages were incubated with Accutase (eBioscience, Asymetrix) for 30 min at 37 ºC, harvested by gentle scraping, washed with 1x PBS and resuspended in FACS buffer (1x PBS, 2% FBS, 0.02% sodium azide), blocked with FACS blocking reagent and resuspended in diluted antibodies for 30 min at 4ºC in the dark: CD14-FITC (BD 555397, clone M5E2, 1:50 dilution), CD86-APC (Exbio 1A-531, clone BU63, 1:25 dilution), and CD163-PE (BD 556018, clone GHI/61, 1:25 dilution). Unstained cells were used as control. Cell surface markers were detected on FACS Canto II (BD Biosciences), using FACS Diva® software, and data were analyzed using FlowJo software v.10.4.

***in silico* analyses |** Nucleotide sequences and mRNA profiles were obtained from NCBI and Ensembl genome browsers. The Ensembl and UCSC genome browsers and the APAdb and Aceview databases were accessed to search for alternative polyadenylation sites on the 3' UTR of human genes.

RNA extraction | Cells were washed with ice-cold PBS and resuspended in 500 µL TRIzol (Invitrogen) to extract total RNA according to manufacturer's instructions, with the exception that all samples were incubated at -80ºC during isopropanol precipitation. Total RNA quantity was determined with a Nanodrop 2000 spectrometer (Thermo Fisher Scientific) or a Qubit Fluorometer, using Qubit RNA HS Assay Kit (ThermoFisher).

cDNA synthesis and Quantitative Real-Time PCR (RT-qPCR) | Total RNA was digested with DNase I (Roche) for 25 min at 37ºC, inactivating the enzyme for 10 min at 80ºC. RNA was reverse transcribed using SuperScript IV (ThermoFisher) and random hexamers, according to manufacturer's instructions. RT-qPCR reactions were performed in triplicate using SYBR Select Master Mix (Applied Biosystems) following the manufacturer's protocol and 0.125 µM of the primer pairs listed in Supplementary Table 3. Negative controls without reverse transcriptase were used to detect possible gDNA contamination. Relative expression was calculated relative to the reference gene *18S*. For quantification of the relative expression of *CCR7* and *TGFB*, RT-qPCR reactions were performed in triplicates using TaqMan Probes and Master Mix (Applied Biosystems). Relative expression was calculated relative to the reference gene *ACTB*. Results were analyzed applying the ΔΔCt method (Livak & Schmittgen, 2001).

Primer Design | For RT-qPCR of APA candidates, primers were designed to the coding and most distal PAS (pA2), as previously described (Anders *et al.*, 2012). Primer sequences used in the RT-qPCRs are listed on Supplementary Table 2.

Chromatin-bound fractionation | Total RNA from macrophages was fractionated as described in Nojima *et al.* 2016. Briefly, $6x10^6$ cells for each condition were washed twice with ice-cold 1x PBS, spun down, and cell pellets were lysed with HLB/NP40 buffer (10 mM Tris-HCl pH 7.5 / 10 mM NaCl / 2.5 mM $MgCl_2$ / 0.05% NP-40 Igepal (Sigma)), carefully underlaid with HLB/NP40/Sucrose (HLB/NP-40 + 25% sucrose) and centrifuged at 208 *g* for 5 minutes at 4ºC to isolate the nuclei from the cytoplasm. The chromatin fraction was isolated via treatment with NUN1 solution (20 mM Tris-HCl pH 7.9 / 75 mM EDTA / 50% v/v glycerol / Protease Inhibitor cOmplete 1x (Roche) added fresh) and NUN2 buffer (20 mM HEPES-KOH pH 7.6 / 300 mM NaCl / 0.2 mM EDTA / 7.5 mM $MgCl_2$ / 1% v/v Igepal / 1 M Urea), with 15 min incubating on ice,

followed by centrifugation at 15680 *g* for 10 minutes at 4ºC, separating from the nucleoplasm supernatant. The RNA-bound chromatin pellet was then resuspended in high salt buffer HSB (10 mM Tris-HCl pH 7.5 / 500 mM NaCl / 10 mM $MgCl_2$) and digested with TURBO DNase (Invitrogen) and Proteinase K (10 mg/mL; Ambion) for 10 min each at 37ºC and 182 *g* for 10 min. All buffers were ice-cold. RNA was then extracted from the cytoplasmic and chromatin-bound fractions with Trizol. To ensure adequate fraction separation was achieved, *MALAT1* RNA levels were measured by RT-qPCR in cytoplasmic and chromatin-bound fractions; *MALAT1* presence was only detected in the chromatin-bound fraction.

RNA-Seq

Library preparation

For ChrRNA-Seq, rRNAs were removed using Ribo-Zero Gold rRNA removal Kit (Human/Mouse/Rat) (Illumina) according to manufacturer's protocol. Chromatin-bound RNA libraries from three biological replicates were generated using NEBNext Ultra II Directional Prep Kit for Illumina (New England Biolabs), according to the manufacturer's protocol, and sequenced with Illumina NextSeq High-Output Kit, 75 cycles, using paired-end 42-nucleotide reads.

For 3'mRNASeq (3'Seq), polyA$^+$ mRNA was obtained from total RNA using Dynabeads mRNA purification kit (ThermoFisher), according to manufacturer's protocol. QuantSeq Rev (Lexogen) mRNA libraries were generated at i3S, Porto, Portugal, using the manufacturer's protocol, quantified using Agilent TapeStation and KAPA Library Quantification Kit (KAPA Biosystems), and sequenced with NextSeq500 using single-end 75-nucleotide reads in the Lexogen Sequencing Facility (Vienna).

For si*NTC* and si*SRSF12*, QuantSeq Rev mRNA libraries were generated from total RNA, using the manufacturer's protocol, quantified using Agilent TapeStation and KAPA Library Quantification Kit and sequenced with NextSeq500 using single-end 75-nucleotide reads in the Lexogen Sequencing Facility.

Data pre-processing

In all datasets, quality control was performed using FastQC and adapters were trimmed with Cutadapt (v1.1), discarding reads under 10 bases.

For ChrRNA-Seq, data were aligned to the reference human genome (hg38) using TopHat (v.2.1) (Trapnell *et al.*, 2009), allowing read pairs to be separated by 3 kb and

only one alignment to the reference genome for each read. Aligned data had 89%-91.2% overall read mapping rate (Supp Table 1).

For 3'Seq gene counts for donors 4 to 6, sequencing data were filtered to detect accurate poly(A) signals, since this sequencing technique may have intrinsic leakiness in polyadenylation signal discovery. Briefly, the input fastq file was mapped to the hg38 reference and three filters were applied in sequence: 1) a Transcript Termination Site (TTS) filter, removing transcripts not lying within ~10 nt of an annotated transcript end site; 2) a Motif filter removing all sequencing peaks whose read start contained a subset of hexamer sequences upstream (Nojima *et al.*, 2015) and 3) a downstream A content filter checked the amount of As in a window downstream of the read start; if a given peak passes the validated threshold, the read is considered internal priming and is removed. All reads passing the three filters are retained as non-internal priming. Total fragments passing all filters ranged from 47.4-70.7% (Suppl Table 2). Data were aligned to the reference human genome (hg38) using STAR (Derti *et al.*, 2012; Gruber *et al.*, 2016; Liu, Hoque, *et al.*, 2017). Aligned data had 75.6%-85.4% overall read mapping rate (Suppl Table 2).

For 3'Seq for donors 7 and 8, the bioinformatic pipeline was equal, with the exception that the initial filtering algorithm was not applied, to include unproductive transcripts in the analysis.

In all datasets, aligned reads were processed with SAMtools (Dobin *et al.*, 2016) and counted with htseq-count (Li *et al.*, 2009) and gene expression differences were calculated using DESeq2 (Anders *et al.*, 2015). Sequencing read distribution through the genome was visualized in IGV, v 7.0, using BedGraphToBigWig.

mRNA isoform expression differences were calculated in the 3'Seq data using DEXSeq (Love *et al.*, 2014). Alternative polyadenylation was considered when and if two or more alternative 3' UTRs were expressed and the second highest mRNA isoform level was at least 10% of the highest isoform, in at least two replicates. For downstream analyses, we focused on isoforms of protein-coding genes, excluding out-of-scope isoforms such as NMD.

To clarify the identity of each mRNA isoform being produced in each condition, 3'seq mRNA isoforms were compared to Chr-bound RNA-Seq data from M1 and M1 + RKO macrophages and to transcripts deposited in the ENSEMBL database.

Candidate gene selection | Criteria for 3'seq candidate gene validation were as follows: DGE candidates were selected for large fold change differences between control and co-cultured macrophages, robustness of response after macrophage co-culture with both CRC cell lines, and relevance to macrophage biology. mRNA isoform candidates were selected according to the following criteria: i) prevalent 3' UTR mRNA isoform shift between the 3' R NA-Seq signal in the two mRNA isoforms with the highest reads, ii) robustness of response after macrophage polarization and co-culture with both cell lines (increase in proximal or distal mRNA isoform) and iii) relevance to macrophage biology and inflammation.

TCGA analysis of patient survival | Datasets for colon carcinoma and normal tissue were procured in the Cancer Genome Atlas (TCGA (*The Cancer Genome Atlas*, n.d.)) and analyzed for post-diagnosis survival data, using TIMER. The normal tissue median values were used as threshold to define "high" and "low" expression levels for each identified DEGs in cancer patients, quantified as FPKM (fragments per Kilobase million). The correlation index (R) indicated a moderate correlation if between 0.25 and 0.35, and a strong correlation if higher than 0.35.

Gene Set Enrichment Analysis (GSEA) | Functional annotation enrichment was performed on the genes with differential expression using GSEA software (Broad Institute).

Enzyme-Linked Immunosorbent Assay (ELISA) | Cytokines IL-1ß, IL-6, and IL12p70, and metabolites epiregulin and thrombospondin (TSP1) were measured in the culture media of mono and co-cultures by ELISA using kits by ThermoFisher (IL1ß), BioLegend (IL-6 and IL12p70) and Abcam (epiregulin and TSP1), according to manufacturer's instructions.

Macrophage siRNA knockdown | Briefly, 50 nM of a pool of 4 *SRSF12* siRNAs (Dharmacon ONTARGETplus SMARTpool si*SRSF12*) or 50 nM of a pool of a non-targeting siRNA control (Dharmacon ONTARGETplus SMARTpool si*NTC*) were transfected into $1.5x10^6$ M1 macrophages in 6-multiwells using 4 µL GenMute for Primary Human Macrophages (SignaGen) as a transfection agent, according to manufacturer's instructions. KD levels were assayed through RT-qPCR.

Western Blot | Macrophage lysates were prepared with RIPA buffer (50 mM Tris-HCl pH 7.5 / 1% NonidetP (NP)-40 / 150 mM NaCl / 2 mM EDTA) with protease inhibitors (Protease Inhibitor cOmplete 1x). Protein concentration was determined through the Bradford method and 25 µg of protein was loaded and run in a 7.5% (for LRP5) or 10% acrylamide gel, which was subsequently transferred into nitrocellulose membranes (GE Healthcare), blocked with 5% non-fat powdered milk or BSA in TBS + 0.1 % Tween 20 (TBS-T) for 1 hour, and incubated overnight with primary antibodies at 4ºC (see STAR Methods Table). HRP-conjugated anti-mouse or anti-rabbit secondary antibodies (SCBT) were incubated for 1 hour at RT. Signal was detected by incubation with ECL Substrate (GE Healthcare), using the Chemidoc Imaging System (BioRad) and band intensity was measured in the ImageLab Software (BioRad).

Statistical analysis | All presented data is mean ± standard deviation (SD). Data was evaluated for normal distribution through the Kolmogorov-Smirnov test. Comparisons between two independent groups were performed using the paired Student's t-test or the Wilcoxon test. Except where otherwise stated, p-values <0.05 were considered statistically significant (* = $p < 0.05$; ** = $p < 0.01$; *** = $p < 0.005$; **** = $p < 0.0001$). Graphs were made in the GraphPad Prism software, using version 7.0a for Mac, GraphPad Software, La Jolla California USA, www.graphpad.com.

Acknowledgements

We thank members of the Gene Regulation and Tumor and Microenvironment Interactions groups at i3S, and the Proudfoot's and Murphy's laboratories at the University of Oxford, for critical discussions.

This work was supported by the Fundação para a Ciência e Tecnologia (FCT) by funding to AM (project "Cancer Research on Therapy Resistance: From Basic Mechanisms to Novel Targets" - NORTE-01-0145-FEDER-000051, supported by Norte Portugal Regional Operational Programme (NORTE 2020), under the PORTUGAL 2020 Partnership Agreement, through the European Regional Development Fund (ERDF); and Programa Operacional Regional do Norte and co-funded by European Regional Development Fund under the project "The Porto

Comprehensive Cancer Center" with the reference NORTE-01-0145-FEDER-072678 - Consórcio PORTO.CCC – Porto.Comprehensive Cancer Center), to NJP (Wellcome Trust Investigator Award [107928/Z/15/Z] and ERC Advanced [339270] grants), to IPC (DL 57/2016/CP1355/CT0016) and to JW by FCT/GABBA PhD fellowship (PD/BD/114168/2016) and FOLSMART fellowship (H2020-NMP-PILOTS-2015-683356-FOLSMART).

The authors acknowledge the Immunohemotherapy Service at Centro Hospitalar Universitário São João for their kind donation of the buffy coats needed for this study. The authors also acknowledge the i3S Scientifics Platforms: María Lázaro from the Bioimaging unit (member of the Portuguese Platform of Bioimaging - PPBI-POCI-01-0145-FEDER-022122), Paula Magalhães and Tânia Meireles from the Cell Culture and Genotyping unit, and Mafalda Rocha and Rob Mensink from the Genomics Unit, and Catarina Meireles from the Translational Cytometry Unit. JW also acknowledges Bruno Pereira for help with the GSEA software (Broad Institute).

Ethical Statement

Buffy coats are waste-products from healthy blood donations that contain high amounts of leukocytes, which are isolated in accordance with protocol 90/19 approved by the Centro Hospitalar Universitário São João Ethics Committee. Anonymized donors filled informed consent forms prior to each blood donation.

Author Contributions

JW performed all molecular biology and transcriptomic experiments with help from IPC (siRNA transfections and chromatin-bound fractionation), JF (FACS analyses), AMC (macrophage polarization RT-qPCR and Western blots) and TN (RNA library preparation). JW, with advice from MT, performed all bioinformatics analyses. JW, MJO, AM, SM and NJP designed the project and wrote the paper.

Data and Code Availability Statement

The datasets generated during this study are available at Gene Expression Omnibus – reference code GSE163726.

References

Abdelwahab, E. M. M., Rapp, J., Feller, D., Csongei, V., Pal, S., Bartis, D., Thickett, D. R., & Pongracz, J. E. (2019). Wnt signaling regulates trans-differentiation of stem cell like type 2 alveolar epithelial cells to type 1 epithelial cells. Respiratory Research, 20(1), 1–9. https://doi.org/10.1186/s12931-019-1176-x

Aghabozorgi, A. S., Bahreyni, A., Soleimani, A., Bahrami, A., Khazaei, M., Ferns, G. A., Avan, A., & Hassanian, S. M. (2019). Role of adenomatous polyposis coli (APC) gene mutations in the pathogenesis of colorectal cancer; current status and perspectives. Biochimie, 157, 64–71. https://doi.org/10.1016/j.biochi.2018.11.003

Ahmed, D., Eide, P. W., Eilertsen, I. A., Danielsen, S. A., Eknæs, M., Hektoen, M., Lind, G. E., & Lothe, R. A. (2013). Epigenetic and genetic features of 24 colon cancer cell lines. Oncogenesis, 2(0424), e71. https://doi.org/10.1038/oncsis.2013.35

Anders, S., Pyl, P. T., & Huber, W. (2015). HTSeq-A Python framework to work with high-throughput sequencing data. Bioinformatics, 31(2), 166–169. https://doi.org/10.1093/bioinformatics/btu638

Anders, S., Reyes, A., & Huber, W. (2012). Detecting differential usage of exons from RNA-seq data. Genome Research, 22(10), 2008–2017. https://doi.org/10.1101/gr.133744.111

Armaghany, T., Wilson, J. D., Chu, Q., & Mills, G. (2012). Genetic alterations in colorectal cancer. Gastrointestinal Cancer Research : GCR, 5(1), 19–27.

Berkovits, B. D., & Mayr, C. (2015). Alternative 3' UTRs act as scaffolds to regulate membrane protein localization. Nature, 522(7556), 363–367. https://doi.org/10.1038/nature14321

Bögels, M., Braster, R., Nijland, P. G., Gül, N., van de Luijtgaarden, W., Fijneman, R. J. A., Meijer, G. A., Jimenez, C. R., Beelen, R. H. J., & van Egmond, M. (2012). Carcinoma origin dictates differential skewing of monocyte function. Oncoimmunology, 1(6), 798–809. https://doi.org/10.4161/onci.20427

Bohlson, S. S., O'Conner, S. D., Hulsebus, H. J., Ho, M.-M., & Fraser, D. a. (2014). Complement, c1q, and c1q-related molecules regulate macrophage polarization. Frontiers in Immunology, 5(August), 402. https://doi.org/10.3389/fimmu.2014.00402

Braz, S. O., Cruz, A., Lobo, A., Bravo, J., Moreira-Ribeiro, J., Pereira-Castro, I., Freitas, J., Relvas, J. B., Summavielle, T., & Moreira, A. (2017). Expression of Rac1 alternative 3′ UTRs is a cell specific mechanism with a function in dendrite outgrowth in cortical neurons. Biochimica et Biophysica Acta - Gene Regulatory Mechanisms, 1860(6), 685–694. https://doi.org/10.1016/j.bbagrm.2017.03.002

Cai, J., Song, X., Wang, W., Watnick, T., Pei, Y., Qian, F., & Pan, D. (2018). A RhoA – YAP – c-Myc signaling axis promotes the development of polycystic kidney disease. Genes & Development, 1–13. https://doi.org/10.1101/gad.315127.118.GENES

Caputo, F., Santini, C., Bardasi, C., Cerma, K., Casadei-Gardini, A., Spallanzani, A., Andrikou, K., Cascinu, S., & Gelsomino, F. (2019). BRAF-mutated colorectal cancer: Clinical and molecular insights. International Journal of Molecular Sciences, 20(21). https://doi.org/10.3390/ijms20215369

Cardoso, A. P., Pinto, M. L. T., Pinto, A. T., Monteiro, C., Oliveira, M. I. M. J., Santos, S. G., Relvas, J. B., Seruca, R., Mantovani, A., Mareel, M., & Barbosa, M. A. (2015). Matrix metalloproteases as maestros for the dual role of LPS- and IL-10-stimulated macrophages in cancer cell behaviour. BMC Cancer, 15, 456. https://doi.org/10.1186/s12885-015-1466-8

Castello, A., Fischer, B., Eichelbaum, K., Horos, R., Beckmann, B. M., Strein, C., Davey, N. E., Humphreys, D. T., Preiss, T., Steinmetz, L. M., Krijgsveld, J., & Hentze, M. W. (2012). Insights into RNA Biology from an Atlas of Mammalian mRNA-Binding Proteins. Cell, 149(6), 1393–1406. https://doi.org/10.1016/j.cell.2012.04.031

Castelo-Branco, P., Furger, A., Wollerton, M., Smith, C., Moreira, A., & Proudfoot, N. (2004). Polypyrimidine tract binding protein modulates efficiency of polyadenylation. Molecular and Cellular Biology, 24(10), 4174–4183. https://doi.org/10.1128/MCB.24.10.4174

Chandler, S. D., Mayeda, A., Yeakley, J. M., Krainer, A. R., & Fu, X. D. (1997). RNA splicing specificity determined by the coordinated action of RNA recognition motifs in SR proteins. Proceedings of the National Academy of Sciences of the United States of America, 94(8), 3596–3601. https://doi.org/10.1073/pnas.94.8.3596

Cowper, A. E., Caceres, J. F., Mayeda, A., & Screaton, G. R. (2001). Serine-Arginine (SR) Protein-like Factors That Antagonize Authentic SR Proteins and Regulate Alternative Splicing. Journal of Biological Chemistry, 276(52), 48908–48914. https://doi.org/10.1074/jbc.M103967200

De Schepper, S., Verheijden, S., Aguilera-Lizarraga, J., Viola, M. F., Boesmans, W., Stakenborg, N., Voytyuk, I., Smidt, I., Boeckx, B., Dierckx de Casterlé, I., Baekelandt, V., Gonzalez Dominguez, E., Mack, M., Depoortere, I., De Strooper, B., Sprangers, B., Himmelreich, U., Soenen, S., Guilliams, M., … Boeckxstaens, G. (2018). Self-Maintaining Gut Macrophages Are Essential for Intestinal Homeostasis. Cell, 175(2), 400-415.e13. https://doi.org/10.1016/j.cell.2018.07.048

Del Valle Morales, D., Trotman, J. B., Bundschuh, R., & Schoenberg, D. R. (2020). Inhibition of cytoplasmic cap methylation identifies 5 top mrnas as recapping targets and reveals recapping sites downstream of native 5 ends. Nucleic Acids Research, 48(7), 3806–3815. https://doi.org/10.1093/NAR/GKAA046

DeNardo, D. G., & Ruffell, B. (2019). Macrophages as regulators of tumour immunity and immunotherapy. Nature Reviews Immunology, 19(6), 369–382. https://doi.org/10.1038/s41577-019-0127-6

Derti, A., Garrett-Engele, P., MacIsaac, K. D., Stevens, R. C., Sriram, S., Chen, R., Rohl, C. A., Johnson, J. M., & Babak, T. (2012). A quantitative atlas of polyadenylation in five mammals. Genome Research, 22(6), 1173–1183. https://doi.org/10.1101/gr.132563.111

Diaz-Muñoz, M. D., Bell, S. E., Fairfax, K., Monzon-Casanova, E., Cunningham, A. F., Gonzalez-Porta, M., Andrews, S. R., Bunik, V. I., Zarnack, K., Curk, T., Heggermont, W. A., Heymans, S., Gibson, G. E., Kontoyiannis, D. L., Ule, J., & Turner, M. (2015). The RNA-binding protein HuR is essential for the B cell antibody response. Nature Immunology, 16(4), 415–425. https://doi.org/10.1038/ni.3115

Dobin, A. (2014). STAR manual 2.4.0.1. 1–33. https://doi.org/10.1093/bioinformatics/bts635

Dobin, A., Gingeras, T. R., Spring, C., Flores, R., Sampson, J., Knight, R., Chia, N., & Technologies, H. S. (2016). Mapping RNA-seq Reads with STAR. Curr Protoc Bioinformatics, 51(4), 586–597. https://doi.org/10.1002/0471250953.bi1114s51.Mapping

Domingues, R. G., Lago-Baldaia, I., Pereira-Castro, I., Fachini, J. M., Oliveira, L., Drpic, D., Lopes, N., Henriques, T., Neilson, J. R., Carmo, A. M., & Moreira, A. (2016). CD5 expression is regulated during human T-cell activation by alternative polyadenylation, PTBP1, and miR-204. European Journal of Immunology, 46(6), 1490–1503. https://doi.org/10.1002/eji.201545663

Dye, M. J., & Proudfoot, N. J. (1999). Terminal exon definition occurs cotranscriptionally and promotes termination of RNA polymerase II. Molecular Cell, 3(3), 371–378. https://doi.org/10.1016/S1097-2765(00)80464-5

Elkon, R., Ugalde, A. P., & Agami, R. (2013). Alternative cleavage and polyadenylation: extent, regulation and function. Nature Reviews Genetics, 14(7), 496–506. https://doi.org/10.1038/nrg3482

Eren, E., Tufekci, K. U., Isci, K. B., Tastan, B., Genc, K., & Genc, S. (2018). Sulforaphane inhibits lipopolysaccharide-induced inflammation, cytotoxicity, oxidative stress, and miR-155 expression and switches to Mox phenotype through activating extracellular signal-regulated kinase 1/2-nuclear factor erythroid 2-related factor 2/an. Frontiers in Immunology, 9(JAN), 1–18. https://doi.org/10.3389/fimmu.2018.00036

Fearon, E. R., & Vogelstein, B. (1990). A genetic model for colorectal tumorigenesis. Cell, 61(5), 759–767. https://doi.org/10.1016/0092-8674(90)90186-I

Feng, Y., Ren, J., Gui, Y., Wei, W., Shu, B., Lu, Q., Xue, X., Sun, X., He, W., Yang, J., & Dai, C. (2018). Wnt/b-catenin–Promoted macrophage alternative activation contributes to kidney fibrosis. Journal of the American Society of Nephrology, 29(1), 182–193. https://doi.org/10.1681/ASN.2017040391

Fischl, H., Neve, J., Wang, Z., Patel, R., Louey, A., Tian, B., & Furger, A. (2019). hnRNPC regulates cancer-specific alternative cleavage and polyadenylation profiles. Nucleic Acids Research, 47(14), 7580–7591. https://doi.org/10.1093/nar/gkz461

Giannakis, M., Mu, X. J., Shukla, S. A., Qian, Z. R., Cohen, O., Nishihara, R., Bahl, S., Cao, Y., Amin-Mansour, A., Yamauchi, M., Sukawa, Y., Stewart, C., Rosenberg, M., Mima, K., Inamura, K., Nosho, K., Nowak, J. A., Lawrence, M. S., Giovannucci, E. L., … Garraway, L. A. (2016). Genomic Correlates of Immune-Cell Infiltrates in Colorectal Carcinoma. Cell Reports, 15(4), 857–865. https://doi.org/10.1016/j.celrep.2016.03.075

Gong, M., Zhuo, X., & Ma, A. (2017). STAT6 Upregulation Promotes M2 Macrophage Polarization to Suppress Atherosclerosis. Medical Science Monitor Basic Research, 23, 240–249. https://doi.org/10.12659/msmbr.904014

Goossens, P., Rodriguez-Vita, J., Etzerodt, A., Masse, M., Rastoin, O., Gouirand, V., Ulas, T., Papantonopoulou, O., Van Eck, M., Auphan-Anezin, N., Bebien, M., Verthuy, C., Vu Manh, T. P., Turner, M., Dalod, M., Schultze, J. L., & Lawrence, T. (2019). Membrane Cholesterol Efflux Drives Tumor-Associated Macrophage Reprogramming and Tumor Progression. Cell Metabolism, 1–14. https://doi.org/10.1016/j.cmet.2019.02.016

Gruber, A. J., Schmidt, R., Ghosh, S., Martin, G., Gruber, A. R., van Nimwegen, E., & Zavolan, M. (2018). Discovery of physiological and cancer-related regulators of 3' UTR processing with KAPAC. Genome Biology, 19(1), 1–17. https://doi.org/10.1186/s13059-018-1415-3

Gruber, A. J., Schmidt, R., Gruber, A. R., Martin, G., Ghosh, S., Belmadani, M., Keller, W., & Zavolan, M. (2016). A comprehensive analysis of 3' end sequencing data sets reveals novel polyadenylation signals and the repressive role of heterogeneous ribonucleoprotein C on cleavage and polyadenylation. Genome Research, 26(8), 1145–1159. https://doi.org/10.1101/gr.202432.115

Gruber, A. R., Martin, G., Muller, P., Schmidt, A., Gruber, A. J., Gumienny, R., Mittal, N., Jayachandran, R., Pieters, J., Keller, W., van Nimwegen, E., & Zavolan, M. (2014). Global 3' UTR shortening has a limited effect on protein abundance in proliferating T cells. Nat Commun, 5, 5465. https://doi.org/10.1038/ncomms6465

Hanahan, D., & Weinberg, R. A. (2000). The Hallmarks of Cancer. 100, 57–70.

Hanahan, D., & Weinberg, R. A. (2011). Hallmarks of cancer: The next generation. Cell, 144(5), 646–674. https://doi.org/10.1016/j.cell.2011.02.013

Hao, N. B., Lü, M. H., Fan, Y. H., Cao, Y. L., Zhang, Z. R., & Yang, S. M. (2012). Macrophages in tumor microenvironments and the progression of tumors. Clinical and Developmental Immunology, 2012. https://doi.org/10.1155/2012/948098

Hardy, J. G., & Norbury, C. J. (2016). Cleavage factor Im (CFIm) as a regulator of alternative polyadenylation. Biochemical Society Transactions, 44(4), 1051–1057. https://doi.org/10.1042/BST20160078

Jia, X., Yuan, S., Wang, Y., Fu, Y., Ge, Y. Y., Ge, Y. Y., Lan, X., Feng, Y., Qiu, F., Li, P., Chen, S., & Xu, A. (2017). The role of alternative polyadenylation in the antiviral innate immune response. Nature Communications, 8, 14605. https://doi.org/10.1038/ncomms14605

Kadl, A., Meher, A., Sharma, P., Lee, M., Doran, A., Johnstone, S., Elliott, M., Gruber, F., Han, J., Chen, W., Kensler, T., Ravichandran, K., & Leitinge, N. (2010). Identification of a novel macrophage phenotype that develops in response to atherogenic phospholipids via Nrf2. Circ Res., 107(6), 737–746. https://doi.org/10.1161/CIRCULATIONAHA.110.956839

Kahles, A., Lehmann, K.-V., Toussaint, N. C., Hüser, M., Stark, S. G., Sachsenberg, T., Stegle, O., Kohlbacher, O., Sander, C., Caesar-Johnson, S. J., Demchok, J. A., Felau, I., Kasapi, M., Ferguson, M. L., Hutter, C. M., Sofia, H. J., Tarnuzzer, R., Wang, Z., Yang, L., … Rätsch, G. (2018). Comprehensive Analysis of Alternative Splicing Across Tumors from 8,705 Patients. Cancer Cell, 0(0), 211–224. https://doi.org/10.1016/J.CCELL.2018.07.001

Kaler, P., Augenlicht, L., & Klampfer, L. (2009). Macrophage-derived IL-1B stimulates Wnt signaling and growth of colon cancer cells: A crosstalk interrupted by vitamin D"3. Oncogene, 28(44), 3892–3902. https://doi.org/10.1038/onc.2009.247

Kamieniarz-Gdula, K., Gdula, M. R., Panser, K., Nojima, T., Monks, J., Wiśniewski, J. R., Riepsaame, J., Brockdorff, N., Pauli, A., & Proudfoot, N. J. (2019). Selective Roles of Vertebrate PCF11 in Premature and Full-Length Transcript Termination. Molecular Cell, 74(1), 158-172.e9. https://doi.org/10.1016/j.molcel.2019.01.027

Kim, M., Lim, J., Lee, J. H., Lee, K. M., Kim, S., Park, K. W., Nho, C. W., & Cho, Y. S. (2018). Understanding the functional role of genistein in the bone differentiation in mouse osteoblastic cell line MC3T3-E1 by RNA-seq analysis. Scientific Reports, 8(1), 1–12. https://doi.org/10.1038/s41598-018-21601-9

Lai, B., Wang, J., Fagenson, A., Sun, Y., Saredy, J., Lu, Y., Nanayakkara, G., Yang, W. Y., Yu, D., Shao, Y., Drummer, C., Johnson, C., Saaoud, F., Zhang, R., Yang, Q., Xu, K., Mastascusa, K., Cueto, R., Fu, H., … Yang, X. (2019). Twenty Novel Disease Group-Specific and 12 New Shared Macrophage Pathways in Eight Groups of 34 Diseases Including 24 Inflammatory Organ Diseases and 10 Types of Tumors. Frontiers in Immunology, 10(November). https://doi.org/10.3389/fimmu.2019.02612

Langmead, B., Trapnell, C., Pop, M., & Salzberg, S. L. (2009). Ultrafast and memory-efficient alignment of short DNA sequences to the human genome. Genome Biology, 10(3). https://doi.org/10.1186/gb-2009-10-3-r25

Larionova, I., Tuguzbaeva, G., Ponomaryova, A., Stakheyeva, M., Cherdyntseva, N., Pavlov, V., Choinzonov, E., & Kzhyshkowska, J. (2020). Tumor-Associated Macrophages in Human Breast, Colorectal, Lung, Ovarian and Prostate Cancers. Frontiers in Oncology, 10(October), 1–34. https://doi.org/10.3389/fonc.2020.566511

Lawrence, T., & Natoli, G. (2011). Transcriptional regulation of macrophage polarization: Enabling diversity with identity. Nature Reviews Immunology, 11(11), 750–761. https://doi.org/10.1038/nri3088

Lee, S. H., Singh, I., Tisdale, S., Abdel-Wahab, O., Leslie, C. S., & Mayr, C. (2018). Widespread intronic polyadenylation inactivates tumour suppressor genes in leukaemia. Nature, 561(7721), 127–131. https://doi.org/10.1038/s41586-018-0465-8

Lee, Y. S., Song, S. J., Hong, H. K., Oh, B. Y., Lee, W. Y., & Cho, Y. B. (2020). The FBW7-MCL-1 axis is key in M1 and M2 macrophage-related colon cancer cell progression: validating the immunotherapeutic value of targeting PI3Kγ. Experimental and Molecular Medicine, 52(5), 815–831. https://doi.org/10.1038/s12276-020-0436-7

Lengauer, C., Kinzler, K. W., & Vogelstein, B. (1997). DNA methylation and genetic instability in colorectal cancer cells. Proceedings of the National Academy of Sciences of the United States of America, 94(6), 2545–2550. https://doi.org/10.1073/pnas.94.6.2545

Li, H., Handsaker, B., Wysoker, A., Fennell, T., Ruan, J., Homer, N., Marth, G., Abecasis, G., Durbin, R., & Subgroup, 1000 Genome Project Data Processing. (2009). The Sequence Alignment/Map format and SAMtools. Bioinformatics, 25(16), 2078–2079. https://doi.org/10.1093/bioinformatics/btp352
Liu, H., Lorenzini, P. A., Zhang, F., Xu, S., Wong, M. S. M., Zheng, J., & Roca, X. (2018). Alternative splicing analysis in human monocytes and macrophages reveals MBNL1 as major regulator. Nucleic Acids Research, 46(May), 1–18. https://doi.org/10.1093/nar/gky401
Liu, X., Freitas, J., Zheng, D., Oliveira, M. S., Hoque, M., Martins, T., Henriques, T., Tian, B., & Moreira, A. (2017). Transcription elongation rate has a tissue-specific impact on alternative cleavage and polyadenylation in Drosophila melanogaster. RNA (New York, N.Y.), 23(12), 258–265. https://doi.org/10.1261/rna.062661.117
Liu, X., Hoque, M., Larochelle, M., Lemay, J.-F., Yurko, N., Manley, J. L., Bachand, F., & Tian, B. (2017). Comparative analysis of alternative polyadenylation in S . cerevisiae and S . pombe. Genome Research, 27(10), 1–11. https://doi.org/10.1101/gr.222331.117.27
Liu, Y. C., Zou, X. B., Chai, Y. F., & Yao, Y. M. (2014). Macrophage polarization in inflammatory diseases. International Journal of Biological Sciences, 10(5), 520–529. https://doi.org/10.7150/ijbs.8879
Livak, K. J., & Schmittgen, T. D. (2001). Analysis of relative gene expression data using real-time quantitative PCR and the 2-ΔΔCT method. Methods, 25(4), 402–408. https://doi.org/10.1006/meth.2001.1262
Locati, M., Mantovani, A., & Sica, A. (2013). Macrophage Activation and Polarization as an Adaptive Component of Innate Immunity. In Advances in Immunology (Vol. 120). https://doi.org/10.1016/B978-0-12-417028-5.00006-5
Logan, C. Y., & Nusse, R. (2004). The Wnt Signaling Pathway in Development and Disease. Annual Review of Cell and Developmental Biology, 20(1), 781–810. https://doi.org/10.1146/annurev.cellbio.20.010403.113126
Love, M. I., Huber, W., & Anders, S. (2014). Moderated estimation of fold change and dispersion for RNA-seq data with DESeq2. Genome Biology, 15(12), 1–21. https://doi.org/10.1186/s13059-014-0550-8
Ma, W., & Mayr, C. (2018). A Membraneless Organelle Associated with the Endoplasmic Reticulum Enables 3′UTR-Mediated Protein-Protein Interactions. Cell, 175(6), 1492-1506.e19. https://doi.org/10.1016/j.cell.2018.10.007
Machacek, C., Supper, V., Leksa, V., Mitulovic, G., Spittler, A., Drbal, K., Suchanek, M., Ohradanova-Repic, A., & Stockinger, H. (2016). Folate Receptor Regulates Integrin CD11b/CD18 Adhesion of a Macrophage Subset to Collagen. The Journal of Immunology, 197(6), 2229–2238. https://doi.org/10.4049/jimmunol.1501878
Mantovani, A., & Locati, M. (2013). Tumor-associated macrophages as a paradigm of macrophage plasticity, diversity, and polarization lessons and open questions. Arteriosclerosis, Thrombosis, and Vascular Biology, 33(7), 1478–1483. https://doi.org/10.1161/ATVBAHA.113.300168
Martin, M. (2011). Cutadapt removes adapter sequences from high-throughput sequencing reads. EMBnet, 7(10), 2803–2809.
Martinez, F. O., Gordon, S., Locati, M., & Mantovani, A. (2006). Transcriptional profiling of the human monocyte-to-macrophage differentiation and polarization: new molecules and patterns of gene expression. Journal of Immunology, 177(10), 7303–7311. https://doi.org/10.4049/jimmunol.177.10.7303
Masckauchán, T. N. H., Shawber, C. J., Funahashi, Y., Li, C.-M., & Kitajewski, J. (2005). Wnt/beta-catenin signaling induces proliferation, survival and interleukin-8 in human endothelial cells. Angiogenesis, 8(1), 43–51. https://doi.org/10.1007/s10456-005-5612-9
Mayr, C. (2017). Regulation by 3′–Untranslated Regions. Annual Review of Genetics, 51(1), annurev-genet-120116-024704. https://doi.org/10.1146/annurev-genet-120116-024704
Mayr, C., & Bartel, D. P. (2009). Widespread Shortening of 3'UTRs by Alternative Cleavage and Polyadenylation Activates Oncogenes in Cancer Cells. Cell, 138(138), 673–684. https://doi.org/10.1016/j.cell.2009.06.016
Mitra, M., Johnson, E. L., & Coller, H. A. (2016). Alternative polyadenylation can regulate post-translational membrane localization. Trends in Cell & Molecular Biology, 10, 37–47.
Németh, Z. H., Lutz, C. S., Csóka, B., Deitch, E. A., Leibovich, S. J., Gause, W. C., Tone, M., Pacher, P., Vizi, E. S., & Haskó, G. (2005). Adenosine Augments IL-10 Production by Macrophages through an A 2B Receptor-Mediated Posttranscriptional Mechanism. The Journal of Immunology, 175(12), 8260–8270. https://doi.org/10.4049/jimmunol.175.12.8260

Nojima, T., Gomes, T., Grosso, A. R. F., Kimura, H., Dye, M. J., Dhir, S., Carmo-Fonseca, M., & Proudfoot, N. J. (2015). Mammalian NET-seq reveals genome-wide nascent transcription coupled to RNA processing. Cell, 161(3), 526–540. https://doi.org/10.1016/j.cell.2015.03.027
Nojima, T., Gomes, T. T., Carmo-Fonseca, M., & Proudfoot, N. J. (2016). Mammalian NET-seq analysis defines nascent RNA profiles and associated RNA processing genome-wide. Nature Protocols, 11(3), 413–428. https://doi.org/10.1038/nprot.2016.012
Ohradanova-Repic, A., Nogueira, E., Hartl, I., Gomes, A. C., Preto, A., Steinhuber, E., Mühlgrabner, V., Repic, M., Kuttke, M., Zwirzitz, A., Prouza, M., Suchanek, M., Wozniak-Knopp, G., Horejsi, V., Schabbauer, G., Cavaco-Paulo, A., & Stockinger, H. (2018). Fab antibody fragment-functionalized liposomes for specific targeting of antigen-positive cells. Nanomedicine: Nanotechnology, Biology, and Medicine, 14(1), 123–130. https://doi.org/10.1016/j.nano.2017.09.003
Pai, A. A., Baharian, G., Pagé Sabourin, A., Brinkworth, J. F., Nédélec, Y., Foley, J. W., Grenier, J. C., Siddle, K. J., Dumaine, A., Yotova, V., Johnson, Z. P., Lanford, R. E., Burge, C. B., & Barreiro, L. B. (2016). Widespread Shortening of 3' Untranslated Regions and Increased Exon Inclusion Are Evolutionarily Conserved Features of Innate Immune Responses to Infection. PLoS Genetics, 12(9), 1–24. https://doi.org/10.1371/journal.pgen.1006338
Pathria, P., Louis, T. L., & Varner, J. A. (2019). Targeting Tumor-Associated Macrophages in Cancer. Trends in Immunology, 40(4), 310–327. https://doi.org/10.1016/j.it.2019.02.003
Pereira-Castro, I., & Moreira, A. (2021). On the function and relevance of alternative 3′-UTRs in gene expression regulation. Wiley Interdisciplinary Reviews: RNA, January, 1–30. https://doi.org/10.1002/wrna.1653
Pinto, A. T., Pinto, M. L., Velho, S., Pinto, M. T., Cardoso, A. P., Figueira, R., Monteiro, A., Marques, M., Seruca, R., Barbosa, M. A., Mareel, M., Oliveira, M. J., & Rocha, S. (2016). Intricate macrophage-colorectal cancer cell communication in response to radiation. PLoS ONE, 11(8), 1–20. https://doi.org/10.1371/journal.pone.0160891
Pinto, M.L., Rios, E., Silva, A. C., Neves, S. C., Caires, H. R., Pinto, A. T., Durães, C., Carvalho, F. A., Cardoso, A. P., Santos, N. C., Barrias, C. C., Nascimento, D. S., Pinto-do-Ó, P., Barbosa, M. A., Carneiro, F., & Oliveira, M. J. (2017). Decellularized human colorectal cancer matrices polarize macrophages towards an anti-inflammatory phenotype promoting cancer cell invasion via CCL18. Biomaterials. https://doi.org/10.1016/j.biomaterials.2017.02.004
Pinto, Marta L., Rios, E., Durães, C., Ribeiro, R., Machado, J. C., Mantovani, A., Barbosa, M. A., Carneiro, F., & Oliveira, M. J. (2019). The Two Faces of Tumor-Associated Macrophages and Their Clinical Significance in Colorectal Cancer. Frontiers in Immunology, 10(August), 1–12. https://doi.org/10.3389/fimmu.2019.01875
Ploeger, D. T., Hosper, N. A., Schipper, M., Koerts, J. A., De Rond, S., & Bank, R. A. (2013). Cell plasticity in wound healing: Paracrine factors of M1/ M2 polarized macrophages influence the phenotypical state of dermal fibroblasts. Cell Communication and Signaling, 11(1). https://doi.org/10.1186/1478-811X-11-29
Quail, D. F., & Joyce, J. A. (2017). Molecular pathways: Deciphering mechanisms of resistance to macrophage-targeted therapies. Clinical Cancer Research, 23(4), 876–884. https://doi.org/10.1158/1078-0432.CCR-16-0133
Roca, X., Krainer, A. R., & Eperon, I. C. (2013). Pick one, but be quick: 5′ splice sites and the problems of too many choices. Genes and Development, 27(2), 129–144. https://doi.org/10.1101/gad.209759.112
Ruiz-López, L., Blancas, I., Garrido, J. M., Mut-Salud, N., Moya-Jódar, M., Osuna, A., & Rodríguez-Serrano, F. (2018). The role of exosomes on colorectal cancer: A review. Journal of Gastroenterology and Hepatology, 33(4), 792–799. https://doi.org/10.1111/jgh.14049
Sandberg, R., Neilson, J. R., Sarma, A., Sharp, P. a, & Burge, C. B. (2008). Proliferating cells express mRNAs with shortened 3' UTRs and fewer microRNA target sites. Science, 320(5883), 1643–1647. https://doi.org/10.1126/science.1155390.Proliferating
Schindelin, J., Arganda-Carreras, I., Frise, E., Kaynig, V., Longair, M., Pietzsch, T., Preibisch, S., Rueden, C., Saalfeld, S., Schmid, B., Tinevez, J. Y., White, D. J., Hartenstein, V., Eliceiri, K., Tomancak, P., & Cardona, A. (2012). Fiji: An open-source platform for biological-image analysis. Nature Methods, 9(7), 676–682. https://doi.org/10.1038/nmeth.2019
Schwich, O. D., Blümel, N., Keller, M., Wegener, M., Setty, S. T., Brunstein, M. E., Poser, I., Mozos, I. R. D. L., Suess, B., Münch, C., Mcnicoll, F., Zarnack, K., Müller-McNicoll, M., & Schwich, O. D. (2021). SRSF3 and SRSF7 modulate 3 ′ UTR length through suppression or activation of proximal polyadenylation sites and regulation of CFIm levels. 1–34.

Serbulea, V., DeWeese, D., & Leitinger, N. (2017). The effect of oxidized phospholipids on phenotypic polarization and function of macrophages. Physiology & Behavior, 176(1), 139–148. https://doi.org/10.1016/j.physbeh.2017.03.040
Shi, Y. (2012). Alternative polyadenylation: new insights from global analyses. RNA (New York, N.Y.), 18(12), 2105–2117. https://doi.org/10.1261/rna.035899.112
Singh, I., Lee, S. H., Sperling, A. S., Samur, M. K., Tai, Y. T., Fulciniti, M., Munshi, N. C., Mayr, C., & Leslie, C. S. (2018). Widespread intronic polyadenylation diversifies immune cell transcriptomes. Nature Communications, 9(1). https://doi.org/10.1038/s41467-018-04112-z
Steele, C. W., Whittle, T., & Joshua Smith, J. (2019). Review: KRAS mutations are influential in driving hepatic metastases and predicting outcome in colorectal cancer. Chinese Clinical Oncology, 8(5), 1–8. https://doi.org/10.21037/cco.2019.08.16
Sutherland, C. (2011). What are the bona fide GSK3 substrates? International Journal of Alzheimer's Disease, 2011. https://doi.org/10.4061/2011/505607
Takagaki, Y., Seipelt, R. L., Peterson, M. L., & Manley, J. L. (1996). The polyadenylation factor CstF-64 regulates alternative processing of IgM heavy chain pre-mRNA during B cell differentiation. Cell, 87(5), 941–952. https://doi.org/10.1016/S0092-8674(00)82000-0
The Cancer Genome Atlas. (n.d.). https://cancergenome.nih.gov/
Tian, B., Hu, J., Zhang, H., & Lutz, C. S. (2005). A large-scale analysis of mRNA polyadenylation of human and mouse genes. Nucleic Acids Research, 33(1), 201–212. https://doi.org/10.1093/nar/gki158
Tian, B., & Manley, J. L. (2016). Alternative polyadenylation of mRNA precursors. Nature Reviews Molecular Cell Biology, 18(1), 18–30. https://doi.org/10.1038/nrm.2016.116
Trapnell, C., Pachter, L., & Salzberg, S. L. (2009). TopHat: discovering splice junctions with RNA-Seq. Bioinformatics, 25(9), 1105–1111. https://doi.org/10.1093/bioinformatics/btp120
Turner, R. E., Henneken, L. M., Liem-Weits, M., Harrison, P. F., Swaminathan, A., Vary, R., Nikolic, I., Simpson, K. J., Powell, D. R., Beilharz, T. H., & Dichtl, B. (2020). Requirement for cleavage factor IIm in the control of alternative polyadenylation in breast cancer cells. Rna, 26(8). https://doi.org/10.1261/RNA.075226.120
Vander Ark, A., Cao, J., & Li, X. (2018). TGF-β receptors: In and beyond TGF-β signaling. Cellular Signalling, 52(September), 112–120. https://doi.org/10.1016/j.cellsig.2018.09.002
Wang, E. T., Sandberg, R., Luo, S., Khrebtukova, I., Zhang, L., Mayr, C., Kingsmore, S. F., Schroth, G. P., & Burge, C. B. (2008). Alternative isoform regulation in human tissue transcriptomes. Nature, 456(7221), 470–476. https://doi.org/10.1038/nature07509
Wang, R., Zheng, D., Wei, L., Ding, Q., & Tian, B. (2019). Regulation of Intronic Polyadenylation by PCF11 Impacts mRNA Expression of Long Genes. Cell Reports, 26(10), 2766-2778.e6. https://doi.org/10.1016/j.celrep.2019.02.049
West, K. O., Scott, H. M., Torres-Odio, S., West, A. P., Patrick, K. L., & Watson, R. O. (2019). The Splicing Factor hnRNP M Is a Critical Regulator of Innate Immune Gene Expression in Macrophages. Cell Reports, 29(6), 1594-1609.e5. https://doi.org/10.1016/j.celrep.2019.09.078
WHO. (2018). Estimated number of cases worldwide , both sexes , all ages. 160.
Wilton, J., Tellier, M., Nojima, T., Costa, A. M., Oliveira, M. J., & Moreira, A. (2021). Simultaneous studies of gene expression and alternative polyadenylation in primary human immune cells. In Methods in Enzymology: Vol. mRNA 3' En (1st ed., Issue June). Elsevier Inc. https://doi.org/10.1016/bs.mie.2021.04.004
Wurth, L., & Gebauer, F. (2015). RNA-binding proteins, multifaceted translational regulators in cancer. Biochimica et Biophysica Acta (BBA) - Gene Regulatory Mechanisms, 1849(7), 881–886. https://doi.org/http://dx.doi.org/10.1016/j.bbagrm.2014.10.001
Xiao, R., Chen, J. Y., Liang, Z., Luo, D., Chen, G., Lu, Z. J., Chen, Y., Zhou, B., Li, H., Du, X., Yang, Y., San, M., Wei, X., Liu, W., Lécuyer, E., Graveley, B. R., Yeo, G. W., Burge, C. B., Zhang, M. Q., … Fu, X. D. (2019). Pervasive Chromatin-RNA Binding Protein Interactions Enable RNA-Based Regulation of Transcription. Cell, 107–121. https://doi.org/10.1016/j.cell.2019.06.001
Xiong, Y., Wang, K., Zhou, H., Peng, L., You, W., & Fu, Z. (2018). Profiles of immune infiltration in colorectal cancer and their clinical significant: A gene expression-based study. Cancer Medicine, 7(9), 4496–4508. https://doi.org/10.1002/cam4.1745
Yahaya, M. A. F., Lila, M. A. M., Ismail, S., Zainol, M., & Afizan, N. A. R. N. M. (2019). Tumour-Associated Macrophages (TAMs) in colon cancer and how to reeducate them. Journal of Immunology Research, 2019. https://doi.org/10.1155/2019/2368249
Yamamoto, H., & Imai, K. (2019). An updated review of microsatellite instability in the era of next-generation sequencing and precision medicine. Seminars in Oncology, 46(3), 261–270. https://doi.org/10.1053/j.seminoncol.2019.08.003

Yang, M., McKay, D., Pollard, J. W., & Lewis, C. E. (2018). Diverse functions of macrophages in different tumor microenvironments. Cancer Research, 78(19), 5492–5503. https://doi.org/10.1158/0008-5472.CAN-18-1367

Yang, X., Wu, J., Xu, W., Tan, S., Chen, C., Wang, X., Sun, J., & Kang, Y. (2018). Genome-wide profiling reveals cancer-related genes with switched alternative polyadenylation sites in colorectal cancer. OncoTargets and Therapy, 11, 5349–5357. https://doi.org/10.2147/OTT.S164233

Yang, Y., Ye, Y. C., Chen, Y., Zhao, J. L., Gao, C. C., Han, H., Liu, W. C., & Qin, H. Y. (2018). Crosstalk between hepatic tumor cells and macrophages via Wnt/β-catenin signaling promotes M2-like macrophage polarization and reinforces tumor malignant behaviors. Cell Death and Disease, 9(8). https://doi.org/10.1038/s41419-018-0818-0

Zheng, D., Wang, R., Ding, Q., Wang, T., Xie, B., Wei, L., Zhong, Z., & Tian, B. (2018). Cellular stress alters 3′UTR landscape through alternative polyadenylation and isoform-specific degradation. Nature Communications, 9(1), 1–14. https://doi.org/10.1038/s41467-018-04730-7

Zhu, Y., Wang, X., Forouzmand, E., Jeong, J., Qiao, F., Sowd, G. A., Engelman, A. N., Xie, X., Hertel, K. J., & Shi, Y. (2017). Molecular mechanisms for CFIm-mediated regulation of mRNA alternative polyadenylation. Molecular Cell, 176(1), 139–148. https://doi.org/10.1016/j.molcel.2017.11.031.Molecular

Zigmond, E., & Jung, S. (2013). Intestinal macrophages: Well educated exceptions from the rule. Trends in Immunology, 34(4), 162–168. https://doi.org/10.1016/j.it.2013.02.001

3.3 *Expression of RAC1 alternative 3' UTR depends on macrophages and CRC cells state*

Paper in preparation.

Introduction

Macrophages are plastic immune cells with diverse functions that are determined by their cellular status and microenvironment. Pro-inflammatory M1 macrophages are specialized in infection and tumor clearance, due to the production of immunomodulatory cytokines and chemokines, ROS and RNS, while anti-inflammatory M2 macrophages are immuno-suppressors that eliminate apoptotic cell debris and damaged molecules (Martinez *et al.*, 2006; Porta *et al*., 2009; Weagel *et al.*, 2015). Therefore, macrophages may act as modulators of cancer dormancy or invasiveness (Mantovani & Locati, 2013).

Tumorigenic progression is characterized by immune evasion and activation of metabolic pathways, among other cancer hallmarks. In cancer cells, gene expression regulation through the production of differential 3' UTR mRNA isoforms alters oncogene activation or metastasis (Andres *et al.*, 2019; Mayr & Bartel, 2009).

Alternative polyadenylation (APA) in the 3' UTR is a cell-type and cell-state specific, co-transcriptional mechanism that regulates gene expression. Alternative 3' UTR usage may occur in up to 70% of human genes in both physiologic and pathologic conditions (Pereira-Castro & Moreira, 2021). Differential usage of polyadenylation signals (PAS) on the 3' UTR lead to the production of several mRNA isoforms that differ on the 3' UTR and thus bind different RNA-binding proteins, which control gene expression, by modulating mRNA stability and translation, and by determining protein subcellular localization (Berkovits & Mayr, 2015; Fischl *et al*., 2019; Lutz & Moreira, 2011; Tian & Manley, 2016). While longer 3' UTRs generated by distal PAS selection frequently have more RBP binding sites and hence are more subject to regulation, cancer cells and activated immune cells have higher expression of mRNAs with short 3' UTRs (Braz *et a*l., 2017; Gruber *et al.*, 2014; Mitra *et al.*, 2016; Sandberg *et al*., 2008).

Hypoxia is one of the main characteristics of the tumor microenvironment. Immediate cellular cytotoxic consequences of hypoxia include production of Reactive Oxygen Species (ROS), immune evasion, modulation of chemotherapy resistance,

tumor regrowth and metastasis (McKeown, 2014; Rey *et al.*, 2017; Sivridis *et al.*, 2005). Research on cancer cell response to hypoxia is growing (D'Ignazio & Rocha, 2016; Martins *et al.*, 2020), but little is known on how hypoxia affects gene expression and APA in primary human macrophages and colorectal cancer cells (CRC). Here, we used human primary cells, THP-1 cell lines and the CRC cell line RKO, to characterize macrophage alternative 3' UTR mRNA isoforms, in hypoxia and normoxia conditions. We found that the short 3' UTRs of most genes is upregulated in M1 macrophages when compared to M0, with the exception of *RAC1*, which shows upregulation of the long 3' UTR, which is consistent with upregulation in protein levels and subcellular delocalization possibly due to YBX1 binding. In hypoxic RKO, upregulation of the short 3'UTR of RAC1 was correlated with increased transcription (ChIP), Rac1 protein downregulation, and found that YBX1 binds the *Rac1* mRNA.
In conclusion, our results show that CRC cells and macrophages produce distinct alternative 3' UTR isoforms when polarized to pro-inflammatory conditions and exposure to long-term oxygen deprivation, with distinct phenotypic effects for each cell type.

Results

Using a previously developed methodology (Wilton *et al.*, 2021), we isolated monocytes from healthy blood donors buffy coats, differentiate them for 7 days and polarized to pro-inflammatory (M1) and anti-inflammatory (M2) macrophage phenotypes, with LPS and IFN-γ or IL-10, respectively (Figure S1).

Pro-inflammatory markers TNFα and CCR7 are upregulated in M1 THP-1 (Figure S2B) and anti-inflammatory markers CD163 and CCL18 are upregulated in M2 THP-1 (Figure S2C). CD80 and TGFβ markers were upregulated respectively in THP-1 M2 and THP-1 M1, indicating that THP-1 polarization follows some of the pathways used primary human macrophage polarization, which enables the use of this cell line as a model system whenever high numbers of primary human macrophage cells are unavailable.

As most tumors are hypoxic, unveiling the mechanisms of gene expression regulation in the tumor-immune microenvironment upon exposure to hypoxia will

mimic more closely the tumor conditions and hence contribute to the identification of novel biomarkers for CRC diagnosis. Therefore, RKO cell co-culture was performed under hypoxic (1 % O_2) and normoxic (21 % O_2) conditions and analyzed the expression and APA profile.

We decided to focus on a set of genes with alternative 3'UTRs in macrophages and RKO cells (listed on Table 1) chosen from previous microarray data and RT-qPCR screens, according to the following criteria:

1. Genes with important functions in CRC and/or immune cells.
2. Genes with few (2-3) polyadenylation signals (PAS) and that true PAS are more than 200 nt apart from each other, to be distinguishable by RT-qPCR.
3. Genes with pleiotropic functions (transcription factors, cell surface receptors, etc.).

Single-gene studies in primary human macrophages were performed through RT-qPCR, preceded by a preliminary study to estimate the Ct values of three housekeeping genes – 18S ribosomal RNA (*18S*), glyceraldehyde 3-phosphate dehydrogenase (*GAPDH*), and beta-actin (b-actin) in M0, M1 and M2 macrophages 24 hours after activation, using 50 ng cDNA (Fig 1A). *18S* was chosen as the housekeeping gene due to the following criteria: low variation of expression after inflammatory stimuli and comparable expression between macrophage donors. Additionally, as beta-actin is a major cytoskeletal component and as shown on Figure 1B on subchapter 4.2, macrophages suffer from extensive cytoskeleton reorganization depending on the inflammatory profile, we decided against using beta-actin as a reference gene.

A gene expression study was performed for YBX1, PTBP1 and ELAVL1 (Figure 1B-D). The RBPs expression in macrophages does not vary significantly, with the exception of a slight upregulation in YBX1 mRNA levels in pro-inflammatory macrophages.

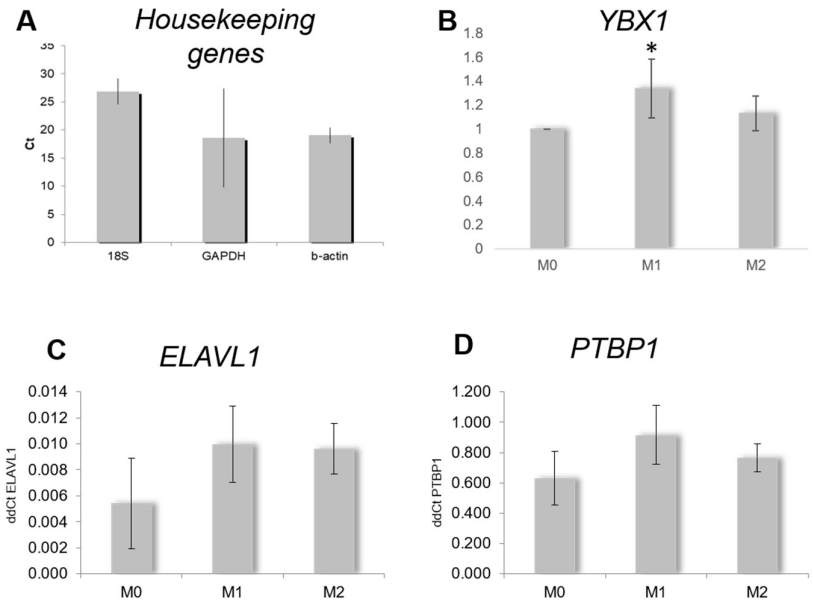


Figure 1 – **A.** Ct values of housekeeping genes 18S, GAPDH and beta-actin in primary human macrophages. n=2 healthy donors of M0 macrophages. **B-D:** Fold change gene expression study in primary human macrophages measuring the coding region of YBX1 (**B**), HuR/ELAVL1 (**C**) and PTBP1 (**D**) by RT-qPCR. RNA binding protein Ybx1 (Y-box binding protein). n=2 (ELAVL1, PTBP1) and n=3 (YBX1). Comparisons were performed using a paired Student's t-test (* $p < 0.05$).

To investigate how 3'UTR-APA is affected by hypoxia, we started to quantify levels of the coding and longer 3' UTR mRNAs of the anti-apoptotic *MCL1* (myeloid cell leukemia), anti-phagocytic cell surface marker *CD47 (*cluster of differentiation 47), pro-inflammatory cytokine *IL1ß* (interleukin 1 beta), GTPase *RAC1* (Ras-related C3 botulinum toxin substrate 1). We used a RT-qPCR-based approach, involving 1 primer pair for coding and 1 primer pair for the longer mRNA isoform (Fischl *et al.*, 2019). Results were normalized to the housekeeping gene *18S* and also to the naïve M0 macrophage levels (Figure 2).

Some assays that require a high number of cells, which is not possible with primary human macrophages, we used the macrophage cell line THP-1 which is extensively used (Spencer *et al.*, 2010; Zhang *et al.*, 2016). We started by characterizing the morphology and inflammatory profile of polarized THP-1 cells and show that PMA addition successfully differentiates THP-1 into adherent cells, but that pro- and anti-inflammatory THP-1 are morphologically similar (Figure S1).

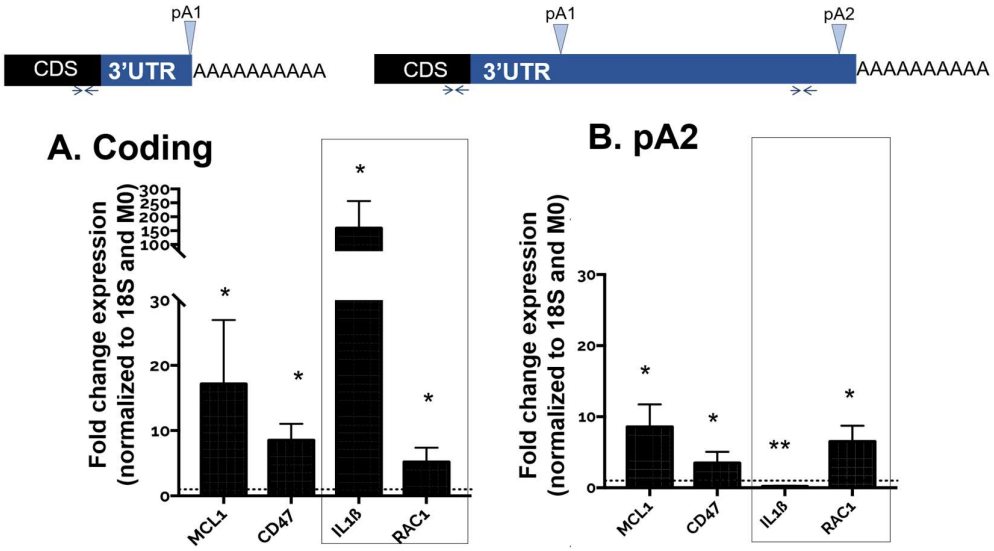


Figure 2 – Fold change gene expression study in primary human macrophages, measuring the coding (A), and distal polyadenylation signal (B) of *MCL1*, *CD47*, *IL1ß* and *RAC1*, by RT-qPCR, with housekeeping gene 18S and unpolarized macrophages as controls. n=4 independent experiments, p-value calculated using Student's t-test * = $p < 0.05$; ** = $p < 0,01$; *** = $p < 0,005$.

Pro-inflammatory M1 macrophages showed upregulation of *MCL1*, *IL1B* and *CD47* gene expression important for macrophage functions (anti-apoptotic, pro-inflammatory cytokine, and anti-phagocytic, respectively) (Figure 2A) and upregulation of the longer 3' UTR of *RAC1* (involved in motility and migration) (Figure 2B). These results prompted us to reanalyze all the RNA-Seq data shown on Subchapter 3.2 and *RAC1* protein expression levels were quantified (Figure 3).

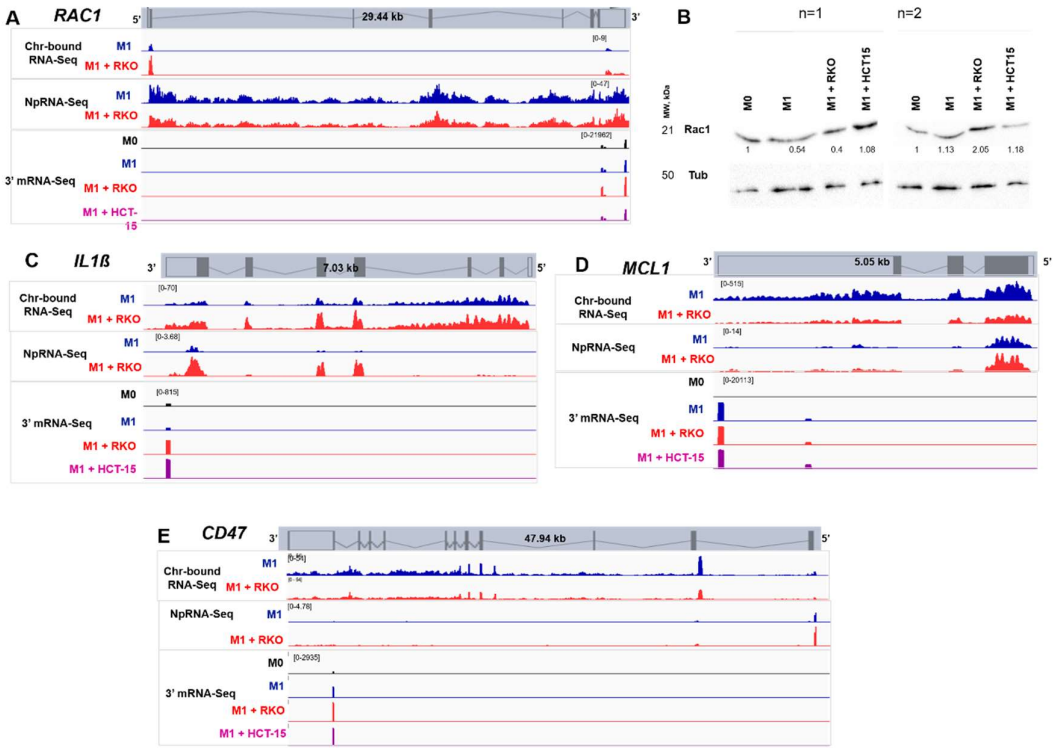


Figure 3 – **A**, **C-E:** IGV gene profile and transcript counts of *RAC1* (**A**), *MCL1* (C), IL*1B* (**D**) and *CD47* (**E**) obtained through ChrRNA-Seq (**top**), NpRNA-Seq (middle) and 3'mRNASeq (**bottom**), of M0 macrophages (**black**), M1 macrophages cultured alone (**blue**) and co-cultured with the CRC cell lines RKO (**red**) or HCT-15 (**lilac**). **B:** Protein levels quantified by western blot of Rac1, using tubulin and GAPDH as loading controls.

All four genes were noticeably upregulated in co-cultured macrophages in comparison to M1, both in the bulk total RNA measured by 3' mRNA-Seq and fractionated RNA samples. In the case of *RAC1*, there is an increase in distal PAS usage upon M1 polarization (Figure 3A). In co-culture with RKO, the expression of *RAC1* long 3'UTR mRNA increases even further, but this effect is not observed in HCT-15 (Figure 3A). These changes do not correlate noticeably to the Rac1 protein levels (Figure 3B).

RAC1 was one of four genes showing an APA switch upon pro-inflammatory stimulation by RT-qPCR, and the only gene that showed a paradigm-defying upregulation of the distal isoform (Figures 2B, 3A). Therefore, the 3' ends of *RAC1* mRNAs were mapped in macrophages before and after polarization, by 3'RACE, in M0, M1 and M2 macrophages (Figure 4). The 3'RACE result confirm that in M1

macrophages the *RAC1* long 3' UTR mRNA isoform is upregulated in contrast to M0; we also show that M2 macrophages preferentially express the short 3'UTR mRNA.

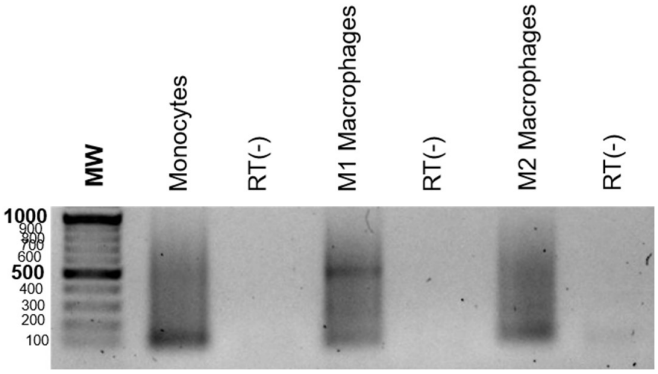


Figure 4 – A. *RAC1* 3'RACE in unpolarized macrophages (M0), pro-inflammatory macrophages (M1), and anti—inflammatory macrophages (M2), with respective reverse transcriptase negative controls.

Taking into account the relevance of RNA binding proteins (RBPs) for the regulation of gene expression and APA (Lutz & Moreira, 2011; Mayr, 2017), we investigated the RBPs that may be involved in the 3' UTR-APA alterations observed, by quantifying *in silico* putative RBP binding sites in the 3' UTR of the selected mRNAs (Table 1).

Table 1 – *In silico* analyses of RBP binding sites in the 3' UTRs of the selected mRNAs in RKO and primary human macrophages, and their relation to the macrophages inflammatory profile, using the databases RBPDB and RBPmap. na = gene is not connected to the inflammatory profile, according to current literature.

mRNA	Ybx1	Ptbp1	ELAVL1	3'UTR size	Number of alternative 3' UTR isoforms	Inflammatory profile
CASC3	1	155	23	1778 nt	5	na
CCL18	1	59	15	991 nt		Anti
CCR7	4	61	4	973 nt	3	Pro
CD47	**5**	264	87	**3945 nt**	21	Pro / Anti
Eef2	1	12	10	498 nt	2	Pro
HIF1A	2	35	25	686 nt	8	Pro
IL1B	**0**	29	14	**610 nt**	2	Pro / Anti
JUNB	1	26	10	500 nt		Pro
MCL1	**14**	167	57	**2824 nt**	4	Anti
MKI67	5	123	19	2530 nt		na
Myc	0	21	15	476 nt	9	Pro
NFKB1	2	20	16	708 nt	4	Anti
PTEN	0	323	170	6459 nt		na
RAC1	**4**	66	24	**1531 nt**	6	Pro / Anti
TFRC	3	135	24	2658 nt		na
TGFB1	1	33	5	196 nt		Anti

Interestingly, both ELAVL1 and PTBP1 bind more frequently to sequences in the 3' UTRs than Ybx1, partly due to their promiscuous motifs (UA-rich and CU-rich respectively). However, as ELAVL1 and PTBP1 RBPs have many binding sites in most human genes, the number of putative binding sites for ELAVL1 and PTBP1 in the 3' UTR of the selected genes is proportional to the rest of the human transcriptome. In contrast, YBX1, an RNA binding protein with relevant functions in tumorigenesis and in regulation of the immune system (Bhullar & Sollars, 2011; Prabhu *et al.*, 2015), has a more specific consensus binding site (UYAUC) (Wu *et al.*, 2015). Interestingly, the 3' UTR of *RAC1*, *CD47*, and *MCL1*, but not *IL1ß*, have predicted binding sites for YBX-1.

Interestingly, YBX1 mRNA levels increased 1.5-fold in M1 macrophages when compared to M0 (Figure 5B). As YBX1 potentially binds to several of the selected genes (Table 1 *in silico* data), we performed RNA Immunoprecipitation (RIP) using specific primers for *RAC1* longer 3' UTR mRNA isoform.

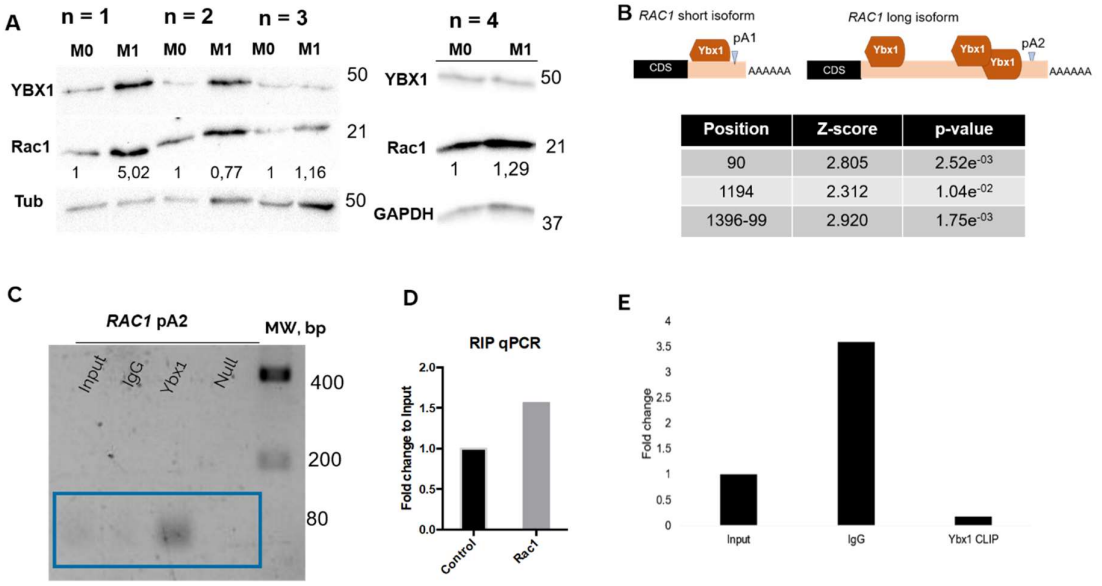


Figure 5 – A. Western blot of YBX1 and Rac1 in M0 and M2 macrophages, using alpha-tubulin and GAPDH as loading controls. **B.** Schematization of the short (left) and long (right) *RAC1* mRNA isoforms (top) and *in silico* prediction of YBX1 binding sites on the 3' UTR of *RAC1* mRNA, using RBPmap (http://rbpmap.technion.ac) indicating position, Z-score (measuring the probability of a binding site occurring in comparison to a background level of 1) and each respective p-value (bottom). **C**. RNA Immunoprecipitation (RIP) in $4x10^7$ M1 THP-1 cells using M0 THP-1 as controls. **D.** Quantification of the bands shown in C by densitometry. **E.** Quantification of RAC1 pA2 YBX1 CLIP in THP-1 M1 cells, by RT-qPCR, comparing to input.

To further investigate the YBX1 binding to the 3' UTR of *RAC1* we performed Cross-Linking ImmunoPrecipitation (CLIP) using primers specific for the longer 3'UTR

(1396-1399 bp) (Figure 5F). In comparison to controls, our results indicate that *YBX1* does not but bind to *RAC1* longer 3'UTR.

Previous results in the Moreira lab showed differential localization of the Rac1 protein in primary mouse neurons, dependent on the 3' UTR isoform (Braz *et al.*, 2017). In macrophages, Rac1 is primarily responsible for regulating cell morphology contributing to membrane ruffling (Wells *et al.*, 2004) and Rac1-deficient bone marrow macrophages show decreased actin polymerization. As macrophage morphology varies upon inflammatory polarization (Wheeler *et al.*, 2006) we investigate a possible role for *RAC1* 3'UTR-APA in Rac1 protein localization in M0, M1 and co-cultured macrophages (Figure 6).

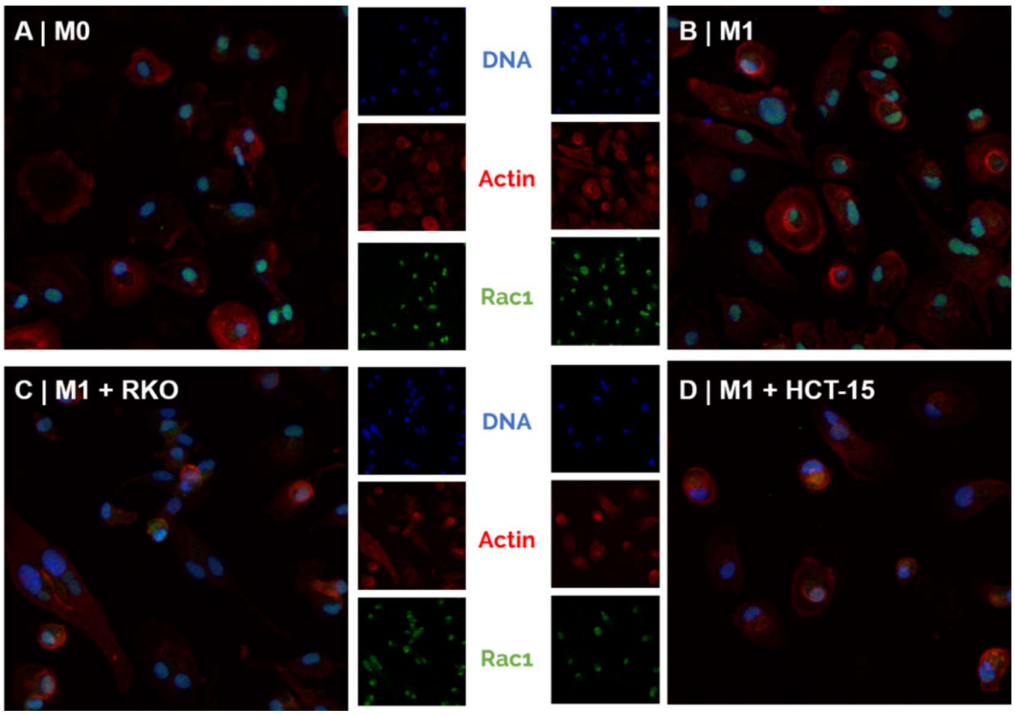


Figure 6 – Immunofluorescence images of unpolarized macrophages (**A**, top left), pro-inflammatory macrophages (**B**, top right), polarized macrophages co-cultured with cell lines RKO (**C**, bottom left) and HCT-15 (**D**, bottom right). DNA is shown with DAPI, actin filaments shown in red and Rac1 protein shown in green.

As seen in Figure 6, Rac1 protein intracellular localization varies with macrophages upon co-culture with CRC cells. While in M0 and in M1 macrophages Rac1 is specifically localized in the nucleus, it partially delocalizes to the cytoplasm and cell periphery in macrophages co-cultured with CRC cells.

CRC cells

Gene expression and 3'UTR-APA imposed by hypoxia were studied using CRC cells.

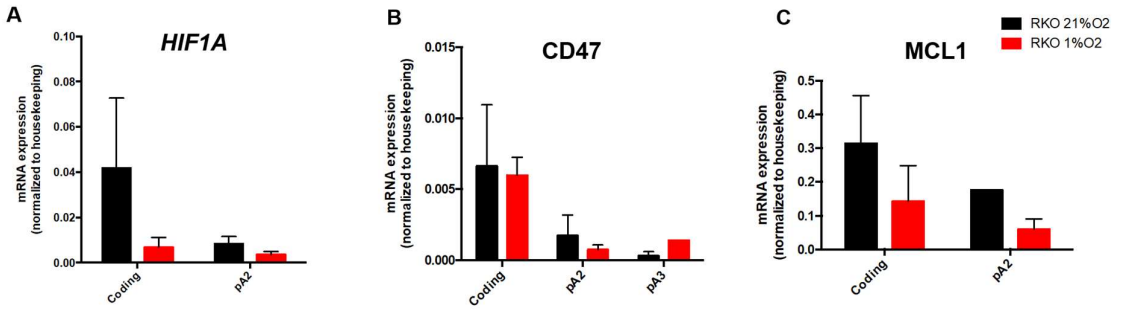


Figure 7 – **A-C:** Fold change expression of coding and longest 3' UTRs of candidate genes *HIF1A* (A), *CD47* (B) and *MCL1* (C) in hypoxic colorectal cancer cell line RKO, normalized to *18S* (housekeeping gene) and normoxic RKO. n=2 independent experiments.

We observed that hypoxia strongly decreases HIF1A expression but does not affect the expression of the longer 3'UTR. Furthermore, in hypoxic RKO, *CD47* and *MCL1* expression is not affected, but the expression of *MCL1* distal 3' UTR isoform decreases (Figure 7). We then investigated how hypoxia affected *RAC1* mRNA, alternative 3' UTR and protein levels in colorectal cancer cells (Figure 8A-C), as well as levels of the previously identified RBPs.

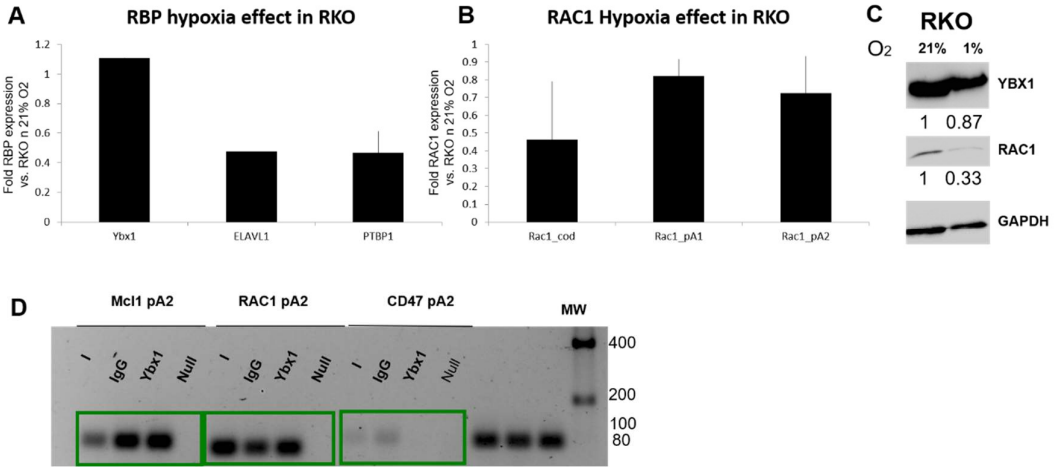


Figure 8 – Fold change expression of RBPs (**A**) and RAC1 (**B**) in hypoxic RKO. C**.** Protein levels of YBX1 in normoxic (N) and hypoxic (H) RKO quantified by western blot. Quantifications were performed through densitometry of YBX1 and RAC1, relative to the housekeeping gene GAPDH, used as a loading control. **D.** *YBX1* RNA Immunoprecipitation (RIP) in $6x10^7$ hypoxic RKO cells with the 3' UTR of MCL1, RAC1 and CD47.

YBX1 mRNA and protein levels were maintained in hypoxic RKO, in contrast with other RBPs that showed a downregulation (Figure 9A). We also observed that total *RAC1* mRNA levels decreased to half upon hypoxic exposure, and were accompanied by a striking decrease in protein levels to a third of the normoxic levels (Figure 8B-C). We then asked if in CRC in hypoxia conditions YBX1 could bind to *RAC1*, *MCL1* and *CD47* mRNAs, using RIP. We show that YBX1 binds to the 3' UTR of *MCL1* and *RAC1* but not to *CD47*, in hypoxic RKO cells (Figure 8D).
After showing that RAC1 undergoes 3' UTR-APA in hypoxic RKO, we analyzed how hypoxia affects RNAPII occupancy along the *RAC1* gene, through chromatin immunoprecipitation (ChIP). Chemical hypoxia was performed in RKO cells by addition of Dfx, which inhibits oxygen-dependent PHD enzymatic degradation of HIF1A (Figure 9A) (G. L. Wang & Semenza, 1993). Dfx concentration was optimized and HIF1A protein levels for 48 hours (Figure 9B).

The *RAC1* RNAPII ChIP results (Figure 9C) indicate that in hypoxia, RNAPII levels are very high at the TSS, indicating that this gene is posed for transcription upon hypoxia. Of note, RNAPII occupancy is high near the pA2, and decreases between pA2 and 1 kb downstream, indicating that transcription termination occurs downstream of pA2 and confirming the preferential selection of pA2 observed in hypoxia conditions

Pilot studies were performed using hypoxic macrophage co-cultures with CRC cells. However, it was technically challenging to obtain homogenous macrophage populations after hypoxia exposure, and thus we also decided to impose a chemically-induced hypoxia to the cells using Dfx.

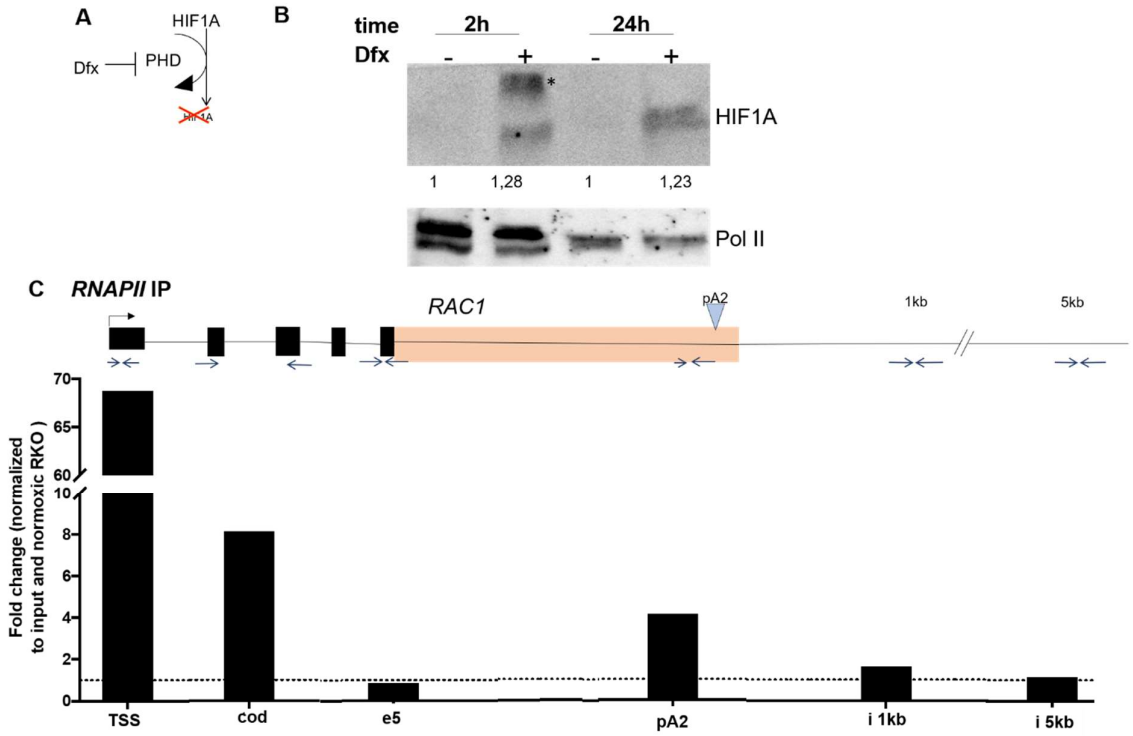


Figure 9 – A. Effect of Dfx addition on HIF1A and inhibition of HIF regulator PHD. **B**. HIF1A before and after Dfx treatment quantified by western blot, using total RNAPII as loading control. The high MW band on HIF1A after 2 h hypoxia is an alternatively spliced isoform. **C**. RNAPII chromatin immunoprecipitation (ChIP) for RAC1 in RKO after 24 hours hypoxia, surveying primer pairs on the transcription start site (TSS), coding region between exons (cod), coding region on the last exon (e5), before the distal PAS (pA2), 1 kilobase downstream of the PAS (I 1kb) and 5 kilobases downstream of the PAS (I 5kb).

The 100 μM Dfx concentration used increased HIF1A levels in RKO. However, the chemically-induced hypoxia had cytotoxic effects that render the investigation of alternative 3' UTR mRNA expression very difficult to achieve.

Discussion

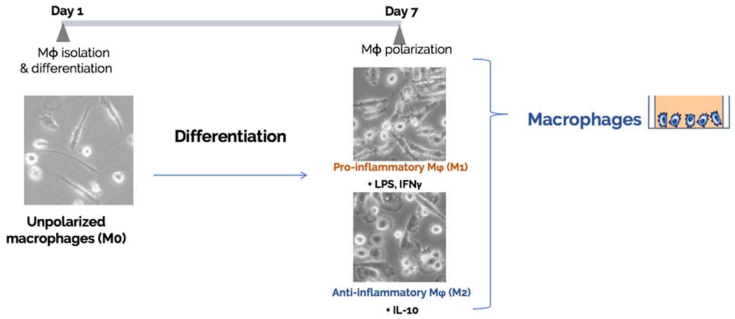
Alternative polyadenylation is a cell-type and cell-state-specific event. Therefore, studying alternative 3'UTR expression in primary human macrophages and CRC cells, in genes relevant for each cell type contributes to the knowledge these mechanisms in the innate immune system and for tumorigenic progression.

Both of the cell types analyzed were more activated than their control counterparts (pro-inflammatory macrophages *vs.* unstimulated macrophages, and hypoxic RKO *vs.* normoxic RKO). Previous literature has established that there is a tendency towards short 3' UTR upregulation in activated cells (Mayr & Bartel, 2009; Pai *et al.*, 2016). We

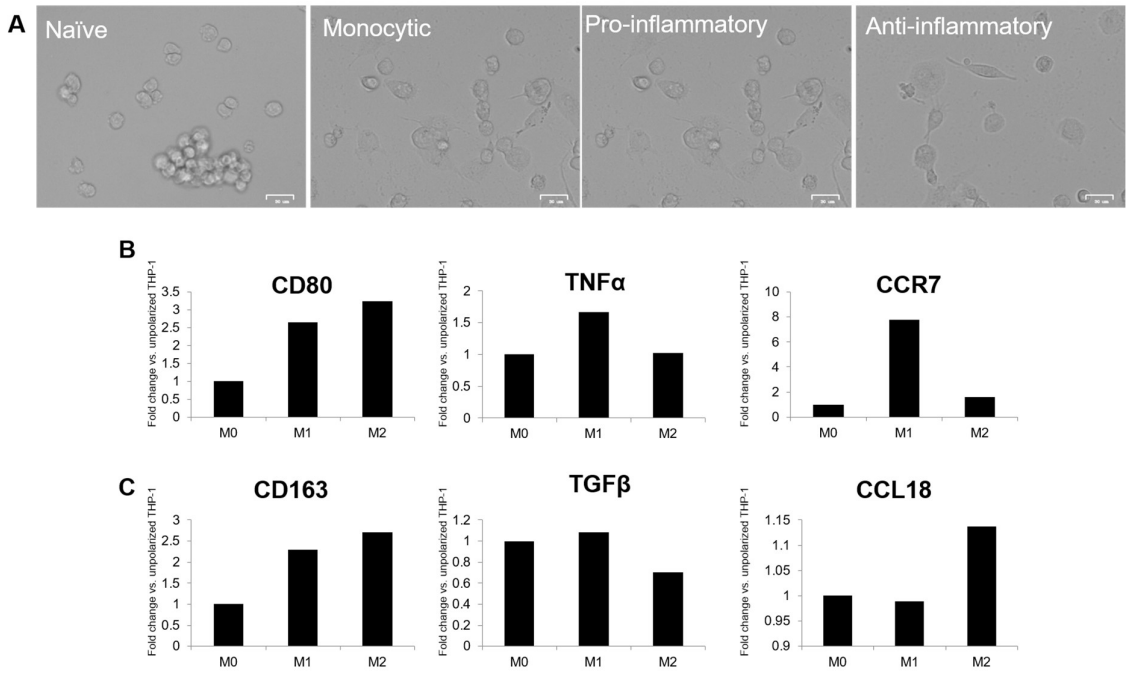
observed the same shortening trend but only in M1 macrophages, in which *RAC1* was the only case showing upregulation of the distal 3' UTR mRNA isoform. However, in hypoxic RKO, we found that each gene is in and of itself an example of several outcomes regarding PAS choice: proximal and distal PAS occurred in the same frequency in the few genes surveyed.

Alternative 3' UTR expression of individual macrophages and CRC genes may have a relevant impact on innate immune and colorectal cell biology and it would be important to identify the physiological function of *RAC1* alternative 3' UTR in macrophages and CRC. It would be possible to use molecular biology tools to deplete *RAC1* pA2 in primary M1 macrophages by siRNA or LNA addition and study protein production, differences in the inflammatory profile, subcellular location, migration and motility, to investigate the function of the longer isoform of *RAC1* in innate immune cells. Similarly, in hypoxic RKO cells, exploring the role of *RAC1* and *HIF1A* longer 3' UTR upregulation could elucidate the importance of oxygen in CRC cells, which is particularly relevant for patients (Martins *et al*., 2020).

Supplementary Figures



Supplementary Figure 1 - Scheme of the macrophage polarization experiment workflow. Day 0: Monocyte isolation and differentiation into macrophages with M-CSF for 7 days, and polarized with LPS and IFNγ (for M1) and IL-10 (for M2).



Supplementary Figure 2 – **A.** Brightfield microscopy showing THP-1 pro-macrophage cell line before and after PMA stimuli (Naïve THP-1 and monocytic THP-1, respectively), and THP-1 polarized to pro- and anti-inflammatory conditions. **B**-**C**. Gene expression study by RT-qPCR of pro-inflammatory markers CD80, TNFα and CCR7 (**B**) and anti-inflammatory markers CD163, TGFβ and CCL18 (**C**), using GAPDH as housekeeping gene and comparing to THP-1 M0 values. n=2 independent experiments.

Materials and Methods

Cell culture | Colorectal cancer cell lines RKO (CRL-2577), purchased from American Type Culture Collection (ATCC, USA), were tested by autosomal short tandem repeat (STR) DNA profiling prior to use. RKO were kept in RPMI 1640 medium with Glutamax (Gibco, Thermo Fisher Scientific) and supplemented with 10% Fetal Bovine Serum (FBS) and 100 U/mL penicillin and 100 µg/mL streptomycin antibiotic solution (Gibco). Cell lines were kept in a humified incubator at 37 ºC with 5 % CO2, subcultured every 3 to 5 days to maintain sub-confluency, and counted in a Neubauer chamber (Marienfeld Superior) with trypan blue exclusion test. When cell lines reached passage 40, they were discarded and a new aliquot was thawed.

Mycoplasma contamination was routinely checked through endpoint PCR, using the following primers: MGSO (fwd): 5’ TGCACCATGTGTCACTCTGTTAACCTC 3’; GPO1 (rev): 5’ ACTCCTACGGGAGGCAGCAGTA 3’. The following PCR program was performed: 5 minutes at 95 ºC, 30 cycles of 30 seconds at 95 ºC, 30 seconds at 56 ºC

and 30 seconds at 72 ºC, final extension of 10 minutes at 72 ºC. Samples were then analyzed on a 1 % agarose gel.
Primary human macrophages were isolated, differentiated and polarized as described in (Wilton et al., 2021). Briefly, CD14+ cells were isolated from PBMCs in buffy coats, seeded in 6-multiwell plates and incubated for 7 days in RPMI medium with glutamine, supplemented with FBS and 100 U/mL penicillin and 100 µg/mL streptomycin. Cells were polarized by adding proinflammatory stimuli to obtain M1 macrophages – LPS 100 ng/mL and IFNγ 25 ng/mL – and by adding anti-inflammatory stimuli to obtain M2 macrophages – IL-10 10 ng/mL.

THP-1 cells were maintained in RPMI 1640 medium with Glutamax supplemented with 10% FBS + 100 U/mL penicillin and 100 µg/mL streptomycin + 1 mM sodium pyruvate. THP-1 differentiation was achieved by seeding 6 multiwell plates in a cell density of 1x106 cells/mL and incubating for 36 hours with 10 ng/mL PMA. Media was renewed and incubated for further 24 hours, before adding polarization stimuli – for M1-like THP-1 macrophages, LPS 100 ng/mL and IFNγ 25 ng/mL were added; for M2-like THP-1 macrophages, IL-10 10 ng/mL was added.

Hypoxia assays | RKO was maintained in 1% O_2 for 72 hours using hypoxic incubators with constant N_2 flow. Hypoxia-induced gene expression changes were determined in comparison to normoxia. RNA and protein extraction were initiated as soon as cells were taken out of the hypoxic chamber, to process the samples, and avoid near-immediate transcriptomic changes due to normoxia shock. For Rac1 ChIP proof-of-concept assay, hypoxia was mimicked through addition of desferrioxamine (Dfx) to RKO cells. Dfx inhibits the action of PHD enzymes and hence keeps high intracellular HIF1A concentrations, mimicking 1 % hypoxic chambers effects (G. L. Wang & Semenza, 1993).

3'Rapid Amplification of cDNA Ends (RACE) | cDNA was synthesized using SuperScript IV Reverse Transcriptase (Invitrogen), according to the manufacturer's protocol. 2.5 µM 3'RACE adapter primer and 0.25-1 µg of total RNA from M0, M1 or M2 primary human macrophages were used. The 3'RACE polymerase chain reaction was performed using Phusion DNA Polymerase (Sigma) according to the manufacturer's protocol. The following PCR program was performed: 1 minute at 98

ºC, 30 cycles of 30 seconds at 98 ºC, 30 seconds at 63 ºC (calculated by the ThermoFisher Scientific primer calculator (*ThermoFisher Primer Tm Calculator*, n.d.)) and 90 seconds at 72 ºC; final extension at 72 ºC for 7 minutes. The PCR products were then separated on a 1 % agarose gel. Primers are listed on table 2 below.

Table 2 - Primer list for *RAC1* 3'RACE assays.

Primer name	Primer sequence (5'→ 3')
Rac1_3'RACE_pfwd1	AGGCAAAGCGACTACAGGAG
Rac1_3'RACE_pfwd2	TGGTCAAGTGACAGTGTCGG
3'RACE adapter primer	AAGCAGTGGTATCAACGCAGAGTAC$(T)_{30}$VN
Oligo anchor primer	GACCAACGCGTATCGATGTCGAC

qPCR: Primer Design and efficiency optimization | For RT-qPCR of gene expression candidates, primers were designed between exons, whenever the sequence specificity and dimer percentages allowed. For RT-qPCR of APA candidates, primers were designed to the coding region (between exons whenever possible) and to the most distal PAS (pA2), as previously described (Pinto et al., 2011). Annealing temperatures were tested by endpoint PCR, using the following program: 95 ºC for 5 minutes, 35 cycles of 95 ºC for 30 seconds, 58 or 60 ºC for 30 seconds, and 72 ºC for 30 seconds, followed by final extension at 72 ºC for 5 minutes. Each primer was tested using two serial cDNA dilutions, and analyzed in a 2 % agarose gel electrophoresis. The annealing temperature that resulted on most intense bands was chosen as optimal for the subsequent RT-qPCR program.

Primer efficiency in RT-qPCR was performed using four serial cDNA dilutions, plotted against the obtained Ct value. If the trend line slope was close to -3.33, corresponding to a near-linear efficiency percentage (90-110 %), the primer pair was considered efficient. Primers used are listed on table 3 below originate from this study, except for previous genes developed in-house - *MCL1*, designed by Isabel Pereira-Castro (cod-F: 5'-AACAAAGAGGCTGGGATGGG-3'; cod-R: 5'-TGCCAAACCAGCTCCTACTC-3'; pA2-F: 5'-GCTTGGGGCAGTGAGGGCT-3'; pA2-R: 5'-ACCACCTGCCTCCTCCTCC-3'); YBX1, designed by Andrea Castro (cod_F: 5' GAAGGAGAAAAGGGTGCGGA 3'; cod_R: 5' TGGTAATTGCGTGGAGGACC 3'); and PTBP1, designed by Vânia Glória (PTBP1_fwd: 5' GTTGGGTCGGTTCCTGCTAT 3';

*PTBP1*_rev: 5' CCGTCCATGGCACACAGAG 3'). In-house housekeeping gene 18S was used as internal control for gene expression. Sequences: 18S_fwd: 5' GCAGAATCCACGCCAGTACAAGA 3'; *18S*_rev: 5' CCCTCTATGGGCCCGAATCTT 3'. The qPCR program used is as follows: 50 ˚C for 2 minutes, 95 ˚C for 2 minutes, 40 cycles of 95 ˚C for 15 seconds and 60 ˚C for 1 minute, then melt curve from 60 ˚C to 95 ˚C with 0.3 ˚C slope.

Table 3 – Primer list for RT-qPCR assays.

Primer name	Primer sequence (5'→ 3')	Tm (ºC)
*HIF1a*_cod_fwd	TGAAGATGACATGAAAGCACAGA	60
*HIF1a*_cod_rev	TCACCATCATCTGTGAGAACCA	60
*HIF1a*_pA2_fwd	TCATTCCTTTTGCTCTTTGTGGT	60
*HIF1a*_pA2_rev	GGTCCACAGAAGATGTTTATTTGA	60
*CD47*_cod_fwd	AACAAGTCCACTGTCCCCAC	60
*CD47*_cod_rev	TCCTGTGTGTGAGACAGCATC	60
*CD47*_pA2_fwd	ACAGGGCTATCCCGTAATTGG	60
*CD47*_pA2_rev	CGTGTTTTGAGCTTTGTTAGTGC	60
*RAC1*_cod_fwd	GAAGCTGACTCCCATCACCTATCC	60
*RAC1*_fwd_rev	CGGGCAGAGGACTGCTCGGATCG	60
*RAC1*_pA2_fwd	ACAAGGAGGCATATTGCTCAG	60
*RAC1*_pA2_rev	ACTGGTTGTTCTGTTAGTCGCT	60
*ELAVL1*_fwd	AGCCTTTCAGGTTTCCCTGG	60
*ELAVL1*_rev	GGGAATCCCGCCTTCCATC	60
*IL1b*_codF	GGCAGGGAACCAGCATC	60
*IL1b*_codR	CCGACCACCACTACAGCAA	60
*IL1b*_pA2_F	ACATTCTGATGAGCAACCGC	60
IL1b_pA2_R	ACACTGCTACTTCTTGCCCC	60

RNA Immunoprecipitation | RNA from macrophages and cancer cells was precipitated using the Magna RIP kit (Sigma), according to manufacturer's instructions. Briefly, cells at 80-90 % confluency were centrifuged at 1500 rpm at 4 ºC, washed twice in ice-cold PBS and lysed for 5 minutes with ice-cold RIP lysis buffer, including protease and RNase inhibitors. Magnetic beads are washed twice with RIP wash buffer and incubated in the antibody/IgG control for 30 minutes at RT, on

rotation, magnetically separated from the supernatant, washed and resuspended in RIP IP buffer. The beads:Ab / IgG complex was added to the RIP lysates, keeping 10 % of the volume as input. Beads : Ab or IgG : lysate complex was incubated overnight at 4 ºC on rotation, separated magnetically as previously described, and washed six times with cold RIP wash buffer. RNA from bead complexes were incubated with Proteinase K for 30 minutes at 55 ºC to, and RNA was purified via phenol:chloroform:isoamyl alcohol extraction, according to manufacturer's instructions. cDNA was synthesized using SuperScript IV Reverse transcriptase, according to manufacturer's instructions. 95 ºC for 5 minutes, 30 cycles of 95 ºC for 30 seconds, 60 ºC for 30 seconds, and 72 ºC for 30 seconds, followed by final extension at 72 ºC for 5 minutes. Samples were then run on an 0.8% agarose gel.

Cross-linking Immunoprecipitation (CLIP) | This protocol was modified from (Hilgers et al., 2012). Briefly, 7 x10^7 RKO cells were crosslinked for 15 minutes at RT, by shaking with 5 mL cross-linking/fixing solution (1.4 % formaldehyde / 50 mM HEPES pH 8.0 / 1 mM EDTA / 0.5 mM EGTA / 100 mM NaCl + n-heptane), centrifuged at 1000 *g* at RT for 1 minute, and washed once each with PBS / 125 mM glycine. Samples were centrifuged at 2000 *g* for 4 minutes at 4 ˚C, supernatant was removed and cells were incubated in ice-cold lysis buffer (50 mM Tris-HCl pH 8.1 / 10 mM EDTA / 1% SDS) for 20 minutes at 4 ˚C. Extracts were sonicated for 20 cycles of 30 seconds on, 30 seconds off, keeping on ice for 30 minutes at midpoint. Extracts were centrifuged at 16000 *g* for 1 minute at 4 ˚C and aliquots were flash-frozen in liquid nitrogen. To perform the IP, 100 µL Protein G Sepharose beads equilibrated in 50 % (v/v) RIPA buffer (10 mM Tris-HCl pH 8 / 140 mM NaCl / 1 mM EDTA / 1 % Triton X-100 / 0.1 % SDS / 0.1 % sodium deoxycholate / 1 x Protease inhibitors / 80 U / mL Ribolock) were incubated for 1 hour at 4 ˚C and centrifuged at 1100 g for 1 minute at 4 ˚C, before resuspending in 100 µL RIPA buffer. Nuclear extracts were pre-cleared with equilibrated beads for 1 hour at 4 ˚C, centrifuged at 3500 rpm for 30 minutes at 4 ˚C and samples were divided: half the pre-clear was incubated with 5 µg anti-YBX1 antibody, and half was incubated with the equivalent control IgG, both o/n with rotation at 4 ˚C. Ab-immunocomplexes were added to the beads, incubated for 4 hours at 4 ˚C with rotation, and washed with 1 mL of the following solutions, centrifuging in between at 16000 g for 30 seconds: twice with RIPA buffer, once with LiCl buffer (250 mM LiCl

/ 10 mM Tris-HCl pH 8.0 / 1 mM EDTA / 0.5 % NP-40 / 0.5 % sodium deoxycholate / 1 x Protease Inhibitors / 80 U / mL Ribolock) and once with TE buffer (10 mM Tris-HCl pH 8.0 / 1 mM EDTA / 1x Protease Inhibitors / 80 U / mL Ribolock). Finally, complexes were resuspended in 100 µL TE buffer, cross-linking was reversed by incubating 1 hour at 68 ˚C. RNA was extracted using Trizol and cDNA was synthesized using SuperScript IV Reverse transcriptase, according to manufacturer's instructions. qPCR was performed using following program: 50 ˚C for 20 seconds, 95 ˚C for 10 minutes, 40 cycles of 95 ˚C for 15 seconds and 60 ˚C for 1 minute, then melt curve from 60 ˚C to 95 ˚C with 1% slope. The following primer set was used: *Rac1*_Ybx1bs1_F: 5' CATGTGTTGCAGCTTTATAGTTTTT 3'; *Rac1*_Ybx1bs1_R – 5' CGGTAATCTGGCAAGACAGTGA 3'.

Western Blotting | Cells were lysed on ice for 15 minutes in soft RIPA buffer (50 mM Tris-HCl pH 8.0 / 150 mM NaCl / 1 % NP-40 Igepal / 0,5 % NaDOC / 0,1 % SDS) with protease inhibitors and phosphatase inhibitors. Cell debris were removed by centrifuging for 10 minutes at 11000 *g* at 4 ºC. Total protein concentration was quantified through the Bradford protein assay (Bio-Rad), using Bovine Serum Albumin (BSA) for the interpolation curve. 25 µg protein per well was used on SDS-PAGE runs, which were transferred into a nitrocellulose membrane with the iBlot Gel transfer device (Invitrogen), for 7 minutes. The membrane was stained with Ponceau S to confirm lane transfer, and blocked for 1 h in 1x Tris-buffered saline (TBS) + 0,01 % Tween20 (TBS+T) containing 5 % powdered milk. After blocking, membranes were incubated overnight at 4 ºC with the antibodies listed below diluted in TBS+T with milk. Membranes were washed three times with TBS+T, incubated with the proper secondary antibodies, washed in TBS+T and signal was detected with the Amersham Enhanced Chemiluminescence (ECL) Prime Western Blotting Detection Reagent (GE Healthcare). Protein semi-quantification was performed using the ImageLab software (Biorad). Antibodies used include anti-tubulin (B-5-1-2, 1: 250K dilution), anti-Ybx1 (ab12148, 1:1000), anti-Rac1 (ab155938, 1: 1000), anti-HIF1A (sc13515, 1:1000), anti-GAPDH (ab9484, 1:250K) and anti-Pol II (8WG16, ab819, 1:1000).

RNAPII Chromatin Immunoprecipitation (ChIP) | Dfx-treated RKO cells at 70 % confluency were cross-linked by incubation with 1 % formaldehyde for 10 minutes at

37 ºC, 50 rpm. Crosslinking was stopped by incubation with 0.125M glycine for 5 minutes. Cells were washed twice in ice-cold PBS, scraped off and centrifuged for 5 minutes at 500 g. The supernatant was discarded and cells were incubated on ice for 10 minutes in cell lysis buffer (PIPES 5 mM / 0.5 % NP-40 / 85 mM KCl with protease inhibitors: 0,5 mM PMSF, PIC 1 x, pepstatin 1 x) and centrifuged at 3000 rpm for 5 minutes at 4 ºC to pellet nuclei. Nucleic extracts were incubated for 10 minutes in ice-cold nuclear lysis buffer (50 mM Tris-HCl pH 8.0 / 0.25 % SDS / 10 mM EDTA with protease inhibitors). Chromatin was sheared using a sonicator, centrifuged at 13000 rpm for 10 minutes at 4 ºC and the supernatant was mixed with IP dilution buffer (16,7 mM Tris-HCl pH 8.0 / 0.01 % SDS / 1.1 % Triton X-100 / 1.2 mM EDTA / 167 mM NaCl with protease inhibitors). 10 % of the sample was reserved as input. The remaining was equally divided into IP and negative control (NO). The PolII Ab 8WG16 was added to the IP sample, and both were incubated o/n under agitation. Washed Protein G Dynabeads were added to IP and NO and incubated for 2 hours on rotation. Beads were purified using a DynaMag magnet according to manufacturer's instructions, and washed once each for 5 minutes with Buffers A-C (Buffer A: 20 mM Tris-HCl pH 8.0 / 2 mM EDTA / 1.1 % SDS / 1 % Triton X-100; 167 mM NaCl; Buffer B: 20 mM Tris-HCl pH 8.0 / 2 mM EDTA / 0.1 % SDS / 1 % Triton X-100 / 500 mM NaCl; Buffer C: 10 mM Tris-HCL pH 8.0 / 1 mM EDTA / 1 % NP-40 / 1 % NaDOC / 500 mM LiCl) and twice with Buffer D (10 mM Tris-HCl pH 8.0 / 1 mM EDTA), at 4 ºC, except the last wash which was performed at RT. Complexes were eluted in IP elution buffer (1 % SDS / 0,1 M $NaHCO_3$), rotating for 20 minutes at room temperature. Crosslinks were reversed by addition of NaCl and RNase A o/n at 65 ºC, and samples were treated with Proteinase K for 2 hours at 45 ºC. Proteinase K was inactivated through incubation for 5 minutes at 65 ºC and DNA was purified by phenol:chloroform:isoamyl alcohol extraction. qPCR was then performed using the program described above using the primers on table 4 below.

Table 4 – Primers used for *RAC1* Chromatin Immunoprecipitation assays.

Primer name	Primer sequence (5'→ 3')
*RAC1*_TSS_fwd	TTCCTCAGCTTTGGGTGGTG
*RAC1*_TSS_rev	CTGCATCAGGGCCGCTC
*RAC1*_Exon5_fwd	ACTGTCCCAACACTCCCATC
*RAC1*_Exon5_rev	TAGACCCTGCGGATAGGTGA
*RAC1*_E2I2-3j_fwd	TAACCTGTTTGTGTTACGGGT
*RAC1*_E2I2-3j_rev	TGTTCATATGAGGATTAAAGATGGC
*RAC1*_intergenic_1kb_fwd	CCGCCTCCAGCTGAGTATTT
*RAC1*_intergenic_1kb_rev	AGTGCAGGAGGCATAGGTTG
*RAC1*_intergenic_5kb_fwd	CTCAGCCTGCTACAGCATTTC
*RAC1*_intergenic_5kb_rev	TTGAGCCCAGGGGTTCACAG

In silico analyses

The ENSEMBL and UCSC genome browsers, and databases APAdb and Aceview were accessed to check for alternative 3' UTR sites of human mRNA. Nucleotide sequences and mRNA profiles were obtained from NCBI and Ensembl databases.

RBP binding sites in alternative 3' UTR mRNAs | RBP databases RBPMap and RBPDB were used to search sequence motifs of RNA-Binding Protein sites in the alternative 3' UTRs of candidate genes. Criteria to consider RBP-RNA interactions were p value < 0.05 and Z-score of 2, meaning that the interaction occurred with twice the probability as in the background 3' UTR nucleotide sequence.

Chapter IV – General Discussion

Chapter IV – General Discussion

Throughout the last hundred years, research on cancer and molecular biology has highlighted the indelible causality between gene expression regulation, environmental factors, and tumor progression. This intricate, complex communication determines patient survival and quality of life, and becomes clearer each day as researchers answer some questions and bring science forth even more.

This PhD thesis aimed to understand the crosstalk between macrophages and colon cancer (CRC) cells, centered on the perspective of RNA biology, particularly gene expression regulation and alternative polyadenylation. We proposed to study the phenotype and gene expression profile of primary human macrophages in opposite ends of the inflammatory spectrum, centering particularly in pro-inflammatory macrophages and in macrophages in co-culture with CRC cancer cells. Furthermore, we aimed to profile mRNA isoforms produced by these cells to infer the association between gene expression regulation and alternative 3' UTR mRNA isoform production, and to determine any possible prognostic hints that could benefit cancer patients. Finally, we identified SRSF12 as a macrophage transcriptomic regulator responsible for 3' UTR-APA isoform diversity in pro-inflammatory macrophages, with a potential protective role *in vivo*.

Understanding the mechanisms regulating gene expression in innate immune cells, such as macrophages, and during their interaction with cancer cells, will provide new insights on tumor immunology and on tumor microenvironment. In particular, APA, a widely described eukaryotic gene regulation mechanism, is almost unexplored in primary human cells (Jia *et al.*, 2017; Pai *et al.*, 2016). However, knowing that transcription and gene expression regulation contribute to macrophage plasticity, we decided to investigate the influence of pro-inflammatory stimuli (LPS and IFNγ) and anti-inflammatory stimuli (CRC cells) on gene expression and alternative polyadenylation in primary human macrophages through an unbiased genome-wide approach. To our knowledge, this was the first genome-wide study using co-cultured primary human macrophages. Studying the transcriptome of macrophages interacting with cancer cells and other components of the tumor microenvironment is crucial to better understand immune evasion and to develop more efficient diagnostic and

therapeutic tools. The strategy applied here involved isolation of macrophages from healthy blood donors, its exposure to pro-inflammatory conditions and then performing indirect co-cultures, which recapitulates macrophage involvement in colon cancer biology and creates an ideal model system for transcriptomic studies.

However, the use of primary human immune cells in transcriptomic studies has been hampered by the plastic nature of these cells and by the different protocols for differentiation and polarization in use that result in diverse outcomes for the cell and consequently affect transcriptomic results. Therefore, macrophage phenotype must be extensively characterized before further studies. It is also important to mention that anti-inflammatory macrophages are inherently functionally heterogeneous (Roszer, 2015) and similar to their naïve M0 counterparts, as previously reported in the literature (Chistiakov *et al.*, 2015; Martinez *et al.*, 2006).

Our first efforts were dedicated to establish a protocol for isolation of human primary monocytes, their polarization into pro-inflammatory macrophages and co-culture with colorectal cancer cells suitable for subsequent gene expression and APA analysis. Using this methodology, it was possible to pinpoint exact mRNA isoform changes observed in the same human donor, and to infer these differences to the nuclear or cytoplasmic fraction. By analyzing the statistical significance of the mRNA isoform changes between conditions, we showed that different genes display different APA profiles and that CRC cells modulate macrophage APA. At this stage, it must be mentioned that one of the limitations of our subcellular fractionation sequencing approach is that while it allows for the discovery of regulatory RNAs such as long non-coding RNA and antisense transcripts genome-wide, it does not enable the identification of ribosomal RNAs from primary human macrophages (Poddar *et al.*, 2013), due to the methods used for mRNA enrichment. Therefore, the analyses of macrophage mRNA translation are true blind spots for this research.

Macrophages are dynamic, plastic immune cells with their gene expression regulation determining functions ranging from defense and detoxification to wound healing. Studying 3’ UTRs in macrophages will increase the spectrum of known alterations in immune cells when exposed to cancer cells or to the hypoxic conditions of the tumor microenvironment. Due to microbiota challenge, intestinal tissue macrophages are mainly circulating macrophages (De Schepper *et al.*, 2018; Zigmond & Jung, 2013), upregulating their pro-inflammatory characteristics to maintain a tight

control on gut microbiome levels. At the onset of colorectal cancer progression, macrophages recognize and attack tumor cells (Bögels *et al.*, 2012). However, the few cells that escape create a tumor-permissive microenvironment in which macrophage polarization is diverted into an anti-inflammatory phenotype. In this context, pro-inflammatory macrophages (M1) have a defined anti-tumoral role, while anti-inflammatory macrophages (M2) are tumor-permissive (Cardoso, Pinto, *et al.*, 2015; Lawrence & Natoli, 2011; Locati *et al*., 2013; Quail & Joyce, 2017).

The described protocol is a low-cost, big data approach for transcriptomic studies adapted to the need and budget of research laboratories, and particularly for the macrophage – CRC model system. Sequencing low quantities of primary macrophages to obtain simultaneous nuclear and total RNA for differential gene expression, as well as novel APA mRNA isoform identification, in Illumina-compatible systems, allows a thorough, unbiased transcriptomic characterization of those plastic immune cells in a relevant pathophysiologic context. Furthermore, with this method one can identify genome-wide signatures relevant for gene expression regulation and with potential diagnostic applications, using relatively few cells. In conclusion, our method provides a basis for transcriptomic analyses using co-cultures of primary human macrophages with cancer cells.

To study the influence of cancer cell communication on macrophage function, we have characterized the morphology, cytoskeletal organization and expression of pro- and anti-inflammatory markers in macrophages cultured alone or with CRC cell lines. Previous results showed that classic M1-like LPS stimulation causes an elongated phenotype with filopodia, while M2-like IL-10 stimulation gives rise to a rounded phenotype (Cardoso, Pinto, *et al.*, 2015; Ploeger *et al.*, 2013). As macrophage morphology is very sensitive to microenvironmental cues (Ploeger *et al.*, 2013), the remarkable phenotypic change observed from ramified, pronounced dendritic-like macrophage monocultures to amoeboid co-cultured macrophages suggests a dynamic transcriptomic response to the molecular factors secreted by the CRC cells. We then sought to uncover their identity and cellular functions.

Using 3’ RNA-seq from total RNA to study the effect of polarization and CRC co-culture on the transcriptome of primary human macrophages, we first observed that

pro-inflammatory macrophages (LPS+IFNγ) sustain substantial transcriptomic changes compared to unstimulated naïve macrophages, with significant differential expression of 3514 genes out of 19,328 expressed genes (18,1%). This surpasses the 5% statistical differential expression previously detected in this populations, in a seminal microarray study performed before the widespread usage of RNA-Seq (Martinez *et al.*, 2006).

CRC modulates gene expression in macrophages

To the best of our knowledge, we performed the first genome-wide transcriptomic study using primary human macrophages polarized as pro-inflammatory M1 and co-cultured with two different CRC cell lines. For that, we have first determined the differential expression of genes in macrophages. Most common DEGs were upregulated in co-cultured macrophages. Moreover, the most upregulated genes were connected to the anti-inflammatory macrophage profile, suggesting that the phenotypic changes observed by confocal microscopy were in fact consistent with the transition from a pro-inflammatory into an anti-inflammatory phenotype. 3' mRNA-Seq was performed in bulk total RNA after co-culture of pro-inflammatory macrophages with CRC cells. Our results demonstrated that co-cultured macrophages presented 35 common DEGs, related to transcription regulation by transcription factor localization, cell-cell exosome signaling, IL-1-mediated signaling pathways, cell-cell adhesion, integrin binding and migration, and MHC class I binding, reinforcing the hypothesis of a reversion of the macrophage inflammatory profile.

Upregulated anti-inflammatory genes included *LRP5,* an integral part of the Wnt pathway (Logan & Nusse, 2004), associated to M2 polarization and immune evasion in macrophages (Cai *et al.*, 2018; Feng *et al.*, 2018; Gong *et al.*, 2017); M2- and TAMs-associated MRC1, which is generally downregulated in pro-inflammatory macrophages (Gordon, 2003; Gundra *et al.*, 2014; Martinez *et al.*, 2006; Roszer, 2015; Pinto *et al.*, 2016), TAMs-associated *FUCA1* (Xu et al., 2020), and modulator ECM component *THBS1*, which triggers IL-10 signaling in macrophages, inhibits angiogenesis via NF-kB and VEGFR, and depending on cellular context, it acts as a pro- or anti-inflammatory mediator (Gutierrez *et al.*, 2011; Zhao *et al.*, 2014). In

addition, upregulation of TAMs-associated EGF ligand EREG was also observed in co-cultured macrophages.

Interestingly, 80 % of genes common in macrophages co-cultured with RKO and HCT-15 code for transmembrane or extracellular proteins, key for macrophage functions. Since our system used indirect co-cultures, it is possible that growth factors secreted by the CRC cells are sufficient to incite these DEG levels in macrophages. Essentially, macrophages convert to anti-inflammatory, detoxifying M2/Mox profile after 24 hours of CRC co-culture, shown by upregulation of the M2 markers listed above and also by the detection of Mox markers in co-cultured macrophages – *IL1B* (Leitinger & Schulman, 2013), *CXCL8* (Parisi *et al.*, 2018), *HMOX* and *SRXN1* (Kadl *et al.*, 2010; Marques *et al.*, 2016) – which is to our knowledge the first time this macrophage population has been identified in the context of the CRC microenvironment. Mox macrophages rebalance redox homeostasis and were previously found in pro-tumor microenvironments such as gastric adenocarcinoma and ulcerative colitis, and induced by anti-inflammatory stimuli (Eren *et al.*, 2018; Kadl *et al.*, 2010; Lai *et al.*, 2019; Serbulea *et al.*, 2017).

Our analysis of ChrRNA-Seq data began by the metaprofile differences between monocultured and co-cultured macrophages, showing a global upregulation of transcription in the latter population, both in the coding region and beyond the TTS. These results are also in agreement with previous data showing increased RNAPII occupancy over the transcription units of the DEGs found in our chromatin-bound data, in M1 macrophages (Ostuni *et al.*, 2013), and also with the upregulation of RNA transcription that occurs upon infection (Pai *et al.*, 2016). We found upregulation of transcription of several receptors relevant for immune system function (*CNR2*, *CD244*, *SPN*), cytoskeleton reorganization (*CTTNBP2*, *ARHGDIB*), transcription factors (*ID3*), ion transporters and binding proteins and amino acid-related enzymes. Moreover, we found that 25% of the 3' mRNA-Seq upregulated genes both in M1+RKO and M1+HCT-15 are also upregulated in the chromatin-bound RNA, indicating that this upregulation is due to co-transcriptional processes. Additionally, upregulated gene ontology in co-cultured macrophages included vesicle-mediated transport and lipid binding, which have been previously associated with pro-tumoral mechanisms stemming from cancer cell crosstalk (Pakiet *et al.*, 2019; Ruiz-López *et al.*, 2018). Our results suggest that not only macrophages switch towards acquiring an anti-

inflammatory phenotype upon co-culture with CRC, but also that they undergo transcriptomic changes towards a Mox detoxifying macrophage phenotype. A pre-existing built-in tendency for increased transcription of the anti-inflammatory genes was revealed in the chromatin-bound RNA fraction, and gene expression was confirmed in several genes by 3' mRNA-Seq. These results argue that as expression of macrophage genes specifically connected to anti-inflammatory or immunomodulatory functions is upregulated after exposure to CRC cells, it may allow for the sustained activation of relevant signaling pathways.

In conclusion, we demonstrate a reversion of the macrophage M1 phenotype presented in monocultures towards a more anti-inflammatory population, both morphologically and transcriptomically, following exposure to CRC cells. Previous studies have shown that macrophage stimuli – such as polarization, autocrine regulation or cancer cell crosstalk (IFNαβ, IFNγ, TGFβ, TNFα, M-CSF, IL-10, IL-4 and IL-13) induce partially overlapping transcriptional programs (Gordon, 2003; Gordon & Martinez, 2010), and it is plausible that the combination of these stimuli may result in this mixed inflammatory phenotype, representing a complex in vivo macrophage population diversity. Furthermore, upregulation of other genes such as *CXCL8* in co-cultured macrophages may be indicative of IL-4 and IL-13-like polarization profile, reinforcing that CRC cells induce a reversal of the M1 pro-inflammatory profile (Turner *et al.*, 2014).

Indeed, several studies have demonstrated that the impact of CRC cells on macrophages differentiation profile is dependent on the tumor-associated macrophage location, and that the microenvironmental-driven polarization profile is predictive of patient survival (Bögels *et al.*, 2012). In CRC, anti-inflammatory-like macrophages tend to be closer to the intra tumor region and the tumor invasive front, while pro-inflammatory-like macrophages are generally closer to the tumor periphery and to the healthy mucosa (Pinto *et al.*, 2019). Such a stratification of macrophage localization may favor tumor cell proliferation, angiogenesis and tumor growth (Hao *et al.*, 2012; Liu *et al*., 2014). Our results clarify the role of macrophage modulation by CRC and identify new therapeutic tools for future cancer treatment.

We explored databases containing *in vivo* results to understand the role of DEGs in CRC patient outcomes, and found that *LRP5* upregulation increased patient

survival, whereas *SEMA6B* and *THBS1* upregulation was correlated with increased macrophage infiltration *in vivo*. As all three genes have been associated with tumorigenesis (Daubon *et al.*, 2019; Larionova *et al.*, 2020; Lindvall *et al.*, 2006), and we found mRNA upregulation in macrophages after only 24 hours co-culture, we propose the inclusion of these as biomarkers for early CRC cancer screening

CRC modulates APA in macrophages

Studying APA and alternative 3' UTRs in macrophages increases the atlas of known innate immune cell transcriptomic alterations and opens doors to uncovering new layers of gene regulation. Before analyzing significant differences in alternative 3' UTR mRNAs expression, an unbiased analysis was conducted in 3'mRNA-Seq data using DEXSeq to quantify the mRNA isoform number in macrophages, upon M1 polarization and co-culture. As previous literature, we applied a stringent expression level criterion to samples: we considered that all mRNA isoforms with 0.1 usage or higher (considering 1.0 as the highest expressed mRNA isoform in each gene) in at least two replicates are indicative of alternative polyadenylation (Singh *et al.*, 2018).

Our unbiased approach aimed to identify physiologically relevant APA events that could enlighten underlying molecular mechanisms in co-cultured macrophages. Additionally, we were able to contribute to the community with the biggest known catalog of alternative 3' UTRs in primary human macrophages after polarization and co-culture stimuli. We found that 50% of genes in naïve and pro-inflammatory macrophages use at least two mRNA isoforms with alternative 3' UTRs, due to the usage of two PAS, irrespectively of their expression. Interestingly, this transcriptomic diversity is abrogated after CRC co-culture, where 75% macrophage genes use only one PAS. This event may not be stochastic, as some of these genes are related to IFNγ, a pro-inflammatory cytokine. Remarkably, these genes tend to choose the distal PAS when in co-culture. As anti-inflammatory macrophages are associated with less proliferation, this observation follows the paradigm established in the field that less proliferative cells choose preferentially distal PAS.

Our data expands the known catalog of alternative 3' UTRs in macrophages upon polarization to 56331 total APA events. Additionally, we identified 46 significant 3' UTR-APA and CR-APA shifts in inflammatory-related genes in pro-inflammatory and co-cultured macrophages.

In accordance to what was found in other cell types (Araki et al., 2018), the total expression of genes that, after CRC exposure, expressed only one long 3' UTR tend to be downregulated. Notably, these genes are involved in gene expression regulation and in immune system development. These lengthened 3' UTR isoforms may be subject to increased regulation by miRNAs and RBPs than shortened 3' UTR isoforms (Castello *et al.*, 2012; Mayr, 2017; Seeley *et al.*, 2018; Tian & Manley, 2016) and hence be available at lower concentrations in the cytoplasm.

Therefore, less prevalent 3' UTR shortening through APA in co-cultured macrophages, particularly in pro-inflammatory, could be associated to lack of adaptability to the CRC cell pressure (Zheng *et al*., 2018), as mRNAs in pre-co-culture pro-inflammatory macrophages tend to use shorter 3' UTRs, which are transcribed and processed quicker. However, whether this observation is a cause or a consequence of macrophage behavior after CRC stimuli is still an unanswered question.

Out of the 46 genes, 33 genes showed upregulation of their shorter 3' UTRs. These genes are connected to inflammation, cell signaling and cell-to-cell communication Interestingly, genes with short 3' UTRs and pro-inflammatory polarization conditions were both previously found to be associated with open chromatin (Li *et al.*, 2016).

Upregulated shorter 3' UTR mRNA isoforms include *MXD1*/*MAD,* a MYC antagonist through competition with binding partner and also shortening APA gene *MAX*, a transcription factor associated with macrophage polarization. *MAX* has been described as an activator when in heterodimer with *MYC* and as an inhibitor when bound to *MXD1* during macrophage differentiation (Hutchinson, 1993; Lambert *et al.*, 2018). Interestingly, *MYC* expression is significantly downregulated after M1 polarization and *MYC* expression levels remain low during co-culture, while there is an upregulation of *MAX* and *MXD1* short 3'UTR mRNAs. It is tempting to speculate that these expression and APA alterations correlate to MYC-MAX function. However, this is, to the best of our knowledge, the first study in which alternative 3' UTRs have been correlated to these gene functions.

The *MXD1* protein product MAD1 is downregulated after pro-inflammatory polarization, concomitantly with upregulation of the shorter mRNA isoform, suggesting that protein levels are increased by 3' UTR shortening. However, not all mRNA changes observed are reflected in their protein products differential expression of 3'

UTRs in *MAP3K8* (*Tpl*-2), an example of CR-APA. *MAP3K8* modulates immune cell function and after pro-inflammatory signaling (Sanz-Garcia *et al.*, 2014) via MAPK, there was no clear correlation with protein expression in co-cultured macrophages, as expression was dependent upon the specific CRC cell line to which macrophages were exposed. In general, our 3'UTR-APA findings are independent of the CRC cell line used. Yet, this is an example in which the secretome of each cell line may be determinant for macrophage response and may be hence further explored for therapy design. Therefore, it is possible that despite genes that undergo APA in M1 but not in co-cultured macrophages mostly choose the distal PAS, the differential APA signature found in M1 is maintained after CRC exposure. For instance, some of the 33 gene subset with preferential proximal PAS selection found in both pro-inflammatory and co-cultured macrophages could apply a similar strategy between to ensure proper protein production.

Upregulated long 3' UTR mRNAs include *PAK1*, a kinase with important functions for macrophage biology. PAK1 is connected to pro-inflammatory polarization and regulates polarity through ERK1/2 activation (Pyronneau *et al.*, 2017). In turn, *IL12RB1*, also an example of CR-APA encodes the ß1 chain of the IL-12 and IL-23 receptors (Zhang *et al.*, 2010).

The low number of mRNA isoforms statistically upregulated in M1 and co-cultured macrophages (33 upregulated shorter 3' UTR isoforms and 13 upregulated longer 3' UTR isoforms) identified in the three biological replicates has also been found in other studies, including in activated immune cells (Gruber *et al.*, 2014; Morris *et al.*, 2012; Pai *et al.*, 2016; Yang *et al.*, 2018) and the relatively small number of alternative 3' UTR genes that undergo statistically significant shifts may be due to primary donor heterogeneity. Additionally, in agreement with previous literature, there was no correlation between gene expression and APA (Jia *et al.*, 2017; Kocabas *et al.*, 2015; Mercer *et al.*, 2011), meaning that these events act independently but in the same pathways, conferring redundancy to macrophage biology.

Similarly to DEGs, we explored the role of some genes undergoing differential APA isoform expression in M1 and co-cultured macrophages in *in vivo* TCGA databases. We found that MAP3K8, MXD1 and IL12RB1 expression in patients decreased patient survival, and we hypothesize that as it has no obvious connection to mRNA upregulation, it could then be connected to the upregulated short 3' UTR (in

MAP3K8 and *MXD1*) or long 3' UTR (in *IL12RB1*) observed in macrophage populations. *MAP3K8* and *IL12RB1* have been implicated in hereditary and metastatic CRC, so we propose they are included in CRC screening in patients (Belhadj *et al.*, 2020; Pyo *et al.*, 2018).

SRSF12 as a macrophage modulator

The RNA Recognition Motif and the SR domain in SRSF12 enable 5' splice site (ss) selection and repression of SR protein action during alternative splicing (Chandler *et al.*, 1997; Cowper *et al.*, 2001; Roca *et al.*, 2013). As the top upregulated gene associated with RNA metabolism in M1 macrophages, *SRSF12* downregulation could have had several cell consequences, as lack of SR repression affects several pathways involved in cell transformation, due to increased levels alternative splicing and NMD (Das & Krainer, 2014; Kim *et al.*, 2015).

SRSF12 siRNA depletion downregulated 334 genes. Interestingly, this is evident for genes connected to the anti-inflammatory profile – *ARMC9*, *SEMA6B*, *MRC1* - suggesting that SRSF12 has a function in modulating 3'UTR-APA in genes with immune-related functions in macrophages.

SRSF12 upregulation in M1 macrophages and specific downregulation of expression of immune-related genes strongly suggests its widespread role in regulating innate immune cell gene expression. Therefore, we hypothesized that SRSF12 could cooperate with other *trans*-acting factors to activate the expression of short 3' UTR mRNAs isoforms in macrophages. For instance, downregulation of *CSTF2* mRNA and protein levels in *siSRSF12* depleted macrophages indicates that SRSF12 activates *CSTF2* expression and hints at a connection to the cleavage and polyadenylation mechanisms. If *CSTF2* is less expressed, its concentration at cleavage sites will be substoichiometric, which has been shown to contribute to increased proximal PAS selection (Shell *et al.*, 2005; Takagaki *et al.*, 1996). Strikingly, *SRSF2*, one of the SR factors on which SRSF12 acts upon, shows upregulation of the short 3' UTR isoform in *siSRSF12* depleted macrophages, possibly indicating a regulatory loop – SRSF2 and SRSF12 could interact differently depending on SRSF12 regulation of the SRSF2 transcript, especially its shorter 3' UTR.

After s*iSRSF12* depletion in macrophages, differences in APA may reflect changes in local 3' end processing factor concentrations, such as CstF2, differences in RBP

binding to the PASs or to *trans*-regulatory factors, such as SRSF12 interactors, with relevant cell consequences. *SRSF12* involvement in the selection of short 3' UTRs of innate immune transcripts in primary human macrophages may serve to hasten mRNA production in innate immune cells, allowing for quicker defense against pathogens or tumor challenge. SRSF12 may act as a macrophage master regulator, being associated to a pro-inflammatory inflammatory profile. Collectively, our data demonstrate that SRSF12 regulates macrophage 3' UTR-APA and gene expression.
Despite SRSF12 being a relatively low abundance SR protein, it was upregulated in in vivo TCGA data and its depletion had a clear effect on the macrophage transcriptome, downregulating gene expression and contributing to decreasing APA. This is reminiscent of hnRNP a0, a low abundance protein present that binds to the 3' UTR of distal transcripts in macrophages (Cok *et al*., 2004; Myer & Steitz, 1995). Furthermore, as SR proteins and hnRNP proteins have antagonistic roles (Expert-Bezançon *et al*., 2004), it is interesting to speculate on the role of SR repressor SRSF12 as closer to that of hnRNP proteins. Further studies are needed to confirm this hypothesis.
Studying the impact of RBPs on dynamic cellular scenarios contributes to an increased understanding of 3' end regulation by *SRSF12* on primary human macrophages.

Individual gene studies

We studied alternative 3'UTRs in individual candidate genes in naïve and pro-inflammatory macrophages prior to performing RNA-Seq, as a proof-of-concept approach. Results demonstrated upregulation of both gene expression and the shorter 3' UTR of *MCL1*, *IL1B* and *CD47* mRNAs, important for macrophage functions (anti-apoptotic molecule, pro-inflammatory cytokine, and anti-phagocytic receptor, respectively). In addition, upregulation of both gene expression and long 3' UTR of *RAC1* (involved in motility and migration) was also observed. RNA-seq data for the genes selected (*RAC1*, *MCL1*, *IL1B* and *CD47*) showed upregulation in co-cultured macrophages, emphasizing that the alternative 3' UTR mRNA isoform expression in cell populations is extremely dependent on cell context such as RBP upregulation.

Conclusion

This PhD work shows that macrophages adapt to CRC stimuli by producing a 35-gene signature consisting of anti-inflammatory, pro-tumoral members, and by decreasing the number of overall available alternative 3' UTR isoforms. Importantly, this work also identified mRNA isoforms significantly upregulated in pro-inflammatory and co-cultured macrophages with differential predictive power of macrophage infiltration levels and overall survival in CRC patients. Simultaneously, this work highlighted the previously unknown role of the SR protein SRSF12 in innate immune gene regulation through selection of proximal PAS signals in pro-inflammatory macrophages through a yet unknown mechanism.

In conclusion, this work sheds new light on alternative 3'UTR isoform expression and regulation by RBPs, which should always be taken into account in transcriptomic studies, when studying innate immune cells and tumor microenvironment, and on a potential novel role for an SR protein involved in alternative splicing, SRSF12.

Chapter V – Future Work

Chapter V – Future work

Validate macrophage genes on human tissue specimens

After characterization of the molecular mechanisms, the next step would be their validation in tissue-matched human samples, available at Hospital São João through immunohistochemistry and classification of samples according to gene expression of the candidate genes and cross with tumor localization on the organ (ascending or descending colon) and with patients' clinicopathological information inferring about possible prognostic effects.

Survey transcriptomic changes in CRC cell lines upon co-culture with macrophages

Studying the transcriptomic changes in the colorectal cancer cell lines RKO and HCT-15, whether in their gene expression or alternative 3' UTRs, would enable us to characterize the converse situation shown here with macrophages, and to deepen our understanding of co-cultures as complex exchanges of information. Moreover, as cancer cell lines are easier to culture *in vitro*, one could reach higher numbers of available cells that would enable the establishment of several timepoints in which we could further elucidate the generation of mRNAs, bringing us to an even higher understanding of this system.

Perform eCLIP in SRSF12 to identify binding sites with nucleotide resolution

It was unfeasible to perform IPs to study SRSF12 due to the lack of good tools, namely appropriate antibodies. However, it would be very interesting to identify mRNAs physically bound to SRSF12 through enhanced cross-linking immunoprecipitation (eCLIP) (Van Nostrand et al., 2016), which uses an RBP antibody to precipitate *in vivo* bound cross-linked RNA. eCLIP enables the high-throughput identification of small nucleotide stretches of identify biologically relevant target mRNAs with reduced sequence bias. If combined with conditional knockout of SRSF12 in mice macrophages, or SRSF12 CRISPR in THP-1, this approach could contribute to increased understanding of the role of SRSF12.

Explore the role of SRSF12 in the CRC co-culture cell context

We revealed a new role of SRSF12 in proximal PAS choice in M1 macrophages. As we have seen that co-cultured macrophages also show several gene expression and alternative 3' UTR choice changes, it would be logical to explore the role of this SR protein in the context of co-culture with RKO and HCT-15 by optimizing the consecutive co-culture/siRNA methodology and performing 3' mRNA-Seq and ChrRNA-Seq in co-culture macrophage populations with SRSF12 depletion, and quantifying DEG and differential alternative 3' UTR levels.

Use of oligonucleotides and ASOs to study alternative 3' UTR choice

Studying RBP binding to individual 3' UTRs in macrophages upon CRC co-culture through ChIRP-MS, which involves pulldown of endogenous RNAs with biotinylated oligonucleotides and subsequent mass spectrometry to identify bound proteins, would enable us to determine the RBPome in interesting innate immune-related or RNA processing genes.

Alternatively, it would be interesting to drive 3' UTR lengthening of genes showing upregulation of short 3' UTRs and related to immune pathways, through the use of antisense oligonucleotides (ASOs). For instance, this approach could be performed in *DICER1*, which shows upregulation of the short 3' UTR in M1 and co-cultured macrophages, with locked nucleic acids or peptide nucleic acids, blocking the proximal PAS and examining effects of forcing the expression of the long 3' UTR of *DICER1* in pro-inflammatory polarization and responses to CRC cell stimuli.

Chapter VI - References

Chapter VI - References

Abdelwahab, E. M. M., Rapp, J., Feller, D., Csongei, V., Pal, S., Bartis, D., Thickett, D. R., & Pongracz, J. E. (2019). Wnt signaling regulates trans-differentiation of stem cell like type 2 alveolar epithelial cells to type 1 epithelial cells. *Respiratory Research*, *20*(1), 1–9. https://doi.org/10.1186/s12931-019-1176-x

Adelman, K., & Lis, J. T. (2012). *Promoter-proximal pausing of RNA polymerase II: emerging roles in Metazoans*. *13*(10), 720–731. https://doi.org/10.1038/nrg3293.Promoter-proximal

Aghabozorgi, A. S., Bahreyni, A., Soleimani, A., Bahrami, A., Khazaei, M., Ferns, G. A., Avan, A., & Hassanian, S. M. (2019). Role of adenomatous polyposis coli (APC) gene mutations in the pathogenesis of colorectal cancer; current status and perspectives. *Biochimie*, *157*, 64–71. https://doi.org/10.1016/j.biochi.2018.11.003

Ahmed, D., Eide, P. W., Eilertsen, I. A., Danielsen, S. A., Eknæs, M., Hektoen, M., Lind, G. E., & Lothe, R. A. (2013). Epigenetic and genetic features of 24 colon cancer cell lines. *Oncogenesis*, *2*(0424), e71. https://doi.org/10.1038/oncsis.2013.35

Ahn, S. H., Kim, M., & Buratowski, S. (2004). Phosphorylation of Serine 2 within the RNA Polymerase II C-Terminal Domain Couples Transcription and 3′ End Processing. *Molecular Cell*, *13*(1), 67–76. https://doi.org/10.1016/S1097-2765(03)00492-1

Akdeli, N., Riemann, K., Westphal, J., Hess, J., Siffert, W., & Bachmann, H. S. (2014). A 3'UTR polymorphism modulates mRNA stability of the oncogene and drug target Polo-like Kinase 1. *Molecular Cancer*, *13*(1), 87. https://doi.org/10.1186/1476-4598-13-87

Alasoo, K., Martinez, F. O., Hale, C., Gordon, S., Powrie, F., Dougan, G., Mukhopadhyay, S., & Gaffney, D. J. (2015). Transcriptional profiling of macrophages derived from monocytes and iPS cells identifies a conserved response to LPS and novel alternative transcription. *Scientific Reports*, *5*(February), 1–12. https://doi.org/10.1038/srep12524

Alberts, B., Johnson, A., Lewis, J., Morgan, D., Raff, M., Roberts, K., & Walter, P. (2008). Molecular Biology of the Cell,6th Edition. In *Medicine & Science in Sports & Exercise* (Vol. 40, Issue 9). https://doi.org/10.1249/mss.0b013e318185ce9d

Alberts, D. S., Marth, C., Alvarez, R. D., Johnson, G., Bidzinski, M., Kardatzke, D. R., Bradford, W. Z., Loutit, J., Kirn, D. H., Clouser, M. C., & Markman, M. (2008). Randomized phase 3 trial of interferon gamma-1b plus standard carboplatin/paclitaxel versus carboplatin/paclitaxel alone for first-line treatment of advanced ovarian and primary peritoneal carcinomas: Results from a prospectively designed analysis of progression-free survival. *Gynecologic Oncology*, *109*(2), 174–181. https://doi.org/10.1016/j.ygyno.2008.01.005

Alexander, R. K., Liou, Y. H., Knudsen, N. H., Starost, K. A., Xu, C., Hyde, A. L., Liu, S., Jacobi, D., Liao, N. S., & Lee, C. H. (2020). Bmal1 integrates mitochondrial metabolism and macrophage activation. *ELife*, *9*, 1–28. https://doi.org/10.7554/eLife.54090

Amend, S. R., & Pienta, K. J. (2015). Ecology meets cancer biology: the cancer swamp promotes the lethal cancer phenotype. *Oncotarget*, *6*(12), 9669–9678. https://doi.org/10.18632/oncotarget.3430

American Cancer Society. (2018a). *Colorectal Cancer Early Detection , Diagnosis , and Staging*. https://www.cancer.org/content/dam/CRC/PDF/Public/8606.00.pdf

American Cancer Society. (2018b). *Treating Colorectal Cancer*. https://www.cancer.org/content/dam/CRC/PDF/Public/8607.00.pdf

Anders, L., Ke, N., Hydbring, P., Choi, Y. J., Widlund, H. R., Joel, M., Zhai, H., Vidal, M., Gygi, S. P., & Braun, P. (2012). *A Systematic Screen for CDK4/6 Substrates Links FOXM1 Phosphorylation to Senescence Suppression in Cancer Cells*. *20*(5), 620–634. https://doi.org/10.1016/j.ccr.2011.10.001.A

Anders, S., Pyl, P. T., & Huber, W. (2015). HTSeq-A Python framework to work with high-throughput sequencing data. *Bioinformatics*, *31*(2), 166–169. https://doi.org/10.1093/bioinformatics/btu638

Anders, S., Reyes, A., & Huber, W. (2012). Detecting differential usage of exons from RNA-seq data. *Genome Research*, *22*(10), 2008–2017. https://doi.org/10.1101/gr.133744.111

Andersen, P. K., Lykke-Andersen, S., & Jensen, T. H. (2012). Promoter-proximal polyadenylation sites reduce transcription activity. *Genes and Development*, *26*(19), 2169–2179. https://doi.org/10.1101/gad.189126.112

Andres, S. F., Williams, K. N., Plesset, J. B., Headd, J. J., Mizuno, R., Chatterji, P., Lento, A. A., Klein-Szanto, A. J., Mick, R., Hamilton, K. E., & Rustgi, A. K. (2019). IMP1 3′ UTR shortening enhances metastatic burden in colorectal cancer. *Carcinogenesis*, *40*(4), 569–579. https://doi.org/10.1093/carcin/bgy153

Antonczyk, A., Krist, B., Sajek, M., Michalska, A., Piaszyk-Borychowska, A., Plens-Galaska, M.,

Wesoly, J., & Bluyssen, H. A. R. (2019). Direct inhibition of IRF-dependent transcriptional regulatory mechanisms associated with disease. *Frontiers in Immunology*, *10*(MAY), 1–23. https://doi.org/10.3389/fimmu.2019.01176

Araki, S., Nakayama, Y., Sano, O., Nakao, S., Shimizu-Ogasawara, M., Toyoshiba, H., Nakanishi, A., & Aparicio, S. (2018). Decoding Transcriptome Dynamics of Genome-Encoded Polyadenylation and Autoregulation with Small-Molecule Modulators of Alternative Polyadenylation. *Cell Chemical Biology*, *25*(12), 1470-1484.e5. https://doi.org/10.1016/j.chembiol.2018.09.006

Armaghany, T., Wilson, J. D., Chu, Q., & Mills, G. (2012). Genetic alterations in colorectal cancer. *Gastrointestinal Cancer Research : GCR*, *5*(1), 19–27.

Bain, C. C., Bravo-Blas, A., Scott, C. L., Gomez Perdiguero, E., Geissmann, F., Henri, S., Malissen, B., Osborne, L. C., Artis, D., & Mowat, A. M. I. (2014). Constant replenishment from circulating monocytes maintains the macrophage pool in the intestine of adult mice. *Nature Immunology*, *15*(10), 929–937. https://doi.org/10.1038/ni.2967

Barclay, A. N., & Brown, M. H. (2006). The SIRP family of receptors and immune regulation. *Nature Reviews Immunology*, *6*(6), 457–464. https://doi.org/10.1038/nri1859

Barsoum, I. B., Smallwood, C. A., Siemens, D. R., & Graham, C. H. (2014). A mechanism of hypoxia-mediated escape from adaptive immunity in cancer cells. *Cancer Research*, *74*(3), 665–674. https://doi.org/10.1158/0008-5472.CAN-13-0992

Beaudoing, E., Freier, S., Wyatt, J. R., Claverie, J. M., & Gautheret, D. (2000). Patterns of variant polyadenylation signal usage in human genes. *Genome Research*, *10*(7), 1001–1010. https://doi.org/10.1101/gr.10.7.1001

Begik, O., Oyken, M., Cinkilli Alican, T., Can, T., & Erson-Bensan, A. E. (2017). Alternative Polyadenylation Patterns for Novel Gene Discovery and Classification in Cancer. *Neoplasia (United States)*, *19*(7), 574–582. https://doi.org/10.1016/j.neo.2017.04.008

Belhadj, S., Terradas, M., Munoz-Torres, P. M., Aiza, G., Navarro, M., Capellá, G., & Valle, L. (2020). Candidate genes for hereditary colorectal cancer: Mutational screening and systematic review. *Human Mutation*, *41*(9), 1563–1576. https://doi.org/10.1002/humu.24057

Ben-Dov, C., Hartmann, B., Lundgren, J., & Valcárcel, J. (2008). Genome-wide analysis of alternative pre-mRNA splicing. *Journal of Biological Chemistry*, *283*(3), 1229–1233. https://doi.org/10.1074/jbc.R700033200

Bennett, C. L., Christie, J., Ramsdell, F., Brunkow, M. E., Ferguson, P. J., Whitesell, L., Kelly, T. E., Saulsbury, F. T., Chance, P. F., & Ochs, H. D. (2001). The immune dysregulation, polyendocrinopathy, enteropathy, X-linked syndrome (IPEX) is caused by mutations of FOXP3. *Nature Genetics*, *27*(1), 20–21. https://doi.org/10.1038/83713

Bentley, D. L. (2005). Rules of engagement: Co-transcriptional recruitment of pre-mRNA processing factors. *Current Opinion in Cell Biology*, *17*(3), 251–256. https://doi.org/10.1016/j.ceb.2005.04.006

Bentley, D. L. (2014). Coupling mRNA processing with transcription in time and space. *Nat Rev Genet*, *15*(3), 163–175. https://doi.org/10.1038/nrg3662.Coupling

Berkovits, B. D., & Mayr, C. (2015). Alternative 3' UTRs act as scaffolds to regulate membrane protein localization. *Nature*, *522*(7556), 363–367. https://doi.org/10.1038/nature14321

Bhullar, J., & Sollars, V. E. (2011). YBX1 expression and function in early hematopoiesis and leukemic cells. *Immunogenetics*, *63*(6), 337–350. https://doi.org/10.1007/s00251-011-0517-9

Bienroth, S., Keller, W., & Wahle, E. (1993). Assembly of a processive messenger RNA polyadenylation complex. *The EMBO Journal*, *12*(2), 585–594. https://doi.org/10.1002/j.1460-2075.1993.tb05690.x

Bilanges, B., & Stokoe, D. (2007). Mechanisms of translational deregulation in human tumors and therapeutic intervention strategies. *Oncogene*, *26*(41), 5973–5990. https://doi.org/10.1038/sj.onc.1210431

Bingle, L., Lewis, C. E., Corke, K. P., Reed, M., & Brown, N. J. (2006). Macrophages promote angiogenesis in human breast tumour spheroids in vivo. *British Journal of Cancer*, *94*(1), 101–107. https://doi.org/10.1038/sj.bjc.6602901

Bochet, L., Meulle, A., Imbert, S., Salles, B., Valet, P., & Muller, C. (2011). Cancer-associated adipocytes promotes breast tumor radioresistance. *Biochemical and Biophysical Research Communications*, *411*(1), 102–106. https://doi.org/10.1016/j.bbrc.2011.06.101

Bögels, M., Braster, R., Nijland, P. G., Gül, N., van de Luijtgaarden, W., Fijneman, R. J. A., Meijer, G. A., Jimenez, C. R., Beelen, R. H. J., & van Egmond, M. (2012). Carcinoma origin dictates differential skewing of monocyte function. *Oncoimmunology*, *1*(6), 798–809. https://doi.org/10.4161/onci.20427

Bohlson, S. S., O'Conner, S. D., Hulsebus, H. J., Ho, M.-M., & Fraser, D. a. (2014). Complement, c1q,

and c1q-related molecules regulate macrophage polarization. *Frontiers in Immunology*, *5*(August), 402. https://doi.org/10.3389/fimmu.2014.00402

Bösken, C. A., Farnung, L., Hintermair, C., Schachter, M. M., Vogel-Bachmayr, K., Blazek, D., Anand, K., Fisher, R. P., Eick, D., & Geyer, M. (2014). The structure and substrate specificity of human Cdk12/Cyclin K. *Nature Communications*, *5*. https://doi.org/10.1038/ncomms4505

Braz, S. O., Cruz, A., Lobo, A., Bravo, J., Moreira-Ribeiro, J., Pereira-Castro, I., Freitas, J., Relvas, J. B., Summavielle, T., & Moreira, A. (2017). Expression of Rac1 alternative 3′ UTRs is a cell specific mechanism with a function in dendrite outgrowth in cortical neurons. *Biochimica et Biophysica Acta - Gene Regulatory Mechanisms*, *1860*(6), 685–694. https://doi.org/10.1016/j.bbagrm.2017.03.002

Brown, K. M., & Gilmartin, G. M. (2003). A Mechanism for the Regulation of Pre-mRNA 3′ Processing by Human Cleavage Factor Im. *Molecular Cell*, *12*(6), 1467–1476. https://doi.org/10.1016/S1097-2765(03)00453-2

Bussink, J., Kaanders, J. H. A. M., & Van Der Kogel, A. J. (2003). Tumor hypoxia at the micro-regional level: Clinical relevance and predictive value of exogenous and endogenous hypoxic cell markers. *Radiotherapy and Oncology*, *67*(1), 3–15. https://doi.org/10.1016/S0167-8140(03)00011-2

Cai, J., Song, X., Wang, W., Watnick, T., Pei, Y., Qian, F., & Pan, D. (2018). A RhoA – YAP – c-Myc signaling axis promotes the development of polycystic kidney disease. *Genes & Development*, 1–13. https://doi.org/10.1101/gad.315127.118.GENES

Calvo, O., & Manley, J. L. (2005). The transcriptional coactivator PC4/Sub1 has multiple functions in RNA polymerase II transcription. *EMBO Journal*, *24*(5), 1009–1020. https://doi.org/10.1038/sj.emboj.7600575

Cao, H., Wang, C., Chai, R., Dong, Q., & Tu, S. (2016). Iron intake, serum iron indices and risk of colorectal adenomas: a meta-analysis of observational studies. *European Journal of Cancer Care*, n/a-n/a. https://doi.org/10.1111/ecc.12486

Capocaccia, R., Gatta, G., & Dal Maso, L. (2015). Life expectancy of colon, breast, and testicular cancer patients: An analysis of US-SEER population-based data. *Annals of Oncology*, *26*(6), 1263–1268. https://doi.org/10.1093/annonc/mdv131

Caputo, F., Santini, C., Bardasi, C., Cerma, K., Casadei-Gardini, A., Spallanzani, A., Andrikou, K., Cascinu, S., & Gelsomino, F. (2019). BRAF-mutated colorectal cancer: Clinical and molecular insights. *International Journal of Molecular Sciences*, *20*(21). https://doi.org/10.3390/ijms20215369

Cardoso, A. P., Gonçalves, R. M., Antunes, J. C., Pinto, M. L., Pinto, A. T., Castro, F., Monteiro, C., Barbosa, M. A., & Oliveira, M. J. (2015). An interferon-??-delivery system based on chitosan/poly(??-glutamic acid) polyelectrolyte complexes modulates macrophage-derived stimulation of cancer cell invasion in vitro. *Acta Biomaterialia*, *23*, 157–171. https://doi.org/10.1016/j.actbio.2015.05.022

Cardoso, A. P., Pinto, M. L. T., Pinto, A. T., Monteiro, C., Oliveira, M. I. M. J., Santos, S. G., Relvas, J. B., Seruca, R., Mantovani, A., Mareel, M., & Barbosa, M. A. (2015). Matrix metalloproteases as maestros for the dual role of LPS- and IL-10-stimulated macrophages in cancer cell behaviour. *BMC Cancer*, *15*, 456. https://doi.org/10.1186/s12885-015-1466-8

Carr, H. S., & Frost, J. A. (2013). Timing is everything: Rac1 controls Net1A localization to regulate cell adhesion. *Cell Adhesion and Migration*, *7*(4), 351–356. https://doi.org/10.4161/cam.25276

Carreau, A., Hafny-Rahbi, B. El, Matejuk, A., Grillon, C., & Kieda, C. (2011). Why is the partial oxygen pressure of human tissues a crucial parameter? Small molecules and hypoxia. *Journal of Cellular and Molecular Medicine*, *15*(6), 1239–1253. https://doi.org/10.1111/j.1582-4934.2011.01258.x

Castello, A., Fischer, B., Eichelbaum, K., Horos, R., Beckmann, B. M., Strein, C., Davey, N. E., Humphreys, D. T., Preiss, T., Steinmetz, L. M., Krijgsveld, J., & Hentze, M. W. (2012). Insights into RNA Biology from an Atlas of Mammalian mRNA-Binding Proteins. *Cell*, *149*(6), 1393–1406. https://doi.org/10.1016/j.cell.2012.04.031

Castelo-Branco, P., Furger, A., Wollerton, M., Smith, C., Moreira, A., & Proudfoot, N. (2004). Polypyrimidine tract binding protein modulates efficiency of polyadenylation. *Molecular and Cellular Biology*, *24*(10), 4174–4183. https://doi.org/10.1128/MCB.24.10.4174

Castro, F., Pinto, M. L., Almeida, R., Pereira, F., Silva, A. M., Pereira, C. L., Santos, S. G., Barbosa, M. A., Gonçalves, R. M., & Oliveira, M. J. (2019). Chitosan/poly(γ-glutamic acid) nanoparticles incorporating IFN-γ for immune response modulation in the context of colorectal cancer. *Biomaterials Science*, *7*(8), 3386–3403. https://doi.org/10.1039/c9bm00393b

Celada, A., Gray, P. W., Rinderknecht, E., & Schreiber, R. D. (1984). Evidence for a gamma-interferon receptor that regulates macrophage tumoricidal activity. *Journal of Experimental Medicine*, *160*(1), 55–74. https://doi.org/10.1084/jem.160.1.55

Chabanon, R. M., Pedrero, M., Lefebvre, C., Marabelle, A., Soria, J. C., & Postel-Vinay, S. (2016). Mutational landscape and sensitivity to immune checkpoint blockers. *Clinical Cancer Research*, *22*(17), 4309–4321. https://doi.org/10.1158/1078-0432.CCR-16-0903

Chan, S. L., Huppertz, I., Yao, C., Weng, L., Moresco, J. J., Yates, J. R., Ule, J., Manley, J. L., & Shi, Y. (2014). CPSF30 and Wdr33 directly bind to AAUAAA in mammalian mRNA 3′ processing. *Genes and Development*, *28*(21), 2370–2380. https://doi.org/10.1101/gad.250993.114

Chandler, S. D., Mayeda, A., Yeakley, J. M., Krainer, A. R., & Fu, X. D. (1997). RNA splicing specificity determined by the coordinated action of RNA recognition motifs in SR proteins. *Proceedings of the National Academy of Sciences of the United States of America*, *94*(8), 3596–3601. https://doi.org/10.1073/pnas.94.8.3596

Chapman, R. D., Heidemann, M., Hintermair, C., & Eick, D. (2008). Molecular evolution of the RNA polymerase II CTD. *Trends in Genetics*, *24*(6), 289–296. https://doi.org/10.1016/j.tig.2008.03.010

Cheung, A. C. M., Sainsbury, S., & Cramer, P. (2011). Structural basis of initial RNA polymerase II transcription. *EMBO Journal*, *30*(23), 4755–4763. https://doi.org/10.1038/emboj.2011.396

Chistiakov, D. A., Bobryshev, Y. V., & Orekhov, A. N. (2015). Changes in transcriptome of macrophages in atherosclerosis. *Journal of Cellular and Molecular Medicine*, *19*(6), 1163–1173. https://doi.org/10.1111/jcmm.12591

Chistiakov, D. A., Kashirskikh, D. A., Khotina, V. A., Grechko, A. V., & Orekhov, A. N. (2019). Immune-Inflammatory Responses in Atherosclerosis: The Role of Myeloid Cells. *Journal of Clinical Medicine*, *8*(11), 1798. https://doi.org/10.3390/jcm8111798

Cho, S. J., Zhang, J., & Chen, X. (2010). RNPC1 modulates the RNA-binding activity of, and cooperates with, HuR to regulate p21 mRNA stability. *Nucleic Acids Research*, *38*(7), 2256–2267. https://doi.org/10.1093/nar/gkp1229

Churchman, L. S., & Weissman, J. S. (2012). Native elongating transcript sequencing (NET-seq). *Current Protocols in Molecular Biology*, *1*(SUPPL.98), 1–17. https://doi.org/10.1002/0471142727.mb0414s98

Claffey, K. P., Shih, S. C., Mullen, A., Dziennis, S., Cusick, J. L., Abrams, K. R., Lee, S. W., & Detmar, M. (1998). Identification of a human VPF/VEGF 3' untranslated region mediating hypoxia-induced mRNA stability. *Molecular Biology of the Cell*, *9*(2), 469–481. https://doi.org/10.1091/mbc.9.2.469

Cok, S. J., Acton, S. J., Sexton, A. E., & Morrison, A. R. (2004). Identification of RNA-binding Proteins in RAW 264.7 Cells That Recognize a Lipopolysaccharide-responsive Element in the 3-Untranslated Region of the Murine Cyclooxygenase-2 mRNA. *Journal of Biological Chemistry*, *279*(9), 8196–8205. https://doi.org/10.1074/jbc.M308475200

Condeelis, J., & Pollard, J. W. (2006). Macrophages: Obligate partners for tumor cell migration, invasion, and metastasis. *Cell*, *124*(2), 263–266. https://doi.org/10.1016/j.cell.2006.01.007

Connelly, S., & Manley, J. L. (1988). A functional mRNA polyadenylation signal is required for transcription termination by RNA polymerase II. *Genes & Development*, *2*(4), 440–452. https://doi.org/10.1101/gad.2.4.440

Core, L., & Lis, J. (2008). Transcription Regulation Through Promoter-Proximal Pausing of RNA Polymerase II. *Science*, *319*(5871), 1791–1792. https://doi.org/10.1038/jid.2014.371

Corrêa, L. H., Corrêa, R., Farinasso, C. M., de Sant'Ana Dourado, L. P., & Magalhães, K. G. (2017). Adipocytes and macrophages interplay in the orchestration of tumor microenvironment: New implications in cancer progression. *Frontiers in Immunology*, *8*(SEP), 1–12. https://doi.org/10.3389/fimmu.2017.01129

Cowper, A. E., Caceres, J. F., Mayeda, A., & Screaton, G. R. (2001). Serine-Arginine (SR) Protein-like Factors That Antagonize Authentic SR Proteins and Regulate Alternative Splicing. *Journal of Biological Chemistry*, *276*(52), 48908–48914. https://doi.org/10.1074/jbc.M103967200

Curinha, A., Oliveira Braz, S., Pereira-Castro, I., Cruz, A., & Moreira, A. (2014). Implications of polyadenylation in health and disease. *Nucleus (Austin, Tex.)*, *5*(6), 508–519. https://doi.org/10.4161/nucl.36360

D'Ignazio, L., Bandarra, D., & Rocha, S. (2016). NF-κB and HIF crosstalk in immune responses. *FEBS Journal*, *283*(3), 413–424. https://doi.org/10.1111/febs.13578

D'Ignazio, L., & Rocha, S. (2016). Hypoxia Induced NF-κB. *Cells*, *5*(1), 10. https://doi.org/10.3390/cells5010010

Dai, Y., Xu, C., & Chen, X. (2017). Nanoparticle design strategies for enhanced anticancer therapy by exploiting the tumour microenvironment. *Chem Soc Rev*, 3830–3852. https://doi.org/10.1039/c6cs00592f

Danckwardt, S., Gantzert, A. S., Macher-Goeppinger, S., Probst, H. C., Gentzel, M., Wilm, M., Gröne, H. J., Schirmacher, P., Hentze, M. W., & Kulozik, A. E. (2011). P38 MAPK Controls Prothrombin Expression by Regulated RNA 3' End Processing. *Molecular Cell*, *41*(3), 298–310.

https://doi.org/10.1016/j.molcel.2010.12.032
Danckwardt, S., Hentze, M. W., & Kulozik, A. E. (2008). 3′ end mRNA processing: Molecular mechanisms and implications for health and disease. *EMBO Journal*, *27*(3), 482–498. https://doi.org/10.1038/sj.emboj.7601932
Danckwardt, S., Kaufmann, I., Gentzel, M., Foerstner, K. U., Gantzert, A.-S., Gehring, N. H., Neu-Yilik, G., Bork, P., Keller, W., Wilm, M., Hentze, M. W., & Kulozik, A. E. (2007). Splicing factors stimulate polyadenylation via USEs at non-canonical 3' end formation signals. *The EMBO Journal*, *26*(11), 2658–2669. https://doi.org/10.1038/sj.emboj.7601699
Das, S., & Krainer, A. R. (2014). Emerging functions of SRSF1, splicing factor and oncoprotein, in RNA metabolism and cancer. *Mol Cancer Res*, *12*(9), 1195–1204. https://doi.org/10.1038/jid.2014.371
Daubon, T., Léon, C., Clarke, K., Andrique, L., Salabert, L., Darbo, E., Pineau, R., Guérit, S., Maitre, M., Dedieu, S., Jeanne, A., Bailly, S., Feige, J. J., Miletic, H., Rossi, M., Bello, L., Falciani, F., Bjerkvig, R., & Bikfalvi, A. (2019). Deciphering the complex role of thrombospondin-1 in glioblastoma development. *Nature Communications*, *10*(1). https://doi.org/10.1038/s41467-019-08480-y
Davidson, L., Muniz, L., & West, S. (2014). 3' end formation of pre-mRNA and phosphorylation of Ser2 on the RNA polymerase II CTD are reciprocally coupled in human cells. *Genes and Development*, *28*(4), 342–356. https://doi.org/10.1101/gad.231274.113
Davies, L. C., Jenkins, S. J., Allen, J. E., & Taylor, P. R. (2014). Tissue-resident macrophages. *Nature Immunol*, *14*(10), 986–995. https://doi.org/10.1038/ni.2705.Tissue-resident
De Schepper, S., Verheijden, S., Aguilera-Lizarraga, J., Viola, M. F., Boesmans, W., Stakenborg, N., Voytyuk, I., Smidt, I., Boeckx, B., Dierckx de Casterlé, I., Baekelandt, V., Gonzalez Dominguez, E., Mack, M., Depoortere, I., De Strooper, B., Sprangers, B., Himmelreich, U., Soenen, S., Guilliams, M., … Boeckxstaens, G. (2018). Self-Maintaining Gut Macrophages Are Essential for Intestinal Homeostasis. *Cell*, *175*(2), 400-415.e13. https://doi.org/10.1016/j.cell.2018.07.048
De Wever, O., Nguyen, Q., Van Hoorde, L., Bracke, M., Bruyneel, E., Gespach, C., & Mareel, M. (2004). Tenascin-C and SF/HGF produced by myofibroblasts in vitro provide convergent proinvasive signals to human colon cancer cells through RhoA and Rac. *The FASEB Journal*, *18*(9), 1016–1018. https://doi.org/10.1096/fj.03-1110fje
Dedon, P. C., & Tannenbaum, S. R. (2004). Reactive nitrogen species in the chemical biology of inflammation. *Archives of Biochemistry and Biophysics*, *423*(1), 12–22. https://doi.org/10.1016/j.abb.2003.12.017
Del Valle Morales, D., Trotman, J. B., Bundschuh, R., & Schoenberg, D. R. (2020). Inhibition of cytoplasmic cap methylation identifies 5 top mrnas as recapping targets and reveals recapping sites downstream of native 5 ends. *Nucleic Acids Research*, *48*(7), 3806–3815. https://doi.org/10.1093/NAR/GKAA046
DeNardo, D. G., Brennan, D. J., Rexhepaj, E., Ruffell, B., Shiao, S. L., Madden, S. F., Gallagher, W. M., Wadhwani, N., Keil, S. D., Junaid, S. A., Rugo, H. S., Shelley Hwang, E., Jirström, K., West, B. L., & Coussens, L. M. (2011). Leukocyte complexity predicts breast cancer survival and functionally regulates response to chemotherapy. *Cancer Discovery*, *1*(1), 54–67. https://doi.org/10.1158/2159-8274.CD-10-0028
DeNardo, D. G., & Ruffell, B. (2019). Macrophages as regulators of tumour immunity and immunotherapy. *Nature Reviews Immunology*, *19*(6), 369–382. https://doi.org/10.1038/s41577-019-0127-6
Derti, A., Garrett-Engele, P., MacIsaac, K. D., Stevens, R. C., Sriram, S., Chen, R., Rohl, C. A., Johnson, J. M., & Babak, T. (2012). A quantitative atlas of polyadenylation in five mammals. *Genome Research*, *22*(6), 1173–1183. https://doi.org/10.1101/gr.132563.111
Devaiah, B. N., Lewis, B. A., Cherman, N., Hewitt, M. C., Albrecht, B. K., Robey, P. G., Ozato, K., Sims, R. J., & Singer, D. S. (2012). BRD4 is an atypical kinase that phosphorylates Serine2 of the RNA Polymerase II carboxy-terminal domain. *Proceedings of the National Academy of Sciences of the United States of America*, *109*(18), 6927–6932. https://doi.org/10.1073/pnas.1120422109
Devaud, C., Westwood, J. A., John, L. B., Flynn, J. K., Paquet-Fifield, S., Duong, C. P. M., Yong, C. S. M., Pegram, H. J., Stacker, S. A., Achen, M. G., Stewart, T. J., Snyder, L. A., Teng, M. W. L., Smyth, M. J., Darcy, P. K., & Kershaw, M. H. (2014). Tissues in different anatomical sites can sculpt and vary the tumor microenvironment to affect responses to therapy. *Molecular Therapy : The Journal of the American Society of Gene Therapy*, *22*(1), 18–27. https://doi.org/10.1038/mt.2013.219
Di Giammartino, D. C., Nishida, K., & Manley, J. L. (2011). Mechanisms and Consequences of Alternative Polyadenylation. *Molecular Cell*, *43*(6), 853–866. https://doi.org/10.1016/j.molcel.2011.08.017

Diaz-Muñoz, M. D., Bell, S. E., Fairfax, K., Monzon-Casanova, E., Cunningham, A. F., Gonzalez-Porta, M., Andrews, S. R., Bunik, V. I., Zarnack, K., Curk, T., Heggermont, W. A., Heymans, S., Gibson, G. E., Kontoyiannis, D. L., Ule, J., & Turner, M. (2015). The RNA-binding protein HuR is essential for the B cell antibody response. *Nature Immunology*, *16*(4), 415–425. https://doi.org/10.1038/ni.3115

DiNapoli, M. R., Calderon, C. L., & Lopez, D. M. (1996). The altered tumoricidal capacity of macrophages isolated from tumor-bearing mice is related to reduced expression of the inducible nitric oxide synthase gene. *Journal of Experimental Medicine*, *183*(4), 1323–1329. https://doi.org/10.1084/jem.183.4.1323

Ding, T., Xu, J., Wang, F., Shi, M., Zhang, Y., Li, S. P., & Zheng, L. (2009). High tumor-infiltrating macrophage density predicts poor prognosis in patients with primary hepatocellular carcinoma after resection. *Human Pathology*, *40*(3), 381–389. https://doi.org/10.1016/j.humpath.2008.08.011

Dobin, A. (2014). *STAR manual 2.4.0.1*. 1–33. https://doi.org/10.1093/bioinformatics/bts635

Dobin, A., Gingeras, T. R., Spring, C., Flores, R., Sampson, J., Knight, R., Chia, N., & Technologies, H. S. (2016). Mapping RNA-seq Reads with STAR. *Curr Protoc Bioinformatics*, *51*(4), 586–597. https://doi.org/10.1002/0471250953.bi1114s51.Mapping

Domingues, R. G., Lago-Baldaia, I., Pereira-Castro, I., Fachini, J. M., Oliveira, L., Drpic, D., Lopes, N., Henriques, T., Neilson, J. R., Carmo, A. M., & Moreira, A. (2016). CD5 expression is regulated during human T-cell activation by alternative polyadenylation, PTBP1, and miR-204. *European Journal of Immunology*, *46*(6), 1490–1503. https://doi.org/10.1002/eji.201545663

Dominguez, D., Freese, P., Alexis, M. S., Su, A., Hochman, M., Palden, T., Bazile, C., Lambert, N. J., Van Nostrand, E. L., Pratt, G. A., Yeo, G. W., Graveley, B. R., & Burge, C. B. (2018). Sequence, Structure, and Context Preferences of Human RNA Binding Proteins. *Molecular Cell*, *70*(5), 854-867.e9. https://doi.org/10.1016/j.molcel.2018.05.001

Duque, G. A., & Descoteaux, A. (2014). Macrophage cytokines: Involvement in immunity and infectious diseases. *Frontiers in Immunology*, *5*(OCT), 1–12. https://doi.org/10.3389/fimmu.2014.00491

Dvorak, H. F. (1986). Tumors: wounds that do not heal. Similarities between tumor stroma generation and wound healing. *The New England Journal of Medicine*, *315*(26), 1650–1659. https://doi.org/10.1056/NEJM198612253152606

Dye, M. J., & Proudfoot, N. J. (1999). Terminal exon definition occurs cotranscriptionally and promotes termination of RNA polymerase II. *Molecular Cell*, *3*(3), 371–378. https://doi.org/10.1016/S1097-2765(00)80464-5

Edge, L., & Macrae, I. (2017). The Long Tail of mRNA Regulation. *Cell*, *168*(3), 335–338. https://doi.org/10.1016/j.cell.2017.01.015

Egloff, S., & Murphy, S. (2008). Cracking the RNA polymerase II CTD code. *Trends in Genetics*, *24*(6), 280–288. https://doi.org/10.1016/j.tig.2008.03.008

Elkon, R., Ugalde, A. P., & Agami, R. (2013). Alternative cleavage and polyadenylation: extent, regulation and function. *Nature Reviews Genetics*, *14*(7), 496–506. https://doi.org/10.1038/nrg3482

Endo, H., Hosono, K., Uchiyama, T., Sakai, E., Sugiyama, M., Takahashi, H., Nakajima, N., Wada, K., Takeda, K., Nakagama, H., & Nakajima, A. (2011). Leptin acts as a growth factor for colorectal tumours at stages subsequent to tumour initiation in murine colon carcinogenesis. *Gut*, *60*(10), 1363–1371. https://doi.org/10.1136/gut.2010.235754

Eren, E., Tufekci, K. U., Isci, K. B., Tastan, B., Genc, K., & Genc, S. (2018). Sulforaphane inhibits lipopolysaccharide-induced inflammation, cytotoxicity, oxidative stress, and miR-155 expression and switches to Mox phenotype through activating extracellular signal-regulated kinase 1/2-nuclear factor erythroid 2-related factor 2/an. *Frontiers in Immunology*, *9*(JAN), 1–18. https://doi.org/10.3389/fimmu.2018.00036

Expert-Bezançon, A., Sureau, A., Durosay, P., Salesse, R., Groeneveld, H., Lecaer, J. P., & Marie, J. (2004). hnRNP A1 and the SR proteins ASF/SF2 and SC35 have antagonistic functions in splicing of β-tropomyosin exon 6B. *Journal of Biological Chemistry*, *279*(37), 38249–38259. https://doi.org/10.1074/jbc.M405377200

Faisal Khan, K. M., & Falcone, D. J. (1997). Role of laminin in matrix induction of macrophage urokinase-type plasminogen activator and 92-kDa metalloproteinase expression. *Journal of Biological Chemistry*, *272*(13), 8270–8275. https://doi.org/10.1074/jbc.272.13.8270

Falleni, M., Savi, F., Tosi, D., Agape, E., Cerri, A., Moneghini, L., & Bulfamante, G. P. (2017). M1 and M2 macrophages' clinicopathological significance in cutaneous melanoma. *Melanoma Research*, *27*(3), 200–210. https://doi.org/10.1097/CMR.0000000000000352

Fearon, E. R., & Vogelstein, B. (1990). A genetic model for colorectal tumorigenesis. *Cell*, *61*(5), 759–

767. https://doi.org/10.1016/0092-8674(90)90186-I
Feng, Y., Ren, J., Gui, Y., Wei, W., Shu, B., Lu, Q., Xue, X., Sun, X., He, W., Yang, J., & Dai, C. (2018). Wnt/b-catenin–Promoted macrophage alternative activation contributes to kidney fibrosis. *Journal of the American Society of Nephrology*, *29*(1), 182–193. https://doi.org/10.1681/ASN.2017040391
Ferrante, C. J., Pinhal-Enfield, G., Elson, G., Cronstein, B. N., Hasko, G., Outram, S., & Leibovich, S. J. (2013). The adenosine-dependent angiogenic switch of macrophages to an M2-like phenotype is independent of interleukin-4 receptor alpha (IL-4Rα) signaling. *Inflammation*, *36*(4), 921–931. https://doi.org/10.1007/s10753-013-9621-3
Fischl, H., Neve, J., Wang, Z., Patel, R., Louey, A., Tian, B., & Furger, A. (2019). hnRNPC regulates cancer-specific alternative cleavage and polyadenylation profiles. *Nucleic Acids Research*, *47*(14), 7580–7591. https://doi.org/10.1093/nar/gkz461
Fong, N., Brannan, K., Erickson, B., Kim, H., Cortazar, M. A., Sheridan, R. M., Nguyen, T., Karp, S., & Bentley, D. L. (2015). Effects of Transcription Elongation Rate and Xrn2 Exonuclease Activity on RNA Polymerase II Termination Suggest Widespread Kinetic Competition. *Molecular Cell*, *60*(2), 256–267. https://doi.org/10.1016/j.molcel.2015.09.026
Franklin, R., & Li, M. (2017). *Ontogeny of Tumor-associated Macrophages and Its Implication in Cancer Regulation*. *2*(1), 20–34. https://doi.org/10.1016/j.trecan.2015.11.004.Ontogeny
Fuda, N. J., Ardehali, M. B., & Lis, J. T. (2009). Defining mechanisms that regulate RNA polymerase II transcription in vivo. *Nature*, *461*(7261), 186–192. https://doi.org/10.1038/nature08449
Fusby, B., Kim, S., Erickson, B., Kim, H., Peterson, M. L., & Bentley, D. L. (2015). Coordination of RNA Polymerase II Pausing and 3' end processing factor recruitment with alternative polyadenylation. *Molecular and Cellular Biology*, *36*(2), MCB.00898-15. https://doi.org/10.1128/mcb.00898-15
Galon, J., Angell, H. K., Bedognetti, D., & Marincola, F. M. (2013). The Continuum of Cancer Immunosurveillance: Prognostic, Predictive, and Mechanistic Signatures. *Immunity*, *39*(1), 11–26. https://doi.org/10.1016/j.immuni.2013.07.008
Genard, G., Lucas, S., & Michiels, C. (2017). Reprogramming of tumor-associated macrophages with anticancer therapies: Radiotherapy versus chemo- and immunotherapies. *Frontiers in Immunology*, *8*(JUL). https://doi.org/10.3389/fimmu.2017.00828
Giannakis, M., Mu, X. J., Shukla, S. A., Qian, Z. R., Cohen, O., Nishihara, R., Bahl, S., Cao, Y., Amin-Mansour, A., Yamauchi, M., Sukawa, Y., Stewart, C., Rosenberg, M., Mima, K., Inamura, K., Nosho, K., Nowak, J. A., Lawrence, M. S., Giovannucci, E. L., … Garraway, L. A. (2016). Genomic Correlates of Immune-Cell Infiltrates in Colorectal Carcinoma. *Cell Reports*, *15*(4), 857–865. https://doi.org/10.1016/j.celrep.2016.03.075
Gilchrist, D. A., Dos Santos, G., Fargo, D. C., Xie, B., Gao, Y., Li, L., & Adelman, K. (2010). Pausing of RNA polymerase II disrupts DNA-specified nucleosome organization to enable precise gene regulation. *Cell*, *143*(4), 540–551. https://doi.org/10.1016/j.cell.2010.10.004
Ginhoux, F., Greter, M., Leboeuf, M., Nandi, S., See, P., Gokhan, S., Mehler, M. M. F., Conway, S. S. J. S., Ng, L. L. G., Stanley, E. R., Samokhvalov, I. I. M. I., & Merad, M. (2010). Fate Mapping Analysis Reveals That Adult Microglia Derive from Primitive Macrophages. *Science*, *330*(6005), 841–845. https://doi.org/10.1038/jid.2014.371
Globocan. (2020a). *Cancer Today. Estimated number of deaths in 2020, worldwide, both sexes, all ages*. *144*, 2020. https://gco.iarc.fr/today/online-analysis-table?v=2020&mode=cancer&mode_population=continents&population=900&populations=900&key=asr&sex=0&cancer=39&type=1&statistic=5&prevalence=0&population_group=0&ages_group%5B%5D=0&ages_group%5B%5D=17&group_cancer=1&i
Globocan. (2020b). *Cancer Today. Estimated number of new cases in 2020, Portugal, both sexes, all ages*. *501*, 2020. https://gco.iarc.fr/today/online-analysis-table?v=2020&mode=cancer&mode_population=continents&population=900&populations=152&key=asr&sex=0&cancer=39&type=0&statistic=5&prevalence=0&population_group=0&ages_group%5B%5D=0&ages_group%5B%5D=17&group_cancer=1&i
Globocan. (2020c). *Cancer Today. Estimated number of new cases in 2020, worldwide, both sexes, all ages*. *419*, 2020. https://gco.iarc.fr/today/online-analysis-table?v=2020&mode=cancer&mode_population=continents&population=900&populations=152&key=asr&sex=0&cancer=39&type=0&statistic=5&prevalence=0&population_group=0&ages_group%5B%5D=0&ages_group%5B%5D=17&group_cancer=1&i
Globocan Observatory, W. (2019). Globocan 2018 - Portugal. *International Agency for Research on Cancer*, *270*, 2018–2019. http://gco.iarc.fr/today/data/factsheets/populations/620-portugal-fact-sheets.pdf.
Glover-Cutter, K., Kim, S., Espinosa, J., & Bentley, D. L. (2008). RNA polymerase II pauses and associates with pre-mRNA processing factors at both ends of genes. *Nature Structural and*

Molecular Biology, *15*(1), 71–78. https://doi.org/10.1038/nsmb1352
Goers, L., Freemont, P., & Polizzi, K. M. (2014). Co-culture systems and technologies: taking synthetic biology to the next level. *Journal of the Royal Society, Interface / the Royal Society*, *11*(96), 20140065-. https://doi.org/10.1098/rsif.2014.0065
Gong, M., Zhuo, X., & Ma, A. (2017). STAT6 Upregulation Promotes M2 Macrophage Polarization to Suppress Atherosclerosis. *Medical Science Monitor Basic Research*, *23*, 240–249. https://doi.org/10.12659/msmbr.904014
González-García, I., Solé, R. V., & Costa, J. (2002). Metapopulation dynamics and spatial heterogeneity in cancer. *Proceedings of the National Academy of Sciences of the United States of America*, *99*(20), 13085–13089. https://doi.org/10.1073/pnas.202139299
Gonzalez, H., Hagerling, C., & Werb, Z. (2018). Roles of the immune system in cancer: From tumor initiation to metastatic progression. *Genes and Development*, *32*(19–20), 1267–1284. https://doi.org/10.1101/GAD.314617.118
Goossens, P., Rodriguez-Vita, J., Etzerodt, A., Masse, M., Rastoin, O., Gouirand, V., Ulas, T., Papantonopoulou, O., Van Eck, M., Auphan-Anezin, N., Bebien, M., Verthuy, C., Vu Manh, T. P., Turner, M., Dalod, M., Schultze, J. L., & Lawrence, T. (2019). Membrane Cholesterol Efflux Drives Tumor-Associated Macrophage Reprogramming and Tumor Progression. *Cell Metabolism*, 1–14. https://doi.org/10.1016/j.cmet.2019.02.016
Gopal, S. K., Greening, D. W., Hanssen, E. G., Zhu, H.-J., Simpson, R. J., & Mathias, R. A. (2016). Oncogenic epithelial cell-derived exosomes containing Rac1 and PAK2 induce angiogenesis in recipient endothelial cells. *Oncotarget*, *7*(15). https://doi.org/10.18632/oncotarget.7573
Gordon, S, & Cohn, Z. A. (1973). The macrophage. *International Review of Cytology*, *36*, 171–214. https://doi.org/10.1016/s0074-7696(08)60218-1
Gordon, Siamon. (2003). Alternative activation of Macrophages. *Nature Reviews Immunology*, *3*, 23–35. https://doi.org/10.1017/CBO9781107415324.004
Gordon, Siamon, & Martinez, F. O. (2010). Alternative activation of macrophages: Mechanism and functions. *Immunity*, *32*(5), 593–604. https://doi.org/10.1016/j.immuni.2010.05.007
Gordon, Siamon, & Plüddemann, A. (2017). Tissue macrophages: Heterogeneity and functions. *BMC Biology*, *15*(1), 1–18. https://doi.org/10.1186/s12915-017-0392-4
Graber, J. H., Cantor, C. R., Mohr, S. C., & Smith, T. F. (1999). In silico detection of control signals: MRNA 3′-end-processing sequences in diverse species. *Proceedings of the National Academy of Sciences of the United States of America*, *96*(24), 14055–14060. https://doi.org/10.1073/pnas.96.24.14055
Graboń, W., Otto-Ślusarczyk, D., Chrzanowska, A., Mielczarek-Puta, M., Joniec-Maciejak, I., Słabik, K., & Barańczyk-Kuźma, A. (2016). Lactate Formation in Primary and Metastatic Colon Cancer Cells at Hypoxia and Normoxia. *Cell Biochemistry and Function*, *34*(7), 483–490. https://doi.org/10.1002/cbf.3211
Greenblatt, J., Nodwell, J. R., & Mason, S. W. (1993). Transcriptional antitermination. *Nature*, *364*(6436), 401–406. https://doi.org/10.1038/364401a0
Gromak, N., West, S., & Proudfoot, N. J. (2006). Pause Sites Promote Transcriptional Termination of Mammalian RNA Polymerase II. *Molecular and Cellular Biology*, *26*(10), 3986–3996. https://doi.org/10.1128/mcb.26.10.3986-3996.2006
Grosso, A. R., Almeida, S. F. De, Braga, J., Almeida, F. De, & Carmo-fonseca, M. (2012). Dynamic transitions in RNA polymerase II density profiles during transcription termination. *Genome Research*, 1447–1456. https://doi.org/10.1101/gr.138057.112
Gruber, A. J., Schmidt, R., Ghosh, S., Martin, G., Gruber, A. R., van Nimwegen, E., & Zavolan, M. (2018). Discovery of physiological and cancer-related regulators of 3' UTR processing with KAPAC. *Genome Biology*, *19*(1), 1–17. https://doi.org/10.1186/s13059-018-1415-3
Gruber, A. J., Schmidt, R., Gruber, A. R., Martin, G., Ghosh, S., Belmadani, M., Keller, W., & Zavolan, M. (2016). A comprehensive analysis of 3' end sequencing data sets reveals novel polyadenylation signals and the repressive role of heterogeneous ribonucleoprotein C on cleavage and polyadenylation. *Genome Research*, *26*(8), 1145–1159. https://doi.org/10.1101/gr.202432.115
Gruber, A. R., Martin, G., Muller, P., Schmidt, A., Gruber, A. J., Gumienny, R., Mittal, N., Jayachandran, R., Pieters, J., Keller, W., van Nimwegen, E., & Zavolan, M. (2014). Global 3' UTR shortening has a limited effect on protein abundance in proliferating T cells. *Nat Commun*, *5*, 5465. https://doi.org/10.1038/ncomms6465
Grünberg, S., & Hahn, S. (2014). Structural insights into transcription initiation by RNA polymerase II. *Bone*, *23*(1), 1–7. https://doi.org/10.1038/jid.2014.371
GTex analysis for SRSF12. (2021). https://www.gtexportal.org/home/gene/SRSF12

Gu, B., Eick, D., & Bensaude, O. (2013). CTD serine-2 plays a critical role in splicing and termination factor recruitment to RNA polymerase II in vivo. *Nucleic Acids Research*, *41*(3), 1591–1603. https://doi.org/10.1093/nar/gks1327

Guenther, M. G., Levine, S. S., Boyer, L. A., Jaenisch, R., & Young, R. A. (2007). A Chromatin Landmark and Transcription Initiation at Most Promoters in Human Cells. *Cell*, *130*(1), 77–88. https://doi.org/10.1016/j.cell.2007.05.042

Gundra, U. M., Girgis, N. M., Ruckerl, D., Jenkins, S., Ward, L. N., Kurtz, Z. D., Wiens, K. E., Tang, M. S., Basu-Roy, U., Mansukhani, A., Allen, J. E., & Loke, P. (2014). Alternatively activated macrophages derived from monocytes and tissue macrophages are phenotypically and functionally distinct. *Blood*, *123*(20), 110–123. https://doi.org/10.1182/blood-2013-08-520619

Guo, J., & Price, D. H. (2013). RNA Polymerase II Transcription Elongation Control. *Chem Rev*, *113*(11), 8583–8603. https://doi.org/10.1038/jid.2014.371

Guo, Q., Wu, Y., Guo, X., Cao, L., Xu, F., Zhao, H., Zhu, J., Wen, H., Ju, X., & Wu, X. (2021). The RNA-Binding Protein CELF2 Inhibits Ovarian Cancer Progression by Stabilizing FAM198B. *Molecular Therapy - Nucleic Acids*, *23*(March), 169–184. https://doi.org/10.1016/j.omtn.2020.10.011

Gutierrez, L. S., Lopez-Dee, Z., & Pidcock, K. (2011). Thrombospondin-1: Multiple paths to inflammation. *Mediators of Inflammation*, *2011*. https://doi.org/10.1155/2011/296069

Hall-Pogar, T., Liang, S., Hague, L. K., & Lutz, C. S. (2007). Specific trans-acting proteins interact with auxiliary RNA polyadenylation elements in the COX-2 3′-UTR. *Rna*, *13*(7), 1103–1115. https://doi.org/10.1261/rna.577707

Hanada, T., Nakagawa, M., Emoto, A., Nomura, T., Nasu, N., & Nomura, Y. (2000). Prognostic value of tumor-associated macrophage count in human bladder cancer. *International Journal of Urology*, *7*(7), 263–269. https://doi.org/10.1046/j.1442-2042.2000.00190.x

Hanahan, D., & Weinberg, R. A. (2000). *The Hallmarks of Cancer*. *100*, 57–70.

Hanahan, D., & Weinberg, R. A. (2011). Hallmarks of cancer: The next generation. *Cell*, *144*(5), 646–674. https://doi.org/10.1016/j.cell.2011.02.013

Hao, N. B., Lü, M. H., Fan, Y. H., Cao, Y. L., Zhang, Z. R., & Yang, S. M. (2012). Macrophages in tumor microenvironments and the progression of tumors. *Clinical and Developmental Immunology*, *2012*. https://doi.org/10.1155/2012/948098

Hardbower, D. M., Coburn, L. A., Asim, M., Singh, K., Sierra, J. C., Barry, D. P., Gobert, A. P., Piazuelo, M. B., Washington, M. K., & Wilson, K. T. (2017). EGFR-mediated macrophage activation promotes colitis-associated tumorigenesis. *Oncogene*, *36*(27), 3807–3819. https://doi.org/10.1038/onc.2017.23

Hardy, J. G., & Norbury, C. J. (2016). Cleavage factor Im (CFIm) as a regulator of alternative polyadenylation. *Biochemical Society Transactions*, *44*(4), 1051–1057. https://doi.org/10.1042/BST20160078

Hashimoto, D., Chow, A., Noizat, C., Teo, P., Beasley, M. B., Leboeuf, M., Becker, C. D., See, P., Price, J., Lucas, D., Greter, M., Mortha, A., Boyer, S. W., Forsberg, E. C., Tanaka, M., van Rooijen, N., García-Sastre, A., Stanley, E. R., Ginhoux, F., … Merad, M. (2013). Tissue-resident macrophages self-maintain locally throughout adult life with minimal contribution from circulating monocytes. *Immunity*, *38*(4), 792–804. https://doi.org/10.1016/j.immuni.2013.04.004

Hatchi, E., Skourti-Stathaki, K., Ventz, S., Pinello, L., Yen, A., Kamieniarz-Gdula, K., Dimitrov, S., Pathania, S., McKinney, K. M., Eaton, M. L., Kellis, M., Hill, S. J., Parmigiani, G., Proudfoot, N. J., & Livingston, D. M. (2015). BRCA1 recruitment to transcriptional pause sites is required for R-loop-driven DNA damage repair. *Molecular Cell*, *57*(4), 636–647. https://doi.org/10.1016/j.molcel.2015.01.011

He, X.-J. J., Zhang, Q. Q., Ma, L.-P. P., Li, N. N., Chang, X.-H. H., & Zhang, Y.-J. J. (2016). Aberrant alternative polyadenylation is responsible for survivin up-regulation in ovarian cancer. *Chinese Medical Journal*, *129*(10), 1140–1146. https://doi.org/10.4103/0366-6999.181965

Herrmann, C. J., Schmidt, R., Kanitz, A., Artimo, P., Gruber, A. J., & Zavolan, M. (2020). PolyASite 2.0: A consolidated atlas of polyadenylation sites from 3′ end sequencing. *Nucleic Acids Research*, *48*(D1), D174–D179. https://doi.org/10.1093/nar/gkz918

Higgs, D. R., Goodbourn, S. E., Lamb, J., Clegg, J. B., Weatherall, D. J., & Proudfoot, N. J. (1983). Alpha-thalassaemia caused by a polyadenylation signal mutation. *Nature*, *306*(5941), 398–400. https://doi.org/10.1038/306398a0

Hilgers, V., Lemke, S. B., & Levine, M. (2012). ELAV mediates 3′ UTR extension in the Drosophila nervous system. *Genes and Development*, *26*(20), 2259–2264. https://doi.org/10.1101/gad.199653.112

Hilska, M., Collan, Y., Peltonen, J., Gullichsen, R., Paajanen, H., & Laato, M. (1998). The distribution of collagen types I, III, and IV in normal and malignant colorectal mucosa. *European Journal of*

Surgery, *164*(6), 457–464. https://doi.org/10.1080/110241598750004274

Hirayama, A., Kami, K., Sugimoto, M., Sugawara, M., Toki, N., Onozuka, H., Kinoshita, T., Saito, N., Ochiai, A., Tomita, M., Esumi, H., & Soga, T. (2009). Quantitative metabolome profiling of colon and stomach cancer microenvironment by capillary electrophoresis time-of-flight mass spectrometry. *Cancer Research*, *69*(11), 4918–4925. https://doi.org/10.1158/0008-5472.CAN-08-4806

Hirose, Y., & Manley, J. L. (1998). RNA polymerase II is an essential mRNA polyadenylation factor. *Nature*, *395*(6697), 93–96. https://doi.org/10.1038/25786

Hoque, M., Ji, Z., Zheng, D., Luo, W., Li, W., You, B., Park, J., Yehia, G., & Tian, B. (2016). Analysis of alternative cleavage and polyadenylation by 3' region extraction and deep sequencing. *Nature Methods*, *10*(2), 133–139. https://doi.org/10.1016/j.physbeh.2017.03.040

Hoshino, K., Takeuchi, O., Kawai, T., Sanjo, H., Ogawa, T., Takeda, Y., Takeda, K., & Akira, S. (1999). Cutting edge: Toll-like receptor 4 (TLR4)-deficient mice are hyporesponsive to lipopolysaccharide: evidence for TLR4 as the Lps gene product. *Journal of Immunology (Baltimore, Md.: 1950)*, *162*(7), 3749–3752. http://www.ncbi.nlm.nih.gov/pubmed/10201887

Houghton, A. M., Quintero, P. A., Perkins, D. L., Kobayashi, D. K., Kelley, D. G., Marconcini, L. A., Mecham, R. P., Senior, R. M., & Shapiro, S. D. (2006). Elastin fragments drive disease progression in a murine model of emphysema -- Houghton et al_ 116 (3) 753 -- Journal of Clinical Investigation. *Journal of Clinical Investigation*, *116*(3), 753. https://doi.org/10.1172/JCI25617.tected

Huang, Y., Du, K. L., Guo, P. Y., Zhao, R. M., Wang, B., Zhao, X. L., & Zhang, C. Q. (2019). IL-16 regulates macrophage polarization as a target gene of mir-145-3p. *Molecular Immunology*, *107*, 1–9. https://doi.org/10.1016/j.molimm.2018.12.027

Hui, L., & Chen, Y. (2015). Tumor microenvironment: Sanctuary of the devil. *Cancer Letters*, *368*(1), 7–13. https://doi.org/10.1016/j.canlet.2015.07.039

Hutchinson, F. (1993). *A switch from Myc : Max to Mad : Max eterocomplexes accompanies monocyte / macrophage differentiation*. 2110–2119.

Hwang, R. F., Moore, T., Arumugam, T., Ramachandran, V., Amos, K. D., Rivera, A., Ji, B., Evans, D. B., & Logsdon, C. D. (2008). Cancer-associated stromal fibroblasts promote pancreatic tumor progression. *Cancer Research*, *68*(3), 918–926. https://doi.org/10.1158/0008-5472.CAN-07-5714

Ibrahim, H. R., Hamasaki, K., & Miyata, T. (2017). Novel peptide motifs from lysozyme suppress pro-inflammatory cytokines in macrophages by antagonizing toll-like receptor and LPS-scavenging action. *European Journal of Pharmaceutical Sciences : Official Journal of the European Federation for Pharmaceutical Sciences*, *107*, 240–248. https://doi.org/10.1016/j.ejps.2017.07.005

Ieda, T., Tazawa, H., Okabayashi, H., Yano, S., Shigeyasu, K., Kuroda, S., Ohara, T., Noma, K., Kishimoto, H., Nishizaki, M., Kagawa, S., Shirakawa, Y., Saitou, T., Imamura, T., & Fujiwara, T. (2019). Visualization of epithelial-mesenchymal transition in an inflammatory microenvironment–colorectal cancer network. *Scientific Reports*, *9*(1), 1–11. https://doi.org/10.1038/s41598-019-52816-z

Inoue, K., Ohno, M., Sakamoto, H., & Shimura, Y. (1989). Effect of the cap structure on pre-mRNA splicing in Xenopus oocyte nuclei. *Genes & Development*, *3*(9), 1472–1479. https://doi.org/10.1101/gad.3.9.1472

Ishii, T., Ueyama, T., Shigyo, M., Kohta, M., Kondoh, T., Kuboyama, T., Uebi, T., Hamada, T., Gutmann, D. H., Aiba, A., Kohmura, E., Tohda, C., & Saito, N. (2017). A novel Rac1-GSPT1 signaling pathway controls astrogliosis following central nervous system injury. *Journal of Biological Chemistry*, *292*(4), 1240–1250. https://doi.org/10.1074/jbc.M116.748871

Itzen, F., Greifenberg, A. K., Bösken, C. A., & Geyer, M. (2014). Brd4 activates P-TEFb for RNA polymerase II CTD phosphorylation. *Nucleic Acids Research*, *42*(12), 7577–7590. https://doi.org/10.1093/nar/gku449

Izban, M. G., & Luse, D. S. (1991). Transcription on nucleosomal templates by RNA polymerase II in vitro: Inhibition of elongation with enhancement of sequence-specific pausing. *Genes and Development*, *5*(4), 683–696. https://doi.org/10.1101/gad.5.4.683

Jacob, F., & Monod, J. (1961). On the Regulation of Gene Activity. *Cold Spring Harb Symp Quant Biol*, *26*, 193–211. https://doi.org/10.1101/SQB.1961.026.01.024

Jetten, N., Verbruggen, S., Gijbels, M. J., Post, M. J., De Winther, M. P. J., & Donners, M. M. P. C. (2014). Anti-inflammatory M2, but not pro-inflammatory M1 macrophages promote angiogenesis in vivo. *Angiogenesis*, *17*(1), 109–118. https://doi.org/10.1007/s10456-013-9381-6

Ji, Z, Luo, W., Li, W., Hoque, M., Pan, Z., Zhao, Y., & Tian, B. (2011). Transcriptional activity regulates alternative cleavage and polyadenylation. *Mol Syst Biol*, *7*(534), 534.

https://doi.org/10.1038/msb.2011.69
Ji, Zhe, Lee, J. Y., Pan, Z., Jiang, B., & Tian, B. (2009). Progressive lengthening of 3' untranslated regions of mRNAs by alternative polyadenylation during mouse embryonic development. *Proceedings of the National Academy of Sciences of the United States of America*, *106*(17), 7028. https://doi.org/10.1073/pnas.0905246106
Jia, X., Yuan, S., Wang, Y., Fu, Y., Ge, Y. Y., Ge, Y. Y., Lan, X., Feng, Y., Qiu, F., Li, P., Chen, S., & Xu, A. (2017). The role of alternative polyadenylation in the antiviral innate immune response. *Nature Communications*, *8*, 14605. https://doi.org/10.1038/ncomms14605
Jones, S., Chen, W.-D. D., Parmigiani, G., Diehl, F., Beerenwinkel, N., Antal, T., Traulsen, A., Nowak, M. A., Siegel, C., Velculescu, V. E., Kinzler, K. W., Vogelstein, B., Willis, J., & Markowitz, S. D. (2008). Comparative lesion sequencing provides insights into tumor evolution. *Proceedings of the National Academy of Sciences of the United States of America*, *105*(11), 4283–4288. https://doi.org/10.1073/pnas.0712345105
Kadl, A., Meher, A., Sharma, P., Lee, M., Doran, A., Johnstone, S., Elliott, M., Gruber, F., Han, J., Chen, W., Kensler, T., Ravichandran, K., & Leitinge, N. (2010). Identification of a novel macrophage phenotype that develops in response to atherogenic phospholipids via Nrf2. *Circ Res.*, *107*(6), 737–746. https://doi.org/10.1161/CIRCULATIONAHA.110.956839
Kafasla, P., Mickleburgh, I., Llorian, M., Coelho, M., Gooding, C., Cherny, D., Joshi, A., Kotik-Kogan, O., Curry, S., Eperon, I. C., Jackson, R. J., & Smith, C. W. J. (2012). Defining the roles and interactions of PTB. *Biochemical Society Transactions*, *40*(4), 815–820. https://doi.org/10.1042/BST20120044
Kahles, A., Lehmann, K.-V., Toussaint, N. C., Hüser, M., Stark, S. G., Sachsenberg, T., Stegle, O., Kohlbacher, O., Sander, C., Caesar-Johnson, S. J., Demchok, J. A., Felau, I., Kasapi, M., Ferguson, M. L., Hutter, C. M., Sofia, H. J., Tarnuzzer, R., Wang, Z., Yang, L., … Rätsch, G. (2018). Comprehensive Analysis of Alternative Splicing Across Tumors from 8,705 Patients. *Cancer Cell*, *0*(0), 211–224. https://doi.org/10.1016/J.CCELL.2018.07.001
Kaida, D., Berg, M. G., Younis, I., Kasim, M., Singh, L. N., Wan, L., & Dreyfuss, G. (2010). U1 snRNP protects pre-mRNAs from premature cleavage and polyadenylation. *Nature*, *468*(7324), 664–668. https://doi.org/10.1038/nature09479
Kaler, P., Augenlicht, L., & Klampfer, L. (2009). Macrophage-derived IL-1B stimulates Wnt signaling and growth of colon cancer cells: A crosstalk interrupted by vitamin D"3. *Oncogene*, *28*(44), 3892–3902. https://doi.org/10.1038/onc.2009.247
Kalluri, R., & Weinberg, R. A. (2009). The basics of epithelial-mesenchymal transition. *Journal of Clinical Investigation*, *119*(6), 1420–1428. https://doi.org/10.1172/JCI39104.1420
Kamieniarz-Gdula, K., Gdula, M. R., Panser, K., Nojima, T., Monks, J., Wiśniewski, J. R., Riepsaame, J., Brockdorff, N., Pauli, A., & Proudfoot, N. J. (2019). Selective Roles of Vertebrate PCF11 in Premature and Full-Length Transcript Termination. *Molecular Cell*, *74*(1), 158-172.e9. https://doi.org/10.1016/j.molcel.2019.01.027
Kang, J. C., Chen, J. S., Lee, C. H., Chang, J. J., & Shieh, Y. S. (2010). Intratumoral macrophage counts correlate with tumor progression in colorectal cancer. *Journal of Surgical Oncology*, *102*(3), 242–248. https://doi.org/10.1002/jso.21617
Kaufmann, I., Martin, G., Friedlein, A., Langen, H., & Keller, W. (2004). Human Fip1 is a subunit of CPSF that binds to U-rich RNA elements and stimulates poly(A) polymerase. *EMBO Journal*, *23*(3), 616–626. https://doi.org/10.1038/sj.emboj.7600070
Kawai, T., & Akira, S. (2011). Toll-like Receptors and Their Crosstalk with Other Innate Receptors in Infection and Immunity. *Immunity*, *34*(5), 637–650. https://doi.org/10.1016/j.immuni.2011.05.006
Kawamura, S., Onai, N., Miya, F., Sato, T., Tsunoda, T., Kurabayashi, K., Yotsumoto, S., Kuroda, S., Takenaka, K., Akashi, K., & Ohteki, T. (2017). Identification of a Human Clonogenic Progenitor with Strict Monocyte Differentiation Potential: A Counterpart of Mouse cMoPs. *Immunity*, *46*(5), 835-848.e4. https://doi.org/10.1016/j.immuni.2017.04.019
Kazemian, M., Ren, M., Lin, J.-X., Liao, W., Spolski, R., & Leonard, W. J. (2015). Comprehensive assembly of novel transcripts from unmapped human RNA-Seq data and their association with cancer. *Molecular Systems Biology*, *11*(8), 826. https://doi.org/10.15252/msb.156172
Kechagia, J. Z., Ivaska, J., & Roca-Cusachs, P. (2019). Integrins as biomechanical sensors of the microenvironment. *Nature Reviews Molecular Cell Biology*, *20*(August). https://doi.org/10.1038/s41580-019-0134-2
Kim, E., Ilagan, J. O., Liang, Y., Daubner, G. M., Stanley, C., Ramakrishnan, A., Li, Y., Chung, Y. R., Micol, J., Murphy, M., Cho, H., Hana, M., Zebari, A. S., Park, C. Y., Buonamici, S., Smith, P. G., Joachim, H., Lobry, C., Aifantis, I., … Abdel-Wahab, O. (2015). SRSF2 mutations contribute to Myelodysplasia through mutant-specific effects on exon recognition. *Cancer Cell*, *27*(5), 617–630.

https://doi.org/10.1016/j.ccell.2015.04.006.SRSF2
Kim, J. S., Park, Y. M., Kim, N. Y., Yun, H. K., Lee, K. J., Kim, B. H., Park, S. J., Yeon, J. W., & Jung, G. (2011). Combination treatment with intrahepatic arterial infusion and intratumoral injection chemotherapy in patients with far-advanced hepatocellular carcinoma and arterioportal or arteriovenous shunts: preliminary results. *The Korean Journal of Hepatology*, *17*(2), 120–129. https://doi.org/10.3350/kjhep.2011.17.2.120
Kim, K., Lu, Z., & Hay, E. D. (2002). Direct evidence for a role of β-catenin/LEF-1 signaling pathway in induction of EMT. *Cell Biology International*, *26*(5), 463–476. https://doi.org/10.1006/cbir.2002.0901
Kim, M., Lim, J., Lee, J. H., Lee, K. M., Kim, S., Park, K. W., Nho, C. W., & Cho, Y. S. (2018). Understanding the functional role of genistein in the bone differentiation in mouse osteoblastic cell line MC3T3-E1 by RNA-seq analysis. *Scientific Reports*, *8*(1), 1–12. https://doi.org/10.1038/s41598-018-21601-9
Kireeva, M. L., Hancock, B., Cremona, G. H., Walter, W., Studitsky, V. M., & Kashlev, M. (2005). Nature of the nucleosomal barrier to RNA polymerase II. *Molecular Cell*, *18*(1), 97–108. https://doi.org/10.1016/j.molcel.2005.02.027
Klostergaard, J. (1987). Role of tumor necrosis factor in monocyte/macrophage tumor cytotoxicity in vitro. *Natural Immunity and Cell Growth Regulation*, *6*(4), 161–166.
Kocabas, A., Duarte, T., Kumar, S., & Hynes, M. A. (2015). Widespread Differential Expression of Coding Region and 3' UTR Sequences in Neurons and Other Tissues. *Neuron*, *88*(6), 1149–1156. https://doi.org/10.1016/j.neuron.2015.10.048
Komarnitsky, P., Cho, E. J., & Buratowski, S. (2000). Different phosphorylated forms of RNA polymerase II and associated mRNA processing factors during transcription. *Genes and Development*, *14*(19), 2452–2460. https://doi.org/10.1101/gad.824700
Konarska, M. M., Grabowski, P. J., Padgett, R. A., & Sharp, P. A. (1985). Characterization of the branch site in lariat RNAs produced by splicing of mRNA precursors. *Nature*, *313*(6003), 552–557. https://doi.org/10.1038/313552a0
Krumm, A., Meulia, T., Brunvand, M., & Groudine, M. (1992). The block to transcriptional elongation within the human c-myc gene is determined in the promoter-proximal region. *Genes and Development*, *6*(11), 2201–2213. https://doi.org/10.1101/gad.6.11.2201
Kumar, A. T., Knops, A., Swendseid, B., Martinez-Outschoom, U., Harshyne, L., Philp, N., Rodeck, U., Luginbuhl, A., Cognetti, D., Johnson, J., & Curry, J. (2019). Prognostic Significance of Tumor-Associated Macrophage Content in Head and Neck Squamous Cell Carcinoma: A Meta-Analysis. *Frontiers in Oncology*, *9*(July), 1–10. https://doi.org/10.3389/fonc.2019.00656
Kwak, Y., Koh, J., Kim, D. W., Kang, S. B., Kim, W. H., & Lee, H. S. (2016). Immunoscore encompassing CD3+ and CD8+ T cell densities in distant metastasis is a robust prognostic marker for advanced colorectal cancer. *Oncotarget*, *7*(49), 81778–81790. https://doi.org/10.18632/oncotarget.13207
Lai, B., Wang, J., Fagenson, A., Sun, Y., Saredy, J., Lu, Y., Nanayakkara, G., Yang, W. Y., Yu, D., Shao, Y., Drummer, C., Johnson, C., Saaoud, F., Zhang, R., Yang, Q., Xu, K., Mastascusa, K., Cueto, R., Fu, H., … Yang, X. (2019). Twenty Novel Disease Group-Specific and 12 New Shared Macrophage Pathways in Eight Groups of 34 Diseases Including 24 Inflammatory Organ Diseases and 10 Types of Tumors. *Frontiers in Immunology*, *10*(November). https://doi.org/10.3389/fimmu.2019.02612
Lai, D.-P., Tan, S., Kang, Y.-N., Wu, J., Ooi, H.-S., Chen, J., Shen, T.-T., Qi, Y., Zhang, X., Guo, Y., Zhu, T., Liu, B., Shao, Z., & Zhao, X. (2015). Genome-wide profiling of polyadenylation sites reveals a link between selective polyadenylation and cancer metastasis. *Human Molecular Genetics*, *24*(12), 3410–3417.
Laitem, C., Zaborowska, J., Isa, N. F., Kufs, J., Dienstbier, M., & Murphy, S. (2015). CDK9 inhibitors define elongation checkpoints at both ends of RNA polymerase II-transcribed genes. *Nature Structural and Molecular Biology*, *22*(5), 396–403. https://doi.org/10.1038/nsmb.3000
Lambert, S. A., Jolma, A., Campitelli, L. F., Das, P. K., Yin, Y., Albu, M., Chen, X., Taipale, J., Hughes, T. R., & Weirauch, M. T. (2018). The Human Transcription Factors. *Cell*, *172*(4), 650–665. https://doi.org/10.1016/j.cell.2018.01.029
Lane, D. J. R., Merlot, A. M., Huang, M. L. H., Bae, D. H., Jansson, P. J., Sahni, S., Kalinowski, D. S., & Richardson, D. R. (2015). Cellular iron uptake, trafficking and metabolism: Key molecules and mechanisms and their roles in disease. *Biochimica et Biophysica Acta - Molecular Cell Research*, *1853*(5), 1130–1144. https://doi.org/10.1016/j.bbamcr.2015.01.021
Langmead, B., Trapnell, C., Pop, M., & Salzberg, S. L. (2009). Ultrafast and memory-efficient alignment of short DNA sequences to the human genome. *Genome Biology*, *10*(3). https://doi.org/10.1186/gb-2009-10-3-r25

Larionova, I., Tuguzbaeva, G., Ponomaryova, A., Stakheyeva, M., Cherdyntseva, N., Pavlov, V., Choinzonov, E., & Kzhyshkowska, J. (2020). Tumor-Associated Macrophages in Human Breast, Colorectal, Lung, Ovarian and Prostate Cancers. *Frontiers in Oncology*, *10*(October), 1–34. https://doi.org/10.3389/fonc.2020.566511

Lawrence, T., & Natoli, G. (2011). Transcriptional regulation of macrophage polarization: Enabling diversity with identity. *Nature Reviews Immunology*, *11*(11), 750–761. https://doi.org/10.1038/nri3088

Le Page, C., Génin, P., Baines, M. G., & Hiscott, J. (2000). Interferon activation and innate immunity. *Reviews in Immunogenetics*, *2*(3), 374–386.

LeBleu, V. S., & Neilson, E. G. (2020). Origin and functional heterogeneity of fibroblasts. *FASEB Journal*, *34*(3), 3519–3536. https://doi.org/10.1096/fj.201903188R

Lee, C. H., Espinosa, I., Vrijaldenhoven, S., Subramanian, S., Montgomery, K. D., Zhu, S., Marinelli, R. J., Peterse, J. L., Poulin, N., Nielsen, T. O., West, R. B., Gilks, C. B., & Van De Rijn, M. (2008). Prognostic significance of macrophage infiltration in leiomyosarcomas. *Clinical Cancer Research*, *14*(5), 1423–1430. https://doi.org/10.1158/1078-0432.CCR-07-1712

Lee, E., Pandey, N. B., & Popel, A. S. (2015). Crosstalk between cancer cells and blood endothelial and lymphatic endothelial cells in tumour and organ microenvironment. *Expert Reviews in Molecular Medicine*, *17*(January), 1–18. https://doi.org/10.1017/erm.2015.2

Lee, J., Breton, G., Oliveira, T. Y. K., Zhou, Y. J., Aljoufi, A., Puhr, S., Cameron, M. J., Sékaly, R. P., Nussenzweig, M. C., & Liu, K. (2015). Restricted dendritic cell and monocyte progenitors in human cord blood and bone marrow. *Journal of Experimental Medicine*, *212*(3), 385–399. https://doi.org/10.1084/jem.20141442

Lee, S. H., Singh, I., Tisdale, S., Abdel-Wahab, O., Leslie, C. S., & Mayr, C. (2018). Widespread intronic polyadenylation inactivates tumour suppressor genes in leukaemia. *Nature*, *561*(7721), 127–131. https://doi.org/10.1038/s41586-018-0465-8

Lee, Y. S., Song, S. J., Hong, H. K., Oh, B. Y., Lee, W. Y., & Cho, Y. B. (2020). The FBW7-MCL-1 axis is key in M1 and M2 macrophage-related colon cancer cell progression: validating the immunotherapeutic value of targeting PI3Kγ. *Experimental and Molecular Medicine*, *52*(5), 815–831. https://doi.org/10.1038/s12276-020-0436-7

Legendre, M., & Gautheret, D. (2003). Sequence determinants in human polyadenylation site selection. *BMC Genomics*, *4*, 1–9. https://doi.org/10.1186/1471-2164-4-7

Leitinger, N., & Schulman, I. G. (2013). Phenotypic polarization of macrophages in atherosclerosis. *Arteriosclerosis, Thrombosis, and Vascular Biology*, *33*(6), 1120–1126. https://doi.org/10.1161/ATVBAHA.112.300173

Lemaitre, B., Nicolas, E., Michaut, L., Reichhart, J. M., & Hoffmann, J. A. (1996). The dorsoventral regulatory gene cassette spatzle/Toll/Cactus controls the potent antifungal response in Drosophila adults. *Cell*, *86*(6), 973–983. https://doi.org/10.1016/S0092-8674(00)80172-5

Lengauer, C., Kinzler, K. W., & Vogelstein, B. (1997). DNA methylation and genetic instability in colorectal cancer cells. *Proceedings of the National Academy of Sciences of the United States of America*, *94*(6), 2545–2550. https://doi.org/10.1073/pnas.94.6.2545

Levental, K. R., Yu, H., Kass, L., Lakins, J. N., Egeblad, M., Erler, J. T., Fong, S. F. T., Csiszar, K., Giaccia, A., Weninger, W., Yamauchi, M., Gasser, D. L., & Weaver, V. M. (2009). Matrix Crosslinking Forces Tumor Progression by Enhancing Integrin Signaling. *Cell*, *139*(5), 891–906. https://doi.org/10.1016/j.cell.2009.10.027

Lewin, B. (2008). *Genes IX* (Jones and Bartlett Publishers (Ed.); 9th (2008)).

Lewis, J. S., Landers, R. J., Underwood, J. C. E., Harris, A. L., & Lewis, C. E. (2000). Expression of vascular endothelial growth factor by macrophages is up-regulated in poorly vascularized areas of breast carcinomas. *Journal of Pathology*, *192*(2), 150–158. https://doi.org/10.1002/1096-9896(2000)9999:9999<::AID-PATH687>3.0.CO;2-G

Li, H., Handsaker, B., Wysoker, A., Fennell, T., Ruan, J., Homer, N., Marth, G., Abecasis, G., Durbin, R., & Subgroup, 1000 Genome Project Data Processing. (2009). The Sequence Alignment/Map format and SAMtools. *Bioinformatics*, *25*(16), 2078–2079. https://doi.org/10.1093/bioinformatics/btp352

Li, P., He, K., Li, J., Liu, Z., & Gong, J. (2017). The role of Kupffer cells in hepatic diseases. *Molecular Immunology*, *85*, 222–229. https://doi.org/10.1016/j.molimm.2017.02.018

Li, W., Park, J. Y., Zheng, D., Hoque, M., Yehia, G., & Tian, B. (2016). Alternative cleavage and polyadenylation in spermatogenesis connects chromatin regulation with post-transcriptional control. *BMC Biology*, *14*(1), 1–17. https://doi.org/10.1186/s12915-016-0229-6

Liepelt, A., Vries, I. S. N., Simons, N., Eichelbaum, K., Föhr, S., Archer, S. K., Castello, A., Usadel, B., Krijgsveld, J., Preiss, T., Marx, G., Hentze, M. W., Ostareck, D. H., Ostareck-lederer, A., Fo, S.,

Archer, S. K., Castello, A., Krijgsveld, J., Preiss, T., … Ostareck-lederer, A. (2016). *Identification of RNA-binding proteins in macrophages by interactome capture*. 2699–2714. https://doi.org/10.1074/mcp.M115.056564

Lim, Z. F., & Ma, P. C. (2019). Emerging insights of tumor heterogeneity and drug resistance mechanisms in lung cancer targeted therapy. *Journal of Hematology and Oncology*, *12*(1), 1–18. https://doi.org/10.1186/s13045-019-0818-2

Lin, Y., Xu, J., & Lan, H. (2019). *Tumor-associated macrophages in tumor metastasis : biological roles and clinical therapeutic applications*. *3*, 1–16.

Lindvall, C., Evans, N. C., Zylstra, C. R., Li, Y., Alexander, C. M., & Williams, B. O. (2006). The Wnt signaling receptor Lrp5 is required for mammary ductal stem cell activity and Wnt1-induced tumorigenesis. *Journal of Biological Chemistry*, *281*(46), 35081–35087. https://doi.org/10.1074/jbc.M607571200

Liu, D., Keijzers, G., & Rasmussen, L. J. (2017). DNA mismatch repair and its many roles in eukaryotic cells. *Mutation Research - Reviews in Mutation Research*, *773*, 174–187. https://doi.org/10.1016/j.mrrev.2017.07.001

Liu, H., Lorenzini, P. A., Zhang, F., Xu, S., Wong, M. S. M., Zheng, J., & Roca, X. (2018). Alternative splicing analysis in human monocytes and macrophages reveals MBNL1 as major regulator. *Nucleic Acids Research*, *46*(May), 1–18. https://doi.org/10.1093/nar/gky401

Liu, X., Freitas, J., Zheng, D., Oliveira, M. S., Hoque, M., Martins, T., Henriques, T., Tian, B., & Moreira, A. (2017). Transcription elongation rate has a tissue-specific impact on alternative cleavage and polyadenylation in Drosophila melanogaster. *RNA (New York, N.Y.)*, *23*(12), 258–265. https://doi.org/10.1261/rna.062661.117

Liu, X., Hoque, M., Larochelle, M., Lemay, J.-F., Yurko, N., Manley, J. L., Bachand, F., & Tian, B. (2017). Comparative analysis of alternative polyadenylation in S . cerevisiae and S . pombe. *Genome Research*, *27*(10), 1–11. https://doi.org/10.1101/gr.222331.117.27

Liu, Y. C., Zou, X. B., Chai, Y. F., & Yao, Y. M. (2014). Macrophage polarization in inflammatory diseases. *International Journal of Biological Sciences*, *10*(5), 520–529. https://doi.org/10.7150/ijbs.8879

Livak, K. J., & Schmittgen, T. D. (2001). Analysis of relative gene expression data using real-time quantitative PCR and the 2-ΔΔCT method. *Methods*, *25*(4), 402–408. https://doi.org/10.1006/meth.2001.1262

Locati, M., Mantovani, A., & Sica, A. (2013). Macrophage Activation and Polarization as an Adaptive Component of Innate Immunity. In *Advances in Immunology* (Vol. 120). https://doi.org/10.1016/B978-0-12-417028-5.00006-5

Logan, C. Y., & Nusse, R. (2004). The Wnt Signaling Pathway in Development and Disease. *Annual Review of Cell and Developmental Biology*, *20*(1), 781–810. https://doi.org/10.1146/annurev.cellbio.20.010403.113126

Long, J. C., & Caceres, J. F. (2009). *The SR protein family of splicing factors : master regulators of gene expression*. *27*, 15–27. https://doi.org/10.1042/BJ20081501

Love, M. I., Huber, W., & Anders, S. (2014). Moderated estimation of fold change and dispersion for RNA-seq data with DESeq2. *Genome Biology*, *15*(12), 1–21. https://doi.org/10.1186/s13059-014-0550-8

Lu, X. J., & Chen, J. (2019). Specific function and modulation of teleost monocytes/ macrophages: polarization and phagocytosis. *Zoological Research*, *40*(3), 146–150. https://doi.org/10.24272/j.issn.2095-8137.2019.035

Luo, W., Johnson, A. W., & Bentley, D. L. (2006). The role of Rat1 in coupling mRNA 3′-end processing to transcription termination: Implications for a unified allosteric-torpedo model. *Genes and Development*, *20*(8), 954–965. https://doi.org/10.1101/gad.1409106

Lutz, C. S., & Moreira, A. (2011). Alternative mRNA polyadenylation in eukaryotes: An effective regulator of gene expression. *Wiley Interdisciplinary Reviews: RNA*, *2*(1), 22–31. https://doi.org/10.1002/wrna.47

Ma, J., Liu, L., Che, G., Yu, N., Dai, F., & You, Z. (2010). The M1 form of tumor-associated macrophages in non-small cell lung cancer is positively associated with survival time. *BMC Cancer*, *10*, 1–9. https://doi.org/10.1186/1471-2407-10-112

Ma, W., & Mayr, C. (2018). A Membraneless Organelle Associated with the Endoplasmic Reticulum Enables 3′UTR-Mediated Protein-Protein Interactions. *Cell*, *175*(6), 1492-1506.e19. https://doi.org/10.1016/j.cell.2018.10.007

MacDonald, C. C., Wilusz, J., & Shenk, T. (1994). The 64-kilodalton subunit of the CstF polyadenylation factor binds to pre-mRNAs downstream of the cleavage site and influences cleavage site location. *Molecular and Cellular Biology*, *14*(10), 6647–6654. https://doi.org/10.1128/mcb.14.10.6647

Machacek, C., Supper, V., Leksa, V., Mitulovic, G., Spittler, A., Drbal, K., Suchanek, M., Ohradanova-Repic, A., & Stockinger, H. (2016). Folate Receptor Regulates Integrin CD11b/CD18 Adhesion of a Macrophage Subset to Collagen. *The Journal of Immunology*, *197*(6), 2229–2238. https://doi.org/10.4049/jimmunol.1501878

Mackaness, G. (1964). The immunological basis of acquired cellular resistance. *J Exp Med*, 105–120.

Malissen, B., Tamoutounour, S., & Henri, S. (2014). The origins and functions of dendritic cells and macrophages in the skin. *Nature Reviews Immunology*, *14*(6), 417–428. https://doi.org/10.1038/nri3683

Mantovani, A., Bottazzi, B., Colotta, F., Sozzani, S., & Ruco, L. (1992). The origin and function of tumor-associated macrophages. *Immunology Today*, *13*(7), 265–270. https://doi.org/10.1016/0167-5699(92)90008-U

Mantovani, A., & Locati, M. (2013). Tumor-associated macrophages as a paradigm of macrophage plasticity, diversity, and polarization lessons and open questions. *Arteriosclerosis, Thrombosis, and Vascular Biology*, *33*(7), 1478–1483. https://doi.org/10.1161/ATVBAHA.113.300168

Mantovani, A., Sica, A., Sozzani, S., Allavena, P., Vecchi, A., & Locati, M. (2004). The chemokine system in diverse forms of macrophage activation and polarization. *Trends in Immunology*, *25*(12), 677–686. https://doi.org/10.1016/j.it.2004.09.015

Mantovani, A., Sozzani, S., Locati, M., Allavena, P., & Sica, A. (2002). Macrophage polarization: Tumor-associated macrophages as a paradigm for polarized M2 mononuclear phagocytes. *Trends in Immunology*, *23*(11), 549–555. https://doi.org/10.1016/S1471-4906(02)02302-5

Mapendano, C. K., Lykke-Andersen, S., Kjems, J., Bertrand, E., & Jensen, T. H. (2010). Crosstalk between mRNA 3′ End Processing and Transcription Initiation. *Molecular Cell*, *40*(3), 410–422. https://doi.org/10.1016/j.molcel.2010.10.012

Marques, L., Negre-Salvayre, A., Costa, L., & Canonne-Hergaux, F. (2016). Iron gene expression profile in atherogenic Mox macrophages. *Biochimica et Biophysica Acta - Molecular Basis of Disease*, *1862*(6), 1137–1146. https://doi.org/10.1016/j.bbadis.2016.03.004

Marshall, N. F., Peng, J., Xie, Z., & Price, D. H. (1996). Control of RNA polymerase II elongation potential by a novel carboxyl- terminal domain kinase. *Journal of Biological Chemistry*, *271*(43), 27176–27183. https://doi.org/10.1074/jbc.271.43.27176

Martin, M. (2011). Cutadapt removes adapter sequences from high-throughput sequencing reads. *EMBnet*, *7*(10), 2803–2809.

Martinez, F. O., Gordon, S., Locati, M., & Mantovani, A. (2006). Transcriptional profiling of the human monocyte-to-macrophage differentiation and polarization: new molecules and patterns of gene expression. *Journal of Immunology*, *177*(10), 7303–7311. https://doi.org/10.4049/jimmunol.177.10.7303

Martins, F., Oliveira, R., Cavadas, B., Pinto, F., Cardoso, A. P., Castro, F., Sousa, B., Pinto, M. L., Silva, A. J., Adão, D., Loureiro, J. P., Pedro, N., Reis, R. M., Pereira, L., Oliveira, M. J., & Costa, A. M. (2020). Hypoxia and macrophages act in concert towards a beneficial outcome in colon cancer. *Cancers*, *12*(4). https://doi.org/10.3390/cancers12040818

Marzluff, W., Wagner, E. J., & Duronio, R. J. (2013). *Metabolism and regulation of canonical histone mRNAs: life without a poly(A) tail William*. *71*(2), 233–236. https://doi.org/10.1038/mp.2011.182.doi

Masckauchán, T. N. H., Shawber, C. J., Funahashi, Y., Li, C.-M., & Kitajewski, J. (2005). Wnt/beta-catenin signaling induces proliferation, survival and interleukin-8 in human endothelial cells. *Angiogenesis*, *8*(1), 43–51. https://doi.org/10.1007/s10456-005-5612-9

Mayr, C. (2016). Evolution and Biological Roles of Alternative 3'UTRs. *Trends in Cell Biology*, *26*(3), 227–237. https://doi.org/10.1016/j.tcb.2015.10.012

Mayr, C. (2017). Regulation by 3′–Untranslated Regions. *Annual Review of Genetics*, *51*(1), annurev-genet-120116-024704. https://doi.org/10.1146/annurev-genet-120116-024704

Mayr, C., & Bartel, D. P. (2009). Widespread Shortening of 3'UTRs by Alternative Cleavage and Polyadenylation Activates Oncogenes in Cancer Cells. *Cell*, *138*(138), 673–684. https://doi.org/10.1016/j.cell.2009.06.016

Mazan-Mamczarz, K., & Gartenhaus, R. B. (2007). Post-transcriptional control of the MCT-1-associated protein DENR/DRP by RNA-binding protein AUF1. *Cancer Genomics and Proteomics*, *4*(3), 233–240.

McCracken, S, Fong, N., Yankulov, K., Ballantyne, S., Pant, G., Greenblattt, J., Patterson, S., Wickens, M., & Bentley, D. L. (1997). The C-terminal domain of RNA polymerase II couples mRNA processing to transcription. *Nature*, *385*, 357–361.

McCracken, Susan, Fong, N., Rosonina, E., Yankulov, K., Brothers, G., Siderovski, D., Hessel, A., Foster, S., Shuman, S., & Bentley, D. L. (1997). 5'-Capping enzymes are targeted to pre-mRNA

by binding to the phosphorylated carboxy-terminal domain of RNA polymerase II. *Genes and Development*, *11*(24), 3306–3318. https://doi.org/10.1101/gad.11.24.3306

McKeown, S. R. (2014). Defining normoxia, physoxia and hypoxia in tumours - Implications for treatment response. *British Journal of Radiology*, *87*(1035), 1–12. https://doi.org/10.1259/bjr.20130676

Medici, M., Hay, E., & Olsen, B. (2008). Snail and Slug Promote Epithelial-Mesenchymal Transition through Beta-Catenin–T-Cell Factor-4-dependent Expression of Transforming Growth Factor-Beta3. *Molecular Biology of the Cell*, *19*(November), 4875–4887. https://doi.org/10.1091/mbc.E08

Mercer, T. R., Wilhelm, D., Dinger, M. E., Soldà, G., Korbie, D. J., Glazov, E. A., Truong, V., Schwenke, M., Simons, C., Matthaei, K. I., Saint, R., Koopman, P., & Mattick, J. S. (2011). Expression of distinct RNAs from 3' untranslated regions. *Nucleic Acids Research*, *39*(6), 2393–2403. https://doi.org/10.1093/nar/gkq1158

Metschnikoff, E. (1892). Untersuchung uber die mesodermalen Phagocyten einiger Wirbeltiere. *Biologicial Centralblatt*, *18*, 560–565.

Millevoi, S., & Vagner, S. (2009). Molecular mechanisms of eukaryotic pre-mRNA 3' end processing regulation. *Nucleic Acids Research*, *38*(9), 2757–2774. https://doi.org/10.1093/nar/gkp1176

Mills, C. D., Kincaid, K., Alt, J. M., Heilman, M. J., & Hill, A. M. (2000). M-1/M-2 Macrophages and the Th1/Th2 Paradigm. *The Journal of Immunology*, *164*(12), 6166–6173. https://doi.org/10.4049/jimmunol.164.12.6166

Misteli, T., Cáceres, J. F., Clement, J. Q., Krainer, A. R., Wilkinson, M. F., & Spector, D. L. (1998). Serine phosphorylation of SR proteins is required for their recruitment to sites of transcription in vivo. *Journal of Cell Biology*, *143*(2), 297–307. https://doi.org/10.1083/jcb.143.2.297

Mitra, M., Johnson, E. L., & Coller, H. A. (2016). Alternative polyadenylation can regulate post-translational membrane localization. *Trends in Cell & Molecular Biology*, *10*, 37–47.

Mittal, D., Gubin, M. M., Schreiber, R. D., & Smyth, M. J. (2014). New insights into cancer immunoediting and its three component phases-elimination, equilibrium and escape. *Current Opinion in Immunology*, *27*(1), 16–25. https://doi.org/10.1016/j.coi.2014.01.004

Miura, P., Shenker, S., Andreu-Agullo, C., Westholm, J. O., & Lai, E. C. (2013). Widespread and extensive lengthening of 3' UTRs in the mammalian brain. *Genome Research*, *23*(5), 812–825. https://doi.org/10.1101/gr.146886.112

Mok, S., Koya, R. C., Tsui, C., Xu, J., Robert, L., Wu, L., Graeber, T. G., West, B. L., Bollag, G., & Ribas, A. (2014). Inhibition of CSF-1 receptor improves the antitumor efficacy of adoptive cell transfer immunotherapy. *Cancer Research*, *74*(1), 153–161. https://doi.org/10.1158/0008-5472.CAN-13-1816

Mola, S., Pandolfo, C., Sica, A., & Porta, C. (2020). The macrophages-microbiota interplay in colorectal cancer (CRC)-related inflammation: Prognostic and therapeutic significance. *International Journal of Molecular Sciences*, *21*(18), 1–30. https://doi.org/10.3390/ijms21186866

Monteleone, M., Stanley, A. C., Chen, K. W., Brown, D. L., Bezbradica, J. S., von Pein, J. B., Holley, C. L., Boucher, D., Shakespear, M. R., Kapetanovic, R., Rolfes, V., Sweet, M. J., Stow, J. L., & Schroder, K. (2018). Interleukin-1β Maturation Triggers Its Relocation to the Plasma Membrane for Gasdermin-D-Dependent and -Independent Secretion. *Cell Reports*, *24*(6), 1425–1433. https://doi.org/10.1016/j.celrep.2018.07.027

Moreira, A., Takagaki, Y., Brackenridge, S., Wollerton, M., Manley, J. L., & Proudfoot, N. J. (1998). The upstream sequence element of the C2 complement poly(A) signal activates mRNA 3' end formation by two distinct mechanisms. *Genes and Development*, *12*(16), 2522–2534. https://doi.org/10.1101/gad.12.16.2522

Morris, A. R., Bos, A., Diosdado, B., Rooijers, K., Elkon, R., Bolijn, A. S., Carvalho, B., Meijer, G. A., & Agami, R. (2012). Alternative cleavage and polyadenylation during colorectal cancer development. *Clinical Cancer Research*, *18*(19), 5256–5266. https://doi.org/10.1158/1078-0432.CCR-12-0543

Mosser, D. M., & Edwards, J. P. (2008). Exploring the full spectrum of macrophage activation. *Nature Reviews Immunology*, *8*(12), 958–969. https://doi.org/10.1038/nri2448.Exploring

Moteki, S., & Price, D. (2002). Functional coupling of capping and transcription of mRNA. *Molecular Cell*, *10*(3), 599–609. https://doi.org/10.1016/S1097-2765(02)00660-3

Müller, M. F., Ibrahim, A. E. K., & Arends, M. J. (2016). Molecular pathological classification of colorectal cancer. *Virchows Archiv*, *469*(2), 125–134. https://doi.org/10.1007/s00428-016-1956-3

Murdoch, C., Giannoudis, A., & Lewis, C. E. (2004). Mechanisms regulating the recruitment of macrophages into hypoxic areas of tumors and other ischemic tissues. *Blood*, *104*(8), 2224–2234. https://doi.org/10.1182/blood-2004-03-1109

Murthy, K. G. K., & Manley, J. L. (1992). Characterization of the multisubunit cleavage-polyadenylation

specificity factor from calf thymus. *Journal of Biological Chemistry*, *267*(21), 14804–14811.
Murthy, K. G. K., & Manley, J. L. (1995). The 160-kD subunit of human cleavage-polyadenylation specificity factor coordinates pre-mRNA 3'-end formation. *Genes and Development*, *9*(21), 2672–2683. https://doi.org/10.1101/gad.9.21.2672
Muse, G. W., Gilchrist, D. A., Nechaev, S., Shah, R., Parker, J. S., Grissom, S. F., Zeitlinger, J., & Adelman, K. (2007). RNA polymerase is poised for activation across the genome. *Nature Genetics*, *39*(12), 1507–1511. https://doi.org/10.1038/ng.2007.21
Myer, V. E., & Steitz, J. A. (1995). Isolation and characterization of a novel, low abundance hnRNP protein - A0. *RNA (New York, N.Y.)*, *1*, 171–182.
Naba, A., Clauser, K. R., Hoersch, S., Liu, H., Carr, S. A., & Hynes, R. O. (2012). The matrisome: In silico definition and in vivo characterization by proteomics of normal and tumor extracellular matrices. *Molecular and Cellular Proteomics*, *11*(4), 1–18. https://doi.org/10.1074/mcp.M111.014647
Nagaike, T., Logan, C., Hotta, I., Rozenblatt-rosen, O., & Manley, J. L. (2012). *Transcriptional activators enhance polyadenylation of mRNA precursors*. *41*(4), 409–418. https://doi.org/10.1016/j.molcel.2011.01.022.Transcriptional
Nakazawa, M. S., Keith, B., & Simon, M. C. (2016). Oxygen availability and metabolic adaptations. *Nature Reviews Cancer*, *16*(10), 663–673. https://doi.org/10.1038/nrc.2016.84
Nath, A., Pal, R., Singh, L. M., Saikia, H., Rahaman, H., Ghosh, S. K., Mazumder, R., & Sengupta, M. (2018). Gold-manganese oxide nanocomposite suppresses hypoxia and augments pro-inflammatory cytokines in tumor associated macrophages. *International Immunopharmacology*, *57*(February), 157–164. https://doi.org/10.1016/j.intimp.2018.02.021
Nechaev, S., Fargo, D., Santos, G., Liu, L., Gao, Y., & Adelman, K. (2010). Global Analysis of Short RNAs Reveals Widespread Promoter- Proximal Stalling and Arrest of Pol II in Drosophila. *Science*, *326*(5963), 335–338. https://doi.org/10.1038/jid.2014.371
Németh, Z. H., Lutz, C. S., Csóka, B., Deitch, E. A., Leibovich, S. J., Gause, W. C., Tone, M., Pacher, P., Vizi, E. S., & Haskó, G. (2005). Adenosine Augments IL-10 Production by Macrophages through an A 2B Receptor-Mediated Posttranscriptional Mechanism . *The Journal of Immunology*, *175*(12), 8260–8270. https://doi.org/10.4049/jimmunol.175.12.8260
Neve, J., Patel, R., Wang, Z., Louey, A., & Furger, A. M. (2017). Cleavage and polyadenylation: Ending the message expands gene regulation. *RNA Biology*, *14*(7), 865–890. https://doi.org/10.1080/15476286.2017.1306171
Newnham, C. M., Hall-Pogar, T., Liang, S., Wu, J., Tian, B., Hu, J., & Carol S. Lutz. (2010). Alternative polyadenylation of MeCP: influence of cis-acting elements and trans-acting factors. *RNA Biology*, *7*(3), 361–372.
Nocito, L., Kleckner, A. S., Yoo, E. J., Jones, A. R., Liesa, M., & Corkey, B. E. (2015). The extracellular redox state modulates mitochondrial function, gluconeogenesis, and glycogen synthesis in murine hepatocytes. *PLoS ONE*, *10*(3), 1–17. https://doi.org/10.1371/journal.pone.0122818
Nojima, T., Gomes, T., Grosso, A. R. F., Kimura, H., Dye, M. J., Dhir, S., Carmo-Fonseca, M., & Proudfoot, N. J. (2015). Mammalian NET-seq reveals genome-wide nascent transcription coupled to RNA processing. *Cell*, *161*(3), 526–540. https://doi.org/10.1016/j.cell.2015.03.027
Nojima, T., Gomes, T. T., Carmo-Fonseca, M., & Proudfoot, N. J. (2016). Mammalian NET-seq analysis defines nascent RNA profiles and associated RNA processing genome-wide. *Nature Protocols*, *11*(3), 413–428. https://doi.org/10.1038/nprot.2016.012
Ohradanova-Repic, A., Nogueira, E., Hartl, I., Gomes, A. C., Preto, A., Steinhuber, E., Mühlgrabner, V., Repic, M., Kuttke, M., Zwirzitz, A., Prouza, M., Suchanek, M., Wozniak-Knopp, G., Horejsi, V., Schabbauer, G., Cavaco-Paulo, A., & Stockinger, H. (2018). Fab antibody fragment-functionalized liposomes for specific targeting of antigen-positive cells. *Nanomedicine: Nanotechnology, Biology, and Medicine*, *14*(1), 123–130. https://doi.org/10.1016/j.nano.2017.09.003
Oliveira, M. S., Freitas, J., Pinto, P. A. B., Jesus, A. De, Tavares, J., Pinho, M., Domingues, R. G., Henriques, T., Lopes, C., Conde, C., Sunkel, C. E., & Moreira, A. (2019). Cell Cycle Kinase Polo is controlled by a widespread 3' Untranslated Region Regulatory Sequence in Drosophila melanogaster. *Molecular and Cellular Biology*, *39*(15), 1–18.
Ostuni, R., Piccolo, V., Barozzi, I., Polletti, S., Termanini, A., Bonifacio, S., Curina, A., Prosperini, E., Ghisletti, S., & Natoli, G. (2013). Latent enhancers activated by stimulation in differentiated cells. *Cell*, *152*(1–2), 157–171. https://doi.org/10.1016/j.cell.2012.12.018
Owen, J., Punt, J., & Stranford, S. (2013). *Kuby Immunology*.
Pagès, F., Mlecnik, B., Marliot, F., Bindea, G., Ou, F. S., Bifulco, C., Lugli, A., Zlobec, I., Rau, T. T., Berger, M. D., Nagtegaal, I. D., Vink-Börger, E., Hartmann, A., Geppert, C., Kolwelter, J., Merkel, S., Grützmann, R., Van den Eynde, M., Jouret-Mourin, A., … Sissy, C. El. (2018). International

validation of the consensus Immunoscore for the classification of colon cancer: a prognostic and accuracy study. *The Lancet*, *391*(10135), 2128–2139. https://doi.org/10.1016/S0140-6736(18)30789-X

Pai, A. A., Baharian, G., Pagé Sabourin, A., Brinkworth, J. F., Nédélec, Y., Foley, J. W., Grenier, J. C., Siddle, K. J., Dumaine, A., Yotova, V., Johnson, Z. P., Lanford, R. E., Burge, C. B., & Barreiro, L. B. (2016). Widespread Shortening of 3' Untranslated Regions and Increased Exon Inclusion Are Evolutionarily Conserved Features of Innate Immune Responses to Infection. *PLoS Genetics*, *12*(9), 1–24. https://doi.org/10.1371/journal.pgen.1006338

Pakiet, A., Kobiela, J., Stepnowski, P., Sledzinski, T., & Mika, A. (2019). Changes in lipids composition and metabolism in colorectal cancer: A review. *Lipids in Health and Disease*, *18*(1), 1–21. https://doi.org/10.1186/s12944-019-0977-8

Palangat, M., Renner, D. B., Price, D. H., & Landick, R. (2005). A negative elongation factor for human RNA polymerase II inhibits the anti-arrest transcript-cleavage factor TFIIS. *Proceedings of the National Academy of Sciences of the United States of America*, *102*(42), 15036–15041. https://doi.org/10.1073/pnas.0409405102

Parisi, L., Gini, E., Baci, D., Tremolati, M., Fanuli, M., Bassani, B., Farronato, G., Bruno, A., & Mortara, L. (2018). Macrophage Polarization in Chronic Inflammatory Diseases: Killers or Builders? *Journal of Immunology Research*, *2018*. https://doi.org/10.1155/2018/8917804

Patel, U., Rajasingh, S., Samanta, S., Cao, T., Dawn, B., & Rajasingh, J. (2017). Macrophage polarization in response to epigenetic modifiers during infection and inflammation. *Drug Discovery Today*, *22*(1), 186–193. https://doi.org/10.1016/j.drudis.2016.08.006.Macrophage

Pathria, P., Louis, T. L., & Varner, J. A. (2019). Targeting Tumor-Associated Macrophages in Cancer. *Trends in Immunology*, *40*(4), 310–327. https://doi.org/10.1016/j.it.2019.02.003

Paul, W. E. (Editor). (2008). Fundamental Immunology, 6th edition. In *Wolters Kluwer, Lippincott Williams & Williams*.

Pereira-Castro, I., & Moreira, A. (2021). On the function and relevance of alternative 3′-UTRs in gene expression regulation. *Wiley Interdisciplinary Reviews: RNA*, *January*, 1–30. https://doi.org/10.1002/wrna.1653

Peterlin, B. M., & Price, D. H. (2006). Controlling the Elongation Phase of Transcription with P-TEFb. *Molecular Cell*, *23*(3), 297–305. https://doi.org/10.1016/j.molcel.2006.06.014

Pinto, A. T., Pinto, M. L., Velho, S., Pinto, M. T., Cardoso, A. P., Figueira, R., Monteiro, A., Marques, M., Seruca, R., Barbosa, M. A., Mareel, M., Oliveira, M. J., & Rocha, S. (2016). Intricate macrophage-colorectal cancer cell communication in response to radiation. *PLoS ONE*, *11*(8), 1–20. https://doi.org/10.1371/journal.pone.0160891

Pinto, M.L., Rios, E., Silva, A. C., Neves, S. C., Caires, H. R., Pinto, A. T., Durães, C., Carvalho, F. A., Cardoso, A. P., Santos, N. C., Barrias, C. C., Nascimento, D. S., Pinto-do-Ó, P., Barbosa, M. A., Carneiro, F., & Oliveira, M. J. (2017). Decellularized human colorectal cancer matrices polarize macrophages towards an anti-inflammatory phenotype promoting cancer cell invasion via CCL18. *Biomaterials*. https://doi.org/10.1016/j.biomaterials.2017.02.004

Pinto, Marta L., Rios, E., Durães, C., Ribeiro, R., Machado, J. C., Mantovani, A., Barbosa, M. A., Carneiro, F., & Oliveira, M. J. (2019). The Two Faces of Tumor-Associated Macrophages and Their Clinical Significance in Colorectal Cancer. *Frontiers in Immunology*, *10*(August), 1–12. https://doi.org/10.3389/fimmu.2019.01875

Pinto, P. A. B., Henriques, T., Freitas, M. O., Martins, T., Domingues, R. G., Wyrzykowska, P. S., Coelho, P. A., Carmo, A. M., Sunkel, C. E., Proudfoot, N. J., & Moreira, A. (2011). RNA polymerase II kinetics in polo polyadenylation signal selection. *The EMBO Journal*, *30*(12), 2431–2444. https://doi.org/10.1038/emboj.2011.156

Ploeger, D. T., Hosper, N. A., Schipper, M., Koerts, J. A., De Rond, S., & Bank, R. A. (2013). Cell plasticity in wound healing: Paracrine factors of M1/ M2 polarized macrophages influence the phenotypical state of dermal fibroblasts. *Cell Communication and Signaling*, *11*(1). https://doi.org/10.1186/1478-811X-11-29

Poddar, D., Basu, A., Baldwin, W. M., Kondratov, R. V., Barik, S., & Mazumder, B. (2013). An Extraribosomal Function of Ribosomal Protein L13a in Macrophages Resolves Inflammation. *The Journal of Immunology*, *190*(7), 3600–3612. https://doi.org/10.4049/jimmunol.1201933

Porta, C., Rimoldi, M., Raes, G., Brys, L., Ghezzi, P., Di Liberto, D., Dieli, F., Ghisletti, S., Natoli, G., De Baetselier, P., Mantovani, A., & Sica, A. (2009). Tolerance and M2 (alternative) macrophage polarization are related processes orchestrated by p50 nuclear factor kappaB. *Proceedings of the National Academy of Sciences of the United States of America*, *106*(35), 14978–14983. https://doi.org/10.1073/pnas.0809784106

Portz, B., Lu, F., Gibbs, E. B., Mayfield, J. E., Rachel Mehaffey, M., Zhang, Y. J., Brodbelt, J. S.,

Showalter, S. A., & Gilmour, D. S. (2017). Structural heterogeneity in the intrinsically disordered RNA polymerase II C-terminal domain. *Nature Communications*, *8*(May), 1–12. https://doi.org/10.1038/ncomms15231

Prabhu, L., Mundade, R., Wang, B., Wei, H., Hartley, A.-V., Martin, M., McElyea, K., Temm, C. J., Sandusky, G., Liu, Y., & Lu, T. (2015). Critical role of phosphorylation of serine 165 of YBX1 on the activation of NF-κB in colon cancer. *Oncotarget*, *6*(30). https://doi.org/10.18632/oncotarget.5120

Proudfoot, N J, & Maniatis, T. (1980). The structure of a human α-globin pseudogene and its relationship to α-globin gene duplication. *Cell*, *21*(2), 537–544. https://doi.org/10.1016/0092-8674(80)90491-2

Proudfoot, Nick J. (2016). Transcriptional termination in mammals: Stopping the RNA polymerase II juggernaut. *Science*, *352*(6291). https://doi.org/10.1126/science.

Proudfoot, Nick J. (2011). Ending the message : poly (A) signals then and now. *Genes & Development*, *25*, 1770–1782. https://doi.org/10.1101/gad.17268411.Freely

Pyo, J.-S., Park, M. J., & Kim, C.-N. (2018). TPL2 expression is correlated with distant metastasis and poor prognosis in colorectal cancer. *Human Pathology*, *79*, 50–56. https://doi.org/10.1016/j.humpath.2018.05.003

Pyronneau, A., He, Q., Hwang, J. Y., Porch, M., Contractor, A., & Zukin, R. S. (2017). Aberrant Rac1-cofilin signaling mediates defects in dendritic spines, synaptic function, and sensory perception in fragile X syndrome. *Science Signaling*, *10*(504), 1–16. https://doi.org/10.1126/scisignal.aan0852

Quail, D F, & Joyce, J. A. (2013). Microenvironmental regulation of tumor progression and metastasis. *Nat Med*, *19*(11), 1423–1437. https://doi.org/10.1038/nm.3394

Quail, Daniela F., & Joyce, J. A. (2017). Molecular pathways: Deciphering mechanisms of resistance to macrophage-targeted therapies. *Clinical Cancer Research*, *23*(4), 876–884. https://doi.org/10.1158/1078-0432.CCR-16-0133

Quezada, S. A., Peggs, K. S., Simpson, T. R., & Allison, J. P. (2011). Shifting the equilibrium in cancer immunoediting: From tumor tolerance to eradication. *Immunological Reviews*, *241*(1), 104–118. https://doi.org/10.1111/j.1600-065X.2011.01007.x

Ramanathan, A., Robb, G. B., & Chan, S. H. (2016). mRNA capping: Biological functions and applications. *Nucleic Acids Research*, *44*(16), 7511–7526. https://doi.org/10.1093/nar/gkw551

Rasmussen, E. B., & Lis, J. T. (1993). In vivo transcriptional pausing and cap formation on three Drosophila heat shock genes. *Proceedings of the National Academy of Sciences of the United States of America*, *90*(17), 7923–7927. https://doi.org/10.1073/pnas.90.17.7923

Ray, A. A., Fountain, J. J., Miller, H. E., Cooper, A. M., & Robinson, R. T. (2015). IL12Rβ1ΔTM is a secreted product of il12rb1 that promotes controlof extrapulmonary tuberculosi. *Infection and Immunity*, *83*(2), 560–571. https://doi.org/10.1128/IAI.01230-13

Rey, S., Schito, L., Wouters, B. G., Eliasof, S., & Kerbel, R. S. (2017). Targeting Hypoxia-Inducible Factors for Antiangiogenic Cancer Therapy. *Trends in Cancer*, *3*(7), 529–541. https://doi.org/10.1016/j.trecan.2017.05.002

Rizvi, N. A., Hellmann, M. D., Snyder, A., Kvistborg, P., Makarov, V., Havel, J. J., Lee, W., Yuan, J., Wong, P., Ho, T. S., Miller, M. L., Rekhtman, N., Moreira, A. L., Ibrahim, F., Bruggeman, C., Gasmi, B., Zappasodi, R., Maeda, Y., Sander, C., … Chan, T. A. (2015). Mutational landscape determines sensitivity to PD-1 blockade in non-small cell lung cancer. *Science*, *348*(6230), 124–128. https://doi.org/10.1126/science.aaa1348

Roca, X., Krainer, A. R., & Eperon, I. C. (2013). Pick one, but be quick: 5′ splice sites and the problems of too many choices. *Genes and Development*, *27*(2), 129–144. https://doi.org/10.1101/gad.209759.112

Rosado-Lugo, J. D., & Hampsey, M. (2014). The Ssu72 phosphatase mediates the RNA polymerase II initiation-elongation transition. *Journal of Biological Chemistry*, *289*(49), 33916–33926. https://doi.org/10.1074/jbc.M114.608695

Rosenberg, S. A., Restifo, N. P., Yang, J. C., Morgan, R. A., & Dudley, M. E. (2008). Adoptive cell transfer: A clinical path to effective cancer immunotherapy. *Nature Reviews Cancer*, *8*(4), 299–308. https://doi.org/10.1038/nrc2355

Rosonina, E., Kaneko, S., & Manley, J. L. (2006). Terminating the transcript: Breaking up is hard to do. *Genes and Development*, *20*(9), 1050–1056. https://doi.org/10.1101/gad.1431606

Roszer, T. (2015). Understanding the Mysterious M2 Macrophage through Activation Markers and Effector Mechanisms. *Mediators of Inflammation*, *2015*, 16–18. https://doi.org/10.1155/2015/816460

Ruiz-López, L., Blancas, I., Garrido, J. M., Mut-Salud, N., Moya-Jódar, M., Osuna, A., & Rodríguez-Serrano, F. (2018). The role of exosomes on colorectal cancer: A review. *Journal of*

Gastroenterology and Hepatology, *33*(4), 792–799. https://doi.org/10.1111/jgh.14049
Ryan, K., & Bauer, D. L. V. (2008). Finishing touches: Post-translational modification of protein factors involved in mammalian pre-mRNA 3′ end formation. *International Journal of Biochemistry and Cell Biology*, *40*(11), 2384–2396. https://doi.org/10.1016/j.biocel.2008.03.016
Ryan, K., Calvo, O., & Manley, J. L. (2004). Evidence that polyadenylation factor CPSF-73 is the mRNA 3′ processing endonuclease. *Rna*, *10*(4), 565–573. https://doi.org/10.1261/rna.5214404
Ryder, M., Ghossein, R. A., Ricarte-Filho, J. C. M., Knauf, J. A., & Fagin, J. A. (2008). Increased density of tumor-associated macrophages is associated with decreased survival in advanced thyroid cancer. *Endocrine-Related Cancer*, *15*(4), 1069–1074. https://doi.org/10.1677/ERC-08-0036
Sandberg, R., Neilson, J. R., Sarma, A., Sharp, P. a, & Burge, C. B. (2008). Proliferating cells express mRNAs with shortened 3' UTRs and fewer microRNA target sites. *Science*, *320*(5883), 1643–1647. https://doi.org/10.1126/science.1155390.Proliferating
Sanz-Garcia, C., Nagy, L. E., Lasunción, M. A., Fernandez, M., & Alemany, S. (2014). Cot/tpl2 participates in the activation of macrophages by adiponectin. *Journal of Leukocyte Biology*, *95*(6), 917–930. https://doi.org/10.1189/jlb.0913486
Schindelin, J., Arganda-Carreras, I., Frise, E., Kaynig, V., Longair, M., Pietzsch, T., Preibisch, S., Rueden, C., Saalfeld, S., Schmid, B., Tinevez, J. Y., White, D. J., Hartenstein, V., Eliceiri, K., Tomancak, P., & Cardona, A. (2012). Fiji: An open-source platform for biological-image analysis. *Nature Methods*, *9*(7), 676–682. https://doi.org/10.1038/nmeth.2019
Schioppa, T., Uranchimeg, B., Saccani, A., Biswas, S. K., Doni, A., Rapisarda, A., Bernasconi, S., Saccani, S., Nebuloni, M., Vago, L., Mantovani, A., Melillo, G., & Sica, A. (2003). Regulation of the chemokine receptor CXCR4 by hypoxia. *The Journal of Experimental Medicine*, *198*(9), 1391–1402. https://doi.org/10.1084/jem.20030267
Schlackow, M., Marguerat, S., Proudfoot, N. J., Bähler, J., Erban, R., & Gullerova, M. (2013). Genome-wide analysis of poly (A) site selection in Schizosaccharomyces pombe. *Rna*, *2013*, 1617–1631. https://doi.org/10.1261/rna.040675.113.
Schlackow, M., Nojima, T., Gomes, T., Dhir, A., Carmo-Fonseca, M., & Proudfoot, N. J. (2017). Distinctive Patterns of Transcription and RNA Processing for Human lincRNAs. *Molecular Cell*, *65*(1), 25–38. https://doi.org/10.1016/j.molcel.2016.11.029
Schneider, M. R., Hoeflich, A., Fischer, J. R., Wolf, E., Sordat, B., & Lahm, H. (2000). Interleukin-6 stimulates clonogenic growth of primary and metastatic human colon carcinoma cells. *Cancer Letters*, *151*(1), 31–38. https://doi.org/10.1016/S0304-3835(99)00401-2
Schönemann, L., Kühn, U., Martin, G., Schäfer, P., Gruber, A. R., Keller, W., Zavolan, M., & Wahle, E. (2014). Reconstitution of CPSF active in polyadenylation: Recognition of the polyadenylation signal by WDR33. *Genes and Development*, *28*(21), 2381–2393. https://doi.org/10.1101/gad.250985.114
Schröder, S., Herker, E., Itzen, F., He, D., Thomas, S., Gilchrist, D. A., Kaehlcke, K., Cho, S., Pollard, K. S., John, A., Schnölzer, M., Cole, P. A., Geyer, M., Bruneau, B. G., Adelman, K., & Ott, M. (2013). Acetylation of RNA Polymerase II Regulates Growth-Factor- Induced Gene Transcription in Mammalian Cells. *Molecular Cell*, *52*(3), 314–324. https://doi.org/10.1016/j.molcel.2013.10.009.Acetylation
Schroeder, S. C., Zorio, D. A. R., Schwer, B., Shuman, S., & Bentley, D. L. (2004). A Function of Yeast mRNA Cap Methyltransferase, Abd1, in Transcription by RNA Polymerase II. *Molecular Cell*, *13*(3), 377–387. https://doi.org/10.1016/S1097-2765(04)00007-3
Schwich, O. D., Blümel, N., Keller, M., Wegener, M., Setty, S. T., Brunstein, M. E., Poser, I., Mozos, I. R. D. L., Suess, B., Münch, C., Mcnicoll, F., Zarnack, K., Müller-mcnicoll, M., & Schwich, O. D. (2021). *SRSF3 and SRSF7 modulate 3 ' UTR length through suppression or activation of proximal polyadenylation sites and regulation of CFIm levels*. 1–34.
Seeley, J. J., Baker, R. G., Mohamed, G., Bruns, T., Hayden, M. S., Deshmukh, S. D., Freedberg, D. E., & Ghosh, S. (2018). Induction of innate immune memory via microRNA targeting of chromatin remodelling factors. *Nature*, *559*(7712), 114–119. https://doi.org/10.1038/s41586-018-0253-5
Serbulea, V., DeWeese, D., & Leitinger, N. (2017). The effect of oxidized phospholipids on phenotypic polarization and function of macrophages. *Physiology & Behavior*, *176*(1), 139–148. https://doi.org/10.1016/j.physbeh.2017.03.040
Shah, Y. M. (2016). The role of hypoxia in intestinal inflammation. *Molecular and Cellular Pediatrics*, *3*(1), 1. https://doi.org/10.1186/s40348-016-0030-1
Shah, Y. M., & Xie, L. (2015). *Hypoxia-Inducible Factors Link Iron Homeostasis and Erythropoiesis*. *146*(3), 630–642. https://doi.org/10.1053/j.gastro.2013.12.031.Hypoxia-Inducible
Shankaran, V., Ikeda, H., Bruce, A. T., White, J. M., Swanson, P. E., Old, L. J., & Shreiber, R. D. (2001). IFNgamma and lymphocytes prevent primary tumour development and shape tumour

immunogenicity. *Nature*, *410*(6832), 1107–1111.
Shatkin, A. J. (1976). Capping of eucaryotic mRNAs. *Cell*, *9*(4), 645–653. https://doi.org/10.1016/0092-8674(76)90128-8
Sheets, M. D., Ogg, S. C., Wickens, M. P., & Program, M. B. (1990). *Point mutations in AAUAAA and the poly (A) addition site: effects on the accuracy and efficiency of cleavage and polyadenylation in vitro*. *18*(19), 5799–5805.
Shell, S. A., Hesse, C., Morris, S. M., & Milcarek, C. (2005). Elevated levels of the 64-kDa cleavage stimulatory factor (CstF-64) in lipopolysaccharide-stimulated macrophages influence gene expression and induce alternative poly(A) site selection. *Journal of Biological Chemistry*, *280*(48), 39950–39961. https://doi.org/10.1074/jbc.M508848200
Sheridan, R. M., Fong, N., D'Alessandro, A., & Bentley, D. L. (2019). Widespread Backtracking by RNA Pol II Is a Major Effector of Gene Activation, 5′ Pause Release, Termination, and Transcription Elongation Rate. *Molecular Cell*, *73*(1), 107-118.e4. https://doi.org/10.1016/j.molcel.2018.10.031
Shi, Y. (2012). Alternative polyadenylation: new insights from global analyses. *RNA (New York, N.Y.)*, *18*(12), 2105–2117. https://doi.org/10.1261/rna.035899.112
Shipitsin, M., Campbell, L. L., Argani, P., Weremowicz, S., Bloushtain-Qimron, N., Yao, J., Nikolskaya, T., Serebryiskaya, T., Beroukhim, R., Hu, M., Halushka, M. K., Sukumar, S., Parker, L. M., Anderson, K. S., Harris, L. N., Garber, J. E., Richardson, A. L., Schnitt, S. J., Nikolsky, Y., … Polyak, K. (2007). Molecular Definition of Breast Tumor Heterogeneity. *Cancer Cell*, *11*(3), 259–273. https://doi.org/10.1016/j.ccr.2007.01.013
Sica, A., & Mantovani, A. (2012). Macrophage Plasticity and Polarization: in vivo veritas. *Journal of Clinical Investigation*, *122*(3), 787–795. https://doi.org/10.1172/JCI59643DS1
Sica, A., Saccani, A., Bottazzi, B., Bernasconi, S., Allavena, P., Gaetano, B., Fei, F., LaRosa, G., Scotton, C., Balkwill, F., & Mantovani, A. (2000). Defective Expression of the Monocyte Chemotactic Protein-1 Receptor CCR2 in Macrophages Associated with Human Ovarian Carcinoma. *The Journal of Immunology*, *164*(2), 733–738. https://doi.org/10.4049/jimmunol.164.2.733
Sica, A., Saccani, A., Bottazzi, B., Polentarutti, N., Vecchi, A., Damme, J. Van, & Mantovani, A. (2000). Autocrine Production of IL-10 Mediates Defective IL-12 Production and NF-κB Activation in Tumor-Associated Macrophages. *The Journal of Immunology*, *164*(2), 762–767. https://doi.org/10.4049/jimmunol.164.2.762
Sims, R. J., Belotserkovskaya, R., & Reinberg, D. (2004). Elongation by RNA polymerase II: The short and long of it. *Genes and Development*, *18*(20), 2437–2468. https://doi.org/10.1101/gad.1235904
Sims, R. J., Rojas, L. A., Beck, D., Bonasio, R., Schüller, R., Drury, W. J., Eick, D., & Reinberg, D. (2011). The C-terminal domain of RNA polymerase II is modified by site-specific methylation. *Science*, *332*(6025), 99–103. https://doi.org/10.1126/science.1202663
Singh, G., Kucukural, A., Cenik, C., Leszyk, J. D., Shaffer, S. A., Weng, Z., & Moore, M. J. (2013). *The Cellular EJC Interactome Reveals Higher Order mRNP Structure and an EJC-SR Protein Nexus*. *151*(4), 750–764. https://doi.org/10.1016/j.cell.2012.10.007.The
Singh, G., Pratt, G., Yeo, G. W., & Moore, M. J. (2015). The Clothes Make the mRNA: Past and Present Trends in mRNP Fashion. *Annual Review of Biochemistry*, *84*(1), 325–354. https://doi.org/10.1146/annurev-biochem-080111-092106
Singh, I., Lee, S. H., Sperling, A. S., Samur, M. K., Tai, Y. T., Fulciniti, M., Munshi, N. C., Mayr, C., & Leslie, C. S. (2018). Widespread intronic polyadenylation diversifies immune cell transcriptomes. *Nature Communications*, *9*(1). https://doi.org/10.1038/s41467-018-04112-z
Sivridis, E., Giatromanolaki, A., & Koukourakis, M. I. (2005). Proliferating fibroblasts at the invading tumour edge of colorectal adenocarcinomas are associated with endogenous markers of hypoxia, acidity, and oxidative stress. *J Clin Pathol*, *58*(10), 1033–1038. https://doi.org/10.1136/jcp.2005.026260
Soni, S., Anand, P., & Padwad, Y. S. (2019). MAPKAPK2: The master regulator of RNA-binding proteins modulates transcript stability and tumor progression. *Journal of Experimental and Clinical Cancer Research*, *38*(1), 1–18. https://doi.org/10.1186/s13046-019-1115-1
Spencer, M., Yao-Borengasser, A., Unal, R., Rasouli, N., Gurley, C. M., Zhu, B., Peterson, C. A., & Kern, P. A. (2010). Adipose tissue macrophages in insulin-resistant subjects are associated with collagen VI and fibrosis and demonstrate alternative activation. *Am J Physiol Endocrinol Metab*, *299*(6), E1016-27. https://doi.org/10.1152/ajpendo.00329.2010
Stacey, S. N., Sulem, P., Jonasdottir, A., Masson, G., Gudmundsson, J., Gudbjartsson, D. F., Magnusson, O. T., Gudjonsson, S. A., Sigurgeirsson, B., Thorisdottir, K., Ragnarsson, R., Benediktsdottir, K. R., Nexø, B. A., Tjønneland, A., Overvad, K., Rudnai, P., Gurzau, E., Koppova, K., Hemminki, K., … Stefansson, K. (2011). A germline variant in the TP53 polyadenylation signal

confers cancer susceptibility. *Nature Genetics*, *43*(11), 1098–1103. https://doi.org/10.1038/ng.926
Stahl, M., Schupp, J., Jaǧer, B., Schmid, M., Zissel, G., Mul̈ler-Quernheim, J., & Prasse, A. (2013). Lung collagens perpetuate pulmonary fibrosis via CD204 and M2 macrophage activation. *PLoS ONE*, *8*(11), 1–10. https://doi.org/10.1371/journal.pone.0081382
Steele, C. W., Whittle, T., & Joshua Smith, J. (2019). Review: KRAS mutations are influential in driving hepatic metastases and predicting outcome in colorectal cancer. *Chinese Clinical Oncology*, *8*(5), 1–8. https://doi.org/10.21037/cco.2019.08.16
Steidl, C., Lee, T., Shah, S., Farinha, P., Han, G., Nayar, T., Delaney, A., Jones, S., Iqbal, J., Weisenburger, D., Bast, M., Rosenwald, A., Muller-Hermelink, H., Rimsza, L., Campo, E., Delabie, J., Braziel, R., Cook, J., Tubbs, R., … Gascoyne, R. (2009). Tumor-Associated Macrophages and survival in Classic Hodgkin's Lymphoma. *The New England Journal of Medicine*, *361*(2), 123–134. https://doi.org/10.1056/NEJMoa0900212
Stout, R., & Suttles, J. (2012). Functional plasticity of macrophages: reversible adaptation to changing microenvironments. *Journal of Leukocyte Biology*, *100*(2), 130–134. https://doi.org/10.1016/j.pestbp.2011.02.012.Investigations
Strese, S., Fryknäs, M., Larsson, R., & Gullbo, J. (2013). Effects of hypoxia on human cancer cell line chemosensitivity. *BMC Cancer*, *13*, 331. https://doi.org/10.1186/1471-2407-13-331
Streuli, C. H., & Bissell, M. J. (1990). Expression of extracellular matrix components is regulated by substratum. *Journal of Cell Biology*, *110*(4), 1405–1415. https://doi.org/10.1083/jcb.110.4.1405
Sutherland, C. (2011). What are the bona fide GSK3 substrates? *International Journal of Alzheimer's Disease*, *2011*. https://doi.org/10.4061/2011/505607
Takagaki, Y., Ryner, L. C., & Manley, J. L. (1989). Four factors are required for 3'-end cleavage of pre-mRNAs. *Genes & Development*, *3*(11), 1711–1724. https://doi.org/10.1101/gad.3.11.1711
Takagaki, Yoshio, & Manley, J. L. (2000). Complex Protein Interactions within the Human Polyadenylation Machinery Identify a Novel Component. *Molecular and Cellular Biology*, *20*(5), 1515–1525. https://doi.org/10.1128/mcb.20.5.1515-1525.2000
Takagaki, Yoshio, Seipelt, R. L., Peterson, M. L., & Manley, J. L. (1996). The polyadenylation factor CstF-64 regulates alternative processing of IgM heavy chain pre-mRNA during B cell differentiation. *Cell*, *87*(5), 941–952. https://doi.org/10.1016/S0092-8674(00)82000-0
Talks, K. L., Turley, H., Gatter, K. C., Maxwell, P. H., Pugh, C. W., Ratcliffe, P. J., & Harris, A. L. (2000). The expression and distribution of the hypoxia-inducible factors HIF-1α and HIF-2α in normal human tissues, cancers, and tumor-associated macrophages. *American Journal of Pathology*, *157*(2), 411–421. https://doi.org/10.1016/S0002-9440(10)64554-3
Tang, R., Ojeda, M., Pouillart, P., Scholl, S., Beuvon, F., & Mosseri, V. (1992). M-CSF (monocyte colony stimulating factor) and M-CSF receptor expression by breast tumour cells: M-CSF mediated recruitment of tumour infiltrating monocytes? *Journal of Cellular Biochemistry*, *50*(4), 350–356. https://doi.org/10.1002/jcb.240500403
Taylor, E. S., McCall, J. L., Girardin, A., Munro, F. M., Black, M. A., & Kemp, R. A. (2016). Functional impairment of infiltrating T cells in human colorectal cancer. *OncoImmunology*, *5*(11), 1–8. https://doi.org/10.1080/2162402X.2016.1234573
Taylor, P. R., Gordon, S., & Martinez-Pomares, L. (2005). The mannose receptor: Linking homeostasis and immunity through sugar recognition. *Trends in Immunology*, *26*(2), 104–110. https://doi.org/10.1016/j.it.2004.12.001
Teresa Pinto, A., Laranjeiro Pinto, M., Patrícia Cardoso, A., Monteiro, C., Teixeira Pinto, M., Filipe Maia, A., Castro, P., Figueira, R., Monteiro, A., Marques, M., Mareel, M., Dos Santos, S. G., Seruca, R., Barbosa, M. A., Rocha, S., & José Oliveira, M. (2016). Ionizing radiation modulates human macrophages towards a pro-inflammatory phenotype preserving their pro-invasive and pro-angiogenic capacities. *Scientific Reports*, *6*(November 2015), 18765. https://doi.org/10.1038/srep18765
The Cancer Genome Atlas. (n.d.). https://cancergenome.nih.gov/
Theil, K., Herzog, M., & Rajewsky, N. (2018). Post-transcriptional Regulation by 3′ UTRs Can Be Masked by Regulatory Elements in 5′ UTRs. *Cell Reports*, *22*(12), 3217–3226. https://doi.org/10.1016/j.celrep.2018.02.094
ThermoFisher primer Tm calculator. (n.d.). https://www.thermofisher.com/pt/en/home/brands/thermo-scientific/molecular-biology/molecular-biology-learning-center/molecular-biology-resource-library/thermo-scientific-web-tools/tm-calculator.html
Thijssen, V. L., Barkan, B., Shoji, H., Aries, I. M., Mathieu, V., Deltour, L., Hackeng, T. M., Kiss, R., Kloog, Y., Poirier, F., & Griffioen, A. W. (2010). Tumor cells secrete galectin-1 to enhance endothelial cell activity. *Cancer Research*, *70*(15), 6216–6224. https://doi.org/10.1158/0008-5472.CAN-09-4150

Thomas, S. S., Makar, K. W., Li, L., Zheng, Y., Yang, P., Levy, L., Rudolph, R. Y., Lampe, P. D., Yan, M., Markowitz, S. D., Bigler, J., Lampe, J. W., & Potter, J. D. (2015). Tissue-specific patterns of gene expression in the epithelium and stroma of normal colon in healthy individuals in an aspirin intervention trial. *Genomics Data*, *6*, 154–158. https://doi.org/10.1016/j.gdata.2015.08.029

Tiainen, S., Tumelius, R., Rilla, K., Hämäläinen, K., Tammi, M., Tammi, R., Kosma, V. M., Oikari, S., & Auvinen, P. (2015). High numbers of macrophages, especially M2-like (CD163-positive), correlate with hyaluronan accumulation and poor outcome in breast cancer. *Histopathology*, *66*(6), 873–883. https://doi.org/10.1111/his.12607

Tian, B., Hu, J., Zhang, H., & Lutz, C. S. (2005). A large-scale analysis of mRNA polyadenylation of human and mouse genes. *Nucleic Acids Research*, *33*(1), 201–212. https://doi.org/10.1093/nar/gki158

Tian, B., & Manley, J. L. (2013). Alternative cleavage and polyadenylation: The long and short of it. *Trends in Biochemical Sciences*, *38*(6), 312–320. https://doi.org/10.1016/j.tibs.2013.03.005

Tian, B., & Manley, J. L. (2016). Alternative polyadenylation of mRNA precursors. *Nature Reviews Molecular Cell Biology*, *18*(1), 18–30. https://doi.org/10.1038/nrm.2016.116

Tigan, A., Bellutti, F., Kollmann, K., Tebb, G., & Sexl, V. (2016). *CDK6 — a review of the past and a glimpse into the future : from cell-cycle control to transcriptional regulation*. *October 2015*, 3083–3091. https://doi.org/10.1038/onc.2015.407

Trapnell, C., Pachter, L., & Salzberg, S. L. (2009). TopHat: discovering splice junctions with RNA-Seq. *Bioinformatics*, *25*(9), 1105–1111. https://doi.org/10.1093/bioinformatics/btp120

Tripathi, C., Tewari, B. N., Kanchan, R. K., Baghel, K. S., Nautiyal, N., Shrivastava, R., Kaur, H., Bramha Bhatt, M. L., & Bhadauria, S. (2014). Macrophages are recruited to hypoxic tumor areas and acquire a Pro-Angiogenic M2-Polarized phenotype via hypoxic cancer cell derived cytokines Oncostatin M and Eotaxin. *Oncotarget*, *5*(14), 5350–5368. https://doi.org/10.18632/oncotarget.2110

Tsukamoto, Y., Helsel, W. E., & Wahl, S. M. (1981). Macrophage production of fibronectin, a chemoattractant for fibroblasts. *The Journal of Immunology*, *127*(2), 673 LP – 678. http://www.jimmunol.org/content/127/2/673.abstract

Turner, M. D., Nedjai, B., Hurst, T., & Pennington, D. J. (2014). Cytokines and chemokines: At the crossroads of cell signalling and inflammatory disease. *Biochimica et Biophysica Acta - Molecular Cell Research*, *1843*(11), 2563–2582. https://doi.org/10.1016/j.bbamcr.2014.05.014

Turner, R. E., Henneken, L. M., Liem-Weits, M., Harrison, P. F., Swaminathan, A., Vary, R., Nikolic, I., Simpson, K. J., Powell, D. R., Beilharz, T. H., & Dichtl, B. (2020). Requirement for cleavage factor IIm in the control of alternative polyadenylation in breast cancer cells. *Rna*, *26*(8). https://doi.org/10.1261/RNA.075226.120

Tymoszuk, P., Evens, H., Marzola, V., Wachowicz, K., Wasmer, M. H., Datta, S., Müller-Holzner, E., Fiegl, H., Böck, G., van Rooijen, N., Theurl, I., & Doppler, W. (2014). In situ proliferation contributes to accumulation of tumor-associated macrophages in spontaneous mammary tumors. *European Journal of Immunology*, *44*(8), 2247–2262. https://doi.org/10.1002/eji.201344304

Ueda, M., Iguchi, T., Nambara, S., Saito, T., Komatsu, H., Sakimura, S., Hirata, H., Uchi, R., Takano, Y., Shinden, Y., Eguchi, H., Masuda, T., Sugimachi, K., Yamamoto, H., Doki, Y., Mori, M., Mimori, K., M., U., T., I., … K., M. (2015). Overexpression of Transcription Termination Factor 1 is Associated with a Poor Prognosis in Patients with Colorectal Cancer. *Annals of Surgical Oncology*, 1490–1498. https://doi.org/10.1245/s10434-015-4652-7

Uniacke, J., Holterman, C. E., Lachance, G., Franovic, A., Jacob, M. D., Fabian, M. R., Payette, J., Holcik, M., Pause, A., & Lee, S. (2012). An oxygen-regulated switch in the protein synthesis machinery. *Nature*, *486*(7401), 126–129. https://doi.org/10.1038/nature11055

Valanne, S., Wang, J.-H., & Rämet, M. (2011). The Drosophila Toll Signaling Pathway . *The Journal of Immunology*, *186*(2), 649–656. https://doi.org/10.4049/jimmunol.1002302

Valcárcel, J., & Gebauer, F. (1997). Post-transcriptional regulation: The dawn of PTB. *Current Biology*, *7*(11), 705–708. https://doi.org/10.1016/s0960-9822(06)00361-7

van Furth, R, & Cohn, Z. (1968). The origin and kinetics of mononuclear phagocytes. *J Exp Med*, *128*(3), 415–435. https://doi.org/10.1017/CBO9781107415324.004

Van Nostrand, E. L., Pratt, G. A., Shishkin, A. A., Gelboin-Burkhart, C., Fang, M. Y., Sundararaman, B., Blue, S. M., Nguyen, T. B., Surka, C., Elkins, K., Stanton, R., Rigo, F., Guttman, M., & Yeo, G. W. (2016). Robust transcriptome-wide discovery of RNA-binding protein binding sites with enhanced CLIP (eCLIP). *Nature Methods*, *13*(6), 508–514. https://doi.org/10.1038/nmeth.3810

van Ravenswaay Claasen, H. H., Kluin, P. M., & Fleuren, G. J. (1992). Tumor infiltrating cells in human cancer. On the possible role of CD16+ macrophages in antitumor cytotoxicity. *Laboratory Investigation; a Journal of Technical Methods and Pathology*, *67*(2), 166—174.

http://europepmc.org/abstract/MED/1501443
Vander Ark, A., Cao, J., & Li, X. (2018). TGF-β receptors: In and beyond TGF-β signaling. *Cellular Signalling*, *52*(September), 112–120. https://doi.org/10.1016/j.cellsig.2018.09.002
Veglia, F., & Gabrilovich, D. I. (2017). Dendritic cells in cancer: the role revisited. *Current Opinion in Immunology*, *45*, 43–51. https://doi.org/10.1016/j.coi.2017.01.002
Victoria, S., Temerozo, J. R., Gobbo, L., Pimenta-Inada, H. K., & Bou-Habib, D. C. (2013). Activation of Toll-like receptor 2 increases macrophage resistance to HIV-1 infection. *Immunobiology*, *218*(12), 1529–1536. https://doi.org/10.1016/j.imbio.2013.06.006
Virchow, R. (1863). *Die krankhaften Geschwülste*. Verlag von August Hirschwald.
Vogelstein, B., Fearon, E. R., Hamilton, S. R., Kern, S. E., Preisinger, A. C., Leppert, M., Nakamura, Y., White, R., Smits, A. M. M., & Bos, J. L. (1988). Genetic alterations during colorectal-tumor development. *New England Journal of Medicine*, *319*(9), 525–532.
Von Furth, Ralph. (1985). Mononuclear Phagocytes - Characteristics, physiology and Function. In *Kluwer Academic Publishers Group* (Vol. 39, Issue 7). https://doi.org/10.1136/jcp.39.7.815-c
Vu, T., & Datta, P. K. (2017). Regulation of EMT in colorectal cancer: A culprit in metastasis. *Cancers*, *9*(12), 1–22. https://doi.org/10.3390/cancers9120171
Wang, D. J., Ratnam, N. M., Byrd, J. C., & Guttridge, D. C. (2014). NF-κB functions in tumor initiation by suppressing the surveillance of both innate and adaptive immune cells. *Cell Reports*, *9*(1), 90–103. https://doi.org/10.1016/j.celrep.2014.08.049
Wang, E. T., Sandberg, R., Luo, S., Khrebtukova, I., Zhang, L., Mayr, C., Kingsmore, S. F., Schroth, G. P., & Burge, C. B. (2008). Alternative isoform regulation in human tissue transcriptomes. *Nature*, *456*(7221), 470–476. https://doi.org/10.1038/nature07509
Wang, G. L., & Semenza, G. L. (1993). Desferrioxamine induces erythropoietin gene expression and hypoxia-inducible factor 1 DNA-binding activity: implications for models of hypoxia signal transduction. *Blood*, *82*(12), 3610–3615.
Wang, K., & Vella, A. T. (2016). Regulatory T Cells and Cancer: A Two-Sided Story. *Immunological Investigations*, *45*(8), 797–812. https://doi.org/10.1080/08820139.2016.1197242
Wang, R., Zheng, D., Wei, L., Ding, Q., & Tian, B. (2019). Regulation of Intronic Polyadenylation by PCF11 Impacts mRNA Expression of Long Genes. *Cell Reports*, *26*(10), 2766-2778.e6. https://doi.org/10.1016/j.celrep.2019.02.049
Wang, T., Yu, H., Hughes, N. W., Liu, B., Kendirli, A., Klein, K., Chen, W. W., Lander, E. S., & Sabatini, D. M. (2017). Gene Essentiality Profiling Reveals Gene Networks and Synthetic Lethal Interactions with Oncogenic Ras. *Cell*, *168*(5), 890-903.e15. https://doi.org/10.1016/j.cell.2017.01.013
Weagel, E., Smith, C., Liu, P., Robison, R., & O'Neill, K. (2015). Macrophage Polarization and Its Role in Cancer. *Journal of Clinical & Cellular Immunology*, *06*(04), 4–11. https://doi.org/10.4172/2155-9899.1000338
Wei, C., Yang, C., Wang, S., Shi, D., Zhang, C., Lin, X., Liu, Q., Dou, R., & Xiong, B. (2019). Crosstalk between cancer cells and tumor associated macrophages is required for mesenchymal circulating tumor cell-mediated colorectal cancer metastasis. *Molecular Cancer*, *18*(1), 1–23. https://doi.org/10.1186/s12943-019-0976-4
Weinberg, R. A. (2008). Twisted epithelial-mesenchymal transition blocks senescence. *Nature Cell Biology*, *10*(9), 1021–1023. https://doi.org/10.1038/ncb0908-1021
Wells, C. M., Walmsley, M., Ooi, S., Tybulewicz, V., & Ridley, A. J. (2004). Rac1-deficient macrophages exhibit defects in cell spreading and membrane ruffling but not migration. *Journal of Cell Science*, *117*(7), 1259–1268. https://doi.org/10.1242/jcs.00997
Welsh, T. J., Green, R. H., Richardson, D., Waller, D. A., O'Byrne, K. J., & Bradding, P. (2005). Macrophage and mast-cell invasion of tumor cell islets confers a marked survival advantage in non-small-cell lung cancer. *Journal of Clinical Oncology*, *23*(35), 8959–8967. https://doi.org/10.1200/JCO.2005.01.4910
Werner, F., & Grohmann, D. (2011). Evolution of multisubunit RNA polymerases in the three domains of life. *Nature Reviews Microbiology*, *9*(2), 85–98. https://doi.org/10.1038/nrmicro2507
West, K. O., Scott, H. M., Torres-Odio, S., West, A. P., Patrick, K. L., & Watson, R. O. (2019). The Splicing Factor hnRNP M Is a Critical Regulator of Innate Immune Gene Expression in Macrophages. *Cell Reports*, *29*(6), 1594-1609.e5. https://doi.org/10.1016/j.celrep.2019.09.078
West, S., Gromak, N., & Proudfoot, N. J. (2004). Human 5′ → 3′ exonuclease Xm2 promotes transcription termination at co-transcriptional cleavage sites. *Nature*, *432*(7016), 522–525. https://doi.org/10.1038/nature03035
West, S., & Proudfoot, N. J. (2008). Human Pcf11 enhances degradation of RNA polymerase II-associated nascent RNA and transcriptional termination. *Nucleic Acids Research*, *36*(3), 905–

914. https://doi.org/10.1093/nar/gkm1112
West, S., & Proudfoot, N. J. (2009). Transcriptional Termination Enhances Protein Expression in Human Cells. *Molecular Cell*, *33*(3), 354–364. https://doi.org/10.1016/j.molcel.2009.01.008
Wheeler, A. P., Wells, C. M., Smith, S. D., Vega, F. M., Henderson, R. B., Tybulewicz, V. L., & Ridley, A. J. (2006). Rac1 and Rac2 regulate macrophage morphology but are not essential for migration. *Journal of Cell Science*, *119*(Pt 13), 2749–2757. https://doi.org/10.1242/jcs.03024
Whitelaw, E., & Proudfoot, N. (1986). Alpha-thalassaemia caused by a poly(A) site mutation reveals that transcriptional termination is linked to 3' end processing in the human alpha 2 globin gene. *The EMBO Journal*, *5*(11), 2915–2922. https://doi.org/10.1002/j.1460-2075.1986.tb04587.x
Whiteside, T. L. (2018). FOXP3+ Treg as a therapeutic target for promoting anti-tumor immunity. *Expert Opinion on Therapeutic Targets*, *22*(4), 353–363. https://doi.org/10.1080/14728222.2018.1451514
WHO. (2018). *Estimated number of cases worldwide , both sexes , all ages*. 160.
Wickens, M. (1990). How the messenger got its tail: addition of poly(A) in the nucleus. *Trends in Biochemical Sciences*, *15*(7), 277–281. https://doi.org/10.1016/0968-0004(90)90054-F
Willingham, S. B., Volkmer, J.-P., Gentles, A. J., Sahoo, D., Dalerba, P., Mitra, S. S., Wang, J., Contreras-Trujillo, H., Martin, R., Cohen, J. D., Lovelace, P., Scheeren, F. A., Chao, M. P., Weiskopf, K., Tang, C., Volkmer, A. K., Naik, T. J., Storm, T. A., Mosley, A. R., … Weissman, I. L. (2012). The CD47-signal regulatory protein alpha (SIRPa) interaction is a therapeutic target for human solid tumors. *Proceedings of the National Academy of Sciences*, *109*(17), 6662–6667. https://doi.org/10.1073/pnas.1121623109
Wilton, J., Tellier, M., Nojima, T., Costa, A. M., Oliveira, M. J., & Moreira, A. (2021). Simultaneous studies of gene expression and alternative polyadenylation in primary human immune cells. In *Methods in Enzymology: Vol. mRNA 3' En* (1st ed., Issue June). Elsevier Inc. https://doi.org/10.1016/bs.mie.2021.04.004
Wissink, E. M., Fogarty, E. A., & Grimson, A. (2016). High-throughput discovery of post-transcriptional cis-regulatory elements. *BMC Genomics*, *17*(1), 1–14. https://doi.org/10.1186/s12864-016-2479-7
Woldai, S. (2014). *The role of CD80 and CD86 in macrophage activation and its regulation following LPS stimulation Seghen Woldai Research report submitted to the Department of Biochemistry , Microbiology and Immunology In partial fulfillment of the requirements for the degr*.
Wu, S. L., Fu, X., Huang, J., Jia, T. T., Zong, F. Y., Mu, S. R., Zhu, H., Yan, Y., Qiu, S., Wu, Q., Yan, W., Peng, Y., Chen, J., & Hui, J. (2015). Genome-wide analysis of YB-1-RNA interactions reveals a novel role of YB-1 in miRNA processing in glioblastoma multiforme. *Nucleic Acids Research*, *43*(17), 8516–8528. https://doi.org/10.1093/nar/gkv779
Wu, X., & Bartel, D. P. (2017). Widespread Influence of 3′-End Structures on Mammalian mRNA Processing and Stability. *Cell*, *169*(5), 905-917.e11. https://doi.org/10.1016/j.cell.2017.04.036
Wurth, L., & Gebauer, F. (2015). RNA-binding proteins, multifaceted translational regulators in cancer. *Biochimica et Biophysica Acta (BBA) - Gene Regulatory Mechanisms*, *1849*(7), 881–886. https://doi.org/http://dx.doi.org/10.1016/j.bbagrm.2014.10.001
Wynn, T. A., Chawla, A., & Pollard, J. W. (2013). Macrophage biology in development, homeostasis and disease. *Nature*, *496*(7446), 445–455. https://doi.org/10.1038/nature12034
Xiao, R., Chen, J. Y., Liang, Z., Luo, D., Chen, G., Lu, Z. J., Chen, Y., Zhou, B., Li, H., Du, X., Yang, Y., San, M., Wei, X., Liu, W., Lécuyer, E., Graveley, B. R., Yeo, G. W., Burge, C. B., Zhang, M. Q., … Fu, X. D. (2019). Pervasive Chromatin-RNA Binding Protein Interactions Enable RNA-Based Regulation of Transcription. *Cell*, 107–121. https://doi.org/10.1016/j.cell.2019.06.001
Xiong, Y., Wang, K., Zhou, H., Peng, L., You, W., & Fu, Z. (2018). Profiles of immune infiltration in colorectal cancer and their clinical significant: A gene expression-based study. *Cancer Medicine*, *7*(9), 4496–4508. https://doi.org/10.1002/cam4.1745
Xu, L., Li, Z., Song, S., Chen, Q., Mo, L., Wang, C., Fan, W., Yan, Y., Tong, X., & Yan, H. (2020). Downregulation of α-l-fucosidase 1 suppresses glioma progression by enhancing autophagy and inhibiting macrophage infiltration. *Cancer Science*, 2284–2296. https://doi.org/10.1111/cas.14427
Yagi, T., Baba, Y., Okadome, K., Kiyozumi, Y., Hiyoshi, Y., Ishimoto, T., Iwatsuki, M., Miyamoto, Y., Yoshida, N., Watanabe, M., Komohara, Y., & Baba, H. (2019). Tumour-associated macrophages are associated with poor prognosis and programmed death ligand 1 expression in oesophageal cancer. *European Journal of Cancer*, *111*, 38–49. https://doi.org/10.1016/j.ejca.2019.01.018
Yahaya, M. A. F., Lila, M. A. M., Ismail, S., Zainol, M., & Afizan, N. A. R. N. M. (2019). Tumour-Associated Macrophages (TAMs) in colon cancer and how to reeducate them. *Journal of Immunology Research*, *2019*. https://doi.org/10.1155/2019/2368249
Yamamoto, H., & Imai, K. (2019). An updated review of microsatellite instability in the era of next-

generation sequencing and precision medicine. *Seminars in Oncology*, *46*(3), 261–270. https://doi.org/10.1053/j.seminoncol.2019.08.003

Yan, Y., Zhang, J., Li, J. H., Liu, X., Wang, J. Z., Qu, H. Y., Wang, J. S., & Duan, X. Y. (2016). High tumor-associated macrophages infiltration is associated with poor prognosis and may contribute to the phenomenon of epithelial–mesenchymal transition in gastric cancer. *OncoTargets and Therapy*, *9*, 3975–3983. https://doi.org/10.2147/OTT.S103112

Yang, M., McKay, D., Pollard, J. W., & Lewis, C. E. (2018). Diverse functions of macrophages in different tumor microenvironments. *Cancer Research*, *78*(19), 5492–5503. https://doi.org/10.1158/0008-5472.CAN-18-1367

Yang, X., Zhao, M., Xia, M., Liu, Y., Yan, J., Ji, H., & Wang, G. (2012). PNAS Plus: Selective requirement for Mediator MED23 in Ras-active lung cancer. *Proceedings of the National Academy of Sciences*, *109*(41), E2813–E2822. https://doi.org/10.1073/pnas.1204311109

Yang, Xiaochen, Wu, J., Xu, W., Tan, S., Chen, C., Wang, X., Sun, J., & Kang, Y. (2018). Genome-wide profiling reveals cancer-related genes with switched alternative polyadenylation sites in colorectal cancer. *OncoTargets and Therapy*, *11*, 5349–5357. https://doi.org/10.2147/OTT.S164233

Yang, Y., Ye, Y. C., Chen, Y., Zhao, J. L., Gao, C. C., Han, H., Liu, W. C., & Qin, H. Y. (2018). Crosstalk between hepatic tumor cells and macrophages via Wnt/β-catenin signaling promotes M2-like macrophage polarization and reinforces tumor malignant behaviors. *Cell Death and Disease*, *9*(8). https://doi.org/10.1038/s41419-018-0818-0

Ye, L., Zhang, T., Kang, Z., Guo, G., Sun, Y., Lin, K., Huang, Q., Shi, X., Ni, Z., Ding, N., Zhao, K. N., Chang, W., Wang, J., Lin, F., & Xue, X. (2019). Tumor-infiltrating immune cells act as a marker for prognosis in colorectal cancer. *Frontiers in Immunology*, *10*(OCT), 1–12. https://doi.org/10.3389/fimmu.2019.02368

Yoshida, D., Ikeda, Y., Waki, K., Shirabe, K., Kakeji, Y., Tsujitani, S., & Maehara, Y. (2012). Different incidence of synchronous liver metastasis between proximal and distal colon cancer. *Surgery Today*, *42*(5), 426–430. https://doi.org/10.1007/s00595-011-0056-x

Yuan, X., Zhang, J., Li, D., Mao, Y., Mo, F., Du, W., & Ma, X. (2017). Prognostic significance of tumor-associated macrophages in ovarian cancer: A meta-analysis. *Gynecologic Oncology*, *147*(1), 181–187. https://doi.org/10.1016/j.ygyno.2017.07.007

Zanganeh, S., Hutter, G., Spitler, R., Lenkov, O., Mahmoudi, M., Shaw, A., Pajarinen, J. S., Nejadnik, H., Goodman, S., Moseley, M., Coussens, L. M., & Daldrup-Link, H. E. (2016). Iron oxide nanoparticles inhibit tumour growth by inducing pro-inflammatory macrophage polarization in tumour tissues. *Nature Nanotechnology*, *11*(11), 986–994. https://doi.org/10.1038/nnano.2016.168

Zaretsky, J. M., Garcia-Diaz, A., Shin, D. S., Escuin-Ordinas, H., Hugo, W., Hu-Lieskovan, S., Torrejon, D. Y., Abril-Rodriguez, G., Sandoval, S., Barthly, L., Saco, J., Moreno, B. H., Mezzadra, R., Chmielowski, B., Ruchalski, K., Shintaku, I. P., Sanchez, P. J., Puig-Saus, C., Cherry, G., … Ribas, A. (2016). Mutations associated with acquired resistance to PD-1 blockade in melanoma. *New England Journal of Medicine*, *375*(9), 819–829. https://doi.org/10.1056/NEJMoa1604958

Zeisberg, M., Shah, A. A., & Kalluri, R. (2005). Bone morphogenic protein-7 induces mesenchymal to epithelial transition in adult renal fibroblasts and facilitates regeneration of injured kidney. *Journal of Biological Chemistry*, *280*(9), 8094–8100. https://doi.org/10.1074/jbc.M413102200

Zeng, Q., Li, S., Chepeha, D. B., Giordano, T. J., Li, J., Zhang, H., Polverini, P. J., Nor, J., Kitajewski, J., & Wang, C. Y. (2005). Crosstalk between tumor and endothelial cells promotes tumor angiogenesis by MAPK activation of Notch signaling. *Cancer Cell*, *8*(1), 13–23. https://doi.org/10.1016/j.ccr.2005.06.004

Zhang, F., Wang, H., Wang, X., Jiang, G., Liu, H., Zhang, G., Wang, H., Fang, R., Bu, X., Cai, S., & Du, J. (2016). TGF-β induces M2-like macrophage polarization via SNAILmediated suppression of a pro-inflammatory phenotype. *Oncotarget*, *7*(32), 52294–52306. https://doi.org/10.18632/oncotarget.10561

Zhang, H., Rigo, F., & Martinson, H. G. (2015). Poly(A) Signal-Dependent Transcription Termination Occurs through a Conformational Change Mechanism that Does Not Require Cleavage at the Poly(A) Site. *Molecular Cell*, *59*(3), 437–448. https://doi.org/10.1016/j.molcel.2015.06.008

Zhang, S., Kim, C. C., Batra, S., McKerrow, J. H., & Loke, P. (2010). Delineation of diverse macrophage activation programs in response to intracellular parasites and cytokines. *PLoS Neglected Tropical Diseases*, *4*(3). https://doi.org/10.1371/journal.pntd.0000648

Zhao, J., Hyman, L., & Moore, C. (1999). Formation of mRNA 3′ Ends in Eukaryotes: Mechanism, Regulation, and Interrelationships with Other Steps in mRNA Synthesis. *Microbiology and Molecular Biology Reviews*, *63*(2), 405–445. https://doi.org/10.1128/mmbr.63.2.405-445.1999

Zhao, Y., Xiong, Z., Lechner, E. J., Klenotic, P. A., Hamburg, B. J., Hulver, M., Khare, A., Oriss, T., Mangalmurti, N., Chan, Y., Zhang, Y., Ross, M. A., Stolz, D. B., Rosengart, M. R., Pilewski, J., Ray, P., Ray, A., Silverstein, R. L., & Lee, J. S. (2014). Thrombospondin-1 triggers macrophage IL-10 production and promotes resolution of experimental lung injury. *Mucosal Immunology*, *7*(2), 440–448. https://doi.org/10.1038/mi.2013.63

Zheng, D., Wang, R., Ding, Q., Wang, T., Xie, B., Wei, L., Zhong, Z., & Tian, B. (2018). Cellular stress alters 3′UTR landscape through alternative polyadenylation and isoform-specific degradation. *Nature Communications*, *9*(1), 1–14. https://doi.org/10.1038/s41467-018-04730-7

Zhu, Yong, Wang, X., Forouzmand, E., Jeong, J., Qiao, F., Sowd, G. A., Engelman, A. N., Xie, X., Hertel, K. J., & Shi, Y. (2017). Molecular mechanisms for CFIm-mediated regulation of mRNA alternative polyadenylation. *Molecular Cell*, *176*(1), 139–148. https://doi.org/10.1016/j.molcel.2017.11.031.Molecular

Zhu, Yu, Herndon, J. M., Sojka, D. K., Kim, K. W., Knolhoff, B. L., Zuo, C., Cullinan, D. R., Luo, J., Bearden, A. R., Lavine, K. J., Yokoyama, W. M., Hawkins, W. G., Fields, R. C., Randolph, G. J., & DeNardo, D. G. (2017). Tissue-Resident Macrophages in Pancreatic Ductal Adenocarcinoma Originate from Embryonic Hematopoiesis and Promote Tumor Progression. *Immunity*, *47*(2), 323-338.e6. https://doi.org/10.1016/j.immuni.2017.07.014

Zigmond, E., & Jung, S. (2013). Intestinal macrophages: Well educated exceptions from the rule. *Trends in Immunology*, *34*(4), 162–168. https://doi.org/10.1016/j.it.2013.02.001